AD_____

Award Number: DAMD17-99-1-9563

TITLE: Multidisciplinary Strategies in the Prevention and Early Detection of Ovarian Cancer

PRINCIPAL INVESTIGATOR: Samuel C. Mok

CONTRACTING ORGANIZATION: Brigham and Women's Hospital
Boston, Massachusetts 02115

REPORT DATE: September 2001

TYPE OF REPORT: Annual

PREPARED FOR: U.S. Army Medical Research and Materiel Command
Fort Detrick, Maryland 21702-5012

DISTRIBUTION STATEMENT: Approved for Public Release;
Distribution Unlimited

The views, opinions and/or findings contained in this report are those of the author(s) and should not be construed as an official Department of the Army position, policy or decision unless so designated by other documentation.

REPORT DOCUMENTATION PAGE

Form Approved
OMB No. 074-0188

1. AGENCY USE ONLY (Leave blank)	2. REPORT DATE	3. REPORT TYPE AND DATES COVERED
	September 2001	Annual (1 Sep 00 - 31 Aug 01)

4. TITLE AND SUBTITLE
Multidisciplinary Strategies in the Prevention and Early Detection of Ovarian Cancer

5. FUNDING NUMBERS
DAMD17-99-1-9563

6. AUTHOR(S)
Samuel C. Mok

7. PERFORMING ORGANIZATION NAME(S) AND ADDRESS(ES)
Brigham and Women's Hospital
Boston, Massachusetts 02115

E-Mail: scmok@rics.bwh.harvard.edu

8. PERFORMING ORGANIZATION REPORT NUMBER

9. SPONSORING / MONITORING AGENCY NAME(S) AND ADDRESS(ES)
U.S. Army Medical Research and Materiel Command
Fort Detrick, Maryland 21702-5012

10. SPONSORING / MONITORING AGENCY REPORT NUMBER

11. SUPPLEMENTARY NOTES

12a. DISTRIBUTION / AVAILABILITY STATEMENT
Approved for Public Release; Distribution Unlimited

12b. DISTRIBUTION CODE

13. ABSTRACT *(Maximum 200 Words)*

This program project consists of 4 research projects. Project I studies genetic changes in microdissected microscopic Stage I ovarian cancer cells, and identify markers for early detection of the disease. Using state of the art technology, we have shown that different histological subtypes of ovarian cancer have different allelic loss profiles. Furthermore, we have also identified several candidate serum markers including prostasin, and GA733 autoantibody, which may be used as markers for early detection of ovarian cancer. Project II evaluates the use of Protease M as early diagnostic marker for ovarian cancer. We have shown that Protease M is secreted by ovarian cancer cells, and is highly expressed in ovarian tumors of different stages and subtypes. Project III studies the effect of hormones on growth and differentiation of normal ovarian surface epithelial cells, evaluate whether they contribute to ovarian carcinogenesis. We have established an *in vitro* system to evaluate the effect the various hormones on the growth of normal ovarian epithelial cells. We have shown that E1, E2, and FSH can induce cell proliferation and enhance colony formation potential in soft agar. Project IV uses lysophospholipids (LPA) to develop a highly sensitive and specific marker for the early detection of ovarian cancer. Using the newly developed ESI-MS-based method, we have found that besides LPA, other lysopgospholipids, including alkyl-LPA, alkenyl-LPA, LPI, SPC, and LPC are also elevated in ascites from patients with ovarian cancer. Receptors of SPC and LPC have also been identified.

14. SUBJECT TERMS	15. NUMBER OF PAGES
Ovarian cancer, carcinogenesis, marker, LPA microdissection	258
	16. PRICE CODE

17. SECURITY CLASSIFICATION OF REPORT	18. SECURITY CLASSIFICATION OF THIS PAGE	19. SECURITY CLASSIFICATION OF ABSTRACT	20. LIMITATION OF ABSTRACT
Unclassified	Unclassified	Unclassified	Unlimited

Table of Contents

INTRODUCTION

Project 1: Early genetic changes in human epithelial ovarian tumors

Ovarian cancer is the fourth cause of death from all cancers among American women and ranks the highest among deaths from gynecologic malignancies. Although the cure rate with stage I ovarian cancer approaches 90%, two-third of patients are diagnosed with advanced intraperitoneal metastatic disease, with five year survival rate of 15 to 20%. Therefore, it is of paramount importance to identify a marker(s) for early diagnosis of the disease. However, it has been rare to identify Stage I disease and to see transition within a malignant tumor from benign to malignant epithelium which might help us to identify early genetic changes during ovarian cancer development. Recent histologic studies on prophylactic ovaries from high-risk individuals showed the presence of microscopic premalignant and malignant epithelia suggesting that they may create an identifiable milieu from which common epithelial tumors of the ovary will mostly likely arise. Molecular genetic study on these microscopic malignant epithelia would provide us with early genetic events during ovarian cancer development. We therefore propose first, to perform LOH study on specific loci on chromosome 1p, 3p, 5q, 6q, 7q, 9p, 11p, 11q, 12p, 12q, 14q, 17p, 17q, 22q and Xq by polymerase chain reaction (PCR) analysis of tandem repeat polymorphisms; second, to perform immunohistochemistry study on specific oncogene and tumor suppressor genes on paraffin sections prepared from ovaries with microscopic malignant serous lesions and to study specific oncogene activation and tumor suppressor gene inactivation by single strand polymorphism (SSCP) analysis and direct PCR sequencing on microdissected malignant serous epithelium obtained from paraffin-embedded ovaries; and third, to perform RNA fingerprinting on mRNA isolated from microdissected normal and malignant ovarian epithelial cells prepared from normal ovarian surface epithelium and early stage serous ovarian carcinoma and to identify differentially expressed genes in these early stage epithelial ovarian cancer cells. We believe that these studies should provide us with early genetic changes during ovarian cancer progression and serum markers which can be used for early diagnosis of the disease which will significantly improve the survival rate of the patient.

Project 2: A Potential Serum Marker for Ovarian Cancer

The poor prognosis of ovarian cancer is mainly due to the lack of sensitive tests for early detection of the disease, which is often asymptomatic. Studies have shown that ovarian cancer detected in early stage has a high five-year survival rate of exceeding 90% (1, 2). Therefore, identification of molecular marker for early stage ovarian cancer detection is of paramount importance. This project is to study a cDNA sequence which we have recently identified by differential display. The encoded protein is highly homologous to trypsin and members of the kallikrein protease family. The novel protease, named as protease M, is highly expressed in many invasive epithelial ovarian cancer tissues and cell lines, but not in normal ovarian cell cultures (3). Since the preliminary data showed that upregulation of protease M was also observed in stage I tumors and the protease was detectable in the conditioned media culturing the tumor cells, the proposed work is to evaluate the potential use of protease M as a serum marker for early detection of ovarian cancer and for monitoring treatment response of ovarian cancer patients, similar to the use of another kallikrein member, prostate-specific antigen (PSA), in the diagnosis and prognosis of prostate cancer (4). The three objectives of this project are: 1) to study the expression level of protease M in normal human ovaries and ovarian tumors of different stages and histological grades; 2) to characterize protease M and to identify the physiological substrates for protease M by an innovative cyclic peptide library screening method; 3) to develop a sensitive, specific, and reproducible method for measuring the circulating protease M in the sera of ovarian cancer patients.

The results of this study will have a significant impact upon developing a substantially more efficient early detection program with an increased probability of reducing mortality from ovarian cancer. The characterization of protease M protein and identification of physiological substrates for protease M may provide insights into the probable function of this novel protease in the pathogenesis of ovarian cancer. The identified optimal peptide substrates with high specificity and affinity for protease M will have significant value in the development of a carrier for targeted delivery of cytotoxic agents to protease M-secreting ovarian cancer cells.

Project 3: Hormones as etiological factors of ovarian carcinogenesis

Ovarian cancer (OC) is the highest-ranking cause of death from gynecological cancers among American women. All cell types of the human ovary may undergo neoplastic transformation; the vast majority (80-90%) of malignant tumors are derived from the single layer of epithelial cells covering the ovarian surface. Although the etiology of OC is still unknown, several theories have been put forth to explain epidemiologic correlates. Nulliparity, lower number of pregnancies, never breast-feeding, and infertility are linked to increased incidence of ovarian cancer. Since these conditions may increase the number of ovulations in a woman's life-time, a unified hypothesis has been proposed to explain the interrelationships between OC and these contributory factors. It has been postulated that "incessant ovulation" leads to neoplastic transformation of HOSE cells. It is believed that following ovulation, ovarian epithelial cells undergo rapid proliferation to repair the ruptured epithelium. While the etiology of OC remains elusive, epidemiological observations have implicated ovarian steroids and/or gonadotropins, particularly when present at abnormal levels during and after menopause, as probable risk factors of OC. Understanding the role of hormones in ovarian carcinogenesis is of utmost importance to combat this deadly disease.

Project 4: Development of a highly sensitive and specific method for the early detection and a strategy for the early intervention of ovarian cancer

Ovarian carcinoma has the worst prognosis of any gynecological malignancy, due to the difficulty of early detection, the high metastatic potential of the tumor and the lack of highly effective treatment for metastatic disease. We have shown previously that lysophosphatidic acid (LPA) may represent a useful marker for the detection of ovarian cancer (5). The method used for LPA determination was a gas chromatographic method, which is cumbersome to perform. We have proposed to develop a mass spectrometry-based method to detect lysophospholipids in human body fluids (Task 1). This method will then be used to analyze lysolipids in blood samples collected from patients with ovarian cancer, other diseases, or healthy controls to determine whether one or more of these lipids may be useful for the detection of ovarian cancer (Task 1). In Task 2, we hypothesize that elevated levels of LPA in blood and ascites from patients with ovarian cancer are due to an abnormality of LPA production and/or degradation. We propose to study the enzymes controlling levels of LPA in ovarian cancer cells and/or body fluids from patients with ovarian cancer. If an abnormal enzymatic activity associated with ovarian cancer is identified, it may represent a target for early intervention, since LPA is likely to be involved in ovarian tumor cell growth, angiogenesis, and metastasis (reviewed in ref 6).

BODY

Project 1: Early genetic changes in human epithelial ovarian tumors

Task 1. Tissue collection, processing and microdissection (months 1-36): A total of 48 stage I epithelial ovarian carcinomas have been collected. Tissue collection will be continued in month 24-36.

Task 2. To perform loss of heterozygosity (LOH) studies on specific loci on chromosome 1p, 3p, 5q, 6q, 7q, 9p, 11p, 11q, 12p, 12q, 14q, 17p, 17q, 22q and Xq in microscopic stage I serous ovarian carcinomas by polymerase chain reaction (PCR) analysis of tandem repeat polymorphisms (months 1-36).

a). Tissue sectioning, and DNA extraction (months 1-12): Tissue sectioning, microdissection, and DNA extraction have been completed.

b). LOH study (months 3-36): also see attached manuscripts in appendix

1. Wang VW, Bell DA, Berkowitz RS, Mok SC: Whole genome amplification and high-throughput allelotyping identified five distinct deletion regions on chromosome 5 and 6 in microdissected early stage ovarian tumors. Cancer Res. 2001:4169-4174.
2. Wang VW, Bell DA, Chung TKH, Wong YF, Hasselblattl K, Minna JD, Schorge JO, Berkowitz RS, Mok SC: Molecular profiling of stage I epithelial ovarian carcinomas by high throughput allelotyping. Submitted.

Using a high-throughput PCR-based method combined with laser capture microdissection and whole genome amplification techniques, we perform allelotyping on DNA isolated from 48 stage I sporadic epithelial ovarian cancer including 15 serous, 9 mucinous, 12 endometrioid, and 12 clear cell carcinomas. Among them, four are microscopically detected tumors (Fig. 1a & b). A total of 20 fluorescent-labeled microsatellite markers spanning chromosome 5 and 6, and 27 markers spanning chromosome 17 were used. The percentage of loss of heterozygosity (LOH) for each marker and the fractional allelic loss (FAL) for each sample were calculated and compared among different histological types. High frequencies of loss on chromosome 5 were identified at loci D5S428 (48%), D5S424 (32%), and D5S630 (32%). Chromosome 6 exhibited high frequencies of LOH at loci D6S1574 (46%), D6S287 (42%), D6S441 (45%), D6S264 (60%) and D6S281 (35%). These results suggest that multiple tumor suppressor genes are located on 5 distinct regions on chromosomes 5 and 6, *i.e.*, 5p15.2, 5q13-21, 6p24-25, 6q21-23 and 6q25.1-27, and may be involved in the early development of ovarian carcinomas. However, there were no significant difference in LOH frequencies among tumors with different sizes, grades, and histological subtypes.

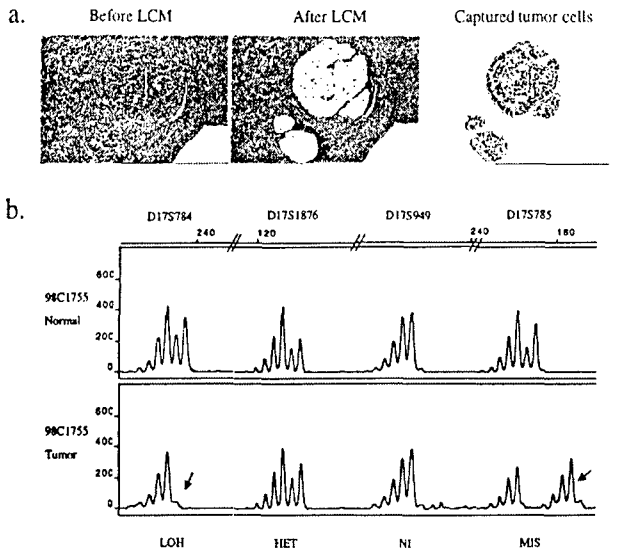

Figure 1. (a) Representative example of LCM of a microscopially identified high grade serous adenocarcinoma. (b). Allelotyping patterns on chromosome 17 in a stage I serous ovarian adenocarcinoma. Shown in this figure are representative electropherogram traces on four loci examined. The top panel depicts the peaks for each of the four loci in the stromal tissue from the same tumor. The bottom panel from left to right shows loss of heterozygosity (LOH), retention of heterozygosity, (HET), uninformative (NI), and microsatellite instability (MIS).

On chromosome 17, allelotyping on all 48 tumors showed high frequencies of LOH (>45%) at loci D17S849 (17p13.2), D17S799 (17p12), and D17S1862 (17q24.3) (Fig. 2). Increased number of loci showed more than 45% LOH rate when the four histological subtypes were analyzed separately. Serous tumors demonstrated significantly higher LOH rate in 7 of 27 loci examined than other tumor types ($p<0.05$). Significant difference in LOH rate was also observed in 18 of 27 loci screened when tumors with different differentiations were compared ($P<0.05$). When the average FAL rate was compared among different tumor types, there was no significant difference among grade I tumors. However, grade 2 serous, mucinous, and clear cell tumors showed significantly higher FAL rate than endometrioid tumors ($p<0.01$); and grade 3 serous and endometrioid tumors showed significantly higher FAL rate than both mucinous and clear cell types ($p<0.01$). Among the microscopic tumors, both grade 3 serous (case 99N51) and endometrioid (case774) adenocarcinomas showed significantly higher FAL than the grade 1 serous (case 3317) ($p<0.0001$) and the grade 2 serous (case 7024) ($p<0.02$) adenocarcinomas (Fig. 2). Significant difference in FAL between the microscopically detected carcinomas and other stage I invasive ovarian carcinomas with the same grade was not detected.

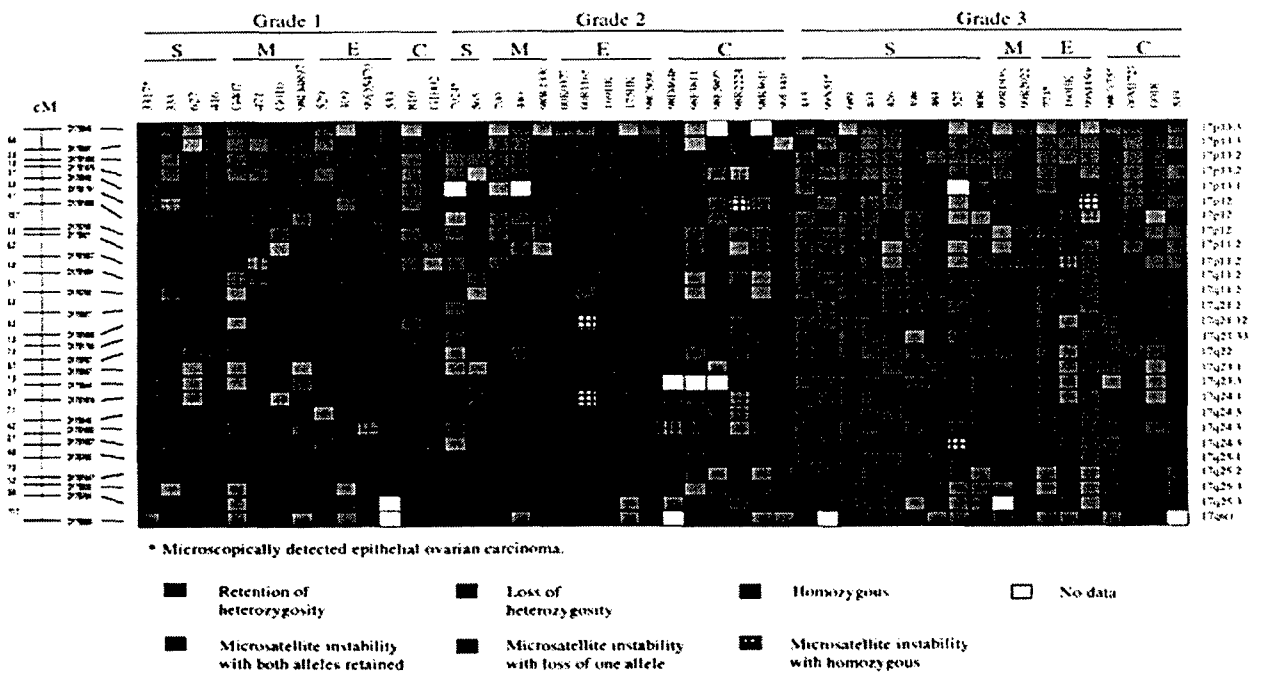

Figure 2. Detailed deletion map of stage I epithelial ovarian tumors. Cases are grouped under different histological types and pathological grades. Microsatellite markers used and the genetic linkage map are shown on the left. Chromosomal localizations of the markers are shown on the right. LOH (Loss of heterozygosity), red box; HET (heterozygous with no loss), green box; NI (homozygous), gray box; MSI (microsatellite instability) with both alleles retained, hatched green box; MSI with loss of one allele, hatched red box; MSI with homozygous, hatched blue box; not test, white box. S, serous; M, mucinous; E, endometrioid; C, clear cell.

Task 3. To study specific proto-oncogene activation and tumor suppressor gene inactivation in microscopic stage I ovarian carcinomas by single strand conformation polymorphism (SSCP) analysis, direct PCR sequencing and immunohistochemistry (months 1-30).
Tissue sectioning (months 1-12)
SSCP analysis and direct PCR sequencing (months 6-24)
Immunostaining of sections (months 18-30) (also see attached manuscript in appendix)

Wang VW, Bell DA, Berkowitz RS, Mok SC: *TP53* is involved in the development of de novo high grade serous ovarian carcinomas. Submitted

Seven microscopically detected stage I ovarian carcinomas were identified. LCM was used to procure tumor cells from tissue sections. DNA was isolated and amplified with primer sets flanking exons 2-11 of the *TP53* gene. Amplified DNA was purified and direct PCR sequencing was performed using the ABI PRISM® BigDye Terminator Cycle Sequencing system (Applied Biosystem, foster City, CA) and the ABI PRISM 310 Genetic Analyzer. Immunolocalization of the p53 protein was also performed on the same cases. The results showed that *TP53* mutations and p53 over-expression were detected in all grade 2 and 3 serous adenocarcinomas but not in the two grade 1 serous adenocarcinomas (case V1834 and 3317), and the grade 3 clear cell adenocarcinoma (case S3854) (Fig. 3, Table 1).

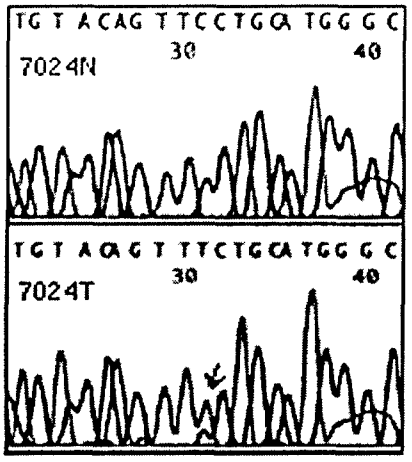

Fig. 3. Electropherogram traces showing TP53 exon 7 sequences in normal (7024N) and tumor tissues (7024T). Arrow indicates a nucleotide change from C to T in the tumor tissue.

Table 1. Mutation and loss of heterozygosity of the TP53 gene and expression of the p53 protein in microscopically detected stage I ovarian tumors

Case No.	Grade	Histological type	Size	Loss of heterozygosity	Immuno-reactivity	Exon-mutated stage (codon)	Nucleotide change	Amino acid change
3317	1	serous	a	L	negative	-	-	-
97-7024	2	serous	8mm	L	positive	7 (241)	TCC to TTC	Ser to Phe
99N51	3	serous	2mm	L	positive	6 (214)	CAT to CGT	His to Arg
774	3	endometrioid	2mm	L	positive	9 (310)	AAC to ACC	Asn to Thr
S3854	3	clear cell	2mm	NL	negative	-	-	-
4613	3	serous	6mm	L	positive	9 (310)	AAC to ACC	Asn to Thr
V1834	1	serous	a	NL	negative	-	-	-

a, several tiny foci too small to measure; L, loss of heterozygosity; NL, no loss

Task 4. To identify differentially expressed genes in microdissected normal ovarian surface epithelial cells and Stage I ovarian carcinoma cells by RNA fingerprinting technique (months 12-36).

Perform RNA fingerprinting (months 12-24)
Characterize differentially expressed sequences (months 16-30) (see attached manuscripts)

1. Kwong-kwok Wong, Cheng RS, Mok SC: Identification of differentially expressed genes from ovarian cancer cells by MICROMAX cDNA microarray system. Biotechnique 2001,30:670-675.
2. Mok SC, Chao J, Skates S, Wong KK, Yiu GK, Muto MG, Berkowitz RS, Cramer DW: Prostasin, a potential serum marker for ovarian cancer, identified through microarray technology. J Natl Cancer Inst, 2001, 93: in press.

3. Kim JH, Herlyn D, Wong KK, Yiu GK, Schorge JO, Lu KH, Berkowitz RS, Mok SC: Ep-CAM autoantibody is a potential serum marker for epithelial ovarian cancer. Submitted.

Using a higher throughput microarray analysis to identify differential expressed genes in early stage ovarian cancer, we have identify a total of 30 putative genes, which are differentially over-expressed in ovarian cancer cells. Two of them, prostasin and Ep-CAM have been validated and further characterized. Prostasin is a serine proteinase normally secreted by the prostate gland. Over-expression of prostasin in ovarian cancer tissues and cell lines was confirmed by real-time PCR and immunostaining. An enzyme linked immunosorbant assay was developed to quantify the amount of prostain in serum samples. The mean (and 95% confidence interval on the mean) serum level of prostasin in ovarian cancer cases was 13.7 (10.5, 16.9) μg/ml compared to 7.5 (6.8, 8.3) μg/ml in 137 controls subjects ($p<0.001$, after adjustment for age and specimen source). In 16 case patients with both pre-operative and postoperative serum samples available, postoperative prostasin levels were statistically significantly lower than pre-operative levels ($p<0.02$). No significant correlation was observed between prostasin and CA-125 in 37 case patients with nonmucinous ovarian cancer and 100 control subjects suggesting that CA-125 may provide complementary information.

Ep-CAM is an epithelial cell adhesion molecule. Microarray analysis showed that this gene exhibited a cancer-to-HOSE ratio of 444. Real time quantitative PCR analysis revealed significant overexpression of Ep-CAM mRNA in cancer cell lines ($P<0.001$) and microdissected cancer tissues ($p=0.035$), compared to that in cultured normal HOSE and microdissected germinal epithelium, respectively. Immuno-histochemical staining of paraffin block sections revealed that Ep-CAM expression was absent in stromal areas of normal ovaries or those with benign disease or cancer. In contrast, a gradient of expression was found in the germinal epithelium with ovaries from women with borderline or invasive cancer displaying the greatest level of expression, normal ovaries the least, and ovaries from women with benign tumors intermediate expression ($p<0.05$). No significant differences in Ep-CAM immuno-histochemical staining were observed among ovarian cancer samples with different histologic types, and grades. Early stage tumors showed significantly stronger staining than late stage tumors. Because Ep-CAM auto-antibody levels have been shown to be elevated in other cancers, such as colon, we examined levels of auto-antibody against Ep-CAM in patients with epithelial ovarian cancer and controls by enzyme-linked immunosorbent assay (ELISA). Ep-CAM auto-antibody levels (measured in units of absorbance at 450nm) were: 0.132 in 52 patients with ovarian cancer, 0.098 in 26 cases with benign gynecologic disease, and 0.090 in 26 normal women ($p<0.05$). When a cut-off value of 0.115 was used, the Ep-CAM auto-antibody assay showed a sensitivity of 71.2% and a specificity of 80.8% whereas the sensitivity and specificity of CA 125 measured in 52% of the same subjects were 84.6% and 88.5% with a CA 125 cut-off of 35U/ml. However, the Ep-CAM auto-antibody assay may be complementary to CA125, as indicated by low correlation coefficient and the fact that combining the test with CA 125 increased the sensitivity to 94.2% and specificity to 100.0%. This investigation has demonstrated the potential value of cDNA microarray analysis in identifying overexpressed genes in ovarian cancer, and suggests that the Ep-CAM auto-antibody may offer a biomarker for ovarian cancer with clinical usefulness.

Project 2: A Potential Serum Marker for Ovarian Cancer

Task 1: Investigation of expression of protease M in clinical samples:

1. Collection of samples: months 1 - 30

Samples are continuously collected by Dr. Samuel Mok and his associates.

2. Gene expression study: months 6 - 36

Table 2 summaries the updated expression data of protease M in ovarian tumor tissues according to different stages of the disease. For the RNA analysis, we have applied real-time quantitative RT-PCR to analyze the expression of protease M in ovarian tumors in comparison with the levels in normal ovarian epithelial primary cultures. Most of the tested tumor RNAs expressed high levels of protease M transcript. Furthermore, many of the early stage and low grade tumor samples showed up-regulation of protease M expression, suggesting that high levels of protease M expression also occur in stage I tumors, especially for invasive epithelial ovarian cancers. Up-regulation of protease M may be an early event during ovarian carcinogenesis. Since our polyclonal antibody does not work for immunohistochemistry, we could only determine the protein expression in a few samples by Western blot analysis. We are now in the process of developing monoclonal antibodies specific to protease M. One goal of this development is to obtain good antibody for detecting protease M in archival tissues by immunohistochemical staining.

	INVASIVE		BORDERLINE	
	RNA	PROTEIN	RNA	PROTEIN
Stage 1	8/9 (89%)	4/6 (67%)	3/4 (75%)	0/1 (0%)
Stage 2	4/7 (57%)	0/1 (0%)	5/6 (83%)	2/2 (100%)
Stage 3	29/33 (88%)	10/18 (56%)	2/2 (100%)	N.D.
Stage 4	7/7 (100%)	1/1 (100%)	N.D.	N.D.

Table 2. Protease M expression in different stages of epithelial ovarian tumors.
Percentage of cases that show protease M RNA and/or protein expression are tabulated according to disease stages.
N.D. = not determined.

Task 2: Substrate screening:

1. Enzymatic assays for protease M and other proteases: months 8 - 16

We have to produce recombinant protease M protein for the enzymatic assays. The COS 7 cells we obtained have been confirmed later that they did not express protease M. We have tried many times of expressing the gene in different cell types without success. Sequencing of the cDNA did not reveal any mutation. The latest strategy was cloning the cDNA together with 5'-noncoding region. Unfortunately the resulting cell lines after transfection were still not producing the recombinant protein. We are now trying to use the TNT® coupled in vitro transcription/translation system (Promega) to confirm that our cDNA is workable and start from there.

We have for the generation of monoclonal antibody purpose produced and purified a prokaryotic protease M recombinant protein in fusion with maltose-binding protein (MBP), which is soluble in native reaction buffer (**Fig. 3A**). Preliminary enzymatic analysis using an EnzChek™ Protease Assay Kit (Molecular Probes) has shown that the protease M fusion protein possesses measurable proteolytic activity (**Fig. 3C**). But the enzymatic activity may be too low for accurate comparison with other proteases, probably due to the hindrance of the nonactive fusion part. Another approach is the development of a prokaryotic recombinant protein with minimal fusion counterpart.

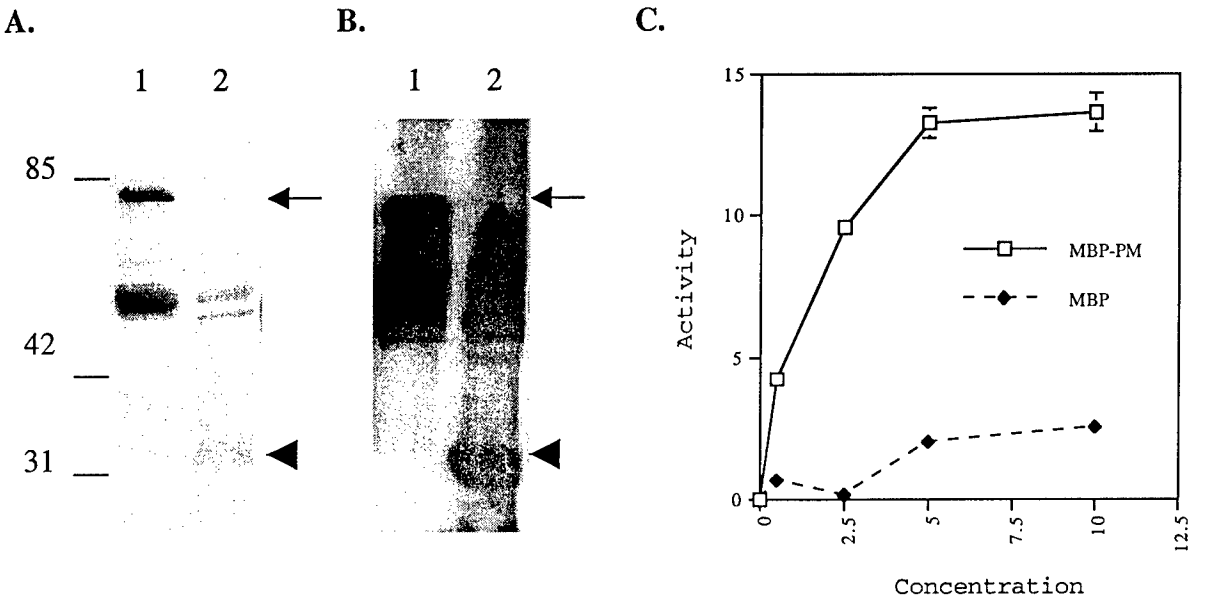

Fig. 3. Production of the maltose-binding protein (MBP)-protease M fusion protein and the proteolytic assay.

A. Coomassie blue staining of the gel. Lane 1: the purified fusion protein; lane 2: The fusion after Factor Xa digestion. Molecular weight markers are shown on the left. The MBP-Protease M fusion protein is indicated by an arrow, whereas the protease M protein released after Factor Xa cleavage is indicated by an arrowhead.

B. Western blot analysis using the protease M-directed polyclonal antibody.

C. Proteolytic assay using an EnzChek™ Protease Assay Kit (Molecular Probes). Proteolytic activity of MBP-protease M fusion protein released the highly fluorescent BODIPY FL dye-labeled peptides. The fluorescence was quantified by a Gemini spectrofluorometer. The plot shown is Activity (arbitrary fluorescence units) versus concentration of the proteins (μg).

2. Enzymatic assays in the presence of protease inhibitors: months 16 - 20

We cannot attempt this without resolving the bottleneck of producing enough recombinant protein. We will hasten the production process to finish this work before the end of this grant.

3. Cyclic peptide library screening: months 14 - 24

Same as above.

4. Confirmation of the optimal peptide motifs by enzymatic assays: months 25 - 30

Not started yet.

Task 3: Detection of protease M in patient blood:

1. Collection of samples and storage: months 1 - 24

Samples are continuously collected by Drs. Samuel Mok and Dan Cramer.

2. Development of detection methods: months 6 - 24

We have developed a prokaryotic protease M fusion protein as mentioned above (Figure 3). We have sent the fusion protein to the company Green Mountain Antibody for immunizing the mice. However, there were very few (about 100) hybrid clones obtained after the fusion of splenocytes with the immortalized myeloma line SN1. Screening of the hybrid clones by ELISA just showed that they produced antibodies either directed only to the maltose-binding protein counterpart or to nothing. The failure of detecting any protease M-directed clones might be due to the dominant effect of the maltose binding protein counterpart to the murine immune system. We have since then changed the strategy by using more immunogen for the immunization and using Factor Xa-released protease M in the boosting of mice. We will test the titer of the antiserum very soon and hope that we will obtain positive clones this time.

3. Assays on the blood samples: months 25 - 30

Not started yet.

4. Data analysis: months 31 - 36

Not started yet.

Project 3: Hormones as etiological factors of ovarian carcinogenesis

The first objective is to determine the efficacies of selected estrogens, to achieve this the HOSE cells will be treated with increasing concentrations of estrogen for five days. The cell proliferation will be measured by MTT assay. To study the synergistic effect of FSH and estrogens cells will be cultured in the absence or presence of FSH and HOSE cell proliferation will be studied. To ascertain whether their mitogenicities are mediated via estrogen receptors receptor blocker will be used.

The second objective is to determine whether the 3 selected estrogens have direct oncogenic potentials and if they could be enhanced by FSH and blocked by the antiestrogen, ICI 182, 780. The HOSE cells will be plated and exposed to different doses of estrogen for two weeks. Soft agar assay will be used to study the transformation potential of estrogens. In a parallel experiment FSH will be added along with estrogen to study the synergistic effect on cell transformation.

The third objective is to pick up a hormonal milieu that will produce the highest frequency of *in vitro* transformation. To ascertain whether progesterone and DHEA exert anti-tumorigenic action by blocking the estrogen and/or FSH-induced neoplastic transformation of HOSE cells, in vitro transformation assay will be used to assay the ability of progesterone and DHEA in inhibiting the estrogen-gonadotropin-induced transformation of HOSE cells.

Results:
Estradiol stimulated cell proliferation is inhibited by antiestrogen: When increasing concentrations (10^{-11}-10^{-6} M) of estrone (E1) or estradiol (E2) were added to primary HOSE 639, HOSE 770, HOSE

783, HOSE 785, and immortalized normal HOSE 642, HOSE 301, HOSE 306, HOSE 12-12, in culture, a dose dependent rise in cell proliferation was observed. About ten to fourteen fold increase was noted by 10^{-6} M E1 or E2 in HOSE 639, HOSE 770, HOSE 783, HOSE 785 cell lines compared to six fold increase in normal immortalized lines HOSE 642, HOSE 301, HOSE 306 and HOSE 12-12 cell lines. E1 and E2 were equally effective in causing cell proliferation in all cell lines except HOSE 12-12 cell line where E1 showed a significant enhancement of cell proliferation compared to E2. Cell lines cultured with FSH and estradiol showed significant cell growth but no additive effect was seen in any cell line tested. The ICI considered as pure antiestrogen, functions specifically by binding to and inactivating the estrogen receptor. When primary and immortalized HOSE cells were incubated with 10^{-8} M E2 A marked enhancement of cell proliferation was seen in all the cell lines with E2 and when cells were cuultured with E2 and two doses (10^{-5} and 10^{-4} M) of ICI for 5 days, addition of ICI to cultures along with E2 markedly attenuated cell proliferation.

FSH and estrogen combination enhance colony formation of HOSE cells.- The first criterion used to select transformed HOSE cells following exposure to estrogen is their ability to proliferate on soft agar. We have established a standard protocol to test the carcinogenicity of hormones on HOSE cells. Briefly, HOSE cells were plated at low density in 24-well plates and exposed to different doses of either estrogen (DES), FSH or combination of both FSH and DES for 14 days. After treatments, cells were removed from the 24-well plates with trypsin and replated in 6-well plates for expansion of potential transformants. Once the cell cultures reached confluence in 6-well plates they are removed and subjected to soft-agar growth selection (Freshney, 1994).. After two-four weeks of soft agar selection, individual clones proliferating on soft agar plates were removed, expanded, and stored for further investigations.

Using this protocol, we discovered that HOSE cells, exposed continuously to diethylstilbestrol (DES), a potent synthetic estrogen, at concentrations between 10^{-9} to 10^{-8} M for 14 days, had acquired ability to grow on soft agar (Table 1). **Approximately 4-6, 3-5 and 8-10 colonies were found in a total of 10^4 FSH treated, DES treated and FSH+DES treated cells plated on soft agar respectively.** Untreated HOSE cells did not form any soft-agar colonies suggesting little or no spontaneous transformation activity. At present, the FSH+DES-induced colonies derived from these preliminary experiments are under passaging to establish stable lines.

Hormones	FSH	DES	FSH+DES
#of colonies	4-6	3-5	8-10

Table 3. Number of colonies obtained by treatment of HOSE Cells with different hormones.

Project 4: Development of a highly sensitive and specific method for the early detection and a strategy for the early intervention of ovarian cancer

Work accomplished as proposed in Task 1:

We have completed work proposed in items a, d, e, f, and g in Task 1. We have collected ascites samples (Task 1, item a) and developed an electrospray ionization mass spectrometry (ESI-MS)-based method for analyzing all lysophospholipids in ascites and in plasma (Task 1, item d, e, f, and g). The work accomplished is published in Anal Biochem (Ref 7; in Appendices). We have optimized conditions to extract lipids from human body fluids and established standard curves to measure each of the lysolipids quantitatively. None of the previous lipid analytical methods, including gas-chromatographic-based, and HLPC-based methods, can analyze many lysophospholipids simultaneously

and quantitatively. The method that we developed is highly effective, reproducible, sensitive, and quantitative.

We have previously shown that lysophosphatidic acid (LPA) is present in ascites and elevated in plasma from patients with ovarian cancer (1). Using the ESI-MS based method developed, we compared lysophospholipid contents isolated in ascitic fluids from patients with ovarian cancer to those from patients with non-malignant diseases. Ascites from ovarian cancer patients contained acyl-, alkyl-, and alkenyl-LPAs, lysophosphatidylinositols (LPIs) and lysophophatidylcholines (LPCs). In addition, we detected both sphingosine-1-phosphate (S1P) and sphingosylphosphorylcholine (SPC) in ascites from patients with ovarian cancer. Overall, ascitic fluids from patients with ovarian cancer contain significantly higher levels of lysophospholipids than those from patients with non-malignant diseases (Ref 7; in Appendices). We have previously shown that LPA stimulates tumor cell proliferation. The high levels of bioactive lipids may play important roles in tumor development and metastasis. Furthermore, these lipids may represent useful diagnostic, prognostic markers and/or novel therapeutic target(s) of ovarian cancer.

The work proposed in items b, c, h, and i in Task 1 has been partially accomplished. We have analyzed lysophospholipid contents in a total of 155 plasma samples, including 15 healthy controls, 24 patients with ovarian cancer, 32 patients with other malignancies, 65 patients with benign gynecological diseases, and 19 patients with family history of ovarian and/or breast cancers. We are in the process of analyzing all data statistically. Fig. 4 (in the appendices) shows that levels of LPA, LPI, and SPC were significantly ($P < 0.05$) elevated in ovarian cancer patients, compared with healthy controls. In contrast, levels of other lipids tested, including LPC and lyso-PAF, were not significantly different in plasma from patients with ovarian cancer and healthy controls. We are in the process of analyzing whether combined measurements of LPA, LPI, and SPC would increase sensitivity and/or specificity of the test.

Work accomplished as proposed in Task 2:

We have proposed to develop a strategy for the early intervention of ovarian cancer through controlling LPA levels. We hypothesize that ovarian cancer cells may be defective in LPA degradation and/or possess the ability to produce abnormally high levels of LPA. Indeed, we have found a lysophospholipase D (LysoPLD) activity in ovarian cancer ascites, but not in ascites from patients with non-malignant diseases (Fig. 5, below). This activity is sensitive to EDTA and EGTA treatment, suggesting that calcium ions are required for the enzymatic activity.

LPA Production in Ascites

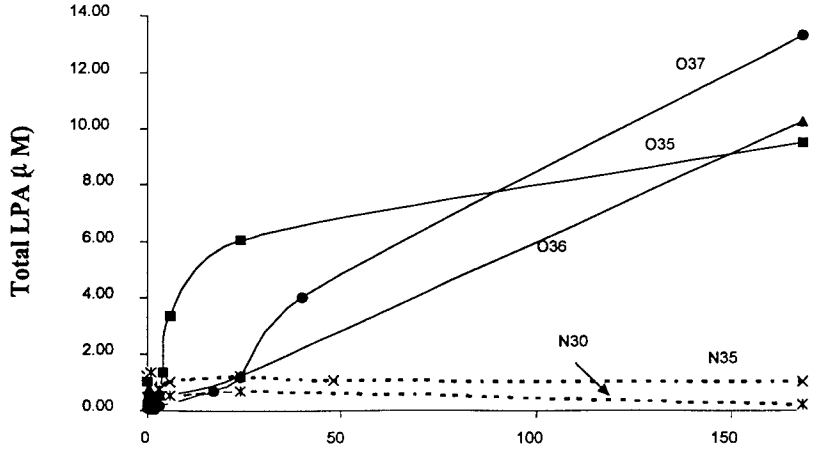

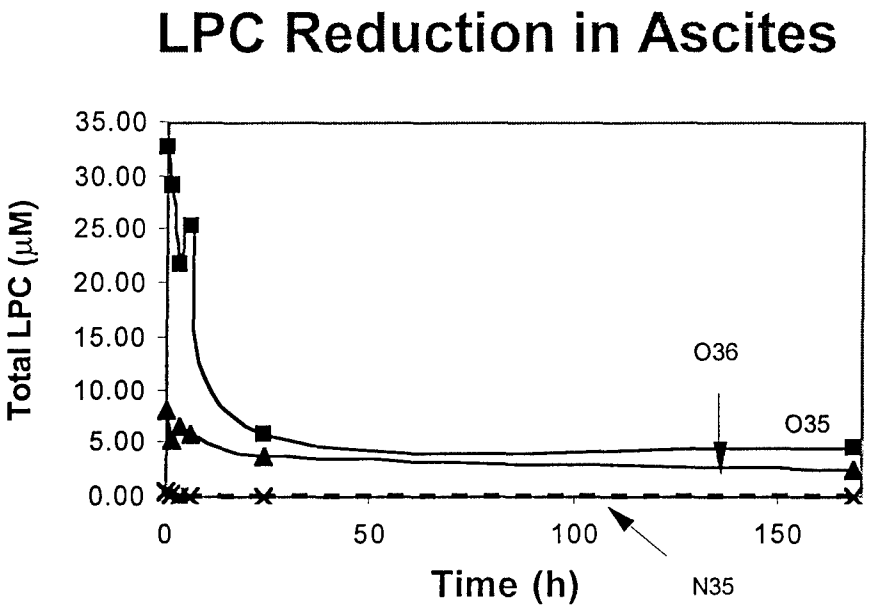

Fig. 5. Ascites samples from patients with ovarian cancer (O35, O36, and O37) and non-malignant diseases (N30 and N35) were incubated at 37°C for times as indicated. LPA and LPC levels were analyzed as described in Ref. 3 (in appendices)

We have performed functional analyses of alkyl- and alkenyl-LPA (al-LPAs) in ovarian cancer cells, and found that they are elevated and stable in ovarian cancer ascites, which represents an *in vivo* environment for ovarian cancer cells. They stimulated DNA synthesis and proliferation of ovarian cancer cells. In addition, they induced cell migration and the secretion of a pro-angiogenic factor, interleukin-8 (IL-8), in ovarian cancer cells. The latter two processes are potentially related to tumor metastasis and angiogenesis, respectively. Al-LPAs induced diverse signaling pathways in ovarian cancer cells. Their mitogenic activity depended on the activation of the $G_{i/o}$ protein, phosphatidylinositol-3 kinase (PI3K), and mitogen-activated protein (MAP) kinase kinase (MEK), but not p38 MAP kinase. The S473 phosphorylation of Akt by these lipids required activation of the $G_{i/o}$ protein, PI3K, MEK, p38 MAP kinase, and Rho. On the other hand, cell migration induced by al-LPAs depended on activities of the $G_{i/o}$ protein, PI3K, and Rho, but not MEK. These data strongly suggest that al-LPAs may play important roles in ovarian cancer development and therefore may represent novel targets for tumor intervention as we proposed in Task 2. A manuscript describing these works is enclosed in the appendices.

We have shown that SPC enhances production of the proangiogenic factor, interleukin-8 (IL-8) (8). LPC may be involved in regulating DNA synthesis and proliferation (our unpublished results). Therefore, these lipids may be useful targets for therapy. While receptors for LPA have been identified in the past few years, the receptors for SPC and LPC were unknown previously. We have recently identified receptors for SPC and LPC (9-11; reprints in the appendices).

KEY RESEARCH ACCOMPLISHMENTS

Project 1: Early genetic changes in human epithelial ovarian tumors

- Six manuscripts have either been published or submitted.
- Techniques including microdissection, whole genome amplification, high throughput allelotyping, and signal amplification system for microarray analysis have been established.
- Two potential serum markers which may be used for early detection of ovarian cancer have been identified.

Project 2: A Potential Serum Marker for Ovarian Cancer

- Gene expression analysis of the tumor samples has demonstrated that protease M is highly expressed in ovarian tumors of various stages and subtypes but not in the normal ovarian epithelial cells.
- Protease M fusion proteins have been made. Different strategies will be tried to produce monoclonal antibodies specific to protease M.

Project 3: Hormones as etiological factors of ovarian carcinogenesis

- One abstract and one manuscript have been published
- An *in vitro* system has been established to evaluate the effect of hormones on the growth of ovarian surface epithelial cells.

Project 4: Development of a highly sensitive and specific method for the early detection and a strategy for the early intervention of ovarian cancer

- Developed a highly sensitive and reproducible electrospray mass spectrometry-based method to analyze lysophospholipids quantitatively.
- Detected for the first time alkyl-LPA and alkenyl-LPA in human body fluids, including plasma and ascites.
- Higher concentrations of bioactive lysophospholipids, including alkyl-, alkenyl-, acyl-LPAs, lysophosphatidylinositol (LPI), lysophosphatidylcholine (LPC), and sphingosylphosphorylcholine (SPC), are present in ascites from patients with ovarian cancer, compared to patients with non-malignant diseases. These lipid molecules 1) may represent useful diagnostic and/or prognostic markers for ovarian cancer; 2) may be useful in clinical management; and 3) may be novel therapeutic targets.
- After analyses of lysophospholipids in plasma samples from patients with ovarian cancer and healthy controls using the ESI-MS method, we confirmed our previous results that LPA levels are elevated in patients with ovarian cancer. In addition, we have found that both LPI and SPC levels were also elevated in plasma from ovarian cancer patients. The clinical significance of these findings are under investigation.
- Identified the first high affinity receptors for SPC and LPC
- Detected a lysoPLD activity in ascites from patients with ovarian cancer, but not from patients with non-malignant diseases. This activity may play a critical role in controlling LPA levels *in vivo*.

REPORTABLE OUTCOMES

Project 1: Early genetic changes in human epithelial ovarian tumors

Manuscript:

1. Wang VW, Bell DA, Berkowitz RS, **Mok SC**: Whole genome amplification and high-throughput allelotyping identified five distinct deletion regions on chromosome 5 and 6 in microdissected early stage ovarian tumors. Cancer Res. 2001,61:4169-4174.
2. Kwong-kwok Wong, Cheng RS, **Mok SC**: Identification of differentially expressed genes from ovarian cancer cells by MICROMAX cDNA microarray system. Biotechnique 2001,30:670-675.
3. **Mok SC**, Chao J, Skates S, Wong KK, Yiu GK, Muto MG, Berkowitz RS, Cramer DW: Prostasin, a potential serum marker for ovarian cancer, identified through microarray technology. J Natl Cancer Inst, 2001, 93: in press.
4. Wang VW, Bell DA, Chung TKH, Wong YF, Hasselblattl K, Minna JD, Schorge JO, Berkowitz RS, **Mok SC**: Molecular profiling of stage I epithelial ovarian carcinomas by high throughput allelotyping. Submitted.
5. Kim JH, Herlyn D, Wong KK, Yiu GK, Schorge JO, Lu KH, Berkowitz RS, **Mok SC**: Ep-CAM autoantibody is a potential serum marker for epithelial ovarian cancer. Submitted.
6. Wang VW, Bell DA, Berkowitz RS, **Mok SC**: *TP53* is involved in the development of de novo high grade serous ovarian carcinomas. Submitted.

Abstract:

1. Garner EIO, Leung SM, Berkowitz RS, Muto MG, Cramer DW, **Mok SC**: Protein profiling of epithelial ovarian tumors by surface enhanced laser desorption/ionization mass spectrometry (SELDI) analysis. (SGO 32nd Annual Meeting, Nashville, TE, March 3-7, 2001).
2. Gibson HE, Wong KK, Yiu GK, Muto MG, Berkowitz RS, Cramer DW, **Mok SC**: Clinical applications of microarray technology. Creatine kinase B is an upregulated gene in epithelial ovarian cancer and shows promise as a serum marker. (SGO 32nd Annual Meeting, Nashville, TE, March 3-7, 2001).
3. Kim JH, Herlyn D, Wong KK, Yiu GK, Schorge JO, Lu KH, Berkowitz RS, **Mok SC**: Ep-CAM autoantibody is a potential serum marker for epithelial ovarian cancer. (AACR 92nd Annual Meeting, New Orlean, LA, March 24-28, 2001).
4. Wang VW, Bell DA, Berkowitz RS, **Mok SC**: Whole genome amplification and high-throughput allelotyping identified five distinct deletion regions on chromosome 5 and 6 in microdissected early stage ovarian tumors. (AACR 92nd Annual Meeting, New Orlean, LA, March 24-28, 2001).
5. **Mok SC**, Chao J, Skates S, Wong KK, Yiu GK, Muto MG, Berkowitz RS, Cramer DW: Prostasin, a potential serum marker for ovarian cancer, identified through microarray technology. (AACR 92nd Annual Meeting, New Orlean, LA, March 24-28, 2001)

Funding applied for based on the work supported by this award:

"Prostasin, a potential serum marker for ovarian cancer " (4/1/02-3/30/07)
Principal Investigator: Samuel C. Mok
Agent : NIH
Type: RO1 ($3,798,254)
To evaluate the potential in using prostasin as a marker for early detection of ovarian cancer

Project 2: A Potential Serum Marker for Ovarian Cancer

None

Project 3: Hormones as etiological factors of ovarian carcinogenesis

Manuscript:

1. Syed V, Ulinski G, Mok SC, Yiu GK, **Ho SM**: Expression of gonadotropin receptor and growth responses to key reproductive hormones in normal and malignant human ovarian surface epithelial cells. Cancer Res 2001, 61:6768-6776.

Abstract:

1. Syed V, Mok SC, **Ho SM**: Hormonal regulation of human ovarian surface epithelial (HOSE) cells. Endocrinology Meeting, June, 2000, Toronto, Canada.

Project 4: Development of a highly sensitive and specific method for the early detection and a strategy for the early intervention of ovarian cancer

Manuscripts:

1. Xiao Y, Schwartz B, Washington M, Kennedy A, Webster K, Belinson J. and **Xu Y**. Electrospray Ionization Mass Spectrometry Analysis of Lysophospholipids in Human Ascitic Fluids: Comparison of the Lysophospholipid Contents in Malignant vs. Non-malignant Ascitic Fluids. Anal Biochem. 290, 302-313, 2001
2. **Xu Y,** Xiao Y, Baudhuin LM, Schwartz BM. The role and clinical applications of bioactive lysolipids in ovarian cancer. *J. Soc. Gyn. Invest* 8,1-13, 2001.
3. Kabarowski JHS, Zhu K, Le LQ, Witte ON, **Xu Y.** Lysophosphatidylcholine as a Ligand for the Immunoregulatory Receptor G2A. Science 293, 702-705 2001
4. Zhu, K., Baudhuin, L., Hong, G. Williams, F.S., Cristina, K.L., Kabarowski, J.H.S., Witte, O.N. and **Xu, Y** Sphingosylphosphorylcholine and lysophosphatidylcholine are ligands for the G protein coupled receptor, GPR4. J. Biol. Chem. In press.
5. Lu J, Baudhuin LM, Hong G, and **Xu, Y**. Role and Signaling Pathways of Ether-linked Lysophosphatidic Acids in Ovarian Cancer Cells. Submitted.

Abstract:

1. Lu J, Xiao Y and **Xu Y**. Roles of Ether-linked Lysophosphatidic Acid in Ovarian Cancer Cells. FASEB Summer Research Conference-Lysophospholipids and Related Bioactive Lipids in Biology & Diseases. Tucson, AZ (6/10/01).
2. Zhu K. and **Xu Y.** Identification of the first two high affinity receptors for Sphingosylphosphorylcholine (SPC) and the first receptor for Lysophosphatidylcholine (LPC) (2001 ASBMB meeting; 3/31-4/4/01, Orlando, FA).
3. Xiao Y, Song, L, Schwartz B Washington M, Kennedy A, Webster K, Belinson J, and **Xu Y.** Alkyl and Alkenyl Lysophosphatidic Acid are elevated in peritoneal washings of patients with early and late stage ovarian Cancer (2001 ASBMB meeting; 3/31-4/4/01, Orlando, FL)
4. Xiao Y, Schwartz B, Washington M, Kennedy A, Webster K, Belinson J. and **Xu Y**. Electrospray Ionization Mass Spectrometry Analysis of Lysophospholipids in Human Ascitic Fluids: Comparison of the Lysophospholipid Contents in Malignant vs. Non-malignant Ascitic Fluids (2000 CCF Retreat, 9/10/00; Research Day, 10/15/00).
5. Zhu K, Baudhuin LM, Hong G, **Xu Y.** Sphingosylphosphorylcholine (SPC) and lysophosphatidylcholine (LPC) are ligands for GRP4 (2000 CCF Retreat, 9/10/00; Research Day, 10/15/00).
6. Lu J, Zhu K, **Xu Y**. Biological Effects of Alkyl- and Alkenyl-lysophosphatidic Acids in Ovarian Cancer Cells (2000 CCF Retreat, 9/10/00).

Presentation:

1 "Role of lysophospholipids in ovarian cancer", an invited talk at Ceretek LLC (8/3/01; Alameda, CA)
2 "Bioactive lysophospholipids in cancers", an invited talk at the Renal Cell Carcinoma SPORE Committee meeting (7/12/01; The Cleveland Clinic Foundation)
3 "Bioactive lysophospholipids in cancers", an invited talk at the Special Symposium: finding a cure to glioblastoma (6/23-6/24/01, The Cleveland Clinic Foundation)
4 "G protein coupled receptors for SPC and LPC", an invited talk at 2001 FASEB Summer Research Conference-Lysophospholipids and Related Bioactive Lipids in Biology & Diseases. (Tucson, AZ, 6/10/01)
5 "The potential clinical applications of lysolipids", an invited talk at Pacific Ovarian Cancer Research Consortium (POCRC) Scientific Seminar (4/17/01, Seattle, WA)
6 "Lysolipids and their receptors", an invited talk at the Department of Anesthesiology at the Cleveland Clinic Foundation (1/30/01)
7 "OGR1 and GPR4 are receptors for SPC and LPC", an invited talk at the Howard Hughes Medical Institute, UCLA (10/12/00).
8 "Bioactive lipids and their receptors in ovarian cancer", an invited talk at University of Virginia, Charlottesville, Sept. 6, 2000)

Funding applied for based on the work supported by this award:
"The Clinical Implication of Lysophosphatidic Acid" (6/1/01-5/31/02)
Principal Investigator: Yan Xu
Agent : Pacific Ovarian Cancer Research Consortium
Type: subcontract ($58,908)
Evaluate the clinical significance of LPA levels in peritoneal washings

CONCLUSIONS

Project 1: Early genetic changes in human epithelial ovarian tumors

High throughput allelotyping on stageI ovarian carcinomas showed that different histological types and grades of sporadic stage I epithelial ovarian cancers have different allelic loss profiles. Allelic loss on chromosome 17 is an early event in the pathogenesis of high grade serous and endometrioid carcinomas. These data support the notion that ovarian cancer represents multiple diseases with different pathogenetic pathways and therefore warrants to be studied separately. The identification of *TP53* mutations and p53 protein over-expression in these microscopically detected high grade serous carcinomas suggest that p53 alteration is an early event in the pathogenesis of high grade serous adenocarcinomas and further suggest that high and low grade ovarian carcinomas may have different pathogenetic pathways. Finally, using microarray analysis, we identified prostasin and Ep-CAM autoantibody as potential serum markers for early detection of ovarian cancer. Characterization of other candidate markers is on-going.

Project 2: A Potential Serum Marker for Ovarian Cancer

Analysis of the tumor samples has demonstrated that protease M is highly expressed in ovarian tumors of various stages and subtypes but not in the normal ovarian epithelial cells. This is important for the development of screening tools for early detection of ovarian cancer. Other objectives are being

pursued to characterize the protease and to develop a sensitive and specific method for detection of circulating protease in the sera of ovarian cancer patients.

Project 3: Hormones as etiological factors of ovarian carcinogenesis

All the cell lines responded equally well to E2 and E1 except HOSE 12-12 cell line, where E1 was more effective than E2 in inducing cell proliferation. Furthermore, No synergism was observed when cultures were challenged simultaneously with FSH and E2. Furthermore, treatment of HOSE cells with FSH and estrogens enhance their colony formation potential on soft agar.

Project 4: Development of a highly sensitive and specific method for the early detection and a strategy for the early intervention of ovarian cancer

We have made important accomplishments in developing a method of detecting, and a strategy for, the early intervention of ovarian cancer. The newly developed ESI-MS-based method is highly sensitive, reproducible, and quantitative. We confirmed that LPA levels are elevated in plasma from patients with ovarian cancer using the MS-based method. Data analyses are in progress to determine the specificity of the test. More clinical samples will be collected in the third year of the grant to further assess the sensitivity and specificity of the test.

Using the MS method, we have found that a number of other lysophospholipids, including alkyl-LPA, alkenyl-LPA, LPI, SPC, and LPC are also elevated in ascites from patients with ovarian cancer, compared with ascites from patients with non-malignant diseases (3). The diagnostic, prognostic, and clinic management signficance of these lipids is under investigation.

Importantly, we have recently identified the first receptors for SPC and LPC (5-7). These discoveries provide an intriguing opportunity and a novel approach to study the roles of SPC and LPC in ovarian cancer. In addition, we have found Lyso-PLD activity in ovarian cancer ascites. To target these receptors and lyso-PLD as an early intervention strategy is under investigation.

REFERENCES

1. Bast, R.C., Jr., Boyer, C.M., Olt, G.J., Berchuck, A., Soper, J.T., Clarke-Pearson, D., Xu, F.J., and Ramakrishnan, S. Identification of marker for early detection of epithelial ovarian cancer. *In*: F. Sharp, W.P. Mason, and R.E. Leake (eds.), Ovarian Cancer Biological and Therapeutic Challenges, pp.265-275., 1990. London, England: Chapman and Hall Medical.
2. Advanced Ovarian Trialists Group. Chemotherapy in advanced ovarian cancer: an overview of randomised clinical trials. Br Med J, 303:884-893, 1991.
3. Anisowicz, A., Sotiropoulou, G., Stenman, G., Mok, S.C., and Sager, R. A novel protease homolog differentially expressed in breast and ovarian cancer. Mol. Med. 2:624-636, 1996.
4. el-Shirbiny, A.M. Prostatic specific antigen. Adv Clin Chem, 31:99-133, 1994.
5. Xu Y, Shen Z, Wiper DW, Wu M, Morton RE, Elson P, Kennedy AW, Belinson J, Markman M, Casey G. Lysophosphatidic acid as a potential biomarker for ovarian and other gynecologic cancers. JAMA 280, 719-723, 1998.
6. Xu Y, Xiao Y, Baudhuin LM, Schwartz BM. The role and clinical applications of bioactive lysolipids in ovarian cancer. J Soc Gyn Invest 8,1-13, 2001.

7. Xiao Y, Schwartz B, Washington M, Kennedy A, Webster K, Belinson J. and Xu Y. Electrospray Ionization Mass Spectrometry Analysis of Lysophospholipids in Human Ascitic Fluids: Comparison of the Lysophospholipid Contents in Malignant vs. Non-malignant Ascitic Fluids. Anal Biochem. 290, 302-313, 2001.
8. Schwartz BM, Hong G, Morrison BH, Wu W, Baudhuin LM, Xiao Y. and Xu Y. Lysophospholipids Increase Interleukin-8 (IL-8) Expression in Ovarian Cancer Cells. Gyn Oncol 81, 291-300, 2001
9. Xu Y, Zhu K, Hong G, Wu W, Baudhuin LM, Xiao Yj, Damron DS. Sphingosylphosphorylcholine is a ligand for ovarian cancer G-protein-coupled receptor 1. *Nat Cell Biol.* 2, 261-267, 2000.
10. Kabarowski JHS, Zhu K, Le LQ, Witte ON, Xu Y. Lysophosphatidylcholine as a Ligand for the Immunoregulatory Receptor G2A. Science 293, 702-705, 2001
11. Zhu, K., Baudhuin, L., Hong, G. Williams, F.S., Cristina, K.L., Kabarowski, J.H.S., Witte, O.N. and Xu, Y Sphingosylphosphorylcholine and lysophosphatidylcholine are ligands for the G protein coupled receptor, GPR4. J. Biol. Chem. In press.

APPENDICES

Manuscript:

1. Wang VW, Bell DA, Berkowitz RS, Mok SC: Whole genome amplification and high-throughput allelotyping identified five distinct deletion regions on chromosome 5 and 6 in microdissected early stage ovarian tumors. Cancer Res. 2001,61:4169-4174.
2. Kwong-kwok Wong, Cheng RS, Mok SC: Identification of differentially expressed genes from ovarian cancer cells by MICROMAX cDNA microarray system. Biotechnique 2001,30:670-675.
3. Mok SC, Chao J, Skates S, Wong KK, Yiu GK, Muto MG, Berkowitz RS, Cramer DW: Prostasin, a potential serum marker for ovarian cancer, identified through microarray technology. J Natl Cancer Inst, 2001, 93: in press.
4. Wang VW, Bell DA, Chung TKH, Wong YF, Hasselblattl K, Minna JD, Schorge JO, Berkowitz RS, Mok SC: Molecular profiling of stage I epithelial ovarian carcinomas by high throughput allelotyping. Submitted.
5. Kim JH, Herlyn D, Wong KK, Yiu GK, Schorge JO, Lu KH, Berkowitz RS, Mok SC: Ep-CAM autoantibody is a potential serum marker for epithelial ovarian cancer. Submitted.
6. Wang VW, Bell DA, Berkowitz RS, Mok SC: *TP53* is involved in the development of de novo high grade serous ovarian carcinomas. Submitted.
7. Syed V, Ulinski G, Mok SC, Yiu GK, Ho SM: Expression of gonadotropin receptor and growth responses to key reproductive hormones in normal and malignant human ovarian surface epithelial cells. Cancer Res 2001, 61:6768-6776.
8. Xiao Y, Schwartz B, Washington M, Kennedy A, Webster K, Belinson J. and Xu Y. Electrospray Ionization Mass Spectrometry Analysis of Lysophospholipids in Human Ascitic Fluids: Comparison of the Lysophospholipid Contents in Malignant vs. Non-malignant Ascitic Fluids. Anal Biochem. 290: 302-313, 2001
9. Xu Y, Xiao Y, Baudhuin LM, Schwartz BM. The role and clinical applications of bioactive lysolipids in ovarian cancer. J Soc Gyn Invest, 8:1-13, 2001.
10. Kabarowski JHS, Zhu K, Le LQ, Witte ON, Xu Y. Lysophosphatidylcholine as a Ligand for the Immunoregulatory Receptor G2A. Science 293: 702-705, 2001
11. Zhu, K., Baudhuin, L., Hong, G. Williams, F.S., Cristina, K.L., Kabarowski, J.H.S., Witte, O.N. and Xu, Y Sphingosylphosphorylcholine and lysophosphatidylcholine are ligands for the G protein coupled receptor, GPR4. J Biol Chem, In press.

12. Lu J, Baudhuin LM, Hong G, and Xu, Y. Role and Signaling Pathways of Ether-linked Lysophosphatidic Acids in Ovarian Cancer Cells. Submitted.

TP53 is involved in the development of de novo high grade serous ovarian carcinomas

Vivian W. Wang, * Debra A. Bell, †‡ Ross S. Berkowitz, *† and Samuel C. Mok *†

From the Division of Gynecologic Oncology, Department of Obstetrics, Gynecology and Reproductive Biology, Brigham and Women's Hospital,* Dana-Farber Harvard Cancer Center,† Department of Pathology,‡ Massachusetts General Hospital, Harvard Medical School, Boston, Massachusetts 02115

Running title: *TP53* alterations in the stage I of ovarian tumor

Footnotes:

Supported by the Army Ovarian Cancer Research Program grant #DAMD17-99-1-9563, the Adler Foundation, the Morse Family Fund, and the Natalie Pihl Fund.

Address reprint requests to Dr. Samuel C. Mok, Department of Obstetrics, Gynecology and Reproductive Biology, Brigham and Women's Hospital, Harvard Medical School, 221 Longwood Avenue, BLI-449, Boston, Massachusetts 02115. Telephone (617) 278-0196, Fax (617) 975-0818. E-mail: scmok@rics.bwh.harvard.edu.

ABSTRACT

The *TP53* gene is considered to be a tumor suppressor gene, and frequent mutations of the gene have been found in a wide variety of human cancers. *TP53* gene alterations have been detected in most advanced stages of ovarian cancer. To evaluate the involvement of *TP53* gene in the development of early stage of ovarian carcinoma, mutation and allelic loss of the *TP53* gene and expression of the p53 protein were investigated in microscopically identified de novo epithelial ovarian carcinomas. Formalin-fixed, paraffin-embedded tumor tissues from 7 patients were examined. DNA was isolated from microdissected tumor cells, whole genome amplification was then performed using a primer-extension pre-amplification method. p53 protein expression was detected with an anti-p53 antibody. *TP53* gene mutations in exons 2-11 were determined by direct DNA sequencing. Loss of heterozygosity *TP53* at the locus was studied using fluorescent-labeled microsatellite markers. Overall, three of the 7 cases (1 grade 2, and 2 grade 3 serous carcinomas) displayed p53 positive staining and *TP53* gene mutation. Missense mutations in exon 6 ($CAT_{214}\rightarrow CGT$), exon 7 ($TCC_{241}\rightarrow TTC$), and exon 8 ($CGT_{273}\rightarrow CCT$) were identified in the three cases, respectively. LOH in the *TP53* locus was also frequent with an average rate of 55%. Our findings indicate that alteration of the p53 gene might be early genetic events in the development of ovarian cancer, particularly in high grade serous ovarian carcinomas.

INTRODUCTION

Ovarian carcinoma is the fifth commonest cancer in women and is the leading cause of death among gynecologic cancers.[1] It tends to present late in its clinical course, with limited prospects for treatment and generally poor survival. However, if the disease is diagnosed and treated at early stages, over 90% of ovarian cancer patients may survival for 5 years or longer.[1]

In spite of all the genetic studies in ovarian cancer, the pathogenetic pathways of ovarian cancer remain unclear. There is still a lack of information regarding the histologic features of early carcinoma or its putative precursor lesions. Bell and Scully [2] identified 14 cases of early ovarian carcinoma detected as microscopic findings in grossly normal ovaries and concluded that at least a subset of ovarian epithelial cancers develops de novo from the ovarian surface epithelium or its inclusion cysts rather from the pre-existing benign epithelial tumors or endometriosis. Genetic changes in these de novo carcinomas remain largely unknown.

It is widely accepted that both activation of protooncogenes and inactivation of tumor suppressor genes are involved in the genesis or progression of various types of human cancers. It has been shown that the *TP53* gene is located on chromosome 17p13.1, and that its mutations play an important role in the development of a wide variety of human cancers.[3-7] Furthermore, over-expression of the p53 protein has been shown to be largely due to the presence of mutations in the evolutionarily conserved regions of the gene that increase the stability of the protein.[8] Ovarian cancer, like most human cancers, is thought to be caused by the accumulation of mutations in multiple genes that are

important for normal cell functions. *TP53* mutations, p53 protein expression and allelic loss at the *TP53* locus have been extensively studied in ovarian cancer.[9-11] However, these changes have not been demonstrated in the early de novo ovarian carcinomas. Here, we describe the use of laser capture microdissection and whole genome amplification techniques to identify *TP53* mutation and allelic loss in these microscopically identified ovarian carcinomas.

MATERIALS AND METHODS

Tissue specimens and microdissection

We examined 7 formalin-fixed, paraffin-embedded microscopiclly identified stage I sporadic epithelial ovarian carcinoma specimens from our archives. The sections stained with hematoxylin and eosin was reviewed and the diagnosis was confirmed. The ovarian carcinomas studied here included 5 serous carcinomas, 1 endometrioid carcinoma, and 1 clear cell carcinoma. The diameters of these microscopic tumors were 1-8 mm. For each tumor, 10-20 serial sections 5 μm were cut. They were deparffinized in xylene, rehydrated in graded ethanols, and stained with hematoxylin and eosin. Approximately 5,000 tumor and non-tumor stromal cells were microdissected using a PixCell II Laser Capture Microdissection system (Arcturus Engineering, Mountain View, CA). The dissected cells were collected into 50μl cell lysis buffer (1 x expand high fidelity buffer from Boehringer Mannheim, Mannheim, Germany, containing 4 mg/ml proteinase K, and 1% Tween 20) and incubated for 72 h at 55 °C. The proteinase K was inactivated by heating at 95 °C for 10 min prior to PCR.

Whole genome amplification

Whole genome amplification was carried out by the modified primer extension preamplification (PEP) method as described previously.[12] Briefly, 50 μl PEP PCR reaction mixture consisted of 0.05 mg/ml gelatin, 40 μM 15-mer random primers (Operon Technologies, Alameda, California), 0.2 mM of each dNTP, 2.5 mM $MgCl_2$, 1 x expand high fidelity buffer, 3.5 units of Taq expand high fidelity polymerase (Boehringer

Mannheim, Mannheim, Germany), and 10 µl of DNA sample. Fifty primer extension cycles were carried out in a Perkin-Elmer 9600 thermocycler after an initial denaturation step at 94 °C for 3 min. Each cycle consisted of 1 min at 94 °C, 2 min at 37 °C, a ramping step of 0.1 °C per second up to 55 °C, a 4 min primer extension step at 55 °C and followed by a 30 s at 68 °C. The PEP reaction products were diluted 2-3 folds, and used as template DNA for *TP53* alteration and allelic loss analysis.

Immunohistochemistry

Immunohistochemical staining of formalin-fixed, paraffin-embedded sections of each tumor was conducted using the anti-p53 monoclonal antibody DO-7 (Dako, Santa Barbara, CA) by using microwave antigen retrieval in citrate buffer. Briefly, Sections were deparaffinized, rehydrated, washed for 2 x 5 min with distilled water and boiled in a microwave oven in 0.01 M citrate buffer for 10 min for antigen retrieval. Endogenous peroxidase activity was blocked by 0.3% hydrogen peroxide for 30 min, followed by washing for 20 min with TBS (100 mM Tris-HCl, pH 7.5; 0.15 M NaCl). After blocking the nonspecific staining with normal mouse serum, tissue sections were incubated with the p53-specific mouse monoclonal antibody at a working dilution of 1:50, 1 h at room temperature. Samples were washed twice for 5 min with TBS and incubated for 30 min with biotinylated secondary antibody (Vectastain ABC Elite Kit, Vector Laboratories, Burlingame, CA). After two washings for 5 min in TBS, the sections were incubated for 30 min in avidinbiotinylated peroxidase complex solution. Sections were washed for 2 x 5 min with TBS, developed with diaminobenzidine tetrahydrochloride substrate (DAB substrate kit, Vector Laboratories, Burlingame, CA) for 7 min, followed by washing with

water for 2 x 5 min, dehydrated, cleared and mounted. Known p53-positive sample was used as positive control, and the same sample processed without the primary antibody was used as a negative control.

Mutation analysis

DNA sequence analyses of each exon contributing to *TP53* open reading frame (exons 2-11) were evaluated by automated DNA sequence analysis. DNA samples were amplified from the entire coding sequence of the p53 gene. The sequences of the primers used are shown in Table 1. Each amplification was performed in a 20 µl reaction medium containing both sense and antisense primers at a final concentration of 1 µM, 0.25 mM of each dNTP, 1 x buffer (50 mM Tris-HCl, pH 8.3; 10 mM KCl), 2.5 mM of $MgCl_2$, 0.5 units AmpliTaq Gold DNA polymerase (Applied Biosystems, Foster City, CA) and 1.5 µl of DNA. Amplification was started with 12 min at 95 °C, followed by 35 cycles composed of 30 sec at 94 °C, 30 sec at 55 °C and 45 sec at 72 °C, and with a final extension at 72 °C for 10 min in a Perkin-Elmer 9600 thermocycler. The products were electrophoresed on a 1.5% agarose gel containing ethidium bromide to assess the purity of each anticipated DNA fragment. The products were purified using a gel extraction kit (Sephaglas BandPrep Kit, Amersham Pharmacia Biotech, Piscataway, NJ) and sequenced directly by using BigDye terminator cycle sequencing kit and capillary electrophoresis in an ABI PRISM 310 automated DNA sequencer (Applied Biosystems, Foster City, CA). All samples with mutations were verified by two independent cycle sequencing PCR reactions and analysis of both sense and antisense DNA strands. The *TP53* DNA sequence in GenBank (accession number HSP53007) was used as references.

Microsatellite analysis

LOH was detected by a set of 3 microsatellite markers mapping to chromosome 17p13.1. All primers were purchased from the Applied Biosystems, Forster City, CA. PCR reactions were performed in a 10 μl volume using 1 μl of whole genome amplified DNA, 0.25-0.5 μM of each primer, 1 x PCR buffer, 2.5 mM $MgCl_2$, 0.25 mM of each dNTP, and 0.5 unit AmpliTaq Gold DNA polymerase. Amplification was started with 12 min at 95 °C, followed by 10 cycles composed of 15 sec at 94 °C, 15 sec at 55 °C and 30 sec at 72 °C, and then 25 cycles composed of 15 sec at 89 °C, 15 sec at 55 °C and 30 sec at 72 °C. Amplified PCR products were run on an ABI PRISM 310 automated DNA sequencer (Applied Biosystems, Forster City, CA). The allelic products were assessed for peak height and peak area using Genescan and Genotyper softwares (Applied Biosystems, Forster City, CA), and the ratios of heterozygous, normal and tumor alleles were calculated as described previously.[12]

RESULTS

p53 protein expression was determined in 7 microscopic ovarian carcinomas by immunohistochemistry. Three of the 7 tumors displayed positive p53 protein immunostaining and were regarded as overexpression or accumulation of p53 protein. The percentage of tumor cell nuclei with positive staining was 40%, 90% and 95% in cases 97-7024, 4613 and 99N51, respectively. These 3 cases were high grade serous type (Table 2). The remaining 4 cases were not found to have positive immunostaining in any tumor cell nuclei, and were considered to be lack of p53 overexpression. Furthermore, the p53 protein positive immunostaining was not observed in the benign components of ovarian carcinomas, including fibrous connective tissue, vessels, and inflammatory cells (Figure 1).

Mutation analysis of the *TP53* open reading frame including exons 2-11 was conducted in all 7 tumors. *TP53* missense mutations were detected in 3 of the 7 (43%) ovarian carcinomas. All these 3 cases showed positive immunostaining for the p53 protein also. The mutations were found in exon 7 (at codon 241 in case 97-7024, grade 2 serous tumor) (Figure 2), exon 6 (at codon 214 in case 99N51, grade 3 serous tumor), and exon 8 (at codon 273 in case 4613, grade 3 serous tumor). Neither *TP53* mutation nor positive p53 protein staining were found in the remaining 4 cases.

LOH in the *TP53* region at 17p13 was observed in most of these microscopic ovarian tumors. LOH at loci D17S938 (17p13.1), D17S1876 (17p13.1-2), and D17S1876 (17p13.1-2) was detected in 4 of 6 (66%), 4 of 7 (57%), and 3 of 7 (42%) informative cases, respectively. However, LOH was observed but p53 protein expression and *TP53*

mutation were not detected in two tumors (case 3317 and case 744). *TP53* gene mutation, p53 protein expression and LOH on 17p13.1 in these microscopically detected stage I ovarian tumors were summarized in Table 2.

The clinical outcome was evaluated by overall survival that was calculated from the day of treatment or treatment start until the date of died of disease. All of the patients were updated to July 2001. Only one case was lost of follow-up. The mean duration of follow-up was 58 months (range, 8-171 months). Case 3317, grade 1 serous adenocarcinoma, followed up to 122 months, and alive with disease. Case S3854, grade 3 clear cell carcinoma, died of disease after alive for 171 months (Table 2).

DISCUSSION

In this study, we identified *TP53* mutations and p53 over-expression in all the early de novo high grade (grade 2 and grade 3) serous carcinoma cases suggesting that high grade serous carcinomas develop directly from ovarian inclusion cysts after acquiring *TP53* mutations. The two early de novo well differentiated serous carcinoma cases showed neither *TP53* mutations nor p53 overexpression, suggesting well differentiated serous carcinomas might have a different pathogenetic pathway (Figure 3). Interestingly, both *TP53* mutation and p53 expression could not be detected in the two high grade endometrioid and clear cell carcinoma cases. Infrequent *TP53* mutation and p53 over-expression have been described in non-serous type of ovarian cancer.[13-17] Ho *et al*[18] studied p53 over-expression in 38 cases of clear cell ovarian carcinomas and found only one positive case. These data further support the hypothesis that both endometrioid and clear cell carcinomas may have different pathogenetic pathways in comparing to the serous histological type.

Previous reports in the literature indicated high LOH frequencies at the *TP53* locus in ovarian tumors.[19-23] In this study, we demonstrated that 86% (6 of 7) of the early de novo ovarian carcinoma cases showed allelic loss in at least one of the three markers located at the *TP53* region. Interestingly, *TP53* mutations and p53 over-expression can only be detected in three of the 6 cases. These data suggest that allelic loss at 17p13.1 is an early event during the pathogenesis of different subtypes of ovarian cancer, and there may be another gene(s) other than *TP53* located in 17p13.1, which may be important for the development of ovarian cancer.

In conclusion, we have detected *TP53* mutation and p53 over-expression in the microscopically detected de novo ovarian carcinoma cases particularly in the high grade serous type. These results strongly suggest that deregulation of p53 function may be one of the early critical events in the development of this type of ovarian carcinoma, and support the notion that different types of ovarian cancer may have different pathogenetic pathways. Genetic changes in a larger set of de novo ovarian carcinoma warrant to be further studied which will provide us insight into the pathogenesis of ovarian cancer and markers for early detection of the disease.

REFERENCES

1. American Cancer Society, Cancer Facts & Figures. American Cancer Society, Inc., 1999
2. Bell DA, Scully RE: Early de novo ovarian carcinoma. Cancer 1994, 73:1859-1864
3. Prosser J, Thompson AL, Cranston G, Evans HJ: Evidence that p53 behaves as a tumor suppressor gene in sporadic breast tumors. Oncogene 1990, 5:1573-1579
4. Mashiyama S, Murakami Y, Yoshimoto T, Sekiya T, Hayashi K: Detection of p53 gene mutations in human brain tumors by single-strand conformation polymorphism analysis of polymerase chain reaction products. Oncogene 1991, 6:1313-1318
5. Goh HS, Chan CS, Khine K, Smith DR: p53 and behaviour of colorectal cancer. Lancet 1994, 344:233-234
6. Ohsaki Y, Toyoshima E, Fujiuchi S, Matsui H, Hirata S, Miakawa N, Kubo Y, Kikuchi K: bcl-2 and p53 protein expression in non-small cell lung cancers: correlation with survival time. Clin Cancer Res 1996, 2:915-920
7. Marks JR, Davidoff AM, Kerns BJ, Humphrey PA, Pence JC, Dodge RK, Clarke-Pearson DL, Iglehart JD, Bast RC Jr, Berchuck A: Overexpression and mutation of p53 in epithelial ovarian cancer. Cancer Res 1991, 51:2979-2984
8. DiCioccio RA, Werness BA, Peng Ruoqi, Allen HJ, Piver MS: Correlation of TP53 mutations and p53 expression in ovarian tumors. Cancer Genet Cytogenet 1998, 105:93-102

9. Okamoto A, Sameshima Y, Yokoyama S, Terashima Y, Sugimura T, Terada M, Yokota J: Frequent allelic losses and mutations of the p53 gene in human ovarian cancer. Cancer Res 1991, 51:5171-5176

10. Quezado MM, Moskaluk CA, Bryant B, Mills SE, Merino MJ: Incidence of loss of heterozygosity at p53 and BRCA1 loci in serous surface carcinoma. Hum Pathol 1999, 30:203-207

11. Wen W, Reles A, Runnebaum IB, Sullivan-Halley J, Bernstein L, Jones LA, Felix JC, Kreienberg R, El-Naggar A, Press MF: p53 mutations and expression in ovarian cancers: correlation with overall survival. Int J Gynecol Pathol 1999, 18:29-41

12. Wang VW, Bell DA, Berkowitz RR, Mok SC: Whole genome amplification and high-throughput allelotyping identified five distinct deletion regions on chromosomes 5 and 6 in microdissected early stage ovarian tumors. Cancer Res 2001, 61:4169-4174

13. Kohler MF, Kerns BJ, Humphrey PA, Marks JR, Bast RC Jr, Berchuck A: Mutation and overexpression of p53 in early-stage epithelial ovarian cancer. Obstet Gynecol 1993, 81:643-650

14. Kupryjanczyk J, Bell DA, Yandell DW, Scully RE, Thor AD: P53 expression in ovarian borderline tumors and stage I carcinomas. Am J Clin Pathol 1994, 102:671-676

15. Righetti SC, Torre GD, Pilotti S, Menard S, Ottone F, Colnaghi MI, Pierotti MA, Lavarino C, Cornarotti M, Oriana S, Bohm S, Bresciani GL, Spatti G, Zunino F: A comparative study of p53 gene mutations, protein accumulation, and response

to cisplatin-based chemotherapy in advanced ovarian carcinoma. Cancer Res 1996, 56:689-693

16. Klemi PJ, Takahashi S, Joensuu H, Kiiholma P, Narimatsu E, Mori M: Immunohistochemical detection of p53 protein in borderline and malignant serous ovarian tumours. Int J Gynecol Pathol 1994, 13:228-233

17. Morita K, Ono Y, Fukui H, Tomita S, Ueda Y, Terano A, Fujimori T: Incidence of p53 and K-ras alterations in ovarian mucinous and serous tumors. Pathol Int 2000, 50:219-223

18. Ho ES, Lai C, Hsieh Y, Chen J, Lin A, Hung M, Liu F: p53 mutation is infrequent in clear cell carcinoma of the ovary. Gynecol Oncol 2001, 80:189-193

19. Otis CN, Krebs PA, Quezado MM, Albuquerque A, Bryant B, Juan XS, Kleiner D, Sobel ME, Merino MJ: Loss of heterozygosity in p53, BRCA1, and estrogen receptor genes and correlation to expression of p53 protein in ovarian epithelial tumors of different cell types and biological behavior. Hum Pathol 2000, 31:233-238

20. Tangir J, Loughridge NS, Berkowitz RS, Muto MG, Bell DA, Welch WR, Mok SC: Frequent microsatellite instability in epithelial borderline ovarian tumors. Cancer Res 1996, 56:2501-2505

21. Wertheim I, Tangir J, Muto MG, Welch WR, Berkowitz RS, Chen WY, Mok SC: Loss of heterozygosity of chromosome 17 in human borderline and invasive epithelial ovarian tumors. Oncogene 1996, 12: 2147-2153

22. Wiper DW, Zanotti KM, Kennedy AW, Belinson JL, Casey G: Analysis of allelic imbalance on chromosome 17p13 in stage I and stage II epithelial ovarian cancers. Gynecol Oncol 1998, 71: 77-82

23. Launonen V, Mannermaa A, Stenback F, Kosma VM, Puistola U, Huusko P, Anttila M, Bloigu R, Saarikoski S, Kauppila A, Winqvist R: Loss of heterozygosity at chromosomes 3, 6, 8, 11, 16, and 17 in ovarian cancer: correlation to clinicopathological variables. Cancer Genet Cytogenet, 2000, 122: 49-54

LEGENDS

Figure 1. p53 expression in microscopically detected stage I ovarian tumors. A, case 3317, grade 1 serous adenocarcinoma, negative for p53 protein staining. B, case 97-7024, grade 2 serous adenocarcinoma, with p53 immunostaining in 40% of tumor cell nuclei. C, case 4613, grade 3 serous adenocarcinoma, with p53 immunostaining in 90% of tumor cell nuclei. D, case S3854, grade 3 clear cell carcinoma, negative for p53 protein staining.

Figure 2. Sequence chromatograms demonstrating mutations in an ovarian carcinoma. A, case 99N51 with exon 6 at codon 214 missense mutation; B, case 97-7024 with exon 7 at codon 241 missense mutation. Upper panel, normal control, lower panel, tumor. Arrows, the position of mutated bases.

Figure 3. Pathogenesis of epithelial ovarian tumors. HOSE, human ovarian surface epithelial cells; IEOC, invasive epithelial ovarian carcinoma.

Table 1. Oligonucleotide primers used in mutation analysis of the TP53 gene in ovarian carcinoma

Exon	Sense primer	Antisense primer	Size of fragment	Codon
2 to 3	5'-TCC TCT TGC AGC AGC CAG ACT GC-3'	5'-AAC CCT TGT CCT TAC CAG AAG GTT G-3'	267	1 to 32
4	5'-CAC CCA TCT ACA GTC CCC CTT GC-3'	5'CTC AGG GCA ACT GAC CGT GCA AG-3'	307	33 to 125
5	5'-CTC TTC CTG CAG TAC TCC CCT GC-3'	5'-GCC CCA GCT GCT CAC CAT CGC TA-3'	211	126 to 186
6	5'-GAT TGC TCT TAG GTC TGG CCC CTC-3'	5'-GGC CAC TGA CAA CCA CCC TTA ACC-3'	185	187 to 224
7	5'-GTG TTG TCT CCT AGG TTG GCT CTG-3'	5'-CAA GTG GCT CCT GAC CTG GAG TC-3'	139	225 to 260
8	5'-ACC TGA TTT CCT TAC TGC CTC TGG C-3'	5'-GTC CTG CTT GCT TAC CTC GCT TAG T-3'	200	261 to 306
9	5'-GCC TCT TTC CTA GCA CTG CCC AAC-3'	5'-CCC AAG ACT TAG TAC CTG AAG GGT G-3'	102	307 to 331
10	5'-TGT TGC TGC AGA TCC GTC GGC GT-3'	5'-GAG GTC ACT CAC CTG GAG TGA GC-3'	131	332 to 367
11	5'-TGT GAT GTC ATC TCT CCT CCC TGC-3'	5'-GGC TGT CAG TGG GGA ACA AGA AGT-3'	153	368 to 393

Table 2. TP53 gene alterations and clinicopathologic characteristics in microscopically identified stage I epithelial ovarian carcinomas

	Histology		Tumor	Follow up	Immuno-	Genomic		Nucleotide	Amino acid	Predicted	Loss of heterozygosity		
Case No.	Grade	Type	Size (mm)	(month)	reactivity	location	Codon	change	change	effect	D17S938	D17S1876	D17S1828
3317	1	Serous	a	Recurrent,122	Negative	—	—	—	—	—	LOH	HET	HET
V1834	1	Serous	a	NED, 8	Negative	—	—	—	—	—	HET	NI	LOH
97-7024	2	Serous	8	—	Positive	Exon 7	241	TCC to TTC	Ser to Phe	Missense	LOH	LOH	LOH
99N51	3	Serous	2	NED, 20	Positive	Exon 6	214	CAT to CGT	His to Arg	Missense	NI	LOH	HET
4613	3	Serous	6	NED, 12	Positive	Exon 8	273	CGT to CCT	Arg to Pro	Missense	NI	LOH	HET
774	3	Endometrioid	6	NED, 15	Negative	—	—	—	—	—	LOH	LOH	LOH
S3854	3	Clear cell	2	DOD, 171	Negative	—	—	—	—	—	HET	HET	HET

a, several tiny foci too small to measure

LOH, loss of heterozygosity; HET, retention of heterozygosity; NI, homozygous

NED, no evidence of disease

DOD, died of disease

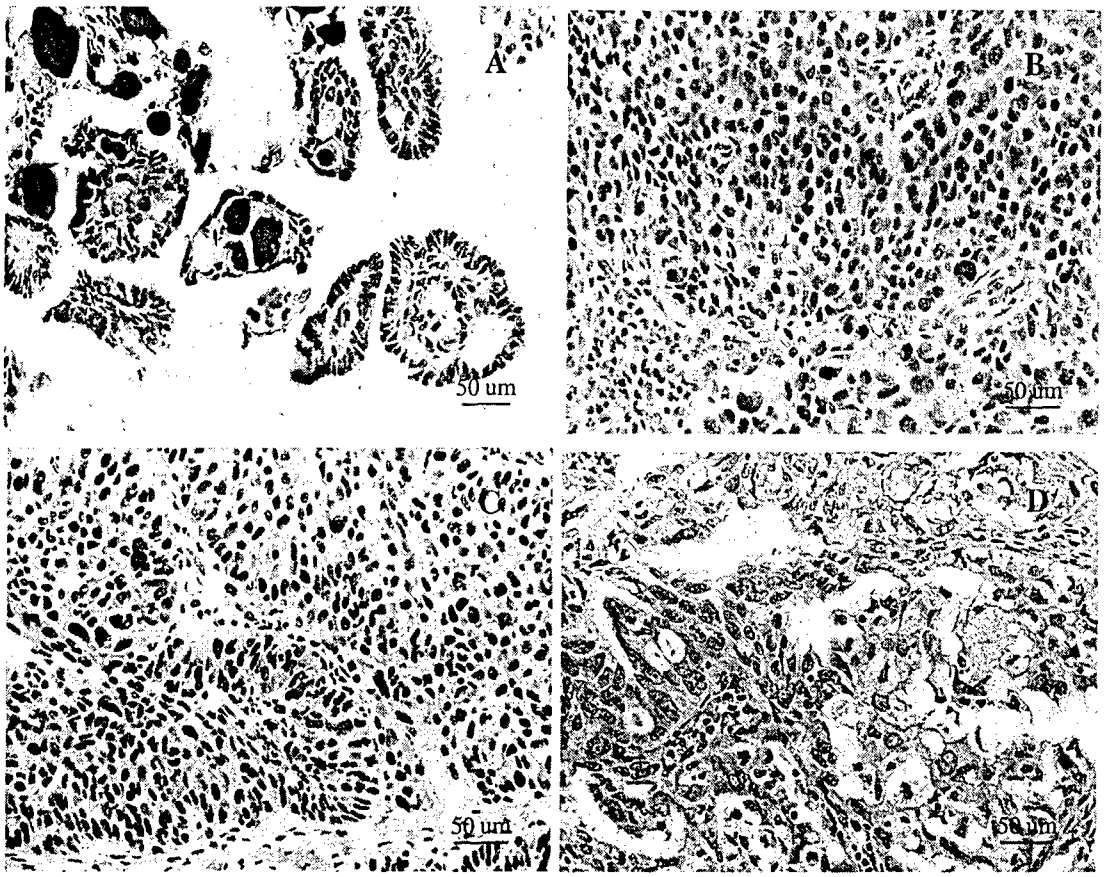
A
50 um
B
50 um
C
50 um
D
50 um

Ep-CAM autoantibody is a potential serum marker for epithelial ovarian cancer

Jae-Hoon Kim,[1,2] Dorothee Herlyn,[3] Kwong-kwok Wong,[4] Gary K Yiu,[1] John O Schorge,[5] Karen H Lu,[6] Ross S. Berkowitz,[1,7] and Samuel C. Mok [1,7]

[1]Department of Obstetrics, Gynecology and Reproductive Biology, Division of Gynecologic Oncology, Brigham and Women's Hospital, Harvard Medical School, Boston, MA,

[2]Department of Obstetrics and Gynecology, Saint Vincent Hospital, The Catholic University of Korea, Suwon, Korea,

[3]The Wistar Institute, Philadelphia, PA,

[4]Department of Pediatrics, Baylor College of Medicine, Houston, TX,

[5]Division of Gynecologic Oncology, Department of Obstetrics and Gynecology, University of Texas Southwestern Medical Center, Dallas, Tx,

[6]Department of Gynecologic Oncology, University of Texas M.D. Anderson Cancer Center, Houston, Tx,

[7]Dana-Farber Harvard Cancer Center, Boston, MA.

Running Title: Ep-CAM is a valuable biomarker with clinical usefulness.

Key words: Ep-CAM, Ovarian Cancer, cDNA microarray, LCM, ELISA

Grant Support: This study was supported by the Ovarian Cancer Research Program grant #DAMD17-99-1-9563 from the Department of Defense, the Early Detection Research Network Grant CA86381 from National Institute of Health, Department of Health and Human Services,

Adler Foundation, Inc., the Ovarian Cancer Research Fund, Inc., the Morse Family Fund, and the Natalie Pihl Fund.

Reprint request: Dr. Samuel C. Mok,

Laboratory of Gynecologic Oncology, Division of Gynecologic Oncology

Department of Obstetrics, Gynecology and Reproductive Biology,

Brigham and Women's Hospital,

221 Longwood Avenue, Boston, MA, 02115.

scmok@rics.bwh.harvard.edu

ABSTRACT

Using the MICROMAX cDNA microarray system and RNA isolated from ovarian cancer cell lines and normal ovarian surface epithelial cells (HOSE), we identified a gene called the epithelial cell adhesion molecule (Ep-CAM) that exhibited a cancer-to-HOSE ratio of 444. Real time quantitative PCR analysis revealed significant overexpression of Ep-CAM mRNA in cancer cell lines ($P<0.001$) and microdissected cancer tissues ($p=0.035$), compared to that in cultured normal HOSE and microdissected germinal epithelium, respectively. Immuno-histochemical staining of paraffin block sections revealed that Ep-CAM expression was absent in stromal areas of normal ovaries or those with benign disease or cancer. In contrast, a gradient of expression was found in the germinal epithelium with ovaries from women with borderline or invasive cancer displaying the greatest level of expression, normal ovaries the least, and ovaries from women with benign tumors intermediate expression ($p<0.05$). No significant differences in Ep-CAM immuno-histochemical staining were observed among ovarian cancer samples with different histologic types and grades. Because Ep-CAM auto-antibody levels have been shown to be elevated in other cancers, such as colon, we examined levels of auto-antibody against Ep-CAM in patients with epithelial ovarian cancer and controls by enzyme-linked immunosorbent assay (ELISA). Ep-CAM auto-antibody levels (measured in units of absorbance at 450nm) were: 0.132 in 52 patients with ovarian cancer, 0.098 in 26 cases with benign gynecologic disease, and 0.090 in 26 normal women ($p<0.05$). When a cut-off value of 0.115 was used, the Ep-CAM auto-antibody assay showed a sensitivity of 71.2% and a specificity of 80.8% whereas the sensitivity and specificity of CA 125 measured in 52% of the same subjects were 84.6% and 88.5% with a CA 125 cut-off of 35U/ml. However, the Ep-CAM auto-antibody assay may be complementary to CA125, as indicated by low correlation coefficient and the fact that combining the test with CA 125 increased the sensitivity to 94.2% and specificity to 100.0%. This investigation has demonstrated the potential value of cDNA microarray analysis in identifying overexpressed

genes in ovarian cancer, and suggests that the Ep-CAM auto-antibody may offer a biomarker for ovarian cancer with clinical usefulness.

INTRODUCTION

Ovarian cancer has the highest mortality rate among all the gynecologic malignancies (1). Every year, 25,000 ovarian cancer cases are being newly diagnosed in the U.S. and approximately 15,000 deaths, secondary to the malignancy, occur annually (2).

Despite intense efforts with cytoreductive surgeries and combined chemotherapeutic modalities, most advanced-stage ovarian cancer patients experience relapses and eventually die from disease (3). There have been continuous efforts in developing new drugs and treatment modalities. Nevertheless, the prognosis for advanced and recurrent ovarian cancers has not substantially changed (4). More than 70% of the patients are in the 3^{rd} or 4^{th} stage at the time of diagnosis (5). Hence, in order to improve survival, it is necessary to develope specific tumor markers that can be used to detect early stages of the disease.

Since most ovarian cancers are of epithelial cell origin, deregulated epithelial antigens may be ideal candidate markers. Ep-CAM has a wide distribution in carcinomas of epithelial origin with exception of squamous cell carcinoma of skin or hepatoma (6). Thus, it has been the focus of immunologic treatment (7-10). Clinical studies in early stage colorectal cancers showed that Ep-CAM could be used as an antigenic target for passive immunotherapy with monoclonal antibody Co 17-1A (9,10). In approaches to active immunotherapy with anti-idiotypic antibodies and recombinant protein, colorectal cancer patients developed humoral and cellular immune responses to the antigen (11,12)

Ep-CAM is a 40-kDa glycoprotein encoded by the GA733-2 gene (13,14). Ep-CAM has been referred to as CO17-1A, MH99, AUA1, MOC31, 323/A3, KS1/4, GA733, HEA125 or KSA, EGP, EGP40 and GA733-2 (14-22). A known biological role of Ep-CAM is its relationship to homophilic cell adhesion (23). Like other adhesion molecules, Ep-CAM is known to be involved in the signaling cascade related to proliferation, differentiation and apoptosis, as well as a regulator of cadherin-mediated functions which is involved in invasion and metastasis (24,25). Furthermore, it has been shown to be associated with proliferation or differentiation secondary to

carcinogenesis and also to play a role in adhesion molecule that suppresses metastasis. Hence, Ep-CAM may have a bi-directional effect in the progression of malignancy.

Here, we demonstrate the use of microarray technology and subsequent validation studies to identify overexpression of Ep-CAM transcript and protein in ovarian cancer cells and tissues, and provide evidence that Ep-CAM autoantibody may be a potential marker for early detection of ovarian cancer.

MATERIALS AND METHODS

Cell lines and culture conditions

All cell lines and cultures were maintained at 37°C in a humidified 5% CO_2 ambient air atmosphere. They were grown in Medium 199 and MCDB 105 (1:1) (Sigma, St Louis, Mo) supplemented with 10% fetal bovine serum (FBS)(Gemini Bio-Products, Calabasas, CA). Normal human ovarian surface epithelial cells (HOSE) cultures were established by scraping the surface of the ovary, as described previously (26). In brief, the scraped cells were spun down, resuspended and cultured in 2.5ml of growth medium. Cells at 75% confluency were then harvested by trypsinization and used for total RNA isolation. Five normal HOSE cells used in this experiment were HOSE695, HOSE697, HOSE713, HOSE726, and HOSE730. Ovarian cancer cell lines were established either by recovery from ascities or explanted from solid tumors as described previously (26). Ten ovarian cancer cell lines were used: OVCA3, OVCA420, OVCA429, OVCA432, OVCA433, OVCA633, CAOV3, DOV13, ALST, as well as SKOV3. All cell cultures and cell lines were established in the Laboratory of Gynecologic Oncology, Brigham and Women's Hospital, except OVCAR-3 and SKOV-3, which were purchased from American Type culture Collection (Rockville, MD).

Antibody and antigen

Monoclonal antibody GA733 against Ep-CAM has been described (27). Ep-CAM (recombinant baculovirus-derived extracellular domain protein) was purified with monoclonal antibody GA733 as described (28).

Tissue and Serum Samples

All patients were treated at the Brigham and Women's Hospital between 1992 and 2000. We randomly retrieved patients with ovarian tumors with different histologic types and grades based on the WHO and the International Federation of Gynecology and Obstetrics criteria. All patient-derived biologic specimens were collected and archived under protocols approved by the Brigham and Women's Human Subjects Committee or studied as an approved use of discarded

human materials. All tumor tissues were collected from the primary ovarian sites and, if possible, metastatic sites from patients undergoing surgery. They contained less than 20% normal tissue.

For fresh frozen sections, fresh specimens collected at the operating room were placed in tissue culture medium, Medium 199 and MCDB 105 (1:1) with 10% FBS, and transported to the laboratory. After removing the nontumorous tissue, the specimens were immediately embedded in Tissue Tek OCT medium (Miles, Elkhart, IN), snap-frozen in liquid nitrogen, and stored at -80 °C until use.

The Archival tissues in paraffin blocks were collected from pathology files in the Laboratory of Gynecologic Oncology at the Brigham and Women's Hospital.

Preoperative serum samples from women with ovarian cancer, and benign gynecologic disorders, and serum samples from non-diseased normals were obtained between 1999 and 2000. These specimen were stored at -80°C without any incident of thawing.

Laser capture microdissection (LCM)

Tissues stored in Tissue Tek OCT medium at -80°C were sectioned at 7 μm in a cryostat (Leica, Allendate, NJ). Sections were mounted on uncoated glass slides and immediately fixed in 70% and 50% ethanol for 30 seconds in each, stained with Hematoxylin and Eosin, dehydrated in an increased series of alcohol and cleared in xylene for 5 minutes in each microdissection. Once air-dried for 3 minutes, the sections were laser microdissected with the PixCell II system(Arctarus, CA). Morphologically normal ovarian epithelial cells and malignant epithelial ovarian cancer cells were procured.

Microarray Probe and Hybridization

The MICROMAX human cDNA system I (NEN Life Science Products, Inc., Boston, MA), which contains 2400 known human cDNA on a 1X3," slide, was used in this study as described (29). Biotin-labeled cDNA was generated from 3 μg total RNA, which was pooled fromHOSE17, HOSE36 and HOSE642. Dinitropheny (DNP)-labeled cDNA was generated from 3 μg total RNA that was pooled from ovarian cancer cell lines OVCA 420, OVCA 433 and SKOV3. Before the

cDNA reaction, an equal amount of RNA control was added to each batch of the RNA samples for normalization. The biotin-labeled and DNP-labeled cDNA were mixed, dried and resuspended in 20 μl hybridization buffer, which was added to the cDNA microarray and covered with a cover slip. Hybridization was carried out overnight at 65°C inside a hybridization cassette (Telechem, Inc. Sunnyvale, CA).

After hybridization, the microarray was washed with 30 ml 0.5X SSC, 0.01% SDS, and then 30 ml 0.06X SSC, 0.01% SDS, and finally, 0.06X SSC alone. The hybridization signal from biotin-labeled cDNA was amplified with streptavidin-horseradish peroxidase and Cy5™-tyramide, while hybridization signal from DNP-labeled cDNA was amplified with anti-DNP-Horseradish peroxidase and Cy3™-tyramide. After the post-hybridization wash, the cDNA microarray was air-dried and signal amplification was detected with a laser scanner.

Laser detection of the Cy3 signal (derived from ovarian cancer cells) and Cy5 signal (derived from HOSE cells) on the microarray was acquired with a confocal laser reader, ScanArray3000 (GSI Lumonics, Watertown, MA). Separate scans were taken for each fluor at a pixel size of 10 μ m. cDNA derived from the control RNA hybridized to 12 specific spots within the Microarray. Cy3 and cy5 signals from these 12 spots should theoretically be equal and were used to normalize the different efficiencies in labeling and detection with the two fluors. The fluorescence signal intensities and the Cy3/Cy5 ratios for each of the 2400 cDNAs were analyzed by the software Imagene 3.0 (Biodiscovery inc, Los Angeles, CA).

Real-time Quantitative RT-PCR

RNA was extracted from the cell lines and tissues using a micro RNA extraction kit as described by the manufacturer (Stratagene, Valenica, CA), and quantified by fluorometry (Gemini Bio-Products). Real-time PCR was performed in duplicate using primer sets specific for Ep-CAM (forward primer: 5'-CGTCAATGCCAGTGTACTTCAGTTG-3'; reverse primer: 5'-TCCAGTAGGTTCTCACTCGCTCAG-3') and a house keeping gene, GAPDH, in an ABI PRISM 5700 Sequence Detector. mRNA was extracted from normal ovarian epithelial cell

cultures (HOSE 695, 697, 713, 726 and 730), ovarian carcinoma cell lines (OVCA3, OVCA420, OVCA429, OVCA432, OVCA433, OVCA633, CAOV3, DOV13, SKOV3 and ALST), three normal ovarian epithelial tissues, and thirteen ovarian cancer tissues.

cDNA was generated from 1 μg total RNA using the TaqMan reverse transcription reagents containing 1X TaqMan RT buffer, 5.5 mM $MgCl_2$, 500 μM dNTP, 2.5 μM random hexamer, 0.4 U/μl Rnase inhibitor, 1.25 U/μl MultiScribe reverse transcriptase (PE Applied Biosystems, Foster City CA) in 100μl. The reaction was incubated at 25°C for 10 minutes, 48°C for 30 minutes and finally at 95°C for 5 minutes.

A total of 0.5 μl of cDNA was used in a 20 μl PCR mix containing 1X SYBR PCR buffer, 3 mM $MgCl_2$, 0.8 mM dNTP, and 0.025 U/μl AmpliTaq Gold (PE Applied Biosystems, Foster City, CA). Amplification was then performed with denaturation for 10 minutes at 95°C, followed by 40 PCR cycles of denaturation at 95°C for 15 seconds and annealing/extension at 60°C for 1 minute. The ABI5700 system software monitored the changes in fluorescence of SYBR Green I dye in every cycle and the threshold cycle (C_T) for each reaction was calculated.

The relative amount of PCR products generated from each primer set was determined based on the threshold cycle or C_T value. GAPDH was used for the normalization of RNA used. Its C_T value was then subtracted from that of each target gene to obtain a ΔC_T value. The difference ($\Delta\Delta C_T$) between the ΔC_T values of the samples for each gene target and the ΔC_T value of the calibrator (HOSE726 and 756HOSE in vitro and in vivo studies, respectively) was determined. The relative quantitative value was expressed as $2^{-\Delta\Delta CT}$. To confirm the specificity of the PCR reaction, PCR products were electrophoresed on a 1.2% agarose gel.

Immunohistochemistry

Specimens used in this experiment consisted of 5 normal ovaries, 17 benign ovarian tumors, 52 borderline ovarian cancers (29 serous, 21 mucinous, 1 endometrioid, and 1 clear cell), and 67 invasive ovarian cancers (31 serous, 20 mucinous, 12 endometrioid, and 4 clear cell).

Immunostaining was performed by the avidin-biotin method. Sections were deparaffinized in xylene and hydrated with graded ethanol concentrations and water. Endogenous peroxide was blocked with 0.3% hydrogen peroxide in methanol for 30 minutes. After blocking nonspecific antigens with normal horse serum for 20 minutes, the sections were incubated with mouse monoclonal antibody GA733 against Ep-CAM (2.35 μg/ml; DAKO, Carpinteria, CA) for 60 minutes at room temperature. The control sections were treated in parallel but incubated with normal mouse serum (as a negative control) instead of the primary antibodies. All sections were incubated in a moist chamber. After being washed two times with tris-buffered saline (TBS) for 10 minutes, sections were then incubated with a biotinylated goat anti-mouse IgG antibody for 30 minutes (Vector Laboratories, Burlingame, CA). The sections were washed again. After incubation in avidin-biotin complex (Vector Laboratories) for 30 minutes, the reaction product was visualized by 3,3-diaminobenzidine tetrahydrochloride (Vector Laboratories). Finally, sections were dehydrated in ethanol, cleared in xylene, and mounted in SP15-500 Permount (Fisher Scientific).

Representative photomicrographs were recorded by a digital camera (Optronics, Goleta, CA). A single person to alleviate technician-induced discrepancies completed all staining. Slides stained with hematoxylin and eosin were available for all specimens.

To evaluate the result, we established a score corresponding to the sum of both staining intensity (strong positive staining in most of cells, 3+; moderate staining in cells, 2+; weak staining in cells, 1+; no evidence of staining, 0), and percentage of positive cells (most of cells demonstrating staining, 3+; half of cells demonstrating staining, 2+; few cells demonstrating staining, 1+; no cells staining, 0), as described elsewhere (30). Differences between groups were evaluated by the sum of intensity and cell count's score. The slides were scored in the absence of any clinical data and the final score reported was the average of the 3 observers.

ELISA

ELISA performed Immunodetection of Ep-CAM autoantibody, as described (31).

Flat-bottomed microtiter enzyme-linked immunosorbent assay (ELISA) plates (Alpha Diagnostic, San Antonio, TX) were incubated at 4 °C overnight with 100 µl purified Ep-CAM (2.5µg/ml) in 0.05 M carbonate buffer, pH 9.7. After washing three times with 5mmol/L Tris buffer, pH7.80 with 0.15 mol of NaCl, 1 mmol of $MgCl_2$ and 0.5 g of sodium azide per liter, the wells were blocked for 1 hour at 37°C with 200 µl 50 mmol/L Tris Buffer, pH7.8 with 10 g of bovine serum albumin (BSA) per liter and washed three times. Serum samples were diluted 1:50 in 50 mmol/L Tris Buffer, pH7.8 with 60g BSA and 0.5 g of sodium azide and incubated overnight at 4°C. After washing six times, the wells were incubated for 2 hours at room temperature with 100 µl horseradish-peroxidase-conjugated goat anti human IgG (Pierce, Rockford, IL) diluted 1:20,000 in 50 mmol/L Tris buffer, pH 7.8 containing 60 g of BSA and 0.5 g of sodium azide per liter. After washing six times, 100 µl TMB substrate solution (Alpha Diagnostic) was added for development at room temperature for 15 minutes. The absorbance at 450nm was measured by an automatic ELISA reader (Biorad, Hercules, CA).

The CA 125 assay was performed by an immunoradiometric assay according to the manufacturer's instructions (Abbot Diagnostics).

Results were expressed as the mean absorbance of triplicate wells after subtraction of background values. Negative controls include the elimination of purified Ep-CAM, patient's serum, secondary antibody or substrate for development in the assay.

Statistical Analysis

Data were expressed as mean ± standard deviation (SD). Mann-Whitney U-test tested statistical significance in real time PCR. Immunohistochemistry and ELISA were tested by one-way analysis of variances (ANOVA) and Turkey's multiple comparison tests among groups. Parameters for tumor marker evaluation were tested by chi-square test and Fisher's exact test. Partial correlation coefficients were calculated between CA 125 and autoantibodies of Ep-CAM, adjusted by age.

The level of critical significance was assigned at $p < 0.05$. All analyses were performed using SPSS version 9.0 (SPSS Inc., Chicago, IL).

RESULTS

Using RNA isolated from 3 normal HOSE cell lines and three ovarian cancer cell lines, we identified thirty genes with a Cy3/Cy5 ratios greater than 5 (25). One of these, with a Cy3/Cy5 ratio of 444, corresponded to tumor related protein called Ep-CAM. It is selectively illustrated in figure 1.

To validate the expression of Ep-CAM, real time PCR was applied to an expanded series of ovarian cancer cell lines and tissues.

Based on the $\Delta\Delta C_T$ relative to the normal cell line, HOSE697, the relative expression levels of Ep-CAM in RNA in other cell lines were calculated. There was a highly significant difference in the expression of Ep-CAM between 5 normal ovarian epithelial cell lines and 10 ovarian cancer cell lines ($p<0.001$). The mean ± SD of normal and cancer cell lines were 2.63 ± 1.79 and 4265.61 ± 2522.14, respectively. Except for DOV13, the expression of EP-CAM in the other ovarian cancer cell lines was 1000-fold greater than that in HOSE 697 (Fig. 2).

Ep-CAM expression in ovarian cancer tissues was also examined. We found a significant difference between the three normal ovarian surface epithelia and 13 ovarian cancer tissues ($p=0.039$). The mean ± SD of the two groups was 3.31 ± 3.65 and 140.92 ± 277.91, respectively. Omental metastasis showed a tendency of lower Ep-CAM expression than cancers involving the ovary; 9.24 ± 4.01 vs. 223.21 ± 335.06 ($p=0.13$). (Fig. 3).

Ep-CAM immunoreactivity was not observed in the stroma of any of the specimens examined. Positive staining was mainly localized to the cellular membrane and cytoplasm (Fig. 4).

The mean ± SD of immunostaining scores in normal ovary, benign ovarian tumor, borderline ovarian tumor, and invasive ovarian cancer were 0.80 ± 1.10, 1,76 ± 1.36, 3,74 ± 1.66, and 3.34 ± 1.47, respectively. This difference among groups was statistically significant ($p<0.001$). There was no statistical difference between borderline tumors and invasive cancers ($p=0.174$) (Table 1).

In the cancer group, no difference in Ep-CAM immunoreactivity among different histological types and grades was observed. However, it appeared that mucinous borderline cases represented

relatively higher Ep-CAM expression, compared to any other cancer groups. Stage III and IV cases showed lower Ep-CAM expression, compared to stage I cases (p=0.007) (Table. 1).

We examined the autoantibody of Ep-CAM by ELISA in sera of 26 normal controls, 26 patients with benign ovarian disease and 52 ovarian cancer patients by ELISA. Normal controls matched for age with patients with benign ovarian disease and ovarian cancer with a mean age of 58 years old (range, 45-76).

Reciprocal serum end-point dilutions ranged between 10 and 1000 among 3 cancer patients (fig. 5).

The cut off positive antibody reactivity against Ep-CAM was 0.140, which was defined as an absorbance greater than 2SDs above the mean value of the normal controls. Another cut off value 0.115, which was defined as an absorbance greater than SD above the mean value of the normal controls, was also used..

The schematic results are shown in Figure 6. The mean ± SD of Ep-CAM autoantibody levels in normal controls, benign ovarian disease, and cancer patients were 0.090 ± 0.025, 0.098 ± 0.026, and 0.132 ± 0.032, respectively. The difference between cancer cases and the other cases was statistically significant (p=0.033). Based on the cut off value as 0.140, 22 ovarian cancer cases (42.3%) were positive, whereas none of the control (0%) and 2 (7.7%) benign ovarian disease cases were positive (fig. 6).

Data obtained from Ep-CAM autoantibody screening showed a sensitivity of 42.3%, a specificity of 100.0%, a positive predictive value of 100.0%, and a negative predictive value of 46.4%. CA125, for which the cut off value is 35 U/ml in accordance with the supplier, showed a sensitivity of 84.6%, a specificity of 88.5%, a positive predictive value of 93.8%, and a negative predictive value of 74.2% in this experiment. In combination, the two markers showed a sensitivity of 88,5%, specificity was 100.0%, positive predictive value 100.0%, and negative predictive value 96.8%. The sensitivity was statistically increased when Ep-CAM was used with CA 125 as compared to CA125 alone ($p<0.01$). When the cut off value of Ep-CAM autoantibody

was lowered to 0.115, combined two markers showed significant increases in sensitivity and negative predictive value than CA125 alone ($p<0.01$, respectively). The combination of CA 125 and Ep-CAM autoantibody showed 92.3% diagnostic efficiency when the cut-off value is 0.140, and 96.2% when the cut-off value is 0.115, which was higher compared than CA 125 alone, 85.9% ($p<0.01$, respectively) (Table 2).

In cancer patient's serum, there were no significant difference in histologic types and grades. The sera of stage IV cases showed lower levels of Ep-CAM autoantibody, compared to either stage I or II ($p=0.039$) (Table 3).

Figure 7 displays a bivariate plot of the autoantibody of Ep-CAM versus CA-125 for normal control subjects with benign ovarian disease, and epithelial ovarian cancer cases. The correlation coefficient for all cases was 0.181 and $p= 0.0073$, and for patients with cancers it was -0.076, $p= 0.59$, respectively (Fig. 7).

DISCUSSION

A tumor marker is generally considered a biochemical substance produced by the tumor and can be used to denote any change in cancer growth behavior. A number of tumor markers are now available to clinical oncologists. They have the potential utility for screening, diagnosis, prognosis, as well as therapeutic monitoring. In epithelial ovarian cancer, many tumor markers have been identified and studied. However, most of these markers have not shown satisfactory sensitivity and specificity, and therefore are not useful as a routine screening method for ovarian cancer. CA 125 is the most extensively researched marker in ovarian cancer, but there is only preliminary evidence that ovarian cancer screening using CA 125 can reduce mortality (32). Therefore, it is of paramount importance to identify new markers, particularly serologic markers, which can be used alone or in combination with CA 125 to improve the sensitivity and the specificity of the screening assay.

Multiple methods have been applied to identify tumor markers. One approach is through the identification of differentially expressed genes in ovarian cancer cells and normal ovarian surface epithelial cells. This is achieved by validation processes to determine whether the differentially expressed protein can be used as a serologic marker. Methods used to identify differentially expressed genes include expression sequencing tags (ESTs) sequencing, serial analysis of gene expression, differential display PCR, and cDNA or oligonucleotide microarray analysis (33-36). In this study, the MICROMAX^{TM} cDNA microarray system, which contains 2,400 known genes with known function, was used. This system, which requires the use of only 1 μg of total RNA, is particularly attractive when small numbers of cells, such as normal HOSE cells are unavoidable. Among all the genes analyzed, Ep-CAM showed the highest Cy3/Cy5 ratio suggesting that it was highly overexpressed in ovarian cancer cells (29).

Ep-CAM is a glycoprotein with a molecular weight of 40 kDa and encoded by the GA733-2 gene located at chromosome 4q (13,15-18). GA733-1 gene product has been known as a unique homologous protein and shares 49% homology with the Ep-CAM amino acid sequence (14). Low

levels of Ep-CAM are detected in all epithelial cells except for squamous stratified epithelium (6). Using real time PCR and immunohistochemistry, we also demonstrate low level of Ep-CAM mRNA and protein expression in normal ovarian surface epithelial cells. Similar to most epithelial derived cancers, ovarian cancers express significantly higher levels of Ep-CAM than normal and benign ovarian epithelia. However, we found no significant difference in Ep-CAM expression in borderline and invasive ovarian tumors with different grades. These data suggest that Ep-CAM may be involved in the development of both borderline and invasive disease and may be associated with an early phase of ovarian carcinogenesis. In contrast to ovarian cancer, other cancers show a different relationship between Ep-CAM expression and degree of differentiation. For example, high-grade transitional cancer of the bladder shows significantly higher Ep-CAM expression than low-grade transitional cancers (37,38). Furthermore, Ep-CAM was expressed at higher level in high-grade cervical intraepithelial neoplasia (CIN) than in low-grade CIN (39).

It is interesting to note that stage III and IV ovarian cancer shows significantly lower Ep-CAM expression than stage I disease. A similar pattern has been observed in laryngeal cancer in which lower expression of Ep-CAM correlates with a high frequency of metastases (40). Furthermore, it has been shown that transfection of murine Ep-CAM into mouse colorectal cancer cells suppressed their metastatic potential (41). These results may be explained by the fact that Ep-CAM also acts as an adhesion protein (23) whose down-regulation may facilitate the metastasis process during cancer progression.

Using an established ELISA, we evaluated the potential of using Ep-CAM autoantibody levels to detect ovarian cancer. Ep-CAM autoantibody levels proved to be significantly higher in ovarian cancer than normal and benign ovarian disease but is less sensitive and less efficient than CA 125 as shown in this experiment. However Ep-CAM autoantibody may be complementary to CA 125 as suggested by the low correlation between the two. Using Ep-CAM autoantibody with CA 125, we found that the sensitivity and diagnostic efficiency were significantly increased as

compared to CA 125 alone without lowering the specificity. Nevertheless, a large study with more cases and controls needs to be performed to confirm the potential diagnostic value of Ep-CAM autoantibody.

In conclusion, this investigation has demonstrated the potential value of the cDNA microarray analysis in identifying overexpressed genes in ovarian cancer, and suggests that Ep-CAM antibodies may be a valuable biomarker with clinical usefulness.

REFERENCE

1. Tortolero-Luna, G., Mitchell, M.F., The epidemiology of ovarian cancer. J. Cell. Biochem. Suppl., *23:* 200-207, 1995.

2. Landis, S.H., Murray, T., Bolden, S., Wingo, P.A. Cancer Statistics. CA. Cancer J. Clin., *49:* 8-31, 1999.

3. Christian, M.C., Trimble, E.L., Salvage chemotherapy for epithelial ovarian carcinoma. Gynecol. Oncol., *55:* S143-150, 1994.

4. Partridge, E.E., Barnes, M.N., Epithelial ovarian cancer: prevention, diagnosis and treatment. CA. Cancer J. Clint., *49:* 297-320, 1999.

5. Cannistra, S.A. Cancer of the ovary. N. Eng. J. Med., *329:* 1550-1559, 1993.

6. Balzar, M., Winter, M.J., de Boer, C.J., Litvinov, S.V. The biology of the 17-1A antigen (Ep-CAM). J. Mol. Med., *77:* 699-712, 1999.

7. Ragnhammar, P., Fagerberg, J., Frodin, J.E., Hjelm, A.L., Lindemalm, C., Magnusson, I., Massuci, G., Melstedt, H. Effect of monoclonal antibody 17-1A and Gm-CSF in patients with advanced colorectal carcinoma--long-lasting complete remissions can be induced. Int. J. Cancer, *53:* 751-758, 1993.

8. Mellstedt, H., Frodin, J.E., Massuci, G., Ragnhammar, P., Fager, J., Hjelm, A.L., Shetye, J., Wersall, P., Osterborg, A. The therapeutic use of monoclonal antibodies in colorectal carcinoma. Semin. Oncol., *18:* 462-477, 1991.

9. Reithmuller, G., Schneider-Gadicke, E., Schlimok, G., Schmiegel, W., Raab, R., Hoeffken, K., Gruber, R., Pichlmaier, H., Hirche, H., Pichlmaier, R., Buggisch, P., Witte, J. Randomized trial of monoclonal antibody for adjuvant therapy of resected Dukes' C colorectal carcinoma. Lancet, *343:* 1177-1183, 1994.

10. Reithmuller, G., Holz, E., Schlimok, G., Schmiegel, W., Raab, R., Hoffken, K., Gruber, R., Funke, I., Pichlmaier, H., Hirche, H., Buggisch, P., Witte, J., Pichlmayr, R. Monoclonal antibody

therapy for resected Dukes'C colorectal cancer: seven-year outcome of a multicenter randomized trial. J. Clin. Oncol., *16:* 1788-1794, 1998.

11. Herlyn, D., Somasundaram, R., Jacob, L., Li, W., Zaloudik, J., Maruyama, H., Benden, A., Harris, D., and Mastrangelo, M. Anti-Idiotypic antibodies that mimic the colorectal cancer antigen CO17-1A/GA733: twelve years of pre-clinical and clinical studies. In: Idiotypes in Medicine-Infections, Autoimmunity and Cancers (Shoenfeld, Kennedy and Ferrone, eds.). Elsevier Pergamone, Holland, 477-489, 1997.

12. Staib, L., Birebent, B., Somasundaram, R., Purev, E., Braumueller, H., Leeser, C., Kuettner, N., Li, W., Zhu, D., Wunner, W., Speicher, D., Beger, H-G., Song, H., Diao, J., and Herlyn, D. Immunogenicity of recombinant GA 733-2E antigen (CO17-1A, EGP, KS1-4, KSA, Ep-CAM) in gastrointestinal carcinoma patients. Int. J. Cancer 92: 79-87, 2001.

13. Linnenbach, A.J., Seng, B.A., Wu, S., Robbins, S., Scollon, M., Pyrc, J.J., Druck, T., Huebner, K. Retroposition in a family of carcinoma associated antigen genes. Mol. Cell. Biol., *13:* 1507-1515, 1993.

14. Szala, S., Froehlich M., Scollon M., Kasai, Y., Steplewski, Z., Koprowski, H., Linnenbach, A.J. Molecular cloning of cDNA for the carcinoma-associated antigen GA733-2. Proc. Natl. Acad. Sci. U.S.A., *87:* 3542-3546, 1990.

15. Herlyn, M., Steplewski, Z., Herlyn, D., Koprowski, H. Colorectal carcinoma-specific antigen: detection by means of monoclonal antibodies. Proc. Natl. Acad. Sci. U.S.A., *76:* 1438-1452, 1979.

16. Durbin, H., Rodrigues, N., Bodmer, W.F. Further characterization, isolation and identification of the epithelial cell-surface antigen defined by monoclonal antibody AUA1. Int. J. Cancer, *45:* 562-565, 1990.

17. Edwards, D.P., Grzyb, K.T., Dressler, L.G., Mansel, R.E., Zava, D.T., Sledge, G.W., McGuire, W.L. Monoclonal antibody identification and characterization of a Mr 43,000 membrane glycoprotein associated with human breast cancer. Cancer Res., *46:* 1306-1317, 1984.

18. Varki, N.M., Reisfeld, R.A., Walker, L.E. Antigens associated with a human lung adenocarcinoma defined by monoclonal antibodies. Cancer Res., *44:* 681-687, 1984.

19. Momburg, F., Moldenhauer, G., Hammerling, G.J., Moller, P. Immunohistochemical study of the expression of a Mr 34,000 human epithelium-specific surface glycoprotein in normal and malignant tissues. Cancer Res., *47:* 2883-2891, 1987.

20. Perez, M.S., Walker, L.E. Isolation and characterization of a cDNA encoding the KS1/4 epithelial carcinoma marker. J. Immunol., *142:* 3662-3667, 1989.

21. Strnad, J., Hamilton, A.E., Beavers, L.S., Gamboa, G.C., Apelgren, L.D., Taber, L.D., Sportsman, J.R., Bumol, T.F., Sharp, J.D., Gadski, R.A. Molecular cloning and characterization of a human adenocarcinoma/epithelial cell surface antigen complementary DNA. Cancer Res., *49:* 314-317, 1989.

22. Simon, B., Podolsky, D.K., Moldenhauer, G., Isselbacher, K.J., Gattoni-Celli, S., Brand, S.J. Epithelial glycoprotein is a member of a family of epithelial cell surface antigens homologous to nidogen, a matrix adhesion protein. Proc. Natl. Acad. Sci. U.S.A., *87:* 2755-2759, 1990.

23. Litvinov, S.V., Velders, M.P., Bakker, H.A., Fleuren, G.J., Warnaar, S.O. Ep-CAM: a human epithelial antigen is a homophilic cell-cell adhesion molecule. J. Cell Biol., 125: 437-446, 1994.

24. Gumbiner, B.M. Cell adhesion: the molecular basis of tissue architecture and morphogenesis. Cell, *84:* 345-357, 1996.

25. Litvinov, S.V., Balzar, M., Winter, M.J., Bakker H.A., Briaire-de Bruijin, I.H., Prins, F., Fleuren, G.J., Warnaar, S.O. Epithelial cell adhesion molecule (Ep-CAM) modulates cell-cell interactions mediated by classic cadherins. J. Cell Biol., *139:* 1337-1348, 1997.

26. Tsao, S.W., Mok, S.C., Fey, E.G., Fletcher, J.A., Wan, T.S., Chew, E.C., Muto, M.G., Knapp, R.C., Berkowitz, R.S. Characterization of human ovarian surface epithelial cells immortalized by human papilloma viral oncogenes (HPV-E6E7 ORFs). Exp. Cell. Res., *218:* 499-507, 1995.

27. Herlyn, D., Herlyn, M., Ross, A. Ernst, C., Atkinson, B., Koprowski, H. Efficient selection of human tumor growth-inhibiting monoclonal antibodies. J. Immunol. Meth. 73: 157-167, 1984.

28. Strassburg, C.P., Kasai, Y., Seng, B.A., Zaloudik, J., Herlyn, D., Koprowski, H., Linnenbach, A.J. Baculovirus recombinant expressing a secreted form of a transmembrane carcinoma-associated antigen. Cancer Res. 52: 815-821, 1992.

29. Wong, K.K., Cheng, R.S., Mok, S.C. Identification of differentially expressed genes from ovarian cancer cells by MICROMAX™ cDNA microarray system. Biotequnique, *30:* 670-675, 2001.

30. Shijubo, N., Uede, T., Kon, S., Maeda, M., Segawa, T., Imada, A., Hirasawa, M., Abe, S. Vascular endothelia growth factor and osteopontin in stage I lung adenocarcinoma. Am. J. Respir. Crit. Care. Med. *160:* 1269-1273, 1999.

31. Mosolits, S., Harmenberg, U., Ruden, U., Ohman, L., Nilsson, B., Wahren, B., Fagerberg, J., Mellstedt, H. Autoantibodies against the tumour-associated antigen GA733-2 in patients with colorectal carcinoma. Cancer Immunol. Immunother., *47:* 315-320, 1999.

32. Jacobs, I.J., Skates, S.J., Macdonald, N., Menon, U., Rosenthal, A., Davies, A.P., Woolas, R., Jeyarajah, A.R., Sibley, K., Lowe, D.G. Oram, D.H. Screening for ovarian cancer: a pilot randomized control trial. Lancet, 353: 1207-1210, 1999.

33. Velculescu, V.E., Zhang, L., Vogelstein, B., Kinzler, K.W. Serial analysis of gene expression. Science, *270:* 484-487, 1995.

34. Zhang, L., Zhou, W., Velculescu, V.E., Kern, S.E., Hruban, R.H., Hamilton, S.R., Vogelstein, B., and Kinzler, K.W. Gene expression profiles in normal and cancer cells. Science, *276:* 1268-1272,1997.

35. Liang, P., Pardee, A.B. Differential display of eukaryotic messenger RNA by means of the polymerase chain reaction. Science, *257:* 967-971, 1992.

36. Lockhart, D.J., Dong, H., Byrne, M.C., Follettie, M.T., Gallo, M.V., Chee, M.S., Mittmann, M., Wang, C., Kobayashi, M., Horton, H., Brown, E.L. Expression monitoring by hybridization to high-density oligonucleotide array. Nat. Biotechnol., *14:* 1675-1680, 1996.

37. Zorzos, J., Zizi, A., Pectasidis, D., Skarlos, D.V., Zorzos, H., Elemenoglou, J., Likourinas, M. Expression of a cell surface antigen recognized by the monoclonal antibody AUA1 in bladder carcinoma: an immunohistochemical study. Eur. Urol., *28:* 251-254, 1995.

38. Tomita, Y., Arakawa, F., Hirose Y., Liao S., Khare P.D., Kuroki M., Yamamoto, T., Ariyoshi A., Kuroki, M. Carcinoma-associated antigens MK-1 and CEA in urological cancers. Anticancer Res., *20:* 793-797, 2000.

39. Litvinov, S.V., van Driel, W., van Rhijin, C.M., Bakker, H.A., van Krieken, H., Fleuren, G.J., Warnaar, S.O. Expression of Ep-CAM in cervical squamous epithelia correlates with an increased proliferation and the disappearance of markers for terminal differentiation. Am. J. Pathol., *148:* 865-875, 1996.

40. Takes, R.P., Baatenburg de Jong, R.J., Schuuring, E., Hermans, J., Vis, A.A. Litvinov, S.V., Van Krieken, J.H. Markers for assessment of nodal metastasis in laryngeal carcinoma. Arch. Otolaryngol., Head Neck Surg., *123:* 412-419, 1997.

41. Basak, S., Speicher, D., Eck, S., Wunner, W., Maul, G., Simmons, M.S., Herlyn, D. Colorectal carcinoma invasion inhibition by CO17-1A/GA733 antigen and its murine homologue. J. Natl. Cancer Inst., *90:* 691-697, 1998.

FIGURE LEGENDS

Fig.1 Microarray analysis using pooled RNA isolated from three normal HOSE cultures and three ovarian cancer cell lines. Arrows indicate spots on two microarrays, which correspond to Ep-CAM.

Fig.2 Relative quantitation of Ep-CAM mRNA in normal and malignant epithelial ovarian cancer cell lines. Statistically significant difference was obtained between normal (HOSE 695, HOSE 697, HOSE 713, HOSE 726, and HOSE 730) and cancer cell lines (ALST, CAOV3, DOV13, OVCA3, OVCA 420, OVCA429, OVCA432, OVCA433, OVCA633) by Mann-Whitney U-test ($p < 0.001$). Each value was expressed as the mean of duplicate determinations.

Fig.3 Relative quantitation of Ep-CAM mRNA in normal and malignant ovarian cancer tissues. Statistically significant difference was obtained between normal (756HOSE, 757HOSE, and 763HOSE) and cancer tissues (330A, 333A, 426C, 427A, 466A, 489C, 629A, 683A, 690C, 720C, 721C, 734A, and 834A; A: ovary, C: omentum) by Mann-Whitney U-test ($p = 0.039$). Each value was expressed as the mean of duplicate determinations.

Fig. 4 Immunolocalization of Ep-CAM in normal and malignant ovarian tissues. (A) Ovarian surface epithelial cells (arrowheads) (B) Benign serous cystadenoma (C) Serous borderline tumor. (D) Serous cystadenocarcinoma. (E) Mucinous borderline ovarian tumor (F) Mucinous cystadenocarcinoma (G) Endometrioid cystadenocarcinoma (H) Clear cell cystadenocarcinoma. Scale bar represents 50 mm.

Fig.5 Absorbance values (mean ± SD) of diluted sera of 3 patients against the Ep-CAM protein. Each value was expressed as the mean ± SD of triplicate determinations.

Fig. 6 Absorbance values of diluted sera of Ep-CAM autoantibody normal controls (n=26), cases with benign lesions (n=26), and cancer(n=52). The results shown are the mean values of triplicate wells. There is a significant difference among three groups by ANOVA (p=0.033) and the differences are significant between cancer cases and the other groups based on Tukey's multiple comparison test.

Fig. 7 Correlation between the Ep-CAM autoantibody and CA-125 (on log scales) in the sera of ovarian cancer cases and controls by partial correlation coefficient. R=partial correlation coefficient adjusted by age. ●: normal (n=26), □: benign ovarian disease (n=26), ▲: cancer (n=52) The horizontal and vertical lines indicate the cut off value for positivity (0.140 for Ep-CAM autoantibody and ≥35 U/ml for CA 125)

Table 1.The expression of Ep-CAM protein in relation to histopathologic characteristics of ovarian tumor

Characteristics	No. of Cases	Scores*	T[#]	*p* value[$]
Diagnosis				
Normal	5	0.80 ± 1.10	a	$p<0.001$
Benign	17	1.76 ± 1.36	b	
Borderline	52	3.67 ± 1.66	c	
Invasive	67	3.34 ± 1.47	c	
Histology of Cancer				
Serous	60	3.36 ± 1.39		$p = 0.32$
Mucinous	41	3.88 ± 1.73		
Endometrioid	13	3.31 ± 1.44		
Clear cell/Other	5	3.00 ± 2.10		
Tumor differntiation				
Borderline	51	3.65 ± 1.79		$p = 0.61$
Well	26	3.83 ± 1.48		
Moderate	14	3.29 ± 1.61		
Poor	28	3.36 ± 1.43		
FIGO stage				
I	54	4.11 ± 1.40	a	$p = 0.007$
II	8	4.33 ± 1.58	a,b	
III	43	3.20 ± 1.70	b	
IV	14	2.90 ± 2.17	b	

* Values are given as mean ± standard deviation

$ Statiistical significances were tested by ANOVA among groups.

The same letters indicate non-significant difference between groups based on Tukey's multiple comparison test.

Table 2. Parameters of the diagnostic evaluation of tumor markers for epithelial ovarian cancer

	CA125	Ep-CAM antibody		CA125 with	Ep-CAM antibody	
	≥35 U/ml	≥ 0.115	≥0.140	≥35 U/ml	≥0.115	≥0.140
Sensitivity (%)	84.6	71.2	42.3		94.2#	88.5#
Specificity (%)	88.5	80.8	100.0		100.0	100.0
Positive predictive value (%)	93.8	90.2	100.0		100.0	100.0
Negative predictive value (%)	74.2	58.3	46.4		87.1#	77.4
Diagnostic efficiency (%)*	85.9	74.4	61.5		96.2	92.3

* true positive + true negative / total patients with or without disease

# $p < 0.01$ *versus* CA 125 alone

Table 3. The levels of Ep-CAM autoantibody in sera in relation to histopathologic characteristics of ovarian cancer

Characteristics	No. of Cases	Scores*	T#	*p* value$
Histology of Cancer				
Serous	26	0.126 ± 0.033		$p = 0.083$
Mucinous	10	0.129 ± 0.017		
Endometrioid	10	0.151 ± 0.024		
Clear cell/Other	6	0.120 ± 0.031		
Tumor differentiation				
Borderline	8	0.119 ± 0.018		$p = 0.061$
Well	6	0.163 ± 0.030		
Moderate	12	0.135 ± 0.024		
Poor	26	0.128 ± 0.035		
FIGO stage				
I	16	0.137 ± 0.030	a	$p = 0.039$
II	6	0.150 ± 0.043	a	
III	26	0.131 ± 0.028	a, b	
IV	4	0.094 ± 0.016	b	

* Values are given as mean ± standard deviation

$ Statistical significances were tested by ANOVA among groups.

The same letters indicate non-significant difference between groups based on Tukey's multiple comparison test

HOSE **CANCER**

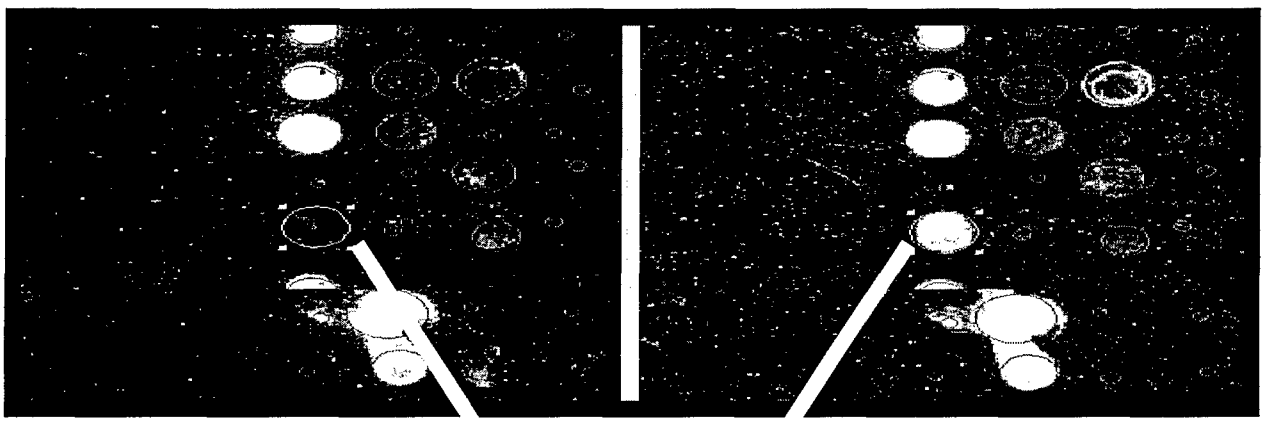

Ep-CAM

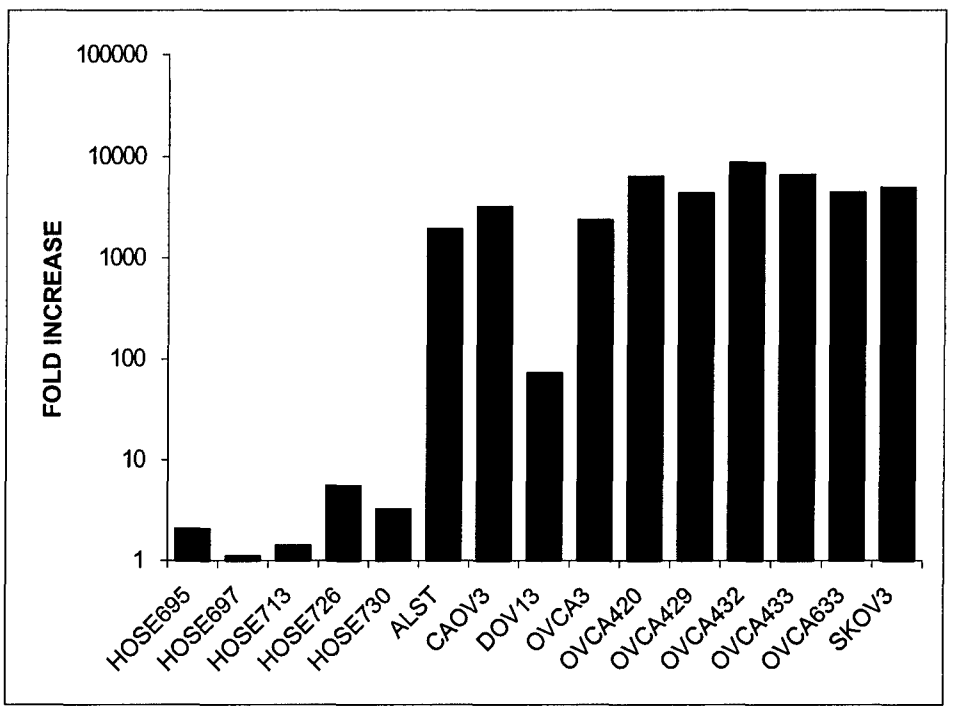
FOLD INCREASE
100000
10000
1000
100
10
1
HOSE695
HOSE697
HOSE713
HOSE726
HOSE730
ALST
CAOV3
DOV13
OVCA3
OVCA420
OVCA429
OVCA432
OVCA433
OVCA633
SKOV3

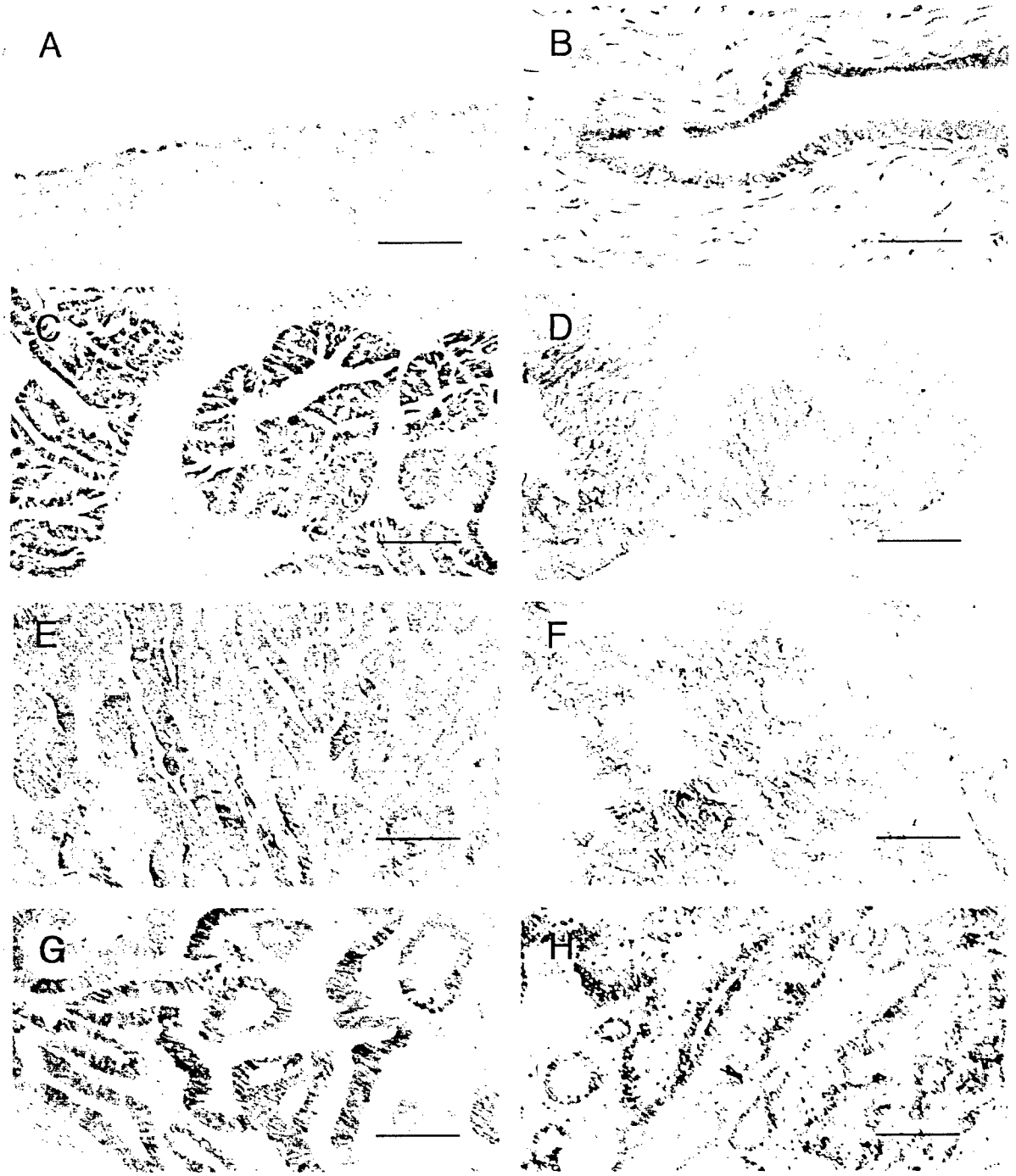
A
B
C
D
E
F
G
H

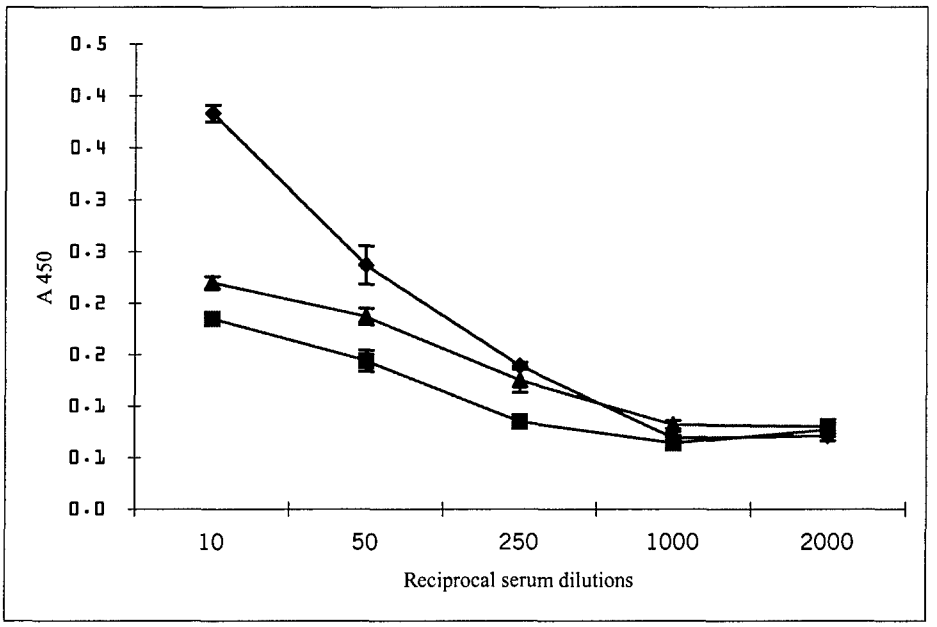
0.5
0.4
0.4
0.3
0.3
0.2
0.2
0.1
0.1
0.0
A 450
10
50
250
1000
2000
Reciprocal serum dilutions

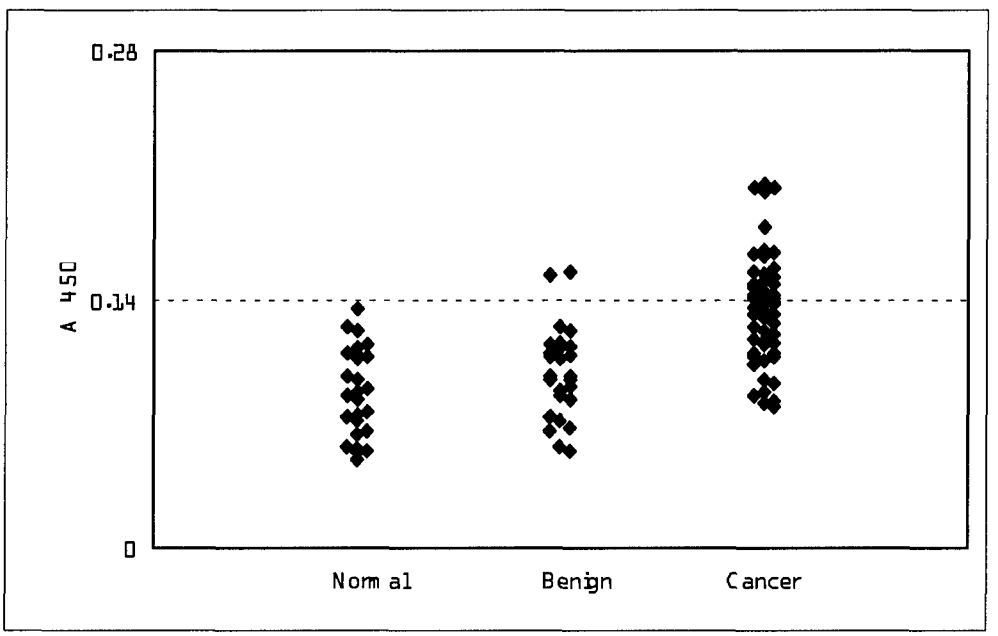
0.28
0.14
0
A 450
Normal
Benign
Cancer

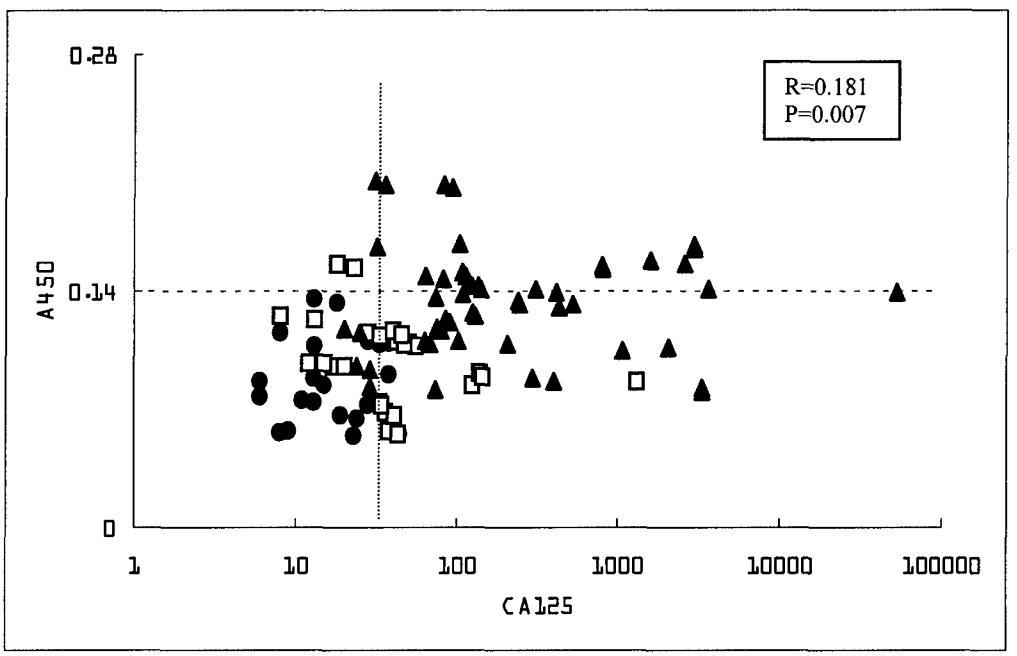
0.28
0.14
0
A450
R=0.181
P=0.007
1
10
100
1000
10000
100000
CA125

Molecular profiling of stage I epithelial ovarian carcinomas by high throughput allelotyping

Vivian W. Wang[1], Debra A. Bell[2,3], Tony K. H. Chung[4], Yick-Fu Wong[4], Kathleen Hasselblatt1[1], John D. Minna[5], John O Schorge[6], Ross S. Berkowitz[1,2], and Samuel C. Mok[1,2]

[1]Division of Gynecologic Oncology, Department of Obstetrics, Gynecology and Reproductive Biology, Brigham and Women's Hospital, Harvard Medical School, Boston, MA,

[2]Dana-Farber Harvard Cancer Center, Boston, MA,

[3]Department of Pathology, Massachusetts General Hospital, Harvard Medical School, Boston, MA,

[4]Department of Obstetrics and Gynecology, The Chinese University of Hong Kong, Shatin.

[5]Hamon Center for Therapeutic Oncology Research, University of Texas Southwestern Medical Center, Dallas, Texas

[6]Division of Gynecologic Oncology, Department of Obstetrics and Gynecology, University of Texas Southwestern Medical Center, Dallas, Texas

Reprint Request: Samuel C. Mok, Ph.D.

Laboratory of Gynecologic Oncology

Brigham and Women's Hospital

221 Longwood Avenue, BLI 449

Boston, MA 02115

Telephone (617) 278-0196, Fax (617) 975-0818

E-mail, scmok@rics.bwh.harvard.edu

Key Words: Epithelial ovarian cancer, allelotyping, chromosome 17, microdissection.

Abbreviations: LCM, laser capture microdissection; LOH, loss of heterozygosity; FAL, fractional allelic loss; PCR, polymerase chain reaction; MSI, microsatellite instability.

Footnotes: This work was supported by the Army Ovarian Cancer Research Program grant #DAMD17-99-1-9563, the Adler Foundation, the Morse Family Fund, and the Natalie Pihl Fund.

ABSTRACT

Background: Epithelial ovarian cancer represents multiple diseases with different histological types and grades exhibiting various degrees of aggressiveness and clinical outcomes. These phenomena may result from different genetic backgrounds in ovarian cancer. Therefore, genetic analyses performed on ovarian cancer, which has been stratified into different histological types and grades, should provide us a more accurate picture in the pathways involved in ovarian pathogenesis.

Methods: DNA was first isolated from microdissected normal and malignant ovarian tissues obtained from forty-eight stage I sporadic epithelial ovarian cancers including 15 serous, 9 mucinous, 12 endometrioid, and 12 clear cell carcinomas. Whole genome amplification was then performed using an improved primer-extension pre-amplification method. High-throughput allelotyping was performed on the amplified DNA using 27 fluorescent-labeled microsatellite markers spanning chromosome 17. The percentage of loss of heterozygosity (LOH) for each marker and the fractional allelic loss (FAL) for each sample were calculated and compared among different histological types.

Results: Allelotyping on all 48 tumors showed high frequencies of LOH (>45%) at loci D17S849 (17p13.2), D17S799 (17p12), and D17S1862 (17q24.3). Increased number of loci showed more than 45% LOH rate when the four histological subtypes were analyzed separately. Serous tumors demonstrated significantly higher LOH rate in 7 of 27 loci examined than other tumor types ($p<0.05$-0.001). Significant difference in LOH rate was also observed in 18 of 27 loci screened when tumors with different differentiations were compared ($P<0.05$-0.001). When the average FAL rate was compared among different tumor types,

there was no significant difference among grade I tumors. However, grade 2 clear cell tumors showed significantly higher FAL rate than endometrioid tumors ($p<0.05$); and grade 3 serous and endometrioid tumors showed significantly higher FAL rate than clear cell types ($p<0.05$).

Conclusions: Different histological types and grades of sporadic epithelial cancers have different allelic loss profiles suggesting that they may have different pathogenetic pathways.

INTRODUCTION

Ovarian cancer is the fifth most common form of cancer in females in the United States. It accounts for 4 percent of the total number of cases and 25 percent of cases occurring in the female genital tract *(1)*. Because of its low rate of cure, it is responsible for 5 percent of all cancer deaths in women and approximately half of the deaths due to cancers of the female genital tract. Epithelial ovarian cancer comprises 97% of ovarian cancer cases. They are classified into four main histological types: serous, mucinous, endometrioid, and clear cell. Serous and mucinous types comprise 50% and 30% of all tumor types respectively. Each histological type can be further grouped into three pathological grades: well differentiated lesion (grade 1), moderately differentiated lesion (grade 2), and poorly differentiated lesion (grade 3).

Due to their relative abundance, most of the molecular genetic studies in ovarian cancer have focused on high grade and late stage serous lesions. However, recent studies show that a significant difference in genetic changes can be identified in ovarian cancer with different histological types and pathological grades. For example, *KRAS* mutation rate is significantly higher in mucinous than in serous adenocarcinoma *(2-4)*. Furthermore, comparative genomic hybridization analysis showed that under-representation of 11p and 13q, and over-representation of 8q and 7p correlated with high grade tumors, while 12p under-representation and 18p overrepresentation were significantly more frequent in well and moderately differentiated tumors *(5)*. These data suggest that the single entity of ovarian cancer represents multiple diseases with different pathogenetic pathways.

In this study, we used an established high throughput PCR based method in combination with LCM and whole genome amplification techniques to generate a high density deletion map on chromosome 17 in 48 stage I epithelial ovarian cancers. In addition, LOH profiles were compared among cases to evaluate whether they correlated with the histological subtype and pathological grade of the tumor.

MATERIALS AND METHODS

Eighteen frozen and 30 formalin-fixed, paraffin-embedded ovarian cancer samples were obtained from the Division of Gynecologic Oncology, Brigham and Women's Hospital, the Department of Pathology, Massachusetts General Hospital, and the Department of Obstetrics and Gynecology, The Chinese University of Hong Kong. All identifying information was removed from each sample prior to its receipt for analysis. According to International Federation of Gynecology and Obstetrics criteria, all 48 cases were stage I epithelial ovarian cancer. Of them, 4 were microscopically identified microinvasive carcinomas. The diameters of these microscopic tumors ranged from 1 to 8 mm. Histologic subtype and pathological grade of the tumors were determined according to the World Health Organization criteria. Fifteen were serous, 9 were mucinous, 12 were endometrioid, and 12 were clear cell adenocarcinomas. Eighteen cases were well differentiated (Grade 1), 14 were moderately differentiated (Grade 2), and 16 were poorly differentiated tumors (Grade 3).

Six-micrometer sections from frozen tissue or paraffin-embedded tissue blocks were cut, mounted onto plain glass slide, and stained with hematoxylin and eosin. Histologic diagnosis for each specimen was confirmed prior to microdissection. Tumor and normal stromal cells were procured by the PixCell II LCM system (Arcturus Engineering, Mountain View, CA). DNA was isolated from the LCM procured cells, microdissected tumor cells and paired stromal cells, and whole genome amplification was carried out as described previously *(6)*. The 27 fluorescent microsatellite markers spanning chromosome 17 used in this study were obtained from the ABI PRISM Linkage

Mapping Set HD-5 (Applied Biosystems, Foster City, CA). Cytogenetic location of the markers was determined by data obtained from the following three websites including UCSC's Genome Brower (http://genome.ucsc.edu), NCBI's Map Viewer (http://www.ncbi.nlm.nic.gov/genome/ guide), and Ensemble (http://www.ensembl.org). PCR reactions were performed in a 10 μl volume using 1 μl of whole genome amplified DNA, 0.25-0.5 μM of each primer, 1 x PCR buffer, 2.5 mM $MgCl_2$, 0.25 mM of each dNTP, and 0.5 unit AmpliTaq Gold DNA polymerase. Amplification was started with 12 min at 95 °C, followed by 10 cycles composed of 15 sec at 94 °C, 15 sec at 55 °C and 30 sec at 72 °C, and then 25 cycles composed of 15 sec at 89 °C, 15 sec at 55 °C and 30 sec at 72 °C. Amplified PCR products for multiple loci were pooled, and run on an ABI PRISM 310 automated capillary electrophoresis DNA sequencer (Applied Biosystems, Foster City, CA).

The allelic products were assessed for peak height and peak area using Genescan and Genotyper softwares (Applied Biosystems, Forster City, CA), and the ratios of heterozygous normal and tumor alleles were calculated as described previously *(6)*. LOH was imputed if the effective decrease in one allele was > 50% (normal : tumor allelic ratios, < 0.5 or >2.0). Retention of both alleles was scored as retention of heterozygosity. A unique peak in both the tumor cells and non-tumor stromal cells was scored as homozygote or not informative. Microsatellite instability (MSI) was defined as a shift of electropherogram tracing in tumor sample when compared with that in the corresponding normal tissue. Representative output of an ovarian cancer case demonstrating allelotyping patterns at loci D17S784, D17S1876, D17S949, and D17S785 are shown in **Figure 1.**

Both LOH percentage for each marker and the FAL for each sample were calculated, and a detailed deletion map was generated using a LOH clustering software as described *(7)*. LOH percentage was measured as the number of samples showing LOH present in a marker divided by the total number of informative (heterozygous) samples. The FAL is a measure of the extent of allele loss in a given tumor sample and was defined as the number of LOH events in a sample divided by the total informative (heterozygous) markers in the corresponding normal DNA sample *(8)*. Pearson's chi-square test and One Way Analysis of Variance were used to evaluate the association between LOH rate or FAL and tumor histologic subtype or pathological grade. Fisher exact test was used to compare FAL among the four microscopically detected tumors. Statistical algorithms were from SPSS 9.0 for windows software (SPSS Inc., Chicago, IL). Probability value was two-tailed, with $p < 0.05$ regarded as statistically significant.

RESULTS

LOH analysis revealed regions of frequent allelic loss in stage I epithelial ovarian cancer. In this study, DNA samples extracted from 48 stage I ovarian cancer cases and their corresponding controls were allelotyped with 27 markers, with an average genetic distance of 5 cM, on chromosome 17. The allelotyping results are shown in Figure 2 and Table 1. Forty-four of 48 (91%) epithelial ovarian cancers displayed LOH of at one or more informative markers. Of these, 5 tumors (3 cases of grade 3 serous adenocarcinoma and 2 cases of grade 3 endometrioid adenocarcinoma) showed LOH at all informative loci. Four tumors (1 case of grade 1 serous adenocarcinoma and 3 cases of grade 1 endometrioid adenocarcinoma) showed all informative alleles on chromosome 17 were retained. The remaining 39 tumors showed partial deletions, suggesting regional losses. The allele loss frequencies of the marker used in all 48 early stage epithelial ovarian tumors are shown in Figure 3. They varied from 13% (D17S928 at 17qter) to 50% (D17S849 at 17p13.3 and D17S799 at 17p12). Frequent losses (>35%) were seen at 12 loci including D17S849 (17p13.3, 50%), D17S831 (17p13.3, 37%), D17S1828 (17p13.2, 42%), D17S1876 (17p13.2, 49%), D17S799 (17p12, 50%), D17S921 (17p11.2, 43%), D17S1857 (17p11.2, 45%), D17S787 (17q22, 45%), D17S944 (17q23.1, 44%), D17S1816 (17q24.1, 38%), D17S1862 (17q24.3, 47%), and D17S836 (17q25.3, 42%). The most prominent regions of allelic loss (>45% loss) were at 17p13.3, 17p13.2, 17p12 and 17q24.3. These regions of loss were confined to one marker or located between two markers. The FAL at 27 loci of chromosome 17 in this set of stage I epithelial ovarian cancers ranged from 0 to 1.0. The average FAL was 0.349.

LOH in different histologic subtypes of stage I epithelial ovarian cancer. LOH of chromosome 17 markers was analyzed according to the histological type as shown in Table 1. A total of 15 serous, 9 mucinous, 12 endometrioid, and 12 clear carcinomas were analyzed. In serous adenocarcinoma, high frequency of LOH (>45%) was detected in 19 loci including D17S1876, D17S1876, D17S799, D17S1857, D17S1824, D17S798, D17S927, D17S1868, D17S1795, D17S787, D17S957, D17S944, D17S1816, D17S1862, D17S1807, D17S785, D17S1847, D17S836 and D17S784. In mucinous adenocarcinoma, high frequency of LOH was detected in 5 loci including D17S849, D17S1828, D17S1876, D17S799 and D17S921. Allelic loss was not detected in any of the markers on 17q21.2-q21.32, and 17q25-qter. In endometrioid adenocarcinoma, only one marker, D17S849 at 17p13.3, showed more than 45% LOH rate. In clear cell adenocarcinoma, high frequency of LOH was detected in 7 loci including D17S849, D17S1791, D17S799, D17S921, D17S787, D17S1862 and D17S836. The average FAL in serous, mucinous, endometrioid, and clear cell adenocarcinoma was 0.447, 0.240, 0.258, and 0.293 respectively. There were significant differences in LOH frequency at 7 individual loci including D17S1824, D17S798, D17S927, D17S1868, D17S944, D17S1807 and D17S785 among the 4 subtypes of cancer ($p<0.05$-0.001) (figure 4). Without further stratification into different pathological grades, the difference of FAL among different histological types of ovarian cancer was not significant ($p>0.05$).

LOH in different pathological grades of stage I epithelial ovarian cancer. LOH of chromosome 17 markers was analyzed according to pathological grades as

shown in Table 1. A total of 14 grade 1, 16 grade 2 and 18 grade 3 tumors were examined. High frequency of LOH (>45%) was detected at 22 loci in poorly differentiated grade 3 cancer, at 3 loci in grade 2 cancer, and at no one locus in grade 1 cancer. There was significant difference in LOH frequency at 18 of 27 loci examined among three pathological grades of stage I ovarian tumor ($p<0.05$-0.001). The LOH frequency at these 18 loci was higher in poorly differentiated tumor than that in other grades (Figure 5). Furthermore, LOH can only be detected at D17S957 on 17q23.1, and D17S928 on 17qter in grade 3 tumors. The average FAL in grade 1, grade 2, and grade 3 was 0.157, 0.208, and 0.624, respectively. Grade 3 tumor showed significantly higher average FAL than grade 2 and grade 1 tumors ($p<0.05$-0.001). When the average FAL was compared among tumors with different grades that were further stratified into different histological types, grade 2 endometrioid tumors showed significantly lower FAL than grade 2 clear cell tumors ($p<0.05$), and lower than grade 2 mucinous and serous tumors ($p=0.051$). Furthermore, grade 3 serous and endometrioid tumors showed significantly higher FAL than grade 3 clear cell tumor ($p<0.05$) (Figure 6).

LOH in microscopically detected stage I epithelial ovarian cancer. To evaluate whether chromosome 17 LOH is an early event in ovarian carcinogenesis, the allelotype profiles from the four microscopically detected ovarian carcinomas were examined (Figure 2). Both grade 3 serous (case 99N51) and endometrioid (case 774) adenocarcinomas showed significantly higher FAL than the grade 1 serous adenocarcinoma (case 3317) ($p<0.001$) and the grade 2 serous adenocarcinoma (case 7024) ($p<0.05$). Significant difference in FAL between the microscopically detected

carcinomas and other stage I invasive ovarian carcinomas with the same grade was not detected.

Microsatellite instability in stage I epithelial ovarian cancer. Fifteen of 48 tumors (31%) exhibited MSI at least in one locus (Figure 2). The number of loci with MSI in these tumors ranged from 1 to 5. One tumor displayed MSI in 5 markers, five tumors had MSI in two markers, while nine tumors had MSI in one marker only. Recurrent changes were not observed in any loci.

DISCUSSION

In this study, we used 27 fluorescent-labeled microsatellite markers and DNA isolated from microdissected normal and malignant ovarian tissues obtained from 48 sporadic stage I epithelial ovarian cancer to generate a high resolution deletion map on chromosome 17. The percentage of LOH for each marker and the FAL for each sample were calculated and compared among different histological types and pathological grades.

Due to their relative abundance, most of the allelotyping have focused on the study of high grade and late stage serous ovarian carcinomas. Detailed deletion mapping of chromosome 17q in ovarian cancers identified at least three distinct commonly deleted regions. They are located at 17q 11.2 (the *NF1* locus), 17q21 (including the *BRCA1* locus) and between 17q25.1 and 17qter *(9-11)*. Multiple common loss regions were also identified on 17p. More than 50% LOH rate at the p53 locus was identified in all types of high grade carcinomas but significantly lower in low grade and early stage tumors *(12-14)*. A site of the chromosome 17p deletions was narrowed to 17p13 where 17 of 21 tumors showing deletions of 17p did not show evidence of *TP53* mutations *(15)*. This suggests that 17p deletions may occur early and precede any *TP53* mutations. Further mapping of the common loss region identified a 15 kB region at 17p13.3 where a number of genes including *OVCA1* and *OVCA2* with potential tumor suppressor function are located *(16, 17)*.

Controversies in LOH percentage exist in ovarian tumors with different histological subtypes and pathological grades. Pieretti *et al. (18)* reported that grade 3

serous tumors had the highest percentage of chromosome 17 loss (89%), followed by grade 2 serous tumors (44%) and grade 3 endometrioid carcinomas (43%). Overall, they detected LOH at 17q in 49% serous, 15% endometrioid, and 4% mucinous neoplasms. Moreover, total loss of chromosome 17 was almost exclusively detected in high grade serous carcinomas. They concluded that chromosome 17 loss is a molecular alteration almost exclusively confined to high-grade and late stage tumors. In contrast, Eccles *et al. (19)* reported high LOH rate at chromosome 17 in early stage ovarian carcinomas. Moreover, Papp *et al. (20)* reported that LOH at 17q was infrequent in tumors with endometrioid, mucinous and clear cell histology. Furthermore, Dodson *et al. (21)* reported a higher percentage of chromosome 17 LOH in low grade tumors. We believe that these controversies are mainly due to the distribution of different histological subtypes and histological grades in their analyses. Using stage I tumor cases with a more even distribution of subtype and grade, our studies clearly demonstrate that within the same stage, ovarian cancers with different pathological grades have different allelic loss profiles. Furthermore, within the same pathological grade, tumors with histological types have different allelic profiles. Both LOH frequency and FAL change dramatically when these tumors are analyzed separately. These data strongly suggest that ovarian tumors with different grades and histological types need to be analyzed separately, and the entity of ovarian cancer represents multiple diseases with different pathogenetic pathways.

In this study, we showed that both microscopic grade 3 serous and endometrioid carcinomas demonstrated significantly higher FAL than the grade 1 serous tumors. These tumors were incidental microscopic findings. The indications for the operations that included oophorectomy were leiomyomas, menorrhagia, and pyometra. None of the

oophorectomies were performed as prophylaxis in women with a family history of ovarian cancer. These tumors represent very early lesions. The identification of significantly higher FAL in the grade 3 serous and endometrioid carcinomas than the low grade microscopic tumors suggests that allelic loss in chromosome 17 is an early event in the pathogenesis of high grade ovarian tumors. Furthermore, it also supports the notion that high grade tumors may develop de novo from premalignant lesions such as inclusion cysts or endosalpingosis without progressing through borderline or low grade stages.

Our study showed that MSI in chromosome 17 is uncommon in stage I ovarian carcinomas. It was identified in tumors with different histological types and pathological grades. One of the tumors (98R2224) showed evidence of MSI at multiple loci. The precise significance of this finding is not yet clear. It may represent an indirect evidence of a mutator phenotype.

In conclusion, this study showed that different histological types and grades of sporadic stage I epithelial ovarian cancers have different allelic loss profiles. Allelic loss on chromosome 17 is an early event in the pathogenesis of high grade serous and endometrioid carcinomas. These data support the notion that ovarian cancer represents multiple diseases with different pathogenetic pathways and therefore warrants to be studied separately.

REFERENCES

(1) American Cancer Society, Cancer Facts & Figures. American Cancer Society, Inc., 1999.

(2) Ichikawa Y, Nishida M, Suzuki H, Yoshida S, Tsunoda H, Kubo T, et al. Mutation of K-ras protooncogene is associated with histological subtypes in human mucinous ovarian tumors. Cancer Res 1994;54:33-5.

(3) Mok SC, Bell DA, Knapp RC, Fishbaugh PM, Welch WR, Muto MG, et al. Mutation of K-ras protooncogene in human ovarian epithelial tumors of borderline malignancy. Cancer Res 1993;53:1489-92.

(4) Enomoto T, Weghorst CM, Inoue M, Tanizawa O, Rice JM. K-ras activation occurs frequently in mucinous adenocarcinomas and rarely in other common epithelial tumors of the human ovary. Am J Pathol 1991;139:777-85.

(5) Kiechle M, Jacobsen A, Schwarz-Boeger U, Hedderich J, Pfisterer J, Arnold N. Comparative genomic hybridization detects genetic imbalances in primary ovarian carcinomas as correlated with grade of differentiation. Cancer 2001;91:534-40.

(6) Wang VW, Bell DA, Berkowitz RR, Mok SC. Whole genome amplification and high-throughput allelotyping identified five distinct deletion regions on chromosomes 5 and 6 in microdissected early stage ovarian tumors. Cancer Res 2001;61(in press).

(7) Girard L, Zöchbauer-Müller S, Virmani AK, Gazdar AF, Minna JD. Genome-wide allelotyping of lung cancer identifies new regions of allelic loss, differences between small cell lung cancer and non-small cell lung cancer, and loci clustering. Cancer Res 2000;60:4894-906.

(8) Vogelstein B, Fearon ER, Kern SE, Hamilton SR, Preisinger AC, Nakamura Y, et al. Allelotype of colorectal carcinomas. Science (Washington DC) 1989;244:207-11.

(9) Narod SA, Feuneun J, Lynch HT, Watson P, Conway T, Lynch J, et al. Familial breast-ovarian cancer locus on chromosome 17q12-q23. Lancet 1991;338:82-3.

(10) Miki Y, Swenson J, Shattuck-Eidens D, Futreal PA, Harshman K, Tavtigan S, et al. A strong candidate gene for the breast and ovarian cancer susceptibility gene BRCA1. Science 1994;266:66-71.

(11) Dion F, Mes-Masson A, Seymour RJ, Provencher D, Tonin PN. Allelotyping defines minimal imbalance at chromosomal region 17q25 in non-serous epithelial ovarian cancers. Oncogene 2000;19:1466-72

(12) Wertheim I, Tangir J, Muto MG, Welch WR, Berkowitz RS, Chen WY, et al. Loss of heterozygosity of chromosome 17 in human borderline and invasive epithelial ovarian tumors. Oncogene 1996;12:2147-53.

(13) Wiper DW, Zanotti KM, Kennedy AW, Belinson JL, Casey G. Analysis of allelic imbalance on chromosome 17p13 in stage I and stage II epithelial ovarian cancers. Gynecol Oncol 1998;71:77-82.

(14) Launonen V, Mannermaa A, Stenback F, Kosma VM, Puistola U, Huusko P, et al. Loss of heterozygosity at chromosomes 3, 6, 8, 11, 16, and 17 in ovarian cancer: correlation to clinicopathological variables. Cancer Genet Cytogenet 2000;122:49-54.

(15) Sakamoto T, Nomura N, Mori H, Wake N. Poor correlation with loss of heterozygosity on chromosome 17p and p53 mutations in ovarian cancers. Gynecol Oncol 1996;63:173-9.

(16) Schultz DC, Vanderveer L, Berman DB, Hamilton TC, Wong AJ, Godwin AK. Identification of two candidate tumor suppressor genes on chromosome 17p13.3. Cancer Res 1996;56:1977-2002.

(17) Phillips NJ, Ziegler MR, Radford DM, Fair KL, Steinbrueck T, Xynos FP, et al. Allelic deletion on chromosome 17p13.3 in early ovarian cancer. Cancer Res 1996;56:606-11.

(18) Pieretti M, Powell DE, Gallion HH, Case EA, Conway PS, Turker MS. Genetic alterations on chromosome 17 distinguish different types of epithelial ovarian tumors. Human Pathology 1995;26:393-7.

(19) Eccles DM, Cranston G, Steel CM, Nakamura Y, Leonard RCF. Allele losses on chromosome 17 in human epithelial ovarian carcinoma. Oncogene 1990;5:1599-1601.

(20) Papp J, Csokay B, Bosze P, Zalay Z, Toth J, Ponder B, et al. Allele loss from large regions of chromosome 17 is common only in certain histological subtypes of ovarian carcinomas. Br J Cancer 1996;74:1592-7.

(21) Dodson MK, Hartmann LC, Cliby WA, DeLacey KA, Keeney GL, Ritland SR, et al. Comparison of loss of heterozygosity patterns in invasive low-grade and high-grade epithelial ovarian carcinomas. Cancer Res 1993;53:4456-60.

LEGENDS

Figure 1. Electropherogram traces on four chromosome 17 loci (D17S784, D17S1876, D17S949, and D17S785) in a clear cell adenocarcinoma (case 98C1755). Top, stromal cells; Bottom, cancer cells. The four panels from left to right show loss of heterozygosity, retention of heterozygosity, homozygous, and microsatellite instability, respectively.

Figure 2. Detailed deletion map of 48 stage I epithelial ovarian cancer cases. Samples are grouped according to tumor grade and histological subtype. Chromosome 17 genetic linkage map and microsatellite markers are shown on the left. Chromosome regional location is shown on the right. S, serous; M, mucinous; E, endometrioid; C, clear cell.

Figure 3. Frequency of allele loss in 27 markers on chromosome 17 in 48 stage I epithelial ovarian tumors.

Figure 4. Graphical representation of LOH frequency at 27 loci on chromosome 17 in 4 histological subtypes of stage I epithelial ovarian tumors.

Figure 5. Graphical representation of LOH frequency at 27 loci on chromosome 17 in varying grades of stage I epithelial ovarian tumors.

Figure 6. Average FAL of each histological subtype and pathological grade on chromosome 17. The error bar depicts the standard deviation of the mean.

Table 1. Correlation of LOH in each locus with pathological features in stage I epithelial ovarian tumors.

Markers	Histology (LOH informative%)					Differentiation (LOH informative%)			
	Serous (n=15)	Mucinous (n=9)	Endometrioid (n=12)	Clear (n=12)	*p* value	Well (n=14)	Moderate (n=16)	Poor (n=18)	*p* value
D17S849	5/12 (42%)	3/6 (50%)	5/8 (63%)	4/8 (50%)	ns	3/11 (27%)	5/10 (50%)	9/13 (69%)	ns
D17S831	5/12 (42%)	4/9 (44%)	4/10 (40%)	2/10 (20%)	ns	3/11 (27%)	2/13 (15%)	10/17 (59%)	< 0.05
D17S1828	10/15 (67%)	4/8 (50%)	3/11 (27%)	2/11 (18%)	ns	3/14 (21%)	4/15 (27%)	12/16 (75%)	< 0.05
D17S1876	8/13 (62%)	5/9 (56%)	3/9 (33%)	5/12 (42%)	ns	5/14 (36%)	5/13 (38%)	11/16 (69%)	ns
D17S938	4/10 (40%)	0/7 (0)	1/7 (14%)	2/10 (20%)	ns	2/14 (14%)	0/8 (0)	5/12 (42%)	< 0.05
D17S1791	5/12 (42%)	1/9 (11%)	2/9 (22%)	6/11 (55%)	ns	4/13 (31%)	3/14 (21%)	7/14 (50%)	ns
D17S1852	4/12 (33%)	4/9 (44%)	2/11 (18%)	1/8 (13%)	ns	1/13 (8%)	4/13 (31%)	6/14 (43%)	ns
D17S799	7/14 (50%)	4/6 (67%)	2/7 (29%)	6/11 (55%)	ns	2/11 (18%)	6/11 (55%)	11/16 (69%)	< 0.05
D17S921	4/9 (40%)	2/3 (67%)	2/9 (22%)	5/9 (56%)	ns	1/9 (11%)	3/10 (30%)	9/11 (82%)	< 0.05
D17S1857	5/10 (50%)	4/9 (44%)	3/8 (38%)	5/11 (45%)	ns	2/9 (22%)	4/14 (29%)	11/15 (73%)	< 0.05
D17S1824	9/13 (69%)	2/8 (25%)	2/12 (17%)	1/9 (11%)	< 0.05	2/13 (15%)	2/12 (17%)	10/17 (59%)	ns
D17S798	7/8 (88%)	0/5 (0)	3/9 (33%)	0/6 (0)	< 0.001	1/7 (14%)	1/7 (14%)	8/14 (57%)	< 0.05
D17S927	6/11 (55%)	0/7 (0)	2/8 (25%)	0/10 (0)	< 0.001	0/11 (0)	1/13 (8%)	7/12 (58%)	< 0.001
D17S1868	6/13 (46%)	0/6 (0)	2/8 (25%)	3/9 (33%)	< 0.05	1/12 (8%)	2/12 (17%)	8/12 (67%)	< 0.05
D17S1795	7/12 (58%)	1/7 (14%)	3/9 (33%)	2/12 (17%)	ns	1/10 (10%)	2/15 (13%)	10/15 (67%)	< 0.05
D17S787	7/10 (70%)	3/8 (38%)	2/10 (20%)	5/10 (50%)	ns	2/11 (18%)	3/14 (21%)	12/13 (92%)	< 0.001
D17S957	2/4 (50%)	0/3 (0)	2/6 (33%)	1/8 (13%)	ns	0/5 (0)	0/8 (0)	5/8 (63%)	< 0.001
D17S944	9/11 (82%)	2/7 (29%)	1/7 (14%)	0/2 (0)	< 0.05	2/9 (22%)	1/7 (14%)	9/11 (82%)	< 0.05
D17S1816	7/12 (58%)	0/6 (0)	3/9 (33%)	4/10 (40%)	ns	1/9 (11%)	6/14 (43%)	7/14 (50%)	ns
D17S949	4/13 (31%)	1/8 (13%)	2/11 (18%)	3/10 (30%)	ns	1/13 (8%)	3/15 (20%)	6/14 (43%)	ns
D17S1862	8/14 (57%)	2/9 (22%)	5/12 (42%)	6/10 (60%)	ns	4/13 (31%)	7/15 (47%)	10/17 (59%)	ns
D17S1807	6/12 (50%)	0/8 (0)	3/12 (25%)	1/12 (8%)	< 0.05	2/13 (15%)	0/15 (0)	8/16 (50%)	< 0.05
D17S785	7/15 (47%)	0/5 (0)	1/11 (9%)	1/12 (8%)	< 0.05	0/12 (0)	1/13 (8%)	8/18 (44%)	< 0.05
D17S1847	4/8 (50%)	0/5 (0)	1/8 (13%)	4/9 (44%)	ns	0/6 (0)	2/11 (18%)	7/13 (54%)	< 0.05
D17S836	7/12 (58%)	0/2 (0)	0/5 (0)	4/7 (57%)	ns	0/5 (0)	2/11 (18%)	9/10 (90%)	< 0.001
D17S784	6/11 (55%)	0/5 (0)	3/7 (43%)	2/9 (22%)	ns	2/11 (18%)	1/9 (11%)	8/12 (67%)	< 0.05
D17S928	4/11 (36%)	0/5 (0)	0/7 (0)	0/7 (0)	ns	0/9 (0)	0/11 (0)	4/10 (40%)	ns

* Well differentiated, grade1; moderately differentiated, grade 2; poorly differentiated, grade 3.
* Statistical significances were tested by Pearson's Chi-Square.
* ns: non-significant.

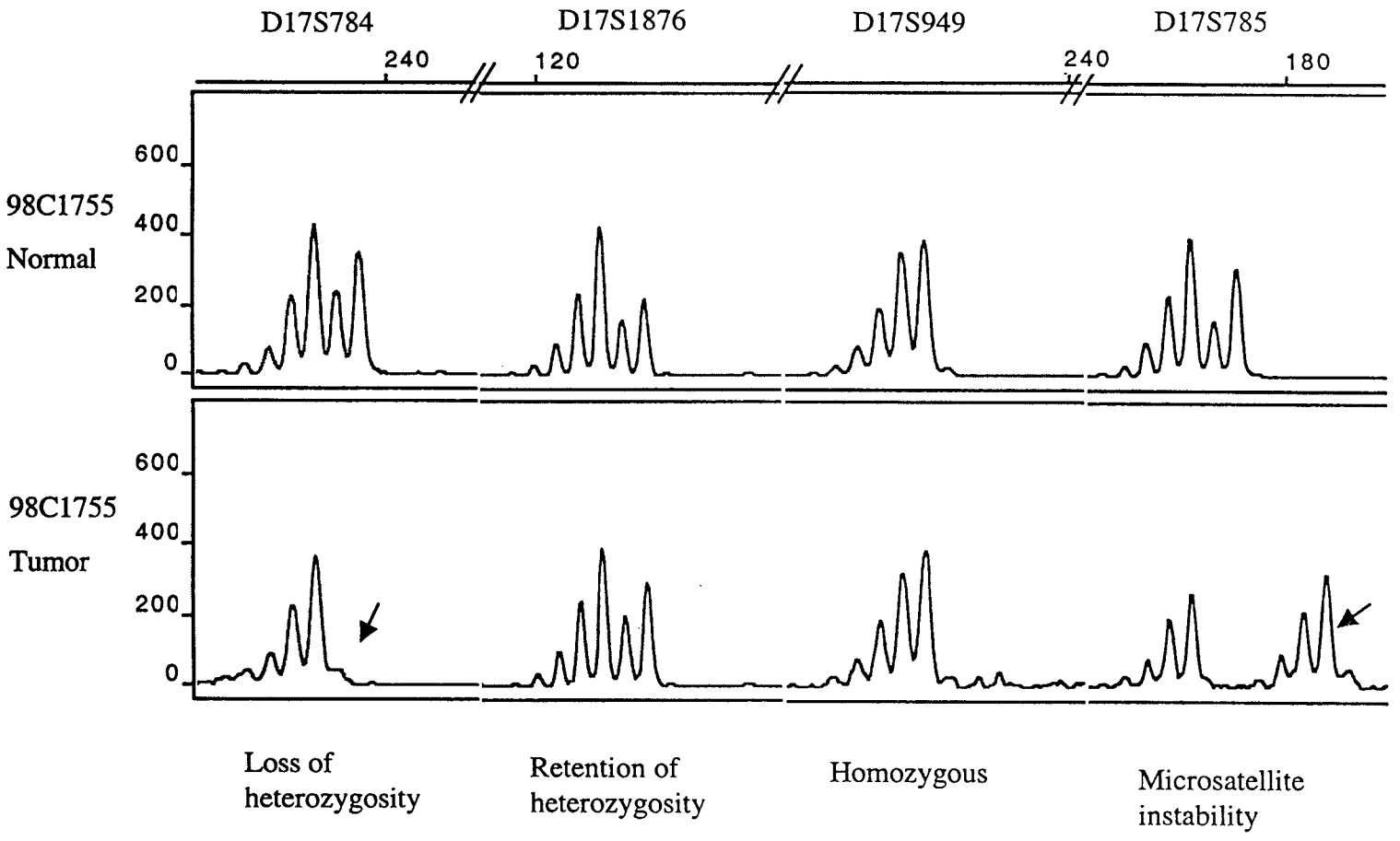
D17S784
D17S1876
D17S949
D17S785
240
120
240
180
600
400
200
0
98C1755
Normal
600
400
200
0
98C1755
Tumor
Loss of heterozygosity
Retention of heterozygosity
Homozygous
Microsatellite instability

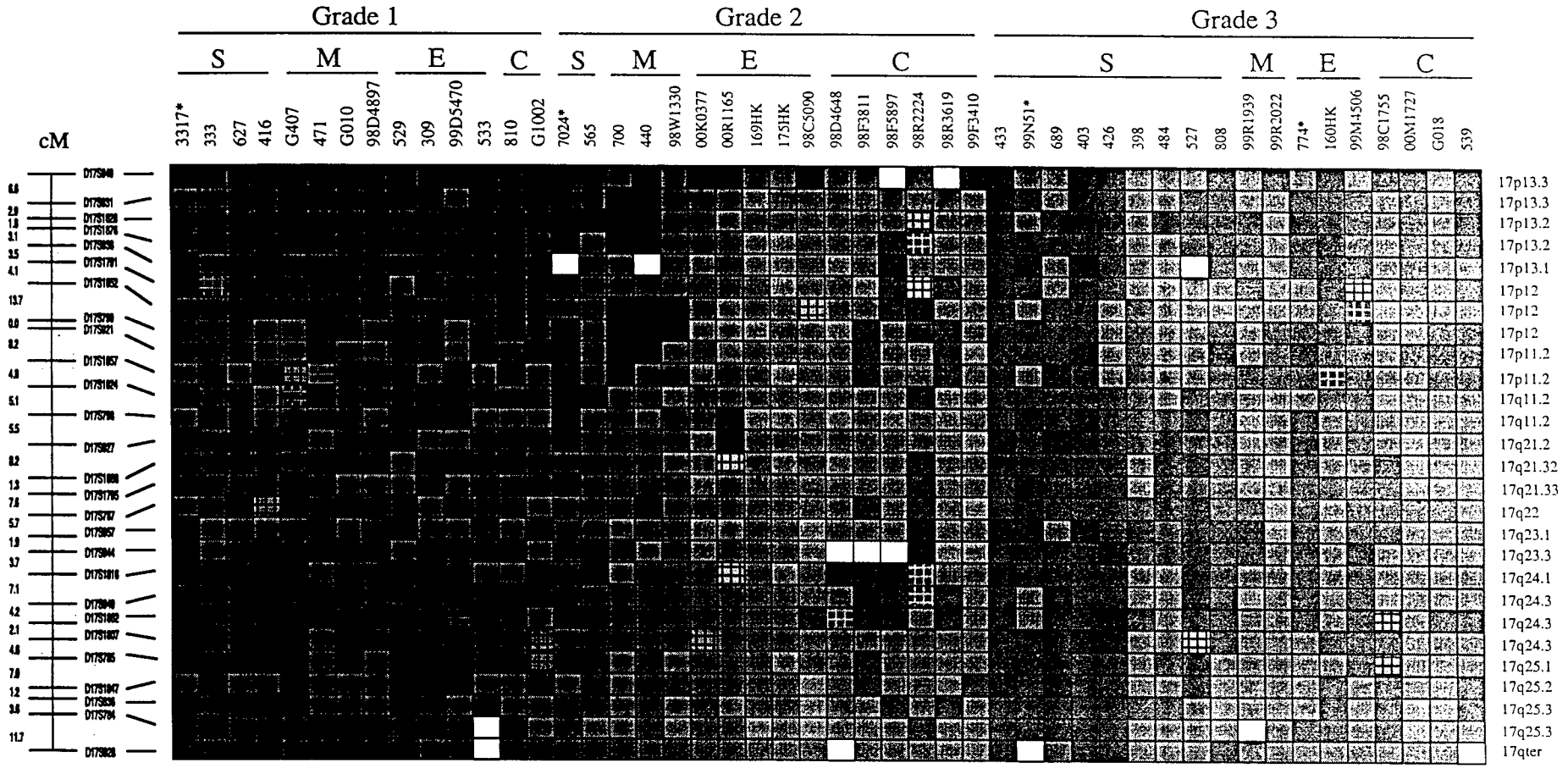

* Microscopically detected epithelial ovarian carcinoma.

Retention of heterozygosity

Loss of heterozygosity

Homozygous

No data

Microsatellite instability with both alleles retained

Microsatellite instability with loss of one allele

Microsatellite instability with homozygous

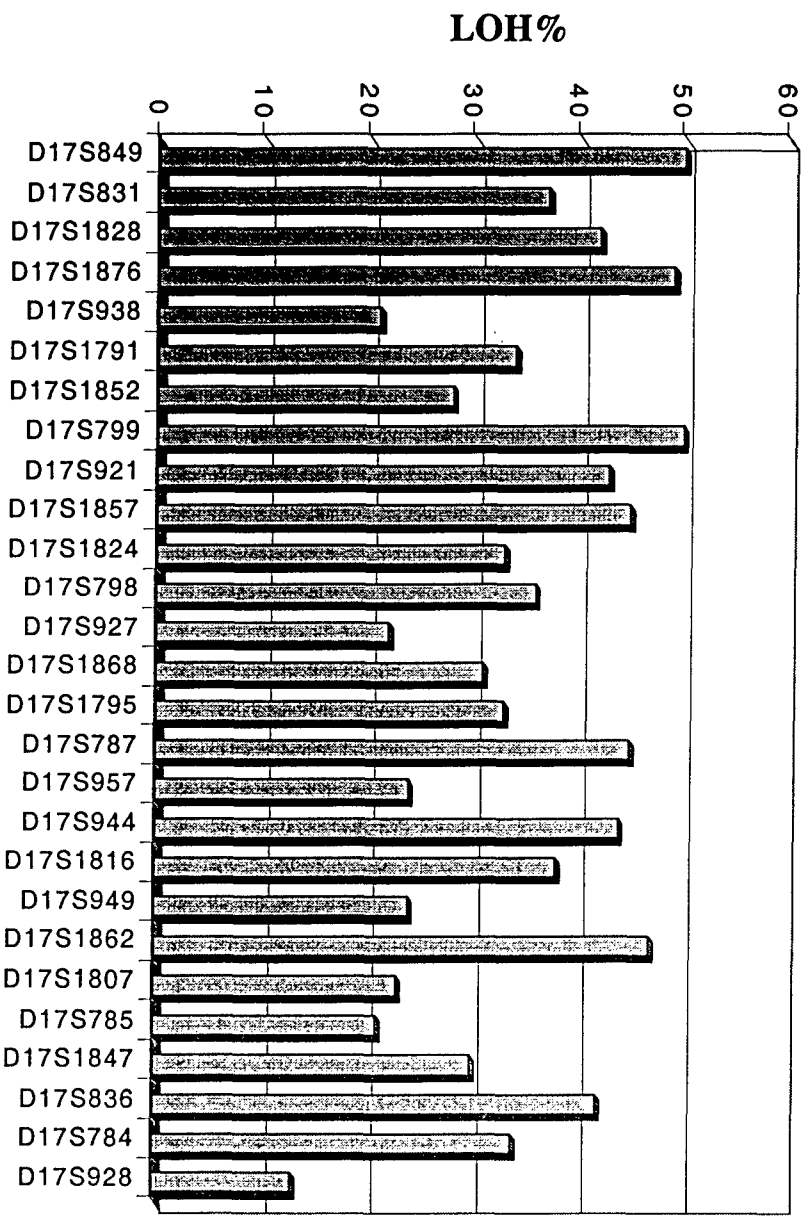
LOH%
0
10
20
30
40
50
60
D17S849
D17S831
D17S1828
D17S1876
D17S938
D17S1791
D17S1852
D17S799
D17S921
D17S1857
D17S1824
D17S798
D17S927
D17S1868
D17S1795
D17S787
D17S957
D17S944
D17S1816
D17S949
D17S1862
D17S1807
D17S785
D17S1847
D17S836
D17S784
D17S928

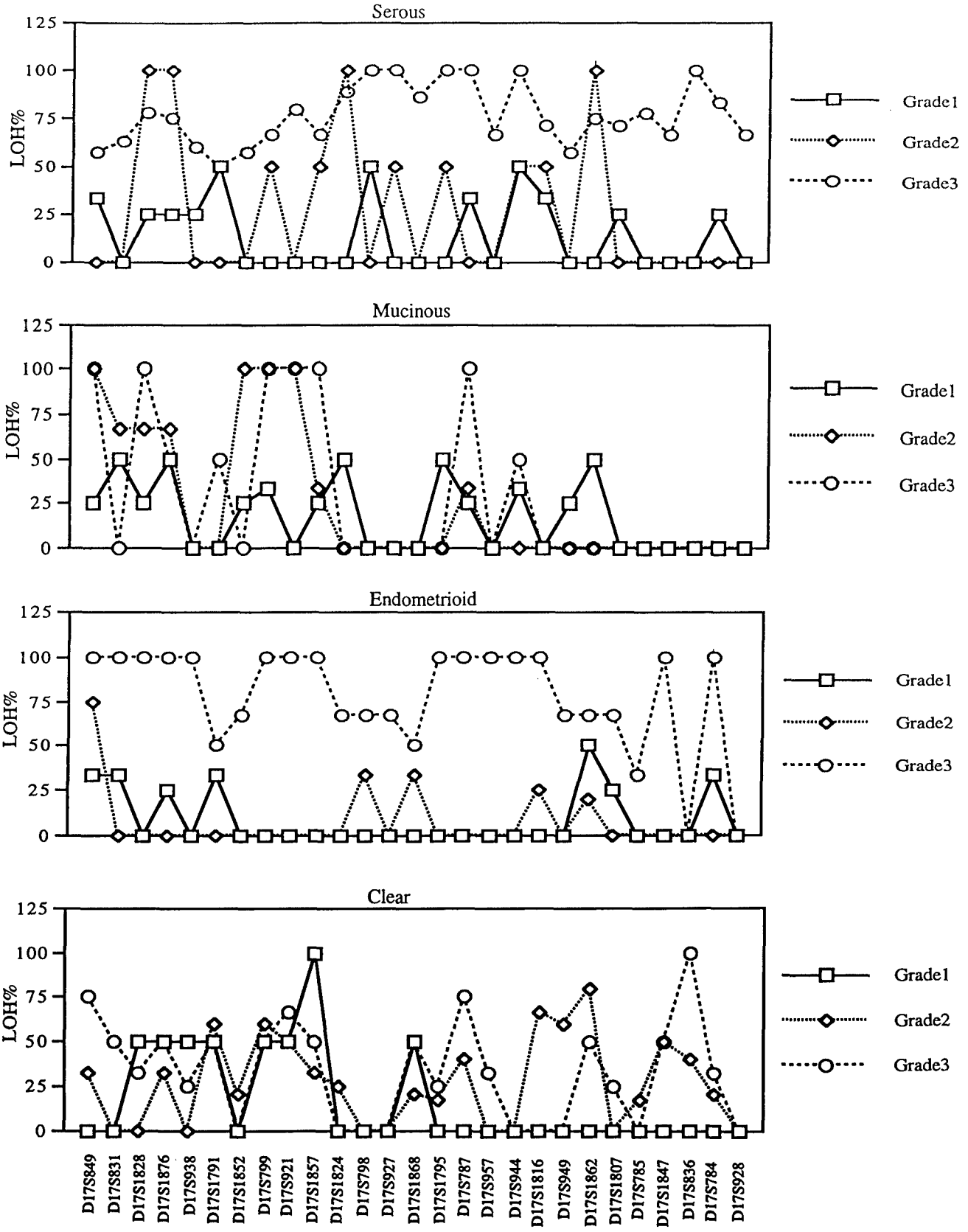
Serous
Mucinous
Endometrioid
Clear
LOH%
125
100
75
50
25
0
Grade1
Grade2
Grade3
D17S849
D17S831
D17S1828
D17S1876
D17S938
D17S1791
D17S1852
D17S799
D17S921
D17S1857
D17S1824
D17S798
D17S927
D17S1868
D17S1795
D17S787
D17S957
D17S944
D17S1816
D17S949
D17S1862
D17S1807
D17S785
D17S1847
D17S836
D17S784
D17S928

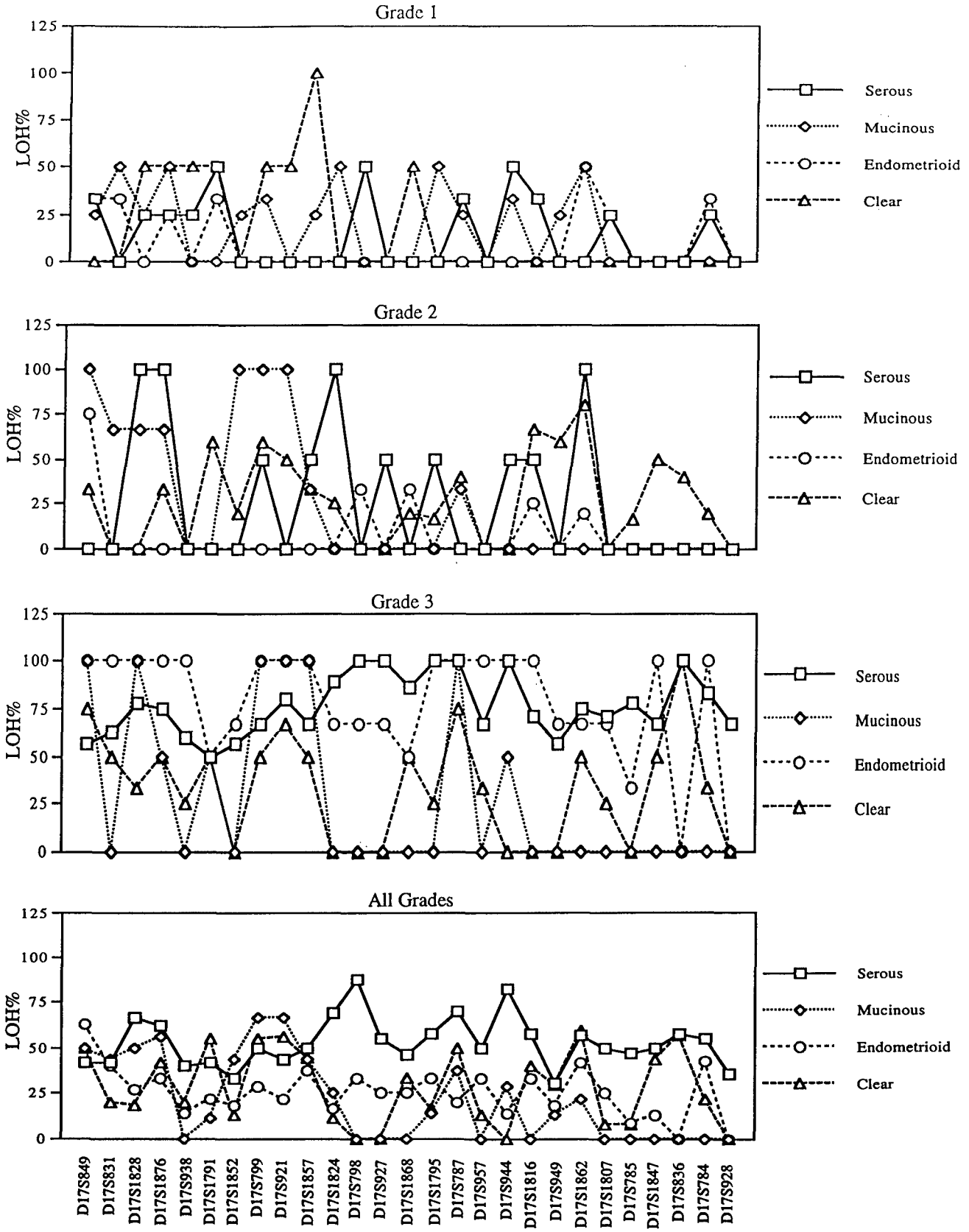
Grade 1
LOH%
125
100
75
50
25
0
Serous
Mucinous
Endometrioid
Clear
Grade 2
LOH%
125
100
75
50
25
0
Serous
Mucinous
Endometrioid
Clear
Grade 3
LOH%
125
100
75
50
25
0
Serous
Mucinous
Endometrioid
Clear
All Grades
LOH%
125
100
75
50
25
0
Serous
Mucinous
Endometrioid
Clear
D17S849
D17S831
D17S1828
D17S1876
D17S938
D17S1791
D17S1852
D17S799
D17S921
D17S1857
D17S1824
D17S798
D17S927
D17S1868
D17S1795
D17S787
D17S957
D17S944
D17S1816
D17S949
D17S1862
D17S1807
D17S785
D17S1847
D17S836
D17S784
D17S928

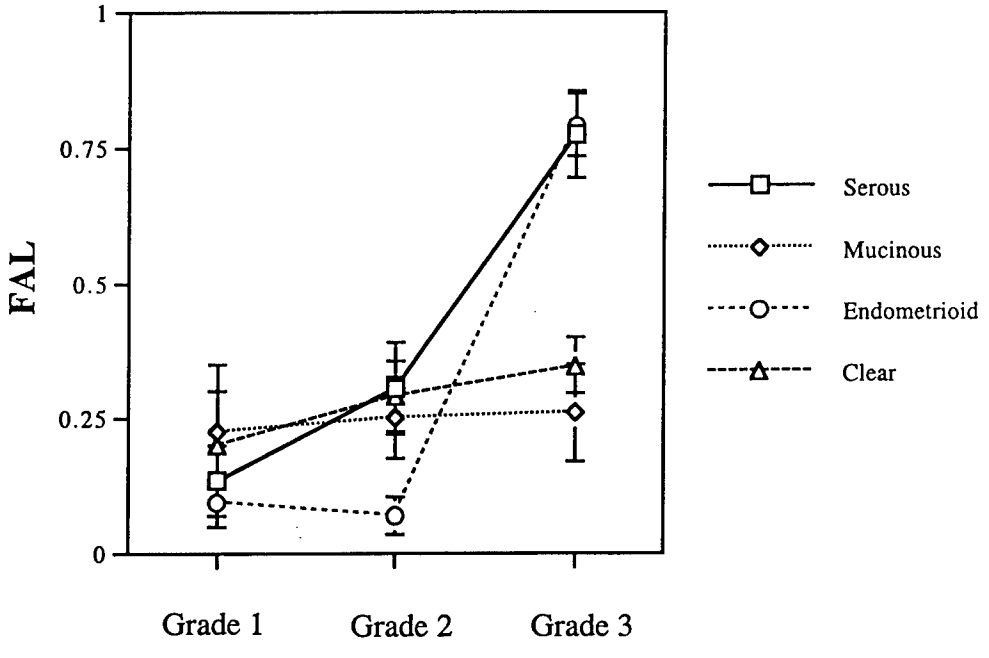
1
0.75
0.5
0.25
0
FAL
Grade 1
Grade 2
Grade 3
Serous
Mucinous
Endometrioid
Clear

ARTICLES

Prostasin, a Potential Serum Marker for Ovarian Cancer: Identification Through Microarray Technology

Samuel C. Mok, Julie Chao, Steven Skates, Kwong-kwok Wong, Gary K. Yiu, Michael G. Muto, Ross S. Berkowitz, Daniel W. Cramer

Background: Screening biomarkers for ovarian cancer are needed because of its late stage at diagnosis and poor survival. We used microarray technology to identify overexpressed genes for secretory proteins as potential serum biomarkers and selected prostasin, a serine protease normally secreted by the prostate gland, for further study. *Methods:* RNA was isolated and pooled from three ovarian cancer cell lines and from three normal human ovarian surface epithelial (HOSE) cell lines. Complementary DNA generated from these pools was hybridized to a microarray slide, and genes overexpressed in the cancer cells were identified. Real-time quantitative polymerase chain reaction was used to examine prostasin gene expression in ovarian cancer and HOSE cell lines. Anti-prostasin antibodies were used to examine prostasin expression and to measure serum prostasin by an enzyme-linked immunosorbent assay in 64 case patients with ovarian cancer and in 137 control subjects. Previously determined levels of CA 125, an ovarian cancer marker, were available from about 70% of all subjects. All statistical tests were two-sided. *Results:* Prostasin was detected by immunostaining more strongly in cancerous ovarian epithelial cells and stroma than in normal ovarian tissue. The mean level of serum prostasin was 13.7 μg/mL (95% confidence interval [CI] = 10.5 to 16.9 μg/mL) in 64 case patients with ovarian cancer and 7.5 μg/mL (95% CI = 6.6 to 8.3 μg/mL) in 137 control subjects ($P<.001$, after adjustment for the subject's age, year of collection, and specimen quality). In 14 of 16 case patients with both preoperative and postoperative serum samples, postoperative prostasin levels were statistically significantly lower than preoperative levels ($P = .004$). In 37 case patients with nonmucinous ovarian cancer and in 100 control subjects for whom levels of CA 125 and prostasin were available, the combination of markers gave a sensitivity of 92% (95% CI = 78.1% to 98.3%) and a specificity of 94% (95% CI = 87.4% to 97.7%) for detecting ovarian cancer. *Conclusions:* Prostasin is overexpressed in epithelial ovarian cancer and should be investigated further as a screening or tumor marker, alone and in combination with CA 125. [J Natl Cancer Inst 2001;93:000–00]

Ovarian cancer ranks closely behind pancreatic cancer as the fifth leading cause of death from cancer in U.S. women and is the most lethal of the gynecologic cancers *(1)*. The majority of women with ovarian cancer are diagnosed when they have distant disease, and the proportion surviving after 5 years is around 28% *(2)*. Alternatively, for the minority of women diagnosed with the disease confined to the ovaries, the proportion surviving after 5 years is about 90% (depending on the tumor grade). Thus, ovarian cancer is an obvious target for better approaches to early detection, including the identification of appropriate molecular markers.

Microarray technology permits the simultaneous comparison of the expression of thousands of genes in samples to allow identification of those that are differentially expressed. The technique has been applied to the molecular classification of tumors *(3–5)* and may also be able to identify overexpressed complementary DNA (cDNA) corresponding to secretory proteins that might serve as serum markers for cancer. In this article, we describe the application of microarray technology to identify novel molecular markers for ovarian cancer and explore the potential clinical value of one of the candidate markers (called prostasin) thus identified.

Materials and Methods

Biologic Specimens

All patient-derived biologic specimens were collected and archived under protocols approved by the Human Subjects Committee of the Brigham and Women's Hospital, Boston, MA, or were approved for study under guidelines covering discarded human materials. Ovarian tissue and cells were freshly collected from women undergoing surgery at the Brigham and Women's Hospital for a diagnosis of primary ovarian cancer or from control subjects having hysterectomy and oophorectomy for benign disease. Cultures of normal human ovarian surface epithelial (HOSE) cells were established by scraping the surface of the ovary and growing recovered cells in a mixture of medium 199 and MCDB105 medium supplemented with 10% fetal calf serum (Sigma Chemical Co., St. Louis, MO) as described previously *(6)*. The following seven normal HOSE cells were used: HOSE17, HOSE636, HOSE642, HOSE697, HOSE713, HOSE726, and HOSE730. Ovarian cancer cell lines were established by recovery from ascites fluid or explanted from solid tumors as described previously *(6)*. The following 10 ovarian cancer cell lines were used: OVCA3, OVCA420, OVCA429, OVCA432, OVCA433, OVCA633, CAOV3, DOV13, ALST, and SKOV3. All of the cell cultures and cell lines were established in the Laboratory of Gynecologic Oncology, Brigham and Women's Hospital, with the exception

Affiliations of authors: S. C. Mok, G. K. Yiu, Department of Obstetrics, Gynecology, and Reproductive Biology, Brigham and Women's Hospital, Harvard Medical School, Boston, MA; J. Chao, Department of Biochemistry and Molecular Biology, Medical University of South Carolina, Charleston; S. Skates, Gillette Center for Women's Cancer, Dana-Farber Cancer Institute, and Biostatistics Center, Massachusetts General Hospital, Boston; K. Wong, Department of Pediatrics, Texas Children's Hospital, Baylor College of Medicine, Houston; M. G. Muto, R. S. Berkowitz, D. W. Cramer, Department of Obstetrics, Gynecology, and Reproductive Biology, Brigham and Women's Hospital, Harvard Medical School, and Gillette Center for Women's Cancer, Dana-Farber Cancer Institute.

Correspondence to: Samuel C. Mok, Ph.D., Laboratory of Gynecologic Oncology, Brigham and Women's Hospital, 221 Longwood Ave., BLI 449, Boston, MA 02115 (e-mail: scmok@rics.bwh.harvard.edu).

See "Notes" following "References."

of SKOV3, which was purchased from the American Type Culture Collection, Manassas, VA. RNA was extracted from individual or pooled cell lines by using a micro RNA extraction kit as described by the manufacturer (Qiagen, Valencia, CA) and quantified by fluorometry (Genital Bio-Products, Inc., Calabasas, VA).

Serum specimens from women with ovarian cancer, other gynecologic cancers, and benign gynecologic disorders requiring hysterectomy and from normal diseased normal women were obtained from discarded specimens and from discarded specimens that were archived during the period from 1983 through 1988 or from specimens collected under more recent protocols since 1996. The archived samples were collected from several studies, from 1983 through 1988, assessing the performance of CA 125 in a variety of diagnostic circumstances, including gynecologically normal subjects as well as subjects having exploratory surgery for pelvic masses that proved to be ovarian, cervical, or endometrial cancer or a benign disease such as fibroid tumors *(7–9)*. These archived specimens were stored at −70 °C. However, during relocation of the Laboratory of Gynecologic Oncology, thawing was known to have occurred once for some of the archived specimens. Archived specimens that had been obtained preoperatively from the case patients and from the surgical control subjects were identified and recovered. The recently collected specimens are those being obtained with written informed consent as part of ongoing studies of ovarian cancer sponsored by the Obstetrics/Gynecology Epidemiology Unit and the Laboratory of Gynecologic Oncology, Brigham and Women's Hospital. These specimens were obtained within the past 5 years and were stored at −70 °C without any incident of thawing. In both specimen banks, serum from case patients with ovarian cancer and serum from control patients were collected concurrently.

Microarray Probe and Hybridization

The MICROMAX™ human cDNA microarray system I (NEN Life Science Products, Inc., Boston, MA), which contains 2400 known human cDNA on a slide 1 inch × 3 inches, was used in this study. Biotin-labeled cDNA was generated from 3 μg of total RNA that was pooled from HOSE17, HOSE636, and HOSE642 cells. Dinitrophenyl-labeled cDNA was generated from 3 μg of total RNA that was pooled from ovarian cancer cell lines OVCA420, OVCA433, and SKOV3. Before the cDNA reaction, equal amounts (5 ng) of *Arabidopsis* control RNA were added to each batch of the RNA samples for the normalization of hybridization signals. The biotin-labeled cDNA and the dinitrophenyl-labeled cDNA were mixed, dried, and resuspended in 20 μL of hybridization buffer (5× standard saline citrate [SSC], 0.1% sodium dodecyl sulfate [SDS], and salmon sperm DNA at 0.1 mg/mL [1× SSC = 0.15 *M* NaCl–0.15 *M* sodium citrate, pH 7]). This mixture was added to the cDNA microarray and was covered with a coverslip. Hybridization was carried out overnight at 65 °C inside a hybridization cassette (Telechem, Inc., Sunnyvale, CA).

After hybridization, the microarray was washed with 30 mL of 0.5× SSC–0.01% SDS, with 30 mL of 0.06× SSC–0.01% SDS, and then with 30 mL of 0.06× SSC alone. The hybridization signal from biotin-labeled cDNA was amplified with streptavidin–horseradish peroxidase and a fluorescent dye, Cy5™-tyramide (NEN Life Science Products, Inc.), and the hybridization signal from the dinitrophenyl-labeled cDNA was amplified with anti-dinitrophenyl–horseradish peroxidase and another fluorescent dye, Cy3™-tyramide (NEN Life Science Products, Inc.). After signal amplification and a posthybridization wash in TNT buffer (i.e., 0.1 *M* Tris–HCl [pH 7.5]–0.15 *M* NaCl–0.15% Tween 20), the microarray was air-dried, and signal amplification was detected with a laser scanner.

Laser detection of the Cy3 signal (derived from ovarian cancer cells) and the Cy5 signal (derived from HOSE cells) on the microarray was acquired with a confocal laser reader, ScanArray3000 (GSI Lumonics, Watertown, MA). Separate scans were taken for each fluor at a pixel size of 10 μm. cDNA derived from the added *Arabidopsis* RNA hybridized to 12 specific spots on the microarray, which were composed of DNA sequences obtained from four different *Arabidopsis*, expressed sequence tags in triplicate (NEN Life Science Products, Inc.). Cy3 and Cy5 signals from these 12 spots should theoretically be equal and were used to normalize the different efficiencies in labeling and detection with the two fluors. The fluorescence signal intensity and the ratio of the signals from Cy3 and Cy5 for each of the 2400 cDNAs were analyzed by the software Imagene 3.0 (Biodiscovery Inc., Los Angeles, CA).

Real-Time Quantitative Reverse Transcription–Polymerase Chain Reaction

Real-time reverse transcription–polymerase chain reaction (RT–PCR) was performed in duplicate by using primer sets specific for the overexpressed gene encoding the secretory protein called prostasin (forward primer = 5′-ACTTGAGGCACTCCTTCCTTCAG-3′; reverse primer = 5′-CTGATGGTC-CCAAAAAGCACAC-3′) and a housekeeping gene, GAPDH, in an ABI PRISM 5700 Sequence Detector (PE Applied Biosystems, Foster City, CA). RNA was first extracted from normal ovarian epithelial cell cultures (HOSE697, HOSE715, HOSE726, and HOSE730) and from 10 ovarian carcinoma cell lines (OVCA3, OVCA420, OVCA429, OVCA432, OVCA433, OVCA633, CAOV3, DOV13, SKOV3, and AI-ST). cDNA was generated from 1 μg of total RNA by using the TaqMan RT reagents containing 1× TaqMan reverse transcriptase buffer, 5.5 m*M* $MgCl_2$, all four deoxyribonucleoside triphosphates (each at 500 μ*M*), 2.5 μ*M* random hexamer, MultiScribe reverse transcriptase (PE Applied Biosystems) at 1.25 U/μL, and RNasin (Promega Corp., Madison, WI) at 0.4 U/μL in 100 μL. The reaction was incubated at 25 °C for 10 minutes, at 48 °C for 30 minutes, and finally at 95 °C for 5 minutes. A total of 1 μg of cDNA was used in a 20-μL PCR mixture containing 1× SYBR® PCR buffer, 3 m*M* $MgCl_2$, all four deoxyribonucleoside triphosphates (each at 0.8 m*M*), and AmpliTaq Gold (all from PE Applied Biosystems). The cDNAs were then amplified by denaturation for 10 minutes at 95 °C, followed by 40 PCR cycles of denaturation at 95 °C for 15 seconds and annealing–extension at 60 °C for 1 minute. The changes in fluorescence of the SYBR Green I dye in every cycle were monitored by ABI5700 system software, and the threshold cycle (C_T), which represents the PCR cycle at which an increase in reporter fluorescence above a baseline signal can first be detected for each reaction, was calculated as described by Heid et al. *(10)*. The relative amount of PCR products generated from each primer set was determined on the basis of the C_T value. GAPDH was used to normalize the quantity of RNA used. Its C_T value was then subtracted from that of each target gene to obtain a ΔC_T value. The difference ($\Delta\Delta C_T$) between the ΔC_T values of the samples for each gene target and the ΔC_T value of a calibrator (sample 697), which served as a physiologic reference, was determined. The relative quantitative value was expressed as $2^{-\Delta\Delta C_T}$. For confirmation of the specificity of the PCR, PCR products were subjected to electrophoresis on a 1.2% agarose gel. A single PCR product with the expected size should be observed in samples that express the gene of interest.

Immunohistochemical Localization of Prostasin

Immunostaining with an anti-prostasin antibody was performed on sections prepared from two normal ovaries, from two serous borderline ovarian tumors, and from two grade 1, two grade 2, and two grade 3 serous ovarian cystadenocarcinomas. This rabbit polyclonal antibody (provided by Dr. Julie Chao's laboratory) also used in the serum assay was prepared from prostasin purified from human seminal fluid as described previously *(11)*. Tissues were fixed in 4% paraformaldehyde and embedded in paraffin. Sections (5 μm) were cut, mounted on Superfrost/Plus microscopic slides (Fisher Scientific, Pittsburgh, PA), and incubated at 50 °C overnight. They were then transferred to Tris-buffered saline (TBS) and quenched in 0.2% H_2O_2 for 20 minutes. After quenching, the sections were washed in TBS for 20 minutes, incubated with normal horse serum for 20 minutes, and then incubated with anti-prostasin polyclonal antibody (diluted 1 : 400) at room temperature for 1 hour. The slides were then washed in TBS for 10 minutes, incubated with diluted biotinylated secondary horse anti-rabbit antibody solution for 30 minutes, washed again in TBS for 10 minutes, incubated with avidin–biotin complex reagent (Vector Laboratories, Inc., Burlingame, CA) for 30 minutes, and washed in TBS for 10 minutes. Stain development was performed for 5 minutes by use of the diaminobenzidine kit (Vector Laboratories, Inc.). Finally, the sections were washed in water for 10 minutes. They were then counterstained with hematoxylin, dehydrated with an ascending series of alcohol solutions, cleared in xylene, and mounted in Permount (Fisher Scientific). The specificity of the staining was confirmed by using preimmunization rabbit serum and by preabsorbing the antibody with the purified peptide (60 mg/mL; Genosys, Woodlands, TX) or prostasin for 2 hours at 37 °C before applying the adsorbed antiserum to the sections.

Measurement of Prostasin and CA 125 in Sera

Sera were available from a total of 201 subjects (64 case patients with ovarian cancer and 137 control subjects, including 24 with other gynecologic cancers, 42 with benign gynecologic diseases, and 71 with no known gynecologic diseases). In all of the case patients and in the 68 control subjects who had surgery, preoperative specimens were available. Serum levels of immunoreactive human prostasin were determined by enzyme-linked immunosorbent assay (ELISA) prepared with the previously described antibody to human prostasin *(11)*. Microtiter plates (96-well) were coated with anti-prostasin immunoglobulin G

(IgG) (1 μg/mL, 100 μL per well) overnight at 4 °C. Purified prostasin standards (0.16–10 ng) or samples were added to individual wells in a total volume of 100 μL of phosphate-buffered saline containing 0.05% Tween 20 and 0.5% gelatin (dilution buffer) and incubated at 37 °C for 90 minutes. Biotin labeled anti-human prostasin IgG was added in each well at a concentration of 1 μg/mL in a total of 100 μL and incubated at 37 °C for 60 minutes. Peroxidase–avidin at a concentration of 1 μL/mL in a total volume of 100 μL was added and incubated at 37 °C for 30 minutes. The color reaction was performed by adding to each well 100 μL of freshly prepared substrate solution [0.03% 2,2'-azino-bis(3-ethylbenzthiazoline-6-sulfonic acid) and 0.03% H_2O_2 in 0.1 M sodium citrate (pH 4.3)] and incubating the mixture at room temperature for 30 minutes. The plates were read at 405 nm with a plate reader (Titertek Instruments Inc., Huntsville, AL).

For 37 case patients with nonmucinous ovarian cancers and for 100 control subjects (about 70% of all subjects), a CA 125 level had been determined previously (from the same specimens) and was available in our database for a comparison standard. These measurements had been performed with the original CA 125 radioimmunoassay from Centocor (Malvern, PA), and the assays were not repeated for this study.

Statistical Analysis

Univariate comparisons for quantitative variables between normal and cancer cell lines or between case and control sera were made by using Student's *t* test. For the analysis of serum levels, adjustment for potential confounding variables, such as the subject's age, year of collection, and whether the specimen had undergone freezing and thawing, was carried out by using general linear modeling. Logistic regression analysis was used to determine the statistical significance of both prostasin and CA 125 as a predictor of case status. Paired Student's *t* test was used to compare the change in postoperative prostasin levels from preoperative levels. Pearson correlation coefficients were calculated between CA 125 and prostasin. Because the distributions of prostasin and CA 125 were skewed positively, log-transformed values were used in the statistical tests. All of the analyses were performed with the Statistical Analyses System (SAS Institute, Cary, NC) or Splus (Insightful Corporation, Seattle, WA). Analyses with a *P* value of .05 or less were considered to be statistically significant. All statistical tests were two-sided, and all confidence intervals (CIs) are 95%.

Results

Fig. 1 shows a selected portion of the microarray analysis of pooled RNA isolated from three normal HOSE cell lines (labeled with the fluorescent dye Cy5) and from three ovarian cancer cell lines (labeled with the fluorescent dye Cy3). Thirty genes with Cy3/Cy5 signal ratios ranging from 5 to 444 were identified, suggesting that these genes were overexpressed in ovarian cancer cells compared with normal HOSE cells, and have been described previously (*12*). Among them, both prostasin and osteopontin encode secretory proteins, which may be potential serum markers. Another gene, creatine kinase B, has been shown to produce a serum marker associated with renal carcinoma and lung cancer (*13,14*). We selected the prostasin gene, with a Cy3/Cy5 ratio of 170, for further study because this gene had an available antibody assay.

To evaluate the differential expression of prostasin in individual normal and malignant ovarian epithelial cell lines from normal and neoplastic ovaries, we performed quantitative PCR analysis on four normal HOSE cultures and on 10 ovarian cancer cell lines (Table 1). The $2^{-\Delta\Delta C_T}$ value, which represents relative prostasin gene expression, ranged from 120.3-fold to 410.1-fold greater for seven of the 10 ovarian cancer cell lines compared with that for HOSE697 cells, but it was only marginally greater for the other three ovarian cancer cell lines (ALST, DOV13, and SKOV3). Overall, there was a highly statistically significant difference between the mean $2^{-\Delta\Delta C_T}$ values for the four normal cell lines compared with those for the 10 ovarian cancer lines ($P<.001$).

For further validation of the expression of prostasin in actual tumor tissue, sections from two normal ovaries, from two serous borderline ovarian tumors, and from two grade 1, two grade 2, and two grade 3 serous ovarian cystadenocarcinomas were immunostained with an anti-prostasin polyclonal antibody. Stronger cytoplasmic staining was detected in cancer cells than in normal HOSE cells, suggesting that prostasin is overexpressed by the ovarian cancer cells (Fig. 2). Prostasin was, however, also detected in normal ovarian tissue by immunostaining.

We next examined prostasin levels detected by ELISA in sera from case patients and control subjects (Table 2). The mean (and 95% CI) prostasin level for all of the case patients was 13.7 μg/mL (95% CI = 10.5 to 16.9 μg/mL) compared with 7.5 μg/mL (95% CI = 6.6 to 8.3 μg/mL) in all of the control subjects. Based on log-transformed values, this difference was statistically significant ($P<.001$) and persisted after adjustment for the subject's age, year of collection, and quality of specimen (possible freeze–thaw damage). Among case patients, there was considerable variability by stage; however, notably, women with stage II disease had the highest level of prostasin, suggesting that

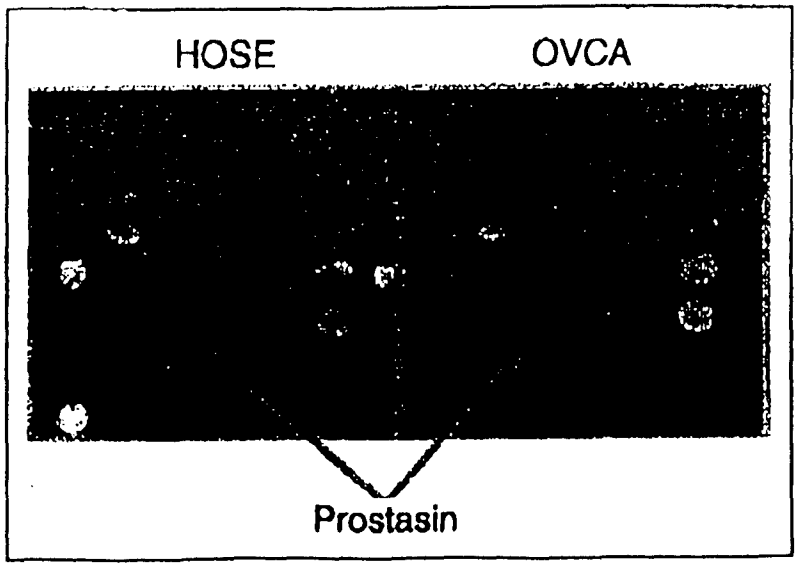

Fig. 1. Microarray analysis using pooled RNA isolated form three normal human ovarian surface epithelial (HOSE) cultures and three ovarian cancer (OVCA) cell lines. Arrows indicate spots on two microarrays that correspond to prostasin. A total of 30 genes have a Cy3/Cy5 signal ratio of ≥5. The GenBank accession numbers of these genes are as follows: M33011, J04765, L41351, L19783, U96759, M57730, L33930, D55672, U97188, L19871, J04991, D00762, U17989, U43148, AF010312, M80244, X99802, U05598, L47647, M55284, X15722, S54005, AB006965, M83653, X12597, M18112, U56816, X06233, D85181, and M31627.

Table 1. Relative quantitation* of prostasin in normal and malignant ovarian epithelial cells

Cell line†	C_T Prostasin	C_T GAPDH	ΔC_T	$\Delta\Delta C_T$	$2^{-\Delta\Delta C_T}$
HOSE697	30.97	17.09	13.88	0	1
HOSE713	31.57	18.32	13.25	−0.63	1.5
HOSE726	30.49	17.26	13.23	−0.65	1.6
HOSE730	30.28	18	12.28	−1.6	3
ALST	28.26	16.99	11.27	−2.61	6.1
CAOV3	23.2	16.24	6.96	−6.92	121.1
DOV13	29.78	17.64	12.14	−1.74	3.3
OVCA3	24.07	17.91	6.16	−7.72	210.8
OVCA420	25.65	18.68	6.97	−6.91	120.3
OVCA429	24.21	17.57	6.64	−7.24	151.2
OVCA432	23.51	18.31	5.2	−8.68	410.1
OVCA433	25.2	19.91	5.29	−8.59	385.3
OVCA633	24.27	18.6	5.67	−8.21	296.1
SKOV3	30.67	19.33	11.34	−2.54	5.8

*$\Delta\Delta C_T$ = ΔC_T relative to HOSE697 (ΔC_T for target gene in HOSE697 cells − ΔC_T for target gene in test cell line). C_T = threshold cycle; ΔC_T = C_T for target gene − C_T for the GAPDH gene; $2^{-\Delta\Delta C_T}$ = measure of the overexpression of prostasin relative to HOSE697 cells.

†HOSE = human ovarian surface epithelial.

prostasin may be of use for early-stage detection. It also appeared that women with mucinous-type ovarian tumors had lower levels of prostasin than women with ovarian tumors of other epithelial types. Among control subjects, there was a statistically significant tendency for the archived specimens to have lower prostasin levels than the current specimens ($P<.001$), but there was no evidence for an effect of age or diagnostic category (i.e., normal tissue, benign gynecologic disease, or other gynecologic cancer). In addition, 60.5% of the archived case specimens and 66.2% of the control specimens had been in the freezer in which freezing and thawing had occurred. There was no evidence of a tendency for these samples to have lower prostasin levels (Table 2).

Fig. 3 shows a box plot of serum prostasin level for case patients with nonmucinous ovarian cancers and for the various control subgroups. Concerning the two control subjects with benign gynecologic disease, who were outliers in Fig. 3, one had uterine fibroid tumors and the other had an extensive family history of ovarian cancer and had been referred to a gynecologic oncologist because pelvic washings at laparoscopy contained "suspicious" mesothelial cells. She was found to have extensive endosalpingiosis at prophylactic oophorectomy.

In 16 women with nonmucinous epithelial ovarian cancers, preoperative and postoperative specimens were available for comparison (Fig. 4). For 14 of these women, a decreased prostasin level was observed after surgery, and, in the entire group of 16, postoperative P levels were statistically significantly lower compared with preoperative levels with the use of a paired t test on the log-transformed values (P = .004).

Fig. 5 displays a bivariate plot of prostasin versus CA 125 for the 37 case patients with nonmucinous ovarian cancers and for the 100 control subjects who had both measurements available. For the case patients with nonmucinous cancers, the correlation was .217 (P = .20). For the control subjects, the correlation was −.004 (P = .97). This lack of correlation suggests that the two may provide complementary information. Indeed, as shown by the curved line in Fig. 5 illustrating the separation that can be obtained between case patients and control subjects with both variables, the combined markers achieved a sensitivity of 34/37 = 92% (95% CI = 78.1% to 98.3%) and a specificity of 94/100 = 94% (95% CI = 87.4% to 97.7%). In contrast, the sensitivity of CA 125 alone at the same specificity was 24/37 = 64.9% (95% CI = 47.5% to 79.8%), and the sensitivity of prostasin alone at the same specificity was 19/37 = 51.4% (95% CI = 34.4% to 68.1%).

Discussion

Using microarray technology on RNA pooled from ovarian cancer and the HOSE cell line, we have identified an overexpressed gene that produces a secretory product, prostasin. We have demonstrated prostasin's potential as a biomarker through real-time PCR in cancer and normal epithelial cell lines and by differential staining in cancer tissue compared with normal tissue. Finally, we demonstrated higher levels of serum prostasin in case patients with ovarian cancer than in control subjects and

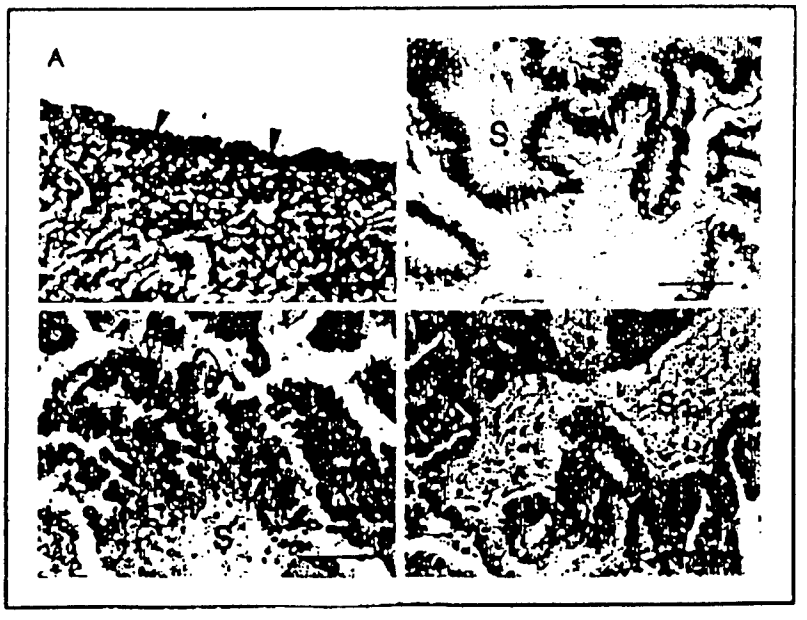

Fig. 2. Immunolocalization of prostasin in normal and malignant ovarian tissues. Normal ovarian surface epithelial cells (arrowheads) (A) and a section of serous borderline ovarian tumor (B) showed low levels of prostasin expression. Increased levels of prostasin expression were observed in a grade 3 tumor (C). A positive signal was not detected in the case sample shown in panel C when preimmune rabbit serum was used (D). S = stroma. Scale bar = 50 μm.

Table 2. Preoperative prostasin levels by selected characteristics of case patients with ovarian cancer and control subjects without ovarian cancer*

	Prostasin level, μg/mL							
	Case patients				Control subjects			
Characteristic	No.	Mean	95% CI	Range	No.	Mean	95% CI	Range
Age, y								
<55	27	9.8	7.2 to 12.5	2.8–30.3	85	7.4	6.1 to 8.7	2.5–41.7
≥55	37	16.5	11.3 to 21.6	1.9–74.9	52	7.6	6.8 to 8.3	2.7–14.2
Specimens†								
Archived 1983–1986	28	13.2	6.8 to 19.4	1.9–74.9	44	5.4	4.6 to 6.2	2.5–13.6
Archived 1987–1988	10	8.1	5.6 to 10.5	3.1–12.8	42	7.4	6.4 to 8.3	2.5–17.5
Current	26	16.4	12.2 to 20.5	5.7–43.9	51	9.3	7.4 to 11.2	3.6–41.7
Histology								
Serous borderline	7	7.6	4.1 to 11.1	3.0–12.8				
Serous invasive	34	16.2	11.7 to 20.6	1.9–47.6				
Mucinous	7	7.1	5.2 to 9.0	2.8–8.7				
Other	16	13.9	5.0 to 22.8	3.7–74.9				
Stage‡								
I	19	8.5	5.8 to 11.1	2.8–25.4				
II	10	20.1	3.4 to 36.8	3.1–74.9				
III	31	15.3	11.3 to 19.5	1.9–43.9				
IV	4	8.8	3.6 to 14.0	5.7–13.1				
Diagnostic category								
Normal GYN					71	7.1	6.4 to 7.9	2.5–17.5
Benign GYN					42	8.3	5.9 to 10.7	2.5–41.7
Other GYN cancers					24	7.0	5.9 to 8.2	3.1–13.6
All subjects	64	13.7	10.5 to 16.9	1.9–74.9	137	7.5	6.6 to 8.3	2.5–41.7

*CI = confidence interval; GYN = gynecologic.

†Of the archived specimens, 23 (60.5%) of 38 case specimens were subjected to freezing and thawing compared with 57 (66.3%) of 86 control specimens. The mean value for case specimens with a freeze–thaw episode was 14.4 μg/mL compared with 7.9 μg/mL without. The mean value for control specimens with a freeze–thaw episode was 6.5 μg/mL compared with 6.3 μg/mL without.

‡Stage I disease is confined to the ovaries; stage II is confined to the pelvis; stage III has spread to the bowel, omentum, or abdominal peritoneum; and stage IV involves distant metastases including liver parenchyma.

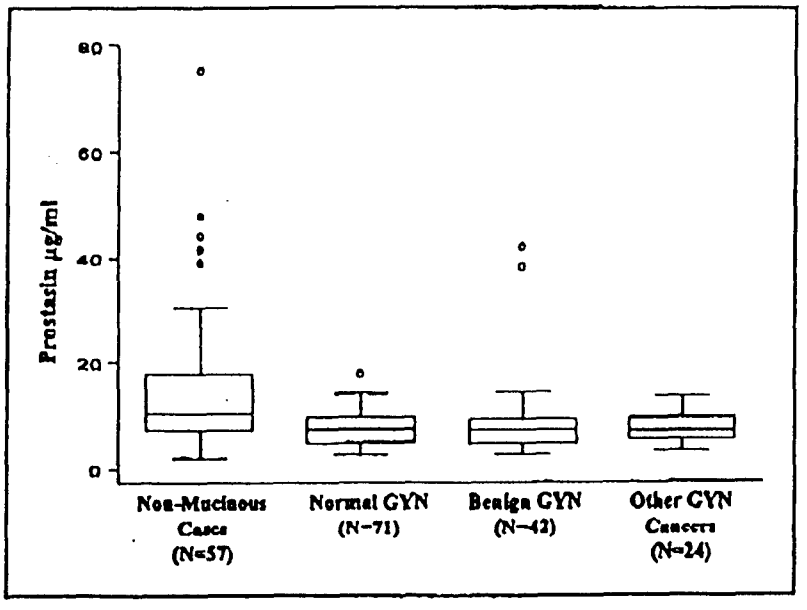

Fig. 3. Box plots of log-transformed prostasin levels in case patients with nonmucinous ovarian cancer and control subject subgroups. The box is bounded above and below by the 25% and 75% percentiles, the median is the line in the box, and the upper and lower error bars indicate about 99% of values. GYN = gynecologic cases.

declining levels of prostasin after surgery for ovarian cancer. Prostasin was isolated originally from human seminal fluid and is present at the highest level in the prostate gland *(10)*. Immunohistochemical studies *(15)* have demonstrated that prostasin is localized in the epithelial cells and ducts of the prostate gland, and it is postulated that prostasin is synthesized in prostatic epithelial cells, secreted into the ducts, and finally excreted into the seminal fluid. The high levels of prostasin found in the prostate gland and in seminal fluid suggest that it may perform important physiologic functions during fertilization, such as liquefaction of semen or activation of other proteinases such as acrosin. Prostasin is also expressed at much lower levels in a variety of human tissues, including kidney, liver, pancreas, salivary gland, lung, bronchus, and colon, but its functions in these

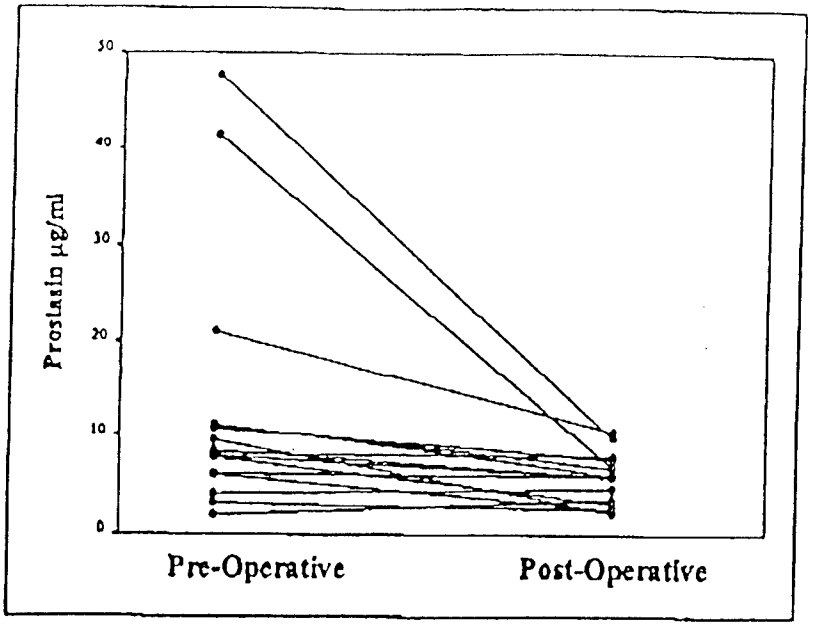

Fig. 4. Comparison of preoperative and postoperative prostasin levels in 16 case patients with ovarian cancer.

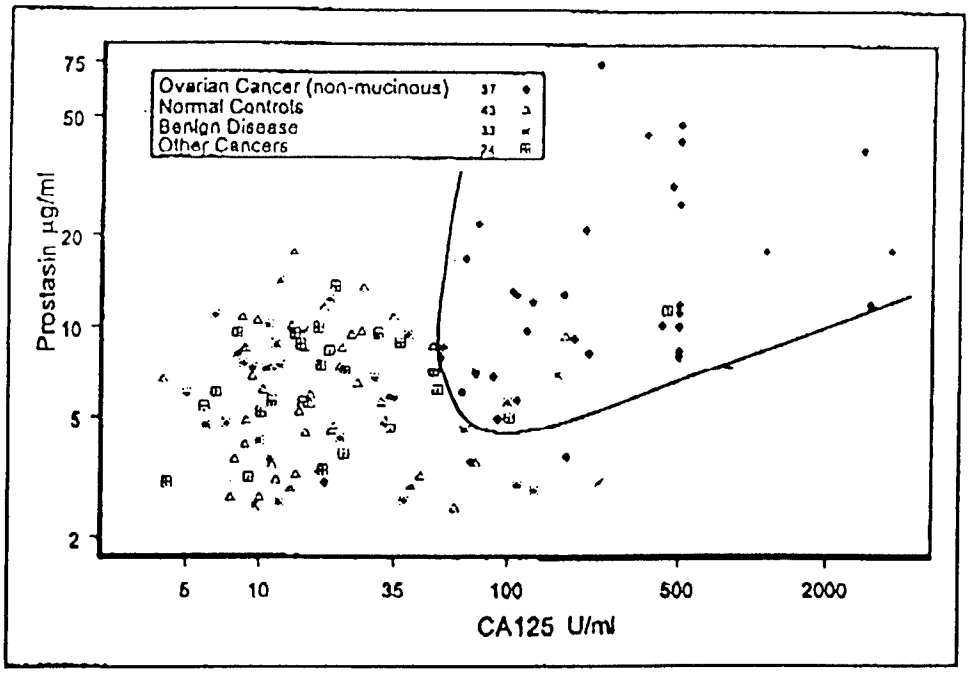

Fig. 5. Correlation between prostasin and CA 125 (on logarithmic scales) in case patients with nonmucinous ovarian tumors and in control subjects. Curve illustrates the separation that can be achieved between case patients and control subjects by a logistic model using both CA 125 and prostasin levels.

tissues have not yet been determined *(15)*. Curiously, prostasin has not been detected in the testis or ovary.

Chemically, prostasin is a trypsin-like serine proteinase with an apparent molecular mass of 40 kd *(11)*. The 20-amino acid sequence at the amino terminus of prostasin is 50%–55% identical to that of human α-tryptase, elastase 2A and 2B, chymotrypsin, acrosin, and the catalytic chains of hepsin, plasma kallikrein, and coagulation factor XI *(11)*. Like the enzymatic activity of other serine proteinases, the enzymatic activity of prostasin is dependent on a catalytic triad of the amino acids histidine, aspartic acid, and serine *(15)*, which are present in motifs that are highly conserved among serine proteinases *(16)*. Similar to acrosin and testisin *(17,18)*, prostasin is likely to be a membrane-anchored protein because there is a putative transmembrane domain of 19 amino acids at the carboxyl terminus that is believed to anchor the protein to the plasma membrane of prostate epithelial cells, from which it is released by cleavage. In view of prostasin's homology with other serine proteases, it is not surprising that several serine proteases are elevated in patients with ovarian cancer; these proteases include certain kallikreins such as protease M/kallikrein 6 *(19)*, prostate-specific antigen *(20)*, hepsin *(21)*, and testisin *(18)*. Our current understanding of prostasin does not provide an explanation of why it or other serine proteinases might be overexpressed in ovarian cancer.

Although we believe that we have demonstrated prostasin's potential value as a biomarker for ovarian cancer, this study has several potential limitations. First, our sample size is relatively small and not ideal for demonstrating the value of prostasin as a screening marker. Although all blood samples were drawn preoperatively, all of the women with ovarian cancer had symptomatic disease and about 55% had stage III disease or greater.

In addition, a majority of the sera were obtained from an archived bank, and some of the specimens had undergone freezing and thawing. We observed no tendency for freezing and thawing to produce lower prostasin levels; however, there was evidence that specimens kept in the freezer longer may have had lower values for prostasin. For this reason, we adjusted for length of freezer storage in the multivariate model, and this adjustment did not negate the difference between case patients with ovarian cancer and control subjects. Our sample did not address prostasin's potential as a marker for tumor recurrence because sera preceding recurrences were not available. Finally, we can only partially address how prostasin might be complementary to other markers for ovarian cancer. It may be complementary to CA 125 as suggested by the low correlation between the two.

We believe that our study also demonstrates the potential value of microarray technology to identify tumor biomarkers that may have clinical usefulness. In this study, we used the MICROMAX cDNA microarray system that contained the 2400 genes with known function at the time of the development of this chip *(13)*. We selected this chip because it was the only chip available at the time that we began this research. Subsequently, microarrays with an even larger collection of genes or expression-sequencing tags have become available, such as the GeneChip™ U95 Set (Affymetrix Inc., Santa Clara, CA) and the GeneAlbum™ GEM™ 1–6 (IncyteGenomics, San Francisco, CA), which represent more than 50 000 genes or expression-sequencing tags. Besides choice of the microarray chip, an important technical issue is the source of the tumor and the normal cDNA for comparison. In this study, we pooled cDNA from several cancer cell lines and compared it with cDNA from normal HOSE cells. The principal advantage of using cell lines is that they provide an abundant source of RNA from the precise cell types involved in epithelial ovarian cancer. Their chief disadvantage is that they are a step removed from the actual cancer *in vivo* and would not detect genes that might be differentially expressed in the stroma of ovarian cancer specimens and that might be important.

Our study also provides a case illustration of the types of validation studies, which are necessary once a differentially expressed gene has been identified through microarray technology. Overexpression of a gene should be confirmed in individual cell lines or in tissues from individuals with cancer or from normal control subjects. Under ideal circumstances, an assay will be available to detect the gene product through either immunostaining of tissues or detection in sera. At each step, these validation studies must be consistent with differential expression associated with the cancer. Thus, although our preliminary study described 30 genes overexpressed in ovarian cancer cell lines when we used the MICROMAX cDNA microarray system *(13)*, we have focused on one of the candidate genes in this study, which we believe has satisfied these additional elements of validation.

In conclusion, we believe that our study demonstrates the potential value of the powerful new technology of cDNA microarray in identifying overexpressed genes in ovarian cancer, and we suggest that prostasin may be a biomarker with clinical potential. Thus, larger studies that can yield more precise estimates of the sensitivity and specificity of prostasin, either alone or in combination with CA 125, will be necessary.

REFERENCES

(1) American Cancer Society. Cancer facts and figures—1999. Atlanta (GA): American Cancer Society; 1999.

(2) Ries LA, Kosary CL, Hankey BF, Miller BA, Edwards BK. SEER cancer statistics review 1973–1995. Bethesda (MD): National Cancer Institute; 1998.

(3) Golub TR, Slonim DK, Tamayo P, Huard C, Gaasenbeek M, Mesirov JP, et al. Molecular classification of cancer: class discovery and class prediction by gene expression monitoring. Science 1999;286:531–7.

(4) Wang T, Hopkins D, Schmidt C, Silva S, Houghton R, Takita H, et al. Identification of genes differentially over-expressed in lung squamous cell carcinoma using combination of cDNA subtraction and microarray analysis. Oncogene 2000;19:1519–28.

(5) Sgroi DC, Teng S, Robinson G, LeVangie R, Hudson JR Jr, Elkahloun AG. *In vivo* gene expression profile analysis of human breast cancer progression. Cancer Res 1999;59:5656–61.

(6) Tsao SW, Mok SC, Fey EG, Fletcher JA, Wan TS, Chew EC, et al. Characterization of human ovarian surface epithelial cells immortalized by human papilloma viral oncogenes (HPV-E6E7 ORFs). Exp Cell Res 1995; 218:499–507.

(7) Bast RC Jr, Klug TL, St John E, Jenison E, Niloff JM, Lazarus H, et al. A radioimmunoassay using a monoclonal antibody to monitor the course of epithelial ovarian cancer. N Engl J Med 1983;309:883–7.

(8) Bast RC Jr, Klug TL, Schaetzl E, Lavin P, Niloff JM, Greber TF, et al. Monitoring human ovarian carcinoma with a combination of CA 125, CA 19-9, and carcinoembryonic antigen. Am J Obstet Gynecol 1984;149:553–9.

(9) Bast RC Jr, Siegal FP, Runowicz C, Klug TL, Zurawski VR Jr, Schonholz D, et al. Elevation of serum CA 125 prior to diagnosis of an epithelial ovarian carcinoma. Gynecol Oncol 1985;22:115–20.

(10) Heid CA, Stevens J, Livak KJ, Williams PM. Real time quantitative PCR. Genome Res 1996;6:986–94.

(11) Yu JX, Chao L, Chao J. Prostasin is a novel human serine proteinase from seminal fluid. Purification, tissue distribution, and localization in prostate gland. J Biol Chem 1994;269:18843–8.

(12) Wong KK, Cheng RS, Mok SC. Identification of differentially expressed genes from ovarian cancer cells by MICROMAX cDNA microarray system. Biotechniques 2001;30:670–5.

(13) Kurtz KJ, Nielsen RD. Serum creatine kinase BB isoenzyme as a diagnostic aid in occult small cell lung cancer. Cancer 1985;56:562–6.

(14) Tukushi M, Zhu Y, Hasegawa S, Kato K. Serum creatine kinase B subunit in patients with renal cell carcinoma. Urol Int 1992;48:144–8.

(15) Yu JX, Chao L, Chao J. Molecular cloning, tissue-specific expression, and cellular localization of human prostasin mRNA. J Biol Chem 1995;270:13483–9.

(16) Perona JJ, Craik CS. Structural basis of substrate specificity in the serine proteases. Protein Sci 1995;4:337–60.

(17) Baba T, Kashiwabara S, Watanabe K, Itoh H, Michikawa Y, Kimura K, et al. Activation and maturation mechanisms of boar acrosin zymogen based on the deduced primary structure. J Biol Chem 1989;264:11920–7.

(18) Shigemasa K, Underwood LJ, Beard J, Tanimoto H, Ohama K, Parmley TH, et al. Overexpression of testin, a serine protease expressed by testicular germ cells, in epithelial ovarian tumor cells. J Soc Gynecolog Investig 2000;7:358–62.

(19) Anisowicz A, Sotiropoulou G, Stenman G, Mok SC, Sager R. A novel protease homolog differentially expressed in breast and ovarian cancer. Mol Med 1996;2:624–36.

(20) Kucera E, Kainz C, Tempfer C, Zeillinger R, Koelbl H, Sliutz G. Prostate specific antigen (PSA) in breast and ovarian cancer. Anticancer Res 1997; 17:4735–7.

(21) Tanimoto H, Yan Y, Clarke J, Korourian S, Shigemasa K, Parmley TH, et al. Hepsin, a cell surface serine protease identified in hepatoma cells, is overexpressed in ovarian cancer. Cancer Res 1997;57:2884–7.

NOTES

Supported in part by Public Health Service grant U01CA86381 from the National Cancer Institute, National Institutes of Health, Department of Health and Human Services; by Army Ovarian Cancer Research Program grant DAMD17-99-1-9563 from the U.S. Department of Defense; by the Adler Foundation; by the Ovarian Cancer Research Fund, Inc.; by the Morse Family Fund; and by the Natalie Phil Fund.

Manuscript received December 26, 2000; revised July 23, 2001; accepted August 1, 2001.

[CANCER RESEARCH 61, 4169–4174, May 15, 2001]

Whole Genome Amplification and High-Throughput Allelotyping Identified Five Distinct Deletion Regions on Chromosomes 5 and 6 in Microdissected Early-Stage Ovarian Tumors[1]

Vivian W. Wang, Debra A. Bell, Ross S. Berkowitz, and Samuel C. Mok[2]

Laboratory of Gynecologic Oncology, Division of Gynecologic Oncology, and Department of Obstetrics, Gynecology and Reproductive Biology, Brigham and Women's Hospital, Dana Farber Harvard Cancer Center; Harvard Medical School, Boston, Massachusetts 02115 [V. W. W., S. C. M., R. S. B.], and Department of Pathology, Massachusetts General Hospital, Dana Farber Harvard Cancer Center; Harvard Medical School, Boston, Massachusetts 02114 [D. A. B.]

ABSTRACT

Investigation of genetic changes in tumors by loss of heterozygosity is a powerful technique for identifying chromosomal regions that may contain tumor suppressor genes. In this study, we determined allelic loss on chromosomes 5 and 6 in 29 primary early-stage epithelial ovarian carcinomas including 3 microscopically identified adenocarcinomas using a high-throughput PCR-based method combined with laser capture microdissection and whole genome amplification techniques. Twenty microsatellite markers spanning chromosomes 5 and 6 at an average distance of 20 cM were examined. High frequencies of loss on chromosome 5 were identified at loci *D5S428* (48%), *D5S424* (32%), and *D5S630* (32%). Our study also showed that chromosome 6 exhibited high frequencies of loss of heterozygosity at loci *D6S1574* (46%), *D6S287* (42%), *D6S441* (45%), *D6S264* (60%), and *D6S281* (35%). These results suggest that multiple tumor suppressor genes are located on five distinct regions on chromosomes 5 and 6, *i.e.*, 5p15.2, 5q13–21, 6p24–25, 6q21–23, and 6q25.1–27, and may be involved in the early development of ovarian carcinomas.

INTRODUCTION

Ovarian cancer is a common gynecological malignancy. Because ovarian cancer is often asymptomatic in its early stages, most patients have widespread disease at the time of diagnosis. Consequently, annual mortality is approximately 65% of the incidence rate (1). Furthermore, patients with early stages of the disease can usually be cured. In recent years, the genetic basis of human tumors has been increasingly elucidated. A growing number of studies have shown that the molecular events controlling tumorigenesis involve abnormal cell growth promoted by activation of proto-oncogenes and/or inactivation of tumor suppressor genes (TSGs)[3] (2, 3). Identification of novel TSGs has been facilitated by LOH studies that have guided the localization of minimally deleted regions on chromosomes. In ovarian carcinoma, the search for LOH has resulted in the identification of several chromosomal regions which may harbor ovarian cancer TSGs (4, 5).

The majority of studies on genetic alterations in malignancies rely on post hoc analysis of tumors identified histologically in sections of fixed, paraffin-embedded tissue. Often, the quantity of material available from paraffin sections is limited, particularly if a tumor lesion is in early stage. Moreover, LOH studies usually require multiple markers. To overcome such limitations, whole genome amplification strategy using PEP has been devised to increase the quantity of target DNA obtained from small samples to facilitate multiple loci analyses (6–9). Neoplastic and nonneoplastic cells are always mixed to some degree in most tumor lesions, necessitating the use of a variety of microdissection techniques to separate the tumor from normal cells (10–12). Such strategy will improve the specificity and reduce the amount of target tissue required for analysis.

In the present study, we have successfully established a protocol combining LCM and whole genome amplification to determine LOH profile in small quantities of archival tumor tissue samples. Using this protocol, we performed a detailed LOH analysis in 29 early-stage epithelial ovarian carcinomas, using 20 microsatellite markers spanning chromosomes 5 and 6. We also correlated LOH with clinicopathological features in these neoplasms.

MATERIALS AND METHODS

Specimen Preparation. Sixteen frozen and 13 Formalin-fixed, paraffin-embedded ovarian cancer specimens were obtained from the Division of Gynecological Oncology, Brigham and Women's Hospital, and the Department of Pathology, Massachusetts General Hospital. According to the International Federation of Gynecology and Obstetrics criteria, all 29 cases were stage I epithelial ovarian cancer (Table 1). Among these 29 cases, 3 were microscopically identified microinvasive carcinomas. The diameters of these microscopic tumors were 1–8 mm. Based on the WHO criteria of histological classification, 14 were serous, 5 mucinous, 3 endometrioid, 3 clear cell, and 4 mixed adenocarcinomas. Twelve cases were well-differentiated, 5 were moderately differentiated, and 12 were poorly differentiated tumors. Six-micrometer sections of frozen or Formalin-fixed, paraffin-embedded tissue were cut and mounted onto plain glass slides. Paraffin tissue was deparaffinized by incubating the slides in xylene for 2 × 10 min and rehydrating in absolute ethanol for 2 × 10 min, in 95% ethanol for 2 × 10 min, and in 70% ethanol for 2 × 10 min. Both slides were stained with H&E.

Microdissection. Stained sections were microdissected using a PixCell II LCM system (Arcturus Engineering, Mountain View, CA). Tumor cells and adjacent nontumor stromal cells were visualized under the microscope and selectively procured by activation of the laser (Fig. 1). Approximately 5000 tumor and nontumor stromal cells were dissected, respectively, in each case. Dissected cells were collected into 50 μl of cell lysis buffer (1× expand high-fidelity buffer from Boehringer Mannheim, Mannheim, Germany, containing 4 mg/ml proteinase K and 1% Tween 20) and incubated for 72 h at 55°C. The proteinase K was inactivated by heating at 95°C for 10 min prior to PCR.

Whole Genome Amplification. Whole genome amplification was performed by an improved PEP described by Dietmaier *et al.* (9), with modifications. Briefly, 50 μl of PEP PCR mixture consisted of 0.05 mg/ml gelatin, 40 μM 15-mer random primers (Operon Technologies, Alameda, CA), 0.2 mM of each dNTP, 2.5 mM $MgCl_2$, 1× expand high-fidelity buffer, 3.5 units of *Taq* expand high-fidelity polymerase (Boehringer Mannheim), and 10 μl of DNA sample. Fifty primer extension cycles were carried out in a Perkin-Elmer 9600 thermocycler (Perkin-Elmer, Norwalk, CT) after an initial 94°C, 3-min denaturation step. Each cycle consisted of 1 min at 94°C, 2 min at 37°C, a ramping step of 0.1°C/s up to 55°C, a 4-min primer extension step at 55°C, followed by 30 s at 68°C. The PEP reaction products were diluted by 3-fold and used as template DNA for LOH analysis.

LOH Analysis. The 20 microsatellite markers used in this study were obtained from the Applied Biosystems Prism Linkage Mapping Set LD-20 (Applied Biosystems, Foster City, CA). The average interval of the loci was

Received 11/22/00; accepted 3/14/01.

The costs of publication of this article were defrayed in part by the payment of page charges. This article must therefore be hereby marked *advertisement* in accordance with 18 U.S.C. Section 1734 solely to indicate this fact.

[1] This work was supported by Army Ovarian Cancer Research Program Grant DAMD17-99-1-9563, the Adler Foundation, the Morse Family Fund, and the Natalie Pihl Fund.

[2] To whom requests for reprints should be addressed, at Department of Obstetrics, Gynecology and Reproductive Biology, Brigham and Women's Hospital, Harvard Medical School, 221 Longwood Avenue, BLI-449, Boston, MA 02115. E-mail: scmok@rics.bwh.harvard.edu.

[3] The abbreviations used are: TSG, tumor suppressor gene; LCM, laser capture microdissection; LOH, loss of heterozygosity; PEP, primer-extension preamplification.

Table 1 *Clinicopathologic features of 29 ovarian tumors studied*

Tumor code	Age (yr)	Histological classification	Tumor grade[a]	Clinical Stage[b]	Tumor size (cm)	Survival duration (mo)
309	74	Endometrioid	1	Ia	11	1
333	59	Serous	1	Ic	15	88
355	36	Endometrioid	2	Ic	2	13
385	50	Mixed (serous + mucinous)	2	Ic	5	98
398	52	Serous	3	Ic	12	86
403	66	Serous	3	Ia	14.5	94
404	62	Mixed (mucinous + endometrioid)	3	Ic	13	78
416	40	Serous	1	Ia	3	27
426	56	Serous	3	Ic	5	85
433	42	Serous	3	Ic	5	84
440	56	Mucinous	2	Ia	32	84
442	36	Mixed (endometrioid + mucinous)	3	Ic	9.5	19
471	43	Mucinous	1	Ia	4	65
484	54	Serous	3	Ib	11	73
526	50	Serous	1	Ic	—[c]	54
529	73	Endometrioid	1	Ib	10	—[c]
533	59	Mixed (endometrioid + mucinous)	1	Ia	5	48
539	57	Clear cell	3	Ic	9	44
565	68	Serous	1	Ic	12	33
627	58	Serous	1	Ia	3	1
689	43	Serous	3	Ic	13	4
700	78	Mucinous	2	Ia	19	1
3317[d]	—[d]	Serous	1	Ia	0.1	—[c]
99N51[d]	—[d]	Serous	3	Ia	0.2	—[c]
97-7024[d]	—[d]	Serous	2	Ia	0.8	—[c]
97G002	47	Clear cell	1	Ia	13	—[c]
98G407	53	Mucinous	1	Ia	21	—[c]
98G018	44	Clear cell	3	Ia	9	—[c]
99G010	50	Mucinous	1	Ia	19	—[c]

[a] Grade 1, well differentiated; grade 2, moderately differentiated; grade 3, poorly differentiated.
[b] Staging based on International Federation of Gynecology and Obstetrics classification.
[c] Data not available.
[d] Microscopically identified microinvasive carcinoma.

about 20 cM. They consisted of fluorescent primer pairs end labeled with fluorochromes 6-carboxyfluorescein, hexachlorinated analogues, or NED that amplify dinucleotide repeat fragments. Optimized PCRs were performed in 10 μl of solution with 1 μl of PEP DNA, 0.25–0.5 μM of each primer, 1× PCR buffer, 2.5 mM $MgCl_2$, 0.25 mM of each dNTP, and 0.5 units of AmpliTaq Gold DNA polymerase (Applied Biosystems). All reactions were carried out in a Perkin-Elmer 9600 thermocycler. Amplification was started with 12 min at 95°C, followed by 10 cycles composed of 15 s at 94°C, 15 s at 55°C, and 30 s at 72°C, and then 25 cycles composed of 15 s at 89°C, 15 s at 55°C, and 30 s at 72°C. Amplified PCR products for multiple loci were pooled and run on an Applied Biosystems Prism 310 automated capillary electrophoresis DNA sequencer (Applied Biosystems). The systems automated size determination, linear quantification of alleles, and computerized discrimination of true alleles. Data were initially processed using Genescan 2.1 software (Applied Biosystems). Result files were then imported into Genotyper (version 2.5, Applied Biosystems), and the data were tabulated according to allele size and allele peak area. The data in this form were analyzed according to a standardized "normal *versus* tumor" template to calculate the normal:tumor allelic ratio. This was typically done using ratios of the allelic peak volume in a form: $(N1/N2)/(T1/T2)$, where N is a normal allele and T is a tumor allele (13). For each particular marker locus, LOH was assessed in the corresponding tumor sample if it was informative (heterozygous) in the normal DNA sample. LOH was imputed if the effective decrease in one allele was >50% (normal:tumor allelic ratios, <0.5 or >2.0). Individual results were classified into homozygous, heterozygous with no loss, and heterozygous with loss.

A validation study of four cases confirmed that the study protocol reliably detected LOH in archival material. The results of LOH determination from four cases at six loci with paraffin-embedded tissue DNA sample were in agreement with those obtained with freshly frozen tissue DNA. The LOH detection was repeated once to check its reproducibility. No difference of repeated score of LOH was found in this series of testing.

Statistical Analysis. Statistical analysis of a possible correlation between detected LOH and histological subtype, clinical stage, and pathological grade was carried out with Pearson's χ^2 test or Fisher's exact test. Probability value was two-tailed, with $P < 0.05$ regarded as statistically significant.

RESULTS

The informative rates of 20 microsatellite markers used in this study were between 52 and 90%. Representative patterns of allelic loss by fluorescent-labeled microsatellite analysis are illustrated in Fig. 2. Fig. 3 shows allelic loss frequencies on chromosomes 5 and 6. Fig. 4 shows common regions of allelic loss found. Among these markers studied, the highest incidence of LOH was at locus *D6S264* (6q25.2–27; 60%). Other loci with frequent LOH (>30%) were *D5S630* (5p15.2; 32%), *D5S424* (5q13–14; 32%), *D5S428* (5q14–21; 48%), *D6S1574* (6p24–25; 46%), D6S287 (6q21–23.3; 42%), *D6S441* (6q25.2–25.3; 45%), and *D6S281* (6q27; 35%).

In 29 cases studied, 3 were microscopically identified microinvasive adenocarcinomas. Their tumor size was 1 mm (case 3317A), 2 mm (case 99N51), and 8 mm (case 97-7024) in diameter, respectively. LOH was detected in all three tumors at locus *D5S630*. Two of three cases showed LOH at loci *D5S428*, *D5S433*, *D6S287*, *D6S264*, and *D6S281*. Total LOH rate showed a trend to increase with tumor size, which was 28, 39, and 53% in cases 3317A, 99N51, and 97-7024, respectively. The LOH rate did not appear to be correlated with cell differentiation in these three tumors.

Table 2 shows correlation between LOH and clinicopathological features. The LOH frequency in these eight loci was >30%. Tumors

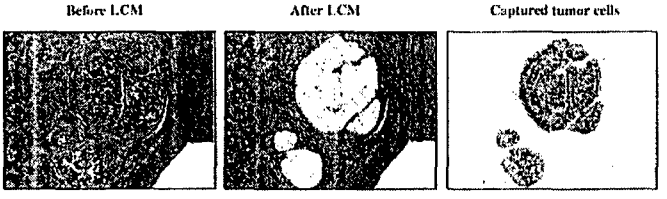

Fig. 1. Representative example of LCM of a microscopically identified ovarian serous adenocarcinoma (case 99N51).

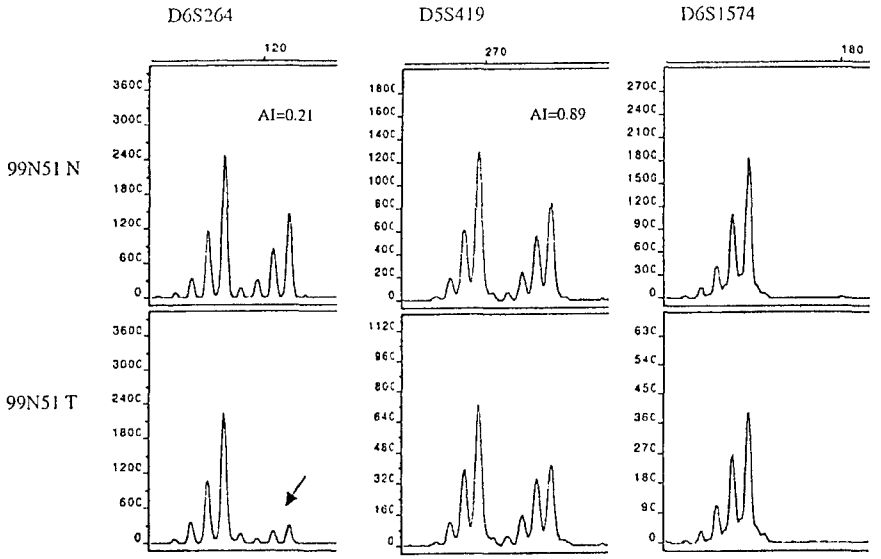

Fig. 2. Representative allelotype analysis of a microscopically identified ovarian serous adenocarcinoma (case 99N51) at three loci on chromosomes 5 and 6. *N*, stromal cell; *T*, tumor cell; *AI*, allelic ratio. *Arrow*, loss of one allele at locus *D6S264* in tumor cells.

were evaluated for LOH with respect to clinical stage, histological subtype, and tumor grade. No significant difference in LOH in a particular locus was found among different substages, histological subtypes, and tumor grades ($P > 0.05$).

DISCUSSION

Over the past decade, it has been shown that LOH is common to most solid neoplasms and that it allows the expression of recessive loss-of-function mutations in TSGs. The detection of nonrandom LOH at a chromosomal region is seen to be prima facie evidence for the localization of candidate TSGs. Several studies have shown that gene alterations appear to play a major role in the development of ovarian cancer. In an effort to identify genomic sites harboring potentially relevant TSGs in ovarian cancer, several groups have studied allelic loss on specific chromosomes. Recent studies have found allelic aberrations on chromosomes 1p, 3p, 5q, 6q, 7p, 8p, 9q, 11p, 13q, 14q, 17p, 17q, 18q, 21q, 22q, and Xp (14–19). In this study, we chose to study allelic loss on chromosomes 5 and 6, which have been shown to have high LOH rates in late-stage tumors. We also correlated LOH with clinicopathological features in these cancers to define the role of allelic loss in the early stage of epithelial ovarian cancer development.

Detection of LOH requires a homogeneous population of tumor cells, because any contamination by adjacent nontumor cells (lymphocytes or stromal cells) would lead to erroneous underestimation of the LOH frequency. LOH can reliably be detected in tumor samples only if the content of tumor cells exceeds 70–80%. Ovarian tumor tissues are often heterogeneous, containing nontumoral as well as neoplastic cells. The technology LCM provides a method whereby individual cells can be harvested from complex tissue. Because the method is reliable and efficient, individual cell capture can be performed rapidly and distinct cell populations can be collected from tissues. However, the screening of multiple loci in tumor cells isolated from microdissected archival tumor specimens is limited by the number of cells available. Most LOH studies need DNA from ~3000 to 6000 cells per genotype, making detailed somatic genetic analyses of small clinical samples impossible (20). Because LOH studies must be done with multiple markers, preamplification of the entire DNA by whole genome amplification would be very helpful. PEP is an *in vitro* procedure developed to duplicate a large fraction of the genome from limited amounts of DNA. Furthermore, it can amplify the genome of a single cell to an estimated minimum of 30 times and may allow as many as 20 locus-specific LOH analyses on as few as 1000 cells (20, 21). This technique has already been shown to be useful in intact sperm cells (6), blastomeres (22, 23), and fetal nucleated erythrocytes (24). Recently, Chung *et al.* (25) reported that PEP amplification

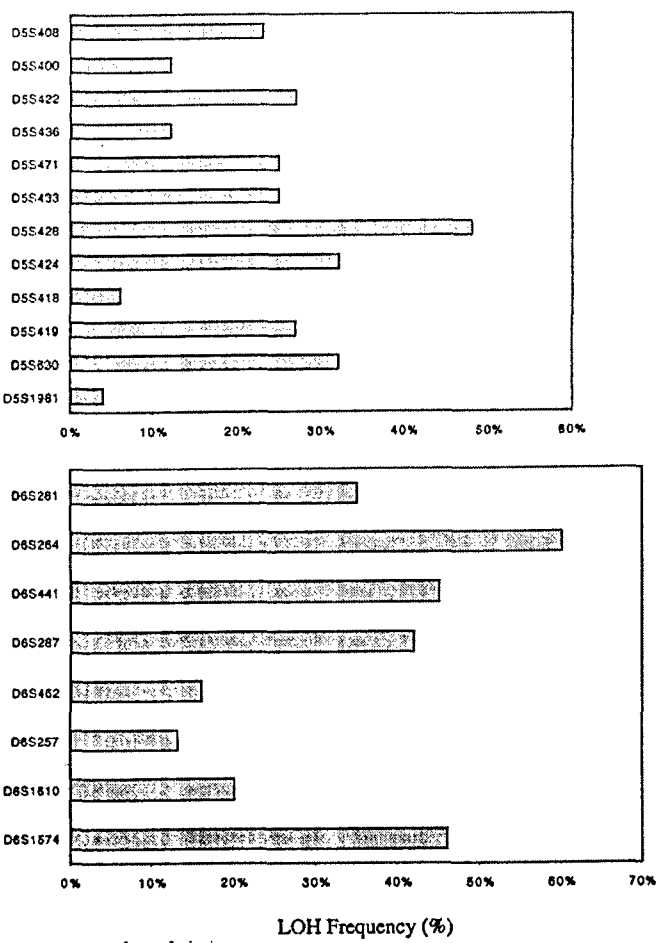

Fig. 3. LOH rate detected at 20 loci on chromosomes 5 and 6. The LOH frequency is expressed as the percentage of total informative cases at each given locus.

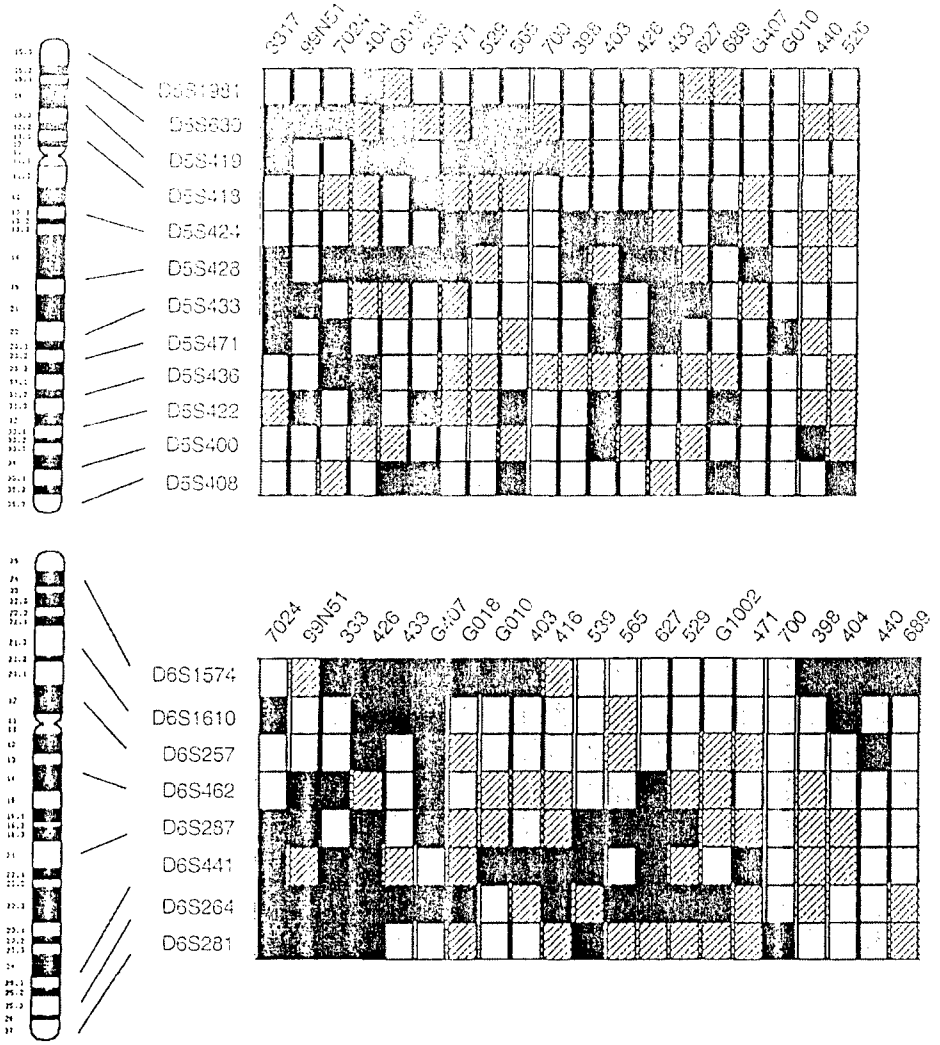

Fig. 4. Deletion map of early-stage epithelial ovarian carcinomas analyzed. ■, heterozygous with loss; ▨, heterozygous with no loss; ▩, homozygous; □, not tested.

could produce accurate and reproducible profiles of LOH in cervical cancers.

We developed a high-throughput strategy for the detection of LOH for this study. LCM was used to enrich the neoplastic cell population and PEP to ensure that adequate amounts of DNA can be produced from a small quantity of archival ovarian tissue. In this study, five minimal deleted regions, including 5p15.2, 5q13–21, 6p24–25, 6q21–23, and 6q25.1–27, were identified on chromosomes 5 and 6. High LOH frequencies on chromosome 5 were identified at loci *D5S630* (32%), *D5S424* (32%), and *D5S428* (48%). The presence of two deleted regions, 5p15.2 and 5q13–21 in the tumors studied, supports the hypothesis that more than one TSG on chromosome 5 may be involved in the development of early-stage ovarian cancer. Several investigators have reported infrequent LOH on chromosome 5q (26–29), whereas others have reported frequent deletions (4, 17, 28). Chuaqui *et al.* examined LOH on 5q 21–22 (*D5S346* locus) in 12

Table 2 *LOH and correlation with clinicopathological features in epithelial ovarian carcinomas*

	No. of LOH/no. of informative cases (%)							
	D5S630(5p15.2)	*D5S424*(5q13-14)	*D5S428*(5q14-21)	*D6S1574*(6p24-25)	*D6S287*(6q21-23.3)	*D6S441*(6q25.1-25.3)	*D6S264*(6q25.2-27)	*D6S281*(6q27)
Stage								
Microinvasive[a]	3/3 (100%)	0/3 (0)	2/3 (67%)	0/2 (0)	2/2 (100%)	1/2 (50%)	2/3 (67%)	2/3 (67%)
Ia	1/7 (14%)	2/6 (33%)	3/8 (38%)	5/9 (56%)	2/5 (40%)	5/9 (56%)	5/9 (56%)	1/6 (17%)
Ib	1/2 (50%)	1/2 (50%)	0/1 (0)	0/2 (0)	1/2 (50%)	0/1 (0)	1/2 (50%)	0/0 (0)
Ic	1/7 (14%)	3/8 (38%)	5/9 (56%)	6/11 (55%)	3/10 (30%)	3/8 (38%)	4/6 (67%)	3/8 (38)
Histological type								
Serous	4/12 (33%)	4/11 (36%)	6/10 (60%)	6/11 (55%)	5/11 (45%)	6/10 (60%)	8/10 (80%)	4/8 (50%)
Mucinous	1/2 (50%)	1/3 (33%)	2/4 (50%)	3/5 (60%)	1/3 (33%)	2/5 (40%)	1/4 (25%)	1/4 (25%)
Endometrioid	1/2 (50%)	1/2 (50%)	0/1 (0)	0/2 (0)	1/2 (50%)	0/1 (0)	1/2 (50%)	0/1 (0)
Clear	0/2 (0)	0/2 (0)	1/2 (50%)	1/3 (33%)	1/1 (100%)	1/1 (100%)	2/2 (100%)	1/1 (100%)
Mixed	0/2 (0)	0/2 (0)	1/4 (25%)	1/3 (33%)	0/2 (0)	0/3 (0)	0/2 (0)	0/3 (0)
Differentiation								
Well	3/9 (33%)	2/7 (29%)	4/7 (57%)	3/8 (38%)	4/6 (67%)	5/9 (56%)	6/9 (67%)	1/5 (20%)
Moderate	1/2 (50%)	0/4 (0)	1/4 (25%)	1/5 (20%)	1/5 (20%)	1/5 (20%)	1/4 (25%)	2/5 (40%)
Poor	2/8 (25%)	4/8 (50%)	5/10 (50%)	7/11 (64%)	3/8 (38%)	3/6 (50%)	5/7 (71%)	3/7 (43%)

[a] Microscopically identified.

synchronous ovarian and appendiceal mucinous lesions and did not detect it in any (29). Weitzel *et al.* (17) found a 50% (10 of 20) LOH rate using markers near the *adenomatous polyposis coli* gene at 5q21. They showed LOH at more than one locus and that most cases showing LOH were stage III or IV (17). Findings from this study are not consistent with the other report, which concluded that 5q LOH was a late event in ovarian carcinogenesis (28). One of the notable findings of this study is the frequent LOH at *D5S630* mapped on 5p15.2. LOH at this locus was detected in all three microscopic serous adenocarcinomas and their pathological grade was well differentiated (case 3317A), moderately differentiated (case 97-7024), and poorly differentiated (case 99N51). Whether such a molecular change represents an early event in the development of ovarian cancer deserves further investigation.

We used eight microsatellite markers on chromosome 6. The LOH patterns were often complex, with a number of stage I cancers exhibiting multiple interstitial losses. LOH patterns of deletion suggesting the existence of three distinct regions of allelic loss were observed. They were defined by 6p24–25 (*D6S1574*), 6q21–23.3 (*D6S287*), and 6q25.1–27 (*D6S441* and *D6S264*). Dodson *et al.* (16) reported chromosome 6p to be frequently lost in low-grade as well as high-grade ovarian epithelial carcinomas, but they did not define deletion regions on 6p (16). Using Southern blot analysis, Gallion *et al.* (30) examined 34 primary ovarian epithelial tumors for the presence of LOH on chromosome 6q and observed LOH at the estrogen receptor site on 6q in only 15% of tumors. This is in contrast to the finding of both Lee *et al.* (14) and Zheung *et al.* (31) who reported allelic loss at the estrogen receptor locus in >50% of ovarian tumors. In our previous study, we used 12 markers spanning a 18-cM region, located between 6q25.1 and 6q26, and found LOH most frequently at the loci defined by markers *D6S473* (44%) and *D6S448* (43%). Detailed mapping of chromosome 6q25-q26 in these tumor samples identified a 4-cM minimal region of LOH between markers *D6S473* and *D6S448* (6q25.1-q25.2) (32). Rey *et al.* (33) found a frequent LOH in the 6q27-qter region in five of eight ovarian carcinomas. Suzuki *et al.* (34) studied LOH in chromosome region 6q27 in 70 ovarian cancers, with particular reference to clear cell adenocarcinoma. LOH at 6q27 was detected in 26 of 48 informative cases using 4 markers (54.2%). In clear cell carcinoma, 6q27 LOH was observed in 5 of 11 informative cases (45%). No significant difference in the incidence of 6q27 LOH was seen in different histological types (34). However, Weitzel *et al.* (17) reported that LOH was infrequently observed at markers on chromosome 6 in ovarian cancer. Taken together, the studies of others and ours suggest the possible presence of several genes on chromosome 6 whose alteration may play a role in tumorigenesis of epithelial ovarian carcinoma.

In this study, the LOH rate seems to increase with tumor size in microinvasive serous adenocarcinoma. However, more cases should be examined before more confident conclusions can be drawn. We correlated LOH with tumor stage, grade, and histological type in this study, but no statistically significant relationship between LOH at a given locus and any of these clinicopathological features was noted.

In summary, concomitant LOH at more than one locus on chromosomes 5 and 6 was observed in most of the stage I ovarian cancers in this study. Although the patterns of LOH on chromosomes 5 and 6 appear to be complex, the results indicate that five regions are frequently altered. Further validation of which regions are relevant to ovarian tumor genesis and progression requires higher density mapping in ovarian neoplasm-derived cell lines and chromosome transfer experiments to identify these cancer-specific TSGs and to correlate regional loss with functional suppression. In addition, the methodology of PCR-based LOH determination using fluorescent-labeled microsatellite markers in combination with primer extension preamplification PCR and LCM techniques developed and validated in this study may increase the potential for molecular analysis of multiple loci in archival microscopically identified tumor samples of any human solid tumor.

REFERENCES

1. Yancik, R. Ovarian cancer: age contrasts in incidence, histology, disease stage at diagnosis, and mortality. Cancer (Phila.), *71*(Suppl. 2): 517–523, 1993.
2. Stanbridge, E. J. Human tumor suppressor genes. Annu. Rev. Genet., *24:* 615–657, 1990.
3. Lasko, D., Cavenee, W., and Nordenskjold, M. Loss of constitutional heterozygosity in human cancer. Annu. Rev. Genet., *25:* 281–314, 1991.
4. Cliby, W., Ritland, S., Hartmann, L., Dodson, M., Halling, K. C., Podratz, K. C., and Jenkins, R. B. Human epithelial ovarian cancer allelotype. Cancer Res., *53:* 2393–2398, 1993.
5. Cooke, I. E., Shelling, A. N., Le Meuth, V. G., Charnock, M. L., and Ganesan, T. S. Allele loss on chromosome arm 6q and fine mapping of the region at 6q27 in epithelial ovarian cancer. Genes Chromosomes Cancer, *15:* 223–233, 1996.
6. Zhang, L., Cui, X., Schmitt, K., Hubert, R., Navidi, W., and Arnheim, N. Whole genome amplification from a single cell: implications for genetic analysis. Proc. Natl. Acad. Sci. USA, *89:* 5847–5851, 1992.
7. Telenius, H., Carter, N. P., Bebb, C. E., Nordenskjold, M., Ponder, B. A., and Tunnacliffe, A. Degenerate oligonucleotide-primed PCR: general amplification of target DNA by a single degenerate primer. Genomics, *13:* 718–725, 1992.
8. Peng, H. Z., Isaacson, P. G., Diss, T. C., and Pan, L. X. Multiple PCR analyses on trace amounts of DNA extracted from fresh and paraffin wax embedded tissues after random hexamer primer PCR amplification. J. Clin. Pathol., *47:* 605–608, 1994.
9. Dietmaier, W., Hartmann, A., Wallinger, S., Heinmoller, E., Kerner, T., Endl, E., Jauch, K., Hofstadter, F., and Ruschoff, J. Multiple mutation analyses in single tumor cells with improved whole genome amplification. Am. J. Pathol., *154:* 83–95, 1999.
10. Emmert-Buck, M. R., Bonner, R. F., Smith, P. D., Chuaqui, R. F., Zhuang, Z., Goldstein, S. R., Weiss, R. A., and Liotta, L. A. Laser capture microdissection. Science (Wash DC), *274:* 998–1001, 1996.
11. Going, J. J., and Lamb, R. F. Practical histological microdissection for PCR analysis. J. Pathol., *179:* 121–124, 1996.
12. Moskaluk, C. A., and Kern, S. E. Microdissection and polymerase chain reaction amplification of genomic DNA from histological tissue sections. Am. J. Pathol., *150:* 1547–1552, 1997.
13. Cawkwell, L., Bell, S. M., Lewis, F. A., Dixon, M. F., Taylor, G. R., and Quirke, P. Rapid detection of allele loss in colorectal tumours using microsatellites and fluorescent DNA technology. Br. J. Cancer, *67:* 1262–1267, 1993.
14. Lee, J. H., Kavanagh, J. J., Wildrick, D. M., Wharton, J. T., and Blick, M. Frequent loss of heterozygosity on chromosomes 6q, 11, and 17 in human ovarian carcinomas. Cancer Res., *50:* 2724–2728, 1990.
15. Ehlen, T., and Dubeau, L. Loss of heterozygosity on chromosomal segments 3p, 6q, and 11p in human ovarian carcinoma. Oncogene, *5:* 219–223, 1990.
16. Dodson, M. K., Hartmann, L. C., Cliby, W. A., de Lacey, K. A., Keeney, G. L., Ritland, S. R., Su, J. Q., Podratz, K. C., and Jenkins, R. B. Comparison of loss of heterozygosity patterns in invasive low-grade and high-grade epithelial ovarian carcinomas. Cancer Res., *53:* 4456–4460, 1993.
17. Weitzel, J. N., Patel, J., Smith, D. M., Goodman, A., Safaii, H., and Ball, H. G. Molecular genetic changes associated with ovarian cancer. Gynecol. Oncol., *55:* 245–252, 1994.
18. Tavassoli, M., Steingrimsdottir, H., Pierce, E., Jiang, X., Alagoz, M., Farzaneh, F., and Campbell, I. G. Loss of heterozygosity on chromosome 5q in ovarian cancer is frequently accompanied by TP53 mutation and identifies a tumour suppressor gene locus at 5q13.1–21. Br. J. Cancer, *74:* 115–119, 1996.
19. Brown, M. R., Chuaqui, R., Vocke, C. D., Berchuck, A., Middleton, A., Emmert-Buck, M. R., and Kohn, E. C. Allelic loss on chromosome arm 8p: analysis of sporadic epithelial ovarian tumors. Gynecol. Oncol., *74:* 98–102, 1999.
20. Barret, M. T., Reid, B. J., and Joslyn, G. Genotypic analysis of multiple loci in somatic cells by whole genome amplification. Nucleic Acids Res., *23:* 3488–3492, 1995.
21. Niederacher, D., Picard, F., van Poyen, C., An, H. X., Bender, H. G., and Beckmann., M. W. Patterns of allelic loss on chromosome 17 in sporadic breast carcinomas detected by fluorescent-labelled microsatellite analysis. Genes Chromosomes Cancer, *18:* 181–192, 1997.
22. Kristjansson, K., Chong, S. S., Van den Veyer, I. B., Subramanian, S., Snabes, M. C., and Hughes, M. R. Preimplantation single cell analyses of dystrophin gene deletions using whole genome amplification. Nat. Genet., *6:* 19–23, 1994.
23. Snabes, M. C., Chong, S. S., Subramanian, S. B., Kristjansson, K., Di Sepio, D., and Hughes, M. R. Preimplantation single-cell analysis of multiple genetic loci by whole-genome amplification. Proc. Natl. Acad. Sci. USA, *91:* 6181–6185, 1994.
24. Sekizawa, A., Watanabe, A., Kimura, T., Saito, H., Yanaihara, T., and Takeshi, S. Prenatal diagnosis of the fetal RhD blood type using a single fetal nucleated erythrocyte from maternal blood. Obstet. Gynecol., *87:* 501–505, 1996.
25. Chung, T. K. H., Cheung, T. H., Lo, W. K., Yu, M. Y., Hampton, G. M., Wong, H. K. T., and Wong, Y. F. Loss of heterozygosity at the short arm of chromosome 3 in microdissected cervical intraepithelial neoplasia. Cancer Lett., *154:* 189–194, 2000.

26. Sato, T., Saito, H., Morita, R., Koi, S., and Nakamura, Y. Allelotype of human ovarian cancer. Cancer Res., *51:* 5118–5122, 1991.
27. Yang-Feng, T. L., Han, H., Chen, K. C., Li, S. B., Claus, E. B., Carcaugin, M. L., Chambers, S. K., Chambers, J. T., and Schwartz, P. E. Allelic loss in ovarian cancer. Int. J. Cancer, *54:* 546–551, 1993.
28. Allan, G. J., Cottrell, S., Trowsdale, J., and Foulkes, W. D. Loss of heterozygosity on chromosome 5 in sporadic ovarian carcinoma is a late event and is not associated with mutations in APC at 5q21–22. Hum. Mutat., *3:* 283–291, 1994.
29. Chuaqui, R. F., Zhuang, Z., Emmert-Buck, M. R., Bryant, B. R., Nogales, F., Tavassoli, F. A., and Merino, M. J. Genetic analysis of synchronous mucinous tumors of the ovary and appendix. Hum. Pathol., *27:* 165–171, 1996.
30. Gallion, H. H., Powell, D. E., Morrow, J. K., Pieretti, M., Case, E., Turker, M. S., De Pariest, P. D., Hunter, J. E., and Van Nagell, J. R. Molecular genetic changes in human epithelial ovarian malignancies. Gynecol. Oncol., *47:* 137–142, 1992.
31. Zheng, J., Robinson, W. R., Ehlen, T., Yu, M. C., and Dubeau, L. Distinction of low grade from high grade human ovarian carcinomas on the basis of losses of heterozygosity on chromosomes 3, 6, and 11 and HER-2/*neu* gene amplification. Cancer Res., *51:* 4045–4051, 1991.
32. Colitti, C. V., Rodabaugh, K. J., Welch, W. R., Berkowitz, R. S., and Mok, S. C. A novel 4 cM minimal deletion unit on chromosome 6q25.1-q25.2 associated with high grade invasive epithelial ovarian carcinomas. Oncogene, *16:* 555–559, 1998.
33. Rey, J. M., Theillet, C., Brouillet, J. P., and Rochefort, H. Stable amino-acid sequence of the mannose-6-phosphate/insulin-like growth-factor-II receptor in ovarian carcinomas with loss of heterozygosity and in breast-cancer cell lines. Int. J. Cancer, *85:* 466–473, 2000.
34. Suzuki, M., Saito, S., Saga, Y., Ohwada, M., and Sato, I. Loss of heterozygosity on chromosome 6q27 and p53 mutations in epithelial ovarian cancer. Med. Oncol., *15:* 119–123, 1998.

This difficulty is overcome with the ASPE assay, which allows multiplexed SNP analysis for any mixtures of allelic variants. This advantage is possible because the "query" nucleotide is part of the ASPE capture probe, while the signal-generating "labeled" nucleotide is free biotin-dCTP. In the SBCE assay, the biotin-ddNTP serves as both "query" and "labeled" nucleotide. Another advantage conferred by the ASPE assay is simplification of the reaction protocol. The residual dNTPs from the target-generating PCR are used for the primer extension, thereby eliminating both the necessity of post-PCR cleanup and the addition of unlabeled nucleotides to the ASPE reaction.

It can be difficult to establish an assay cost per SNP because that cost will vary dramatically depending on how the assay is employed. Cost parameters include the total number of assays run, the number of simultaneous assays performed (multiplex factor), and whether many SNPs are assayed on few patients (genome-wide scan) or whether few SNPs are assayed on many patients (targeted genomic region). The microspheres and coupling reagents are inexpensive compared to reagents such as enzymes or fluorescent nucleotides. We estimate our average cost is less than US $0.20 per SNP, excluding the cost of generating the PCR target. SBCE and ASPE reactions are comparable in cost. Attempts to reduce assay costs further have concentrated on minimizing reagent consumption, especially that of the enzyme and fluorochrome. Recently, we have successfully generated short target DNAs in 50-plex PCRs and have also migrated from 20-plex to 50-plex SBCE reactions. Even higher levels of complexity are theoretically possible using the complete 100-microsphere set.

In an attempt to minimize the subjectivity of genotypic calls, various data clustering algorithms are currently under development that will allow automatic assignment of genotypes to the different clusters. Observed challenges to automated allele scoring include variability in tightness of data clustering, dissimilar signal intensities between the two alleles, and the formation of extraneous data clusters due to previously undetected polymorphisms within the probe sequence. Extensive testing on large data sets will not only allow refinement of these algorithms but also may identify characteristics of problematic markers that can be avoided in future probe design.

ACKNOWLEDGMENTS

The authors thank Terri Fleming for the bioinformatics support for high-throughput operations, the Glaxo Wellcome Genotyping Facility, and the Glaxo Wellcome Sequencing Core Facility for their services. Thanks also are due to Dan Burns of the Genetics Directorate and Ralph McDade, Van Chandler, Mark Chandler, Jim Jacobson, and Christy Weiss of Luminex Corporation for many helpful discussions.

REFERENCES

1. **Brinson, E.C., T. Adriano, W. Bloch, C.L. Brown, C.C. Chang, J. Chen, F.A. Eggerding, P.D. Grossman et al.** 1997. Introduction to PCR/OLA/SCS, a multiplex DNA test and its application to cystic fibrosis. Genet. Test. *1*:61-68.
2. **Chen, J., M.A. Iannone, M.-S. Li, J.D. Taylor, P. Rivers, A.J. Nelsen, K.A. Slentz-Kesler, A. Roses, and M.P. Weiner.** 2000. A microsphere-based assay for single nucleotide polymorphism analysis using single base chain extension. Genome Res. *10*:549-557.
3. **Chen, X.N., L. Levine, and P.Y. Kwok.** 1999. Fluorescence polarization in homogeneous nucleic acid analysis. Genome Res. *9*:492-498.
4. **Cooper, D.N., B.A. Smith, H.J. Cooke, S. Niemann, and J. Schmidtke.** 1985. An estimate of unique DNA sequence heterozygosity in the human genome. Hum. Genet. *69*:201-205.
5. **Eggerding, F.A.** 1995. A one-step coupled amplification and oligonucleotide ligation procedure for multiplex genetic typing. PCR Methods Appl. *4*:337-345.
6. **Fu, D.J., K. Tang, A. Braun, D. Reuter, B. Darnhofer-Demar, D.P. Little, M.J. O'Donnell, C.R. Cantor, and H. Koster.** 1998. Sequencing exons 5 to 8 of the p53 gene by MALDI-TOF mass spectrometry. Nat. Biotechnol. *16*:381-384.
7. **Fulton, R.J., R.L. McDade, P.L. Smith, L.J. Kienker, and J.R. Kettman, Jr.** 1997. Advanced multiplexed analysis with the FlowMetrix system. Clin. Chem. *43*:1749-1756.
8. **Gilles, P.N., D.J. Wu, C.B. Foster, P.J. Dillon, and S.J. Chanock.** 1999. Single nucleotide polymorphic discrimination by an electronic dot blot assay on semiconductor microchips. Nat. Biotechnol. *17*:365-370.
9. **Iannone, M.A., J.D. Taylor, J. Chen, M.-S. Li, P. Rivers, K.A. Slentz-Kesler, and M.P. Weiner.** 2000. Multiplexed single nucleotide polymorphism genotyping by oligonucleotide ligation and flow cytometry. Cytometry *39*:131-140.
10. **Kettman, J.R., T. Davies, D. Chandler, K.G. Oliver, and R.J. Fulton.** 1998. Classification and properties of 64 multiplexed microsphere sets. Cytometry *33*:234-243.
11. **Lai, E., J. Riley, I. Purvis, and A. Roses.** 1998. A 4-MB high-density single nucleotide polymorphism-based map around human APOE. Genomics *54*:31-38.
12. **Landegren, U., R. Kaiser, J. Sanders, and L. Hood.** 1988. A ligase-mediated gene detection technique. Science *241*:1077-1080.
13. **Livak, K.J., J. Marmaro, and J.A. Todd.** 1995. Towards full automated genome-wide polymorphism screening. Nat. Genet. *9*:341-342.
14. **McDade, R.L. and R.J. Fulton.** 1997. True multiplexed analysis by computer-enhanced flow cytometry. Med. Dev. Diag. Indust. *19*:75-82.
15. **McHugh, T.M.** 1994. Flow microsphere immunoassay for the quantitative and simultaneous detection of multiple soluble analytes. Methods Cell Biol. *42*:575-595.
16. **Mein, C.A., B.J. Barratt, M.G. Dunn, T. Siegmund, A.N. Smith, L. Esposito, S. Nutland, H.E. Stevens et al.** 2000. Evaluation of single nucleotide polymorphism typing with Invader on PCR amplicons and its automation. Genome Res. *10*:330-343.
17. **Orita, M., H. Iwahana, H. Kanazawa, K. Hayashi, and T. Sekiya.** 1989. Detection of polymorphisms of human DNA by gel electrophoresis as single-strand conformation polymorphisms. Proc. Natl. Acad. Sci. USA *86*:2766-2770.
18. **Parker, L.T., H. Zakeri, Q. Deng, S. Spurgeon, P.-Y. Kwok, and D.A. Nickerson.** 1996. AmpliTaq® DNA polymerase, FS dye-terminator sequencing: analysis of peak height patterns. BioTechniques *21*:694-699.
19. **Saiki, R.K., P.S. Walsh, C.H. Levenson, and H.A. Erlich.** 1989. Genetic analysis of amplified DNA with immobilized sequence-specific oligonucleotide probes. Proc. Natl. Acad. Sci. USA *86*:6230-6234.
20. **Syvanen, A.C.** 1999. From gels to chips: "minisequencing" primer extension for analysis of point mutations and single nucleotide polymorphisms. Hum. Mutat. *13*:1-10.
21. **Tyagi, S., D.P. Bratu, and F.R. Kramer.** 1998. Multicolor molecular beacons for allele discrimination. Nat. Biotechnol. *16*:49-53.

Received 20 April 2000; accepted 13 October 2000.

Address correspondence to:

J. David Taylor
Glaxo Wellcome, Inc.
5 Moore Drive
Research Triangle Park
NC 27709-3398, USA
e-mail: jdt6451@glaxowellcome.com

DRUG DISCOVERY
AND GENOMIC TECHNOLOGIES

Product Application Focus

Identification of Differentially Expressed Genes from Ovarian Cancer Cells by MICROMAX™ cDNA Microarray System

Kwong-Kwok Wong, Rita S. Cheng, and Samuel C. Mok[1]
Pacific Northwest National Laboratory, Molecular Biosciences, Richland, WA, and [1]Laboratory of Gynecologic Oncology, Brigham and Women's Hospital, Harvard Medical School, Boston, MA, USA

BioTechniques 30:670-675 (March 2001)

ABSTRACT

Using the MICROMAX™ cDNA microarray system, we were able to identify genes that are differentially overexpressed in ovarian cancer. A total of 30 putative genes, which are differentially overexpressed in ovarian cancer cell lines, were identified. The differential expression of some of these genes was further confirmed by real-time RT-PCR. Using this strategy, we have identified genes that either overexpress in all cancer cell lines or in only some cancer cell lines. Further characterization of these genes will allow them to be exploited in diagnosis, prognosis, anticancer therapy, and molecular classification of ovarian cancer.

INTRODUCTION

Ovarian cancer is the leading cause of death among women from gynecologic malignancies (1). Previously, we have successfully applied RAP-PCR (differential display) technology to identify differentially expressed genes in ovarian cancer, and only a few genes have been identified in the last few years (5–7).

cDNA microarray technology is a very sensitive method that allows one to analyze thousands of genes simultaneously (2,3,9). Several commercial human cDNA microarray systems are currently available. Here, we discuss the use of the MICROMAX™ system (NEN® Life Science Products, Boston, MA, USA) to identify genes that are differentially overexpressed in ovarian cancer cells. The use of an efficient tyramide signal amplification (TSA) system in the MICROMAX system enables us to use 20–100 times less total RNA than the currently used method. The use of a lower amount of RNA is very desirable in microarray analysis of precious RNA samples extracted from primary cell cultures or microdissected tissue samples.

MATERIALS AND METHODS

Cell Culture

Cultures of the normal human ovarian surface epithelial (HOSE) cells were established by scraping the HOSE cells from the ovary and growing in a mixture of Medium 199 and MCDB105 supplemented with 10% fetal calf serum (Sigma, St. Louis, MO, USA) as described previously (7). The seven HOSE cells used were HOSE17, HOSE636, HOSE642, HOSE695, HOSE697, HOSE713, and HOSE726. The ovarian cancer cell lines used were OVCA3, OVCA420, OVCA432, OVCA433, OVCA633, SKOV3, and ALST. All cell cultures and cell lines were established in the Laboratory of Gynecologic Oncology, Brigham and Women's Hospital, except SKOV3, which was purchased from ATCC (Manassas, VA, USA).

Microarray Probe and Hybridization

MICROMAX human cDNA microarray system, which contains 2400 known human cDNA on a 1 × 3 inch slide, was used in this study. Microarray probe and hybridization were performed as described in the instruction manual. In brief, biotin-labeled cDNA was generated from 3 μg total RNA, which was pooled from HOSE17, HOSE636, and HOSE642. Dinitropheny (DNP)-labeled cDNA was generated from 3 μg total RNA that was pooled from ovarian cancer cell lines OVCA 420, OVCA 433, and SKOV3. Before the cDNA reaction, an equal amount of RNA control was added to each batch of the RNA samples for normalization during data analysis. Biotin-labeled and DNP-labeled cDNA were mixed, dried, and resuspended in 20 μL hybridization buffer, which was added to the cDNA microarray and covered with a cover-

Table 1. List of Genes Differentially Overexpressed in Ovarian Cancer Cells More than Tenfold

Accession No.	Description	Before Extensive Washing (Cy3/Cy5)	After Extensive Washing (Cy3/Cy5)	Cy3 Signal Intensity
M33011	Carcinoma-associated antigen GA733-2	472	444	1249
J04765	Osteopontin	156	184	11851
L41351	Prostasin	44	170	3172
L19783	GPI-H	4	88	916
U96759	Von Hippel-Lindau binding protein (VBP-1)	60	59	1377
M57730	B61	20	49	5514
L33930	CD24 signal transducer and 3′ region	24	47	26722
D55672	hnRNP D	45	44	950
U97188	Putative RNA binding protein KOC	223	38	3599
L19871	ATF3	9	37	3507
J04991	p18	15	34	9914
D00762	mRNA for proteasome subunit HC8	17	29	4703
U17989	Nuclear autoantigen GS2NA	5	28	721
U43148	Patched homolog (PTC)	10	28	4155
AF010312	Pig7 (PIG7)	13	23	17379
M80244	E16	18	21	4180
X99802	mRNA for ZYG homologue	14	21	2086
U05598	Dihydrodiol dehydrogenase	10	18	21595
L47647	Creatine kinase B.	7	18	787
M55284	Protein kinase C-L (PRKCL)	7	16	863
X15722	mRNA for glutathione reductase	23	14	794
S54005	Thymosin beta-10	6	13	1476
AB006965	mRNA for Dnm1p/Vps1p-like protein	7	13	4183
M83653	Cytoplasmic phosphotyrosyl protein phosphatase	6	13	2156
X12597	mRNA for high mobility group-1 protein (HMG-1)	7	12	2785
M18112	poly(ADP-ribose) polymerase	6	12	9277
U56816	Kinase Myt1 (Myt1)	4	11	1773
X06233	mRNA for calcium-binding protein in macrophages (MRP-14)	7	11	3007
D85181	mRNA for fungal sterol-C5-desaturase homolog	6	11	3571
M31627	X box binding protein-1 (XBP-1)	5	10	12151

slip. Hybridization was carried out overnight at 65°C inside a hybridization cassette (Telechem, Sunnyvale, CA, USA).

Posthybridization and Cyanine-3 (Cy3™) and Cyanine-5 (Cy5™) TSA

After hybridization, the microarray was washed with 30 mL 0.5× SSC, 0.01% SDS, and then with 30 mL 0.06× SSC, 0.01% SDS. Finally, the microarray was washed with 0.06× SSC. Hybridization signal from biotin-labeled cDNA was amplified with streptavidin-horseradish peroxidase (HRP) and Cy5-tyramide, while hybridization signal from DNP-labeled cDNA was amplified with anti-DNP-HRP and Cy3 tyramide. After signal amplification and posthybridization wash, the cDNA microarray was air-dried and detected with a laser scanner.

Image Acquisition and Data Analysis

Cy3 signal was derived from ovarian cancer cells, and Cy5 signal was derived from HOSE cells. Laser detection of the Cy3 and Cy5 signal on the microarray was acquired with a confocal laser reader, ScanArray® 3000 (GSI Lumonics,

Table 2. Cy3 versus Cy5 Ratio for a Set of Genes that Are Previously Shown to Express at Relatively Constant Level (2)

Accession No.	Description	Before Extensive Washing (Cy3/Cy5)	After Extensive Washing (Cy3/Cy5)
X06323	MRL3 mRNA for ribosomal protein L3 homologue	3.31	5.22
AF006043	3-phosphoglycerate dehydrogenase	3.81	4.8
M37400	Cytosolic aspartate aminotransferase	3.03	3.66
D30655	mRNA for eukaryotic initiation factor 4AII	4.17	3.48
J04208	inosine-5'-monophosphate dehydrogenase (IMP)	1.13	2.15
M17885	Acidic ribosomal phosphoprotein P0	2.74	2.09
X54326	mRNA for glutaminyl-tRNA synthetase	1.17	2.01
J04973	Cytochrome bc-1 complex core protein II	0.98	1.6
D13900	mitochondrial short-chain enoyl-CoA hydratase	0.91	1.52
Z11531	mRNA for elongation factor-1-gamma	0.76	0.89
D78361	mRNA for ornithine decarboxylase antizyme	0.51	0.82
U13261	eIF-2-associated p67 homolog	0.41	0.82
X15183	mRNA for 90-kDa heat-shock protein	0.8	0.75
M36340	ADP-ribosylation factor 1 (ARF1)	0.5	0.66
X91257	mRNA for seryl-tRNA synthetase	0.75	0.52
AF047470	Malate dehydrogenase precursor (MDH) mRNA	0.41	0.51
D13748	mRNA for eukaryotic initiation factor 4AI	0.33	0.43
L36151	Phosphatidylinositol 4-kinase	0.26	0.38
X04297	mRNA for Na,K-ATPase alpha-subunit	0.27	0.34
X79535	mRNA for beta tubulin, clone nuk_278	0.18	0.28
J04173	Phosphoglycerate mutase (PGAM-B)	0.14	0.23

Watertown, MA, USA). Separate scans were taken for each fluor at a pixel size of 10 µm. cDNA derived from the control RNA hybridized to 12 specific spots within the microarray. Cy3 and Cy5 signals from these 12 spots should theoretically be equal and were used to normalize the different efficiencies in labeling and detection with the two fluors. The fluorescence signal intensities and the Cy3/Cy5 ratios for each of the 2400 cDNAs were analyzed by the software Imagene 3.0™ (Biodiscovery, Los Angeles, CA, USA).

Real-Time Quantitative RT-PCR

Real-time PCR was performed in duplicate using primers sets specific to GA733-2, osteopontin, prostasin, creatine kinase B, CEA, KOC, and a housekeeping gene, cyclosporin, in an ABI PRISM™ 5700 Sequence Detector (Applied Biosystems, Foster City, CA, USA). RNA was first extracted form normal ovarian epithelial cell cultures (HOSE 695, 697, 713, and 726) and six ovarian carcinoma cell lines (OVCA3, OVCA432, OVCA433, OVCA633, SKOV3, and ALST). cDNA was generated from 1 µg total RNA using the TaqMan® reverse transcription reagents containing 1× TaqMan reverse transcription buffer, 5.5 mM $MgCl_2$, 500 µM dNTP, 2.5 µM random hexamer, 0.4 U/µL RNase inhibitor, 1.25 U/µL MultiScribe™ reverse transcriptase (Applied Biosystems) in 100 µL. The reaction was incubated at 25°C for 10 min, 48°C for 30 min, and finally at 95°C for 5 min. Briefly, 0.5 µL cDNA was used in a 20-µL PCR mixture containing 1× SYBR® PCR buffer, 3 mM $MgCl_2$, 0.8 mM dNTP, and 0.025 U/µL AmpliTaq Gold® (Applied Biosystems). Amplification was then performed with denaturation for 10 min at 95°C, followed by 40 cycles of denaturation at 95°C for 15 s and annealing/extension

at 60°C for 1 min. The changes in fluorescence of SYBR Green I dye in every cycle was monitored by the ABI 5700 system software, and the threshold cycle (C_T) for each reaction was calculated. The relative amount of PCR products generated from each primer set was determined based on the C_T value. Cyclosporin was used for the normalization of quantity of RNA used. Its C_T value was then subtracted from that of each target gene to obtain a ΔC_T value. The difference ($\Delta\Delta C_T$) between the ΔC_T values of the samples for each gene target and the ΔC_T value of the calibrator (HOSE726) was determined. The relative quantitative value was expressed as $2^{-\Delta\Delta CT}$.

RESULTS AND DISCUSSION

The MICROMAX System

The MICROMAX system allows the simultaneous analysis of the expression level of 2400 known genes. The use of TSA in the MICROMAX system after hybridization reduces the amount of total RNA needed to a few micrograms, which is about 20–100 times less than currently used method. The detail of TSA has been described previously for chromosome mapping of PCR-labeled probes less than 1 kb by FISH (10). In this study, we were able to identify 30 putative differentially overexpressed genes (excluding nine ribosomal genes) in ovarian cancer cell lines (Table 1). Using high-density cDNA array on membrane, Schummer et al. (11) have identified 32 known genes that exhibit tumor-to-HOSE ratios of more than 2.5-fold. Fourteen of these 32 genes were present in the MICROMAX cDNA microarray, but only five of them were more than threefold in our study. This difference may be due to the use of cancer cell lines in our study versus the use of bulk tumor tissues in the study by Schummer et al. (11).

In this study, biotin-labeled cDNA was made from ovarian cancer cell lines, while DNP-labeled cDNA was made from HOSE cells. The differential TSA of the hybridization signal depends on the use of streptavidin-HRP conjugate or anti-DNP-HRP conjugate in a sequential step. At each step, Cy5-Tyramide or Cy3-Tyramide can be added, and the HRP will then catalyze the deposit of Cy3 or Cy5 onto the hybridized cDNA nonspecifically. As a result, we can choose to have either Cy3 or Cy5 signal for the cDNA derived from ovarian cancer cell lines, and vice versa for HOSE cells. Thus, we do not have to make two different sets of probes if we want to compare the effect of Cy3 or Cy5 fluorescence as a result of their differences in extinction coefficients and quantum yields. We also found that the Cy3 and Cy5 signals on the processed slides were stable for more than six months.

Normalization of Signals

The MICROMAX system has three nonhuman genes as internal controls. Each of the control genes has been spotted four times on the microarray. Equal amounts of polyA RNA derived from these control genes were spiked into the total RNA samples derived from both HOSE and ovarian cancer cell lines during cDNA synthesis. Thus, hybridization signals from these control genes in two RNA samples should theoretically be the same. The Cy3-to-Cy5 ratios for these control genes varied from 0.4 to 4.0, and the average ratio was 1.5 ± 1.1 (data not shown). From a prior microarray analysis of human cancer cells, 88 genes have been identified to express at relatively constant levels in many cell types (2). The MICROMAX microarray also contains 58 of these 88 genes and 21 of these genes with a signal-to-noise ratio more than threefold were analyzed (Table 2). The ratios varied from 0.23 to 5.22. The average ratio is 1.6 ± 1.5. Thus, the result of internal control RNA for normalizing signal was similar to that of genes that express at a relatively constant level in different cell types. The set of nonhuman control genes will be useful as control for other custom-designed chips.

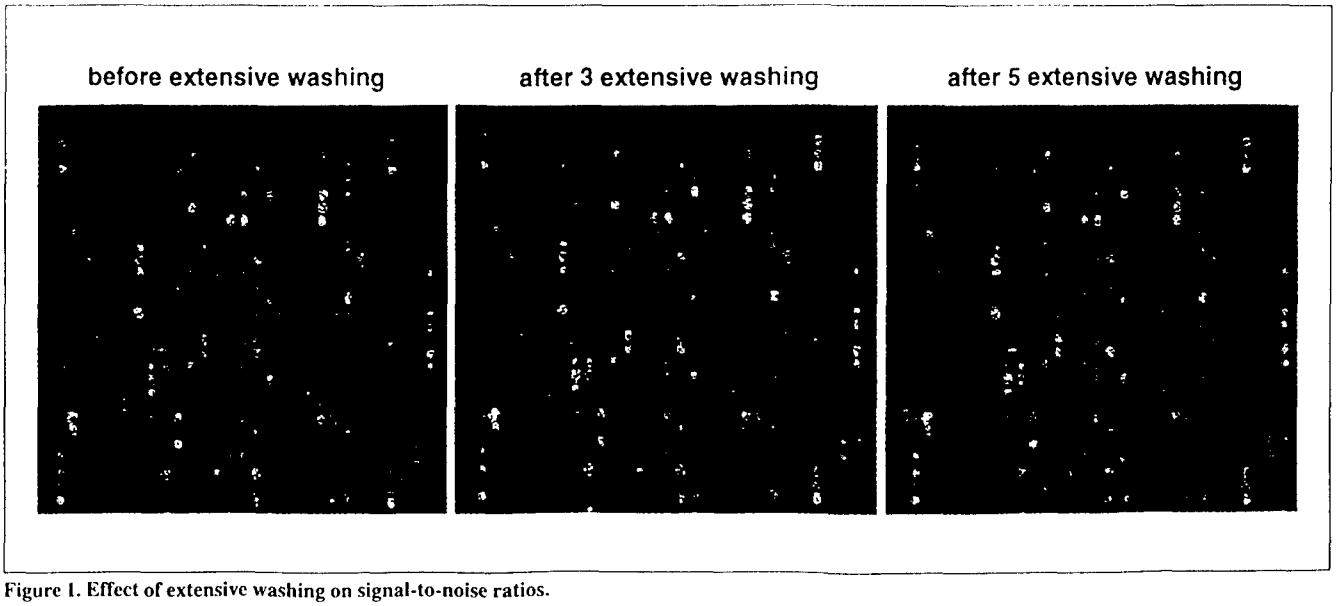

Figure 1. Effect of extensive washing on signal-to-noise ratios.

Table 3. Real-Time Quantitative RT-PCR Analysis of a Few Selected Genes[a]

	GA733-2	Osteopontin	KOC	Prostasin	Creatine kinase B	CEA	RGS
Normal ovarian cells							
HOSE695	4	21	5	28	0.4	5	32
HOSE697	1	1	2	4	0.4	3	18
HOSE713	1	20	7	5	1	16	25
HOSE726	1	1	1	1	1	1	1
Average (HOSE)	2	11	4	9	1	6	19
Ovarian cancer cell lines							
OVCA3	419	6	4	61	393	1	4
OVCA432	136	0	0	17	8	0	1
OVCA433	2048	0	52	57	12	1	4
OVCA633	2917	13777	3	228	4	15	27
SKOV3	2856	265	10	2	31	6	13
ALST	3875	6081	78	10	1	2	5
Average (OVCA)	2042	3355	24	62	75	4	9
OVCA/HOSE (average)	1361	310	6	7	103	1	0.5

[a]Each gene was analyzed using an identical panel of 10 cDNA samples that were comprised off our normal ovarian surface epithelial cells and six ovarian cancer cell lines. The expression of each gene for each cDNA sample was normalized against cyclosporin. Duplicated reactions were performed for each of the genes, and similar results were obtained.

Effect of Background Signal on the Identification of Differentially Expressed Genes

In our study, 1357 of the 2400 genes on the microarray have Cy3 signals (from ovarian cancer cell lines) that were at least twofold higher than the background, or 740 genes have Cy3 signals that were at least threefold higher than the background. After posthybridization washes, there was still significant background intensity for the Cy3 signal (Figure 1) but very low background for Cy5 (data not shown). Subsequently, we washed the microarray again in 30 mL TNT buffer at 42°C for 20 min instead of at room temperature, followed by 30 mL 0.006× SSC for 1 min. The washed microarray was then dried and rescanned. This process was repeated several times until the number of genes with signal-to-noise ratios at least threefold remained the same. The extensive washing steps decreased the background intensity significantly, but there were no obvious changes in the signal intensity. As a result, the number of genes with at least threefold signal-to-noise ratios has increased from 740 to 791 genes. Moreover, the differential expression ratios, in general, have increased as shown in both Table 1 and Table 2. More importantly, after the extensive washing, we were able to detect the differential expression of two weakly expressed genes, thiol-specific antioxidant protein (4.5-fold) and elongation factor-1-β (9.7-fold), which were previously identified by Schummer et al. (11). Thus, we suggest that extensive posthybridization washing and rescanning of signals may be necessary to decrease background signal, especially in the case of differentially expressed genes with low expression level.

Confirmation of Differential Expression by Real-Time Quantitative PCR

To further validate the differential expression, we chose five interesting genes, GA733-2, osteopontin, *koc*, prostasin, and creatine kinase B, for real-time PCR analysis. All of these genes are either surface antigens or secreted proteins. Thus, they may be useful as tumor markers for ovarian cancer. GA733-2 is a cell surface 40-kDa glycoprotein associated with human carcinomas of various origins (13). Osteopontin is a secreted glycoprotein with a conserved Arg-Gly-Asp (RGD) integrin-binding motif and is expressed predominantly in bone but has been found in breast cancer and thyroid carcinoma with enhanced invasiveness (12,15). Prostasin is a novel secreted serine proteinase that was originally identified in seminal fluid (16). The *koc* transcript is highly overexpressed in pancreatic cancer cell lines and in pancreatic cancer. It is speculated that koc may assume a role in the regulation of tumor cell proliferation by interfering with tran-

scriptional and or posttranscriptional processes (8). Creatine kinase B is a serum marker associated with renal carcinoma and lung cancer (4,14). Moreover, two randomly selected genes, CEA and RGS, were used as negative controls.

The results (Table 3) showed that all the tested ovarian cancer cell lines expressed higher levels of GA733-2. However, osteopontin, prostasin, KOC, and creatine kinase B were overexpressed in only some of the cancer cell lines. Since we were using pools of RNA, the differential expression that we have observed is an average of the gene expression from three independent HOSE cells or three different cancer cell lines. This strategy allows us to capture genes that overexpress in either some or all of the cell lines. Genes that only overexpress in some of the ovarian cancer cell lines may be useful for molecular classification of ovarian cancer cells. Since as little as 10 pg cDNA is enough for real-time quantitative RT-PCR, RNA extracted from microdissected tissue would be enough for thousands of such real-time quantitative RT-PCR analyses.

ACKNOWLEDGMENTS

This work is partly supported by Laboratory Directed Research and Development from Department of Energy under contract no. DE-AC06-76RLO 1830, and by Department of Defense under contract no. DAMD17-99-1-9563. We also thank Dr. Walter Tian for reading the manuscript.

REFERENCES

1. **Boring, C.C., T.S. Squires, T. Tong and S. Montgomery.** 1994. Cancer statistics, 1994. Cancer J. Clin. *44*:7-26.
2. **DeRisi, J., L. Penland, P.O. Brown, M.L. Bittner, P.S. Meltzer, M. Ray, Y. Chen, Y.A. Su and J.M. Trent.** 1996. Use of a cDNA microarray to analyse gene expression patterns in human cancer. Nat. Genet. *14*:457-460.
3. **Iyer, V.R., M.B. Eisen, D.T. Ross, G. Schuler, T. Moore, J.C.F. Lee, J.M. Trent, L.M. Staudt, J. Hudson, Jr., M.S. Boguski, D. Lashkari, D. Shalon, D. Botstein and P.O. Brown.** 1999. The transcriptional program in the response of human fibroblasts to serum. Science *283*:83-287.
4. **Kurtz, K.J. and R.D. Nielsen.** 1985. Serum creatine kinase BB isoenzyme as a diagnostic aid in occult small cell lung cancer. Cancer *56*:562-566.
5. **Mok, S.C., W.Y. Chan, K.K. Wong, K.K. Cheung, C.C. Lau, S.W. Ng, A. Baldini, C.V. Colitti, C.O. Rock and R.S. Berkowitz.** 1998. DOC-2, a candidate tumor suppressor gene in human epithelial ovarian cancer. Oncogene *16*:2381-2387.
6. **Mok, S.C., W.Y. Chan, K.K. Wong, M.G. Muto and R.S. Berkowitz.** 1996. SPARC, an extracellular matrix protein with tumor-suppressing activity in human ovarian epithelial cells. Oncogene *12*:1895-1901.
7. **Mok, S.C., K.K. Wong, R.K. Chan, C.C. Lau, S.W. Tsao, R.C. Knapp and R.S. Berkowitz.** 1994. Molecular cloning of differentially expressed genes in human epithelial ovarian cancer. Gynecol. Oncol. *52*:247-252.
8. **Mueller-Pillasch, F., U. Lacher, C. Wallrapp, A. Micha, F. Zimmerhackl, H. Hameister, G. Varga, H. Friess, M. Buchler, H.G. Beger, M.R. Vila, G. Adler and T.M. Gress.** 1997. Cloning of a gene highly overexpressed in cancer coding for a novel KH-domain containing protein. Oncogene *14*:2729-2733.
9. **Schena, M., D. Shalon, R.W. Davis and P.O. Brown.** 1995. Quantitative monitoring of gene expression patterns with a complementary DNA microarray. Science *270*:467-470.
10. **Schriml, L.M., H.M. Padilla-Nash, A. Coleman, P. Moen, W.G. Nash, J. Menninger, G. Jones, T. Ried and M. Dean.** 1999. Tyramide signal amplification (TSA)-FISH applied to mapping PCR-labeled probes less than 1 kb in size. BioTechniques *27*:608-611.
11. **Schummer, M., W.V. Ng, R.E. Bumgarner, P.S. Nelson, B. Schummer, D.W. Bednarski, L. Hassell, R.L. Baldwin, B.Y. Karlan and L. Hood.** 1999. Comparative hybridization of an array of 215000 ovarian cDNAs for the discovery of genes overexpressed in ovarian carcinomas. Gene *238*:375-385.
12. **Sharp, J.A., V. Sung, J. Slavin, E.W. Thompson and M.A. Henderson.** 1999. Tumor cells are the source of osteopontin and bone sialoprotein expression in human breast cancer. Lab. Invest. *79*:869-877.
13. **Szala, S., M. Froehlich, M. Scollon, Y. Kasai, Z. Steplewski, H. Koprowski and A.J. Linnenbach.** 1990. Molecular cloning of cDNA for the carcinoma-associated antigen GA733-2. Proc. Natl. Acad. Sci. USA *87*:3542-3546.
14. **Takashi, M., Y. Zhu, S. Hasegawa and K. Kato.** 1992. Serum creatine kinase B subunit in patients with renal cell carcinoma. Urol. Int. *48*:144-148.
15. **Tuck, A.B., D.M. Arsenault, F.P. O'Malley, C. Hota, M.C. Ling, S.M. Wilson and A.F. Chambers.** 1999. Osteopontin induces increased invasiveness and plasminogen activator expression of human mammary epithelial cells. Oncogene *18*:4237-4246.
16. **Yu, J.X., L. Chao and J. Chao.** 1994. Prostasin is a novel human serine proteinase from seminal fluid. Purification, tissue distribution, and localization in prostate gland. J. Biol. Chem. *269*:18843-18848.

Address correspondence to Dr. Kwong-Kwok Wong, Molecular Biosciences, P7-56, Pacific Northwest National Laboratory, 902 Battelle Boulevard, Richland, WA 99352, USA, e-mail: kk.wong@pnl.gov

[CANCER RESEARCH 61, 6768–6776, September 15, 2001]

Expression of Gonadotropin Receptor and Growth Responses to Key Reproductive Hormones in Normal and Malignant Human Ovarian Surface Epithelial Cells[1]

Viqar Syed, Gregory Ulinski, Samuel C. Mok, Gary K. Yiu, and Shuk-Mei Ho[2]

Department of Surgery, Division of Urology [V. S., G. U., S-M. H.] and Department of Cell Biology [S-M. H.], University of Massachusetts Medical School, Worcester, Massachusetts 01655, and Laboratory of Gynecologic Oncology, Department of Obstetrics, Gynecology and Reproductive Biology, Brigham and Women's Hospital, Harvard Medical School Boston, Massachusetts 02115 [S. C. M., G. K. Y.]

ABSTRACT

Epidemiological data have implicated reproductive hormones as probable risk factors for ovarian cancer (OCa) development. Although pituitary and sex hormones have been reported to regulate OCa cell growth, no information is available regarding whether and how they influence normal ovarian surface epithelial (OSE) cell proliferation. To fill this data gap, this study has compared cell growth responses to gonadotropins and sex steroids in primary cultures of human OSE (HOSE) cells with those observed in immortalized, nontumorigenic HOSE cells and in OCa cell lines. Both malignant and normal cell lines/cultures responded equally well to the stimulatory actions of luteinizing hormone and follicle-stimulating hormone and to 17β-estradiol and estrone, although the latter estrogen has a much lower affinity for estrogen receptor than does the former estrogen. In normal HOSE cell cultures/lines, 5α-dihydrotestosterone was found to be more effective than testosterone in stimulating cell growth, but in OCa cell lines, 5α-dihydrotestosterone and testosterone are equally potent. One OCa cell line, OVCA 433, was found to be nonresponsive to androgen stimulation. In general, primary cultures of normal HOSE cells exhibited the greatest hormone-stimulated growth responses (>10-fold enhancement), followed by immortalized HOSE cell lines (4–5-fold enhancement) and by OCa cell lines (2–4-fold enhancement). Interestingly, progesterone (P4), at low concentrations (10^{-11} to 10^{-10} M), was stimulatory to HOSE and OCa cell growth, but at high doses (10^{-8} to 10^{-6} M), P4 exerted marked inhibitory effects. In all cases, cotreatment of a cell culture/line with a hormone and its specific antagonist blocked the effect of the hormone, confirming specificity of the hormonal action. Taken together, these data support the hypothesis that reproductive states associated with rising levels of gonadotropins, estrogen, and/or androgen promote cell proliferation in the normal OSE, which favors neoplastic transformation. Conversely, those states attended by high levels of circulating P4, such as that seen during pregnancy, induce OSE cell loss and offer protection against ovarian carcinogenesis.

INTRODUCTION

OCa[3] varies widely in frequency among different geographic regions and ethnic groups, with high incidences observed in the Scandinavia, Western Europe, and North American and low incidences found in Asian countries (1). The majority of cases are sporadic, whereas about 5–10% of OCa cases are familial. Although all cell types of the human ovary may undergo neoplastic transformation, the vast majority (80–90%) of benign and malignant tumors are derived from the OSE and its cystic derivatives (2). The origin of OSE could be traced to the mesothelium of the embryonic gonads, or the Mullerian epithelium; therefore, ovarian tumors often resemble those of the fallopian tube, endometrium, and endocervix (2, 3).

Although the etiology of OCa remains poorly understood, evidence is mounting to indicate the involvement of gonadotropins and/or sex hormones in its etiology. Because OCa incidence increases dramatically in women above the age of 45 years and peaks at 10–20 years after menopause, it has been suggested that elevated levels of gonadotropins during this reproductive period are risk factors for the cancer (4–7). The gonadotropin theory is further supported by several case studies reporting development of OCa shortly after ovulation induction with fertility drugs such as clomiphene citrate or gonadotropins (7, 8). It has also been proposed that entrapment of OSE cells in inclusion cysts increases the odds of OSE neoplastic transformation, possibly due to exposure of these cells to a stromal hormonal milieu rich in androgens (2, 9, 10). In support of the androgen theory is the observation that women with polycystic ovary syndrome have a higher risk of developing OCa, which is likely attributable to the higher levels of androgen present in their circulation. With regard to estrogens, earlier data are in inconclusive in demonstrating a positive relationship between estrogen usage and OCa risk (11–15). However, recent large-scale epidemiological studies (16–18) consistently demonstrate that postmenopausal usage of estrogen elevates OCa incidence in a manner dependent on usage duration. Finally, epidemiological data have established pregnancy, particularly one that occurs in late life, as a protective factor against OCa development (19). These findings, in conjunction with laboratory studies (20, 21) demonstrating induction of apoptosis in OCa cell lines by P4, raise the possibility that progestins are protective against ovarian carcinogenesis. Taken together, these theories strongly argue for major roles played by reproductive hormones, such as those associated with the female cycle, pregnancy, perimenopause, and postmenopause, in ovarian carcinogenesis.

According to modern concept of hormonal carcinogenesis (22), endogenous and exogenous hormones enhance cell proliferation and thus enhance the opportunity for the accumulation of random genetic errors and the emergence of malignancy. Previous studies on hormones and OCa were focused primarily on the effects of pituitary and/or sex hormones on OCa cell growth (23–38). To the best of our knowledge, no information is available regarding whether and how key reproductive hormones regulate the growth of normal OSE cells. Answers to these questions are critical to our understanding of hormone-induced tumor initiation in the OSE. To fill this data gap, in this study, we have simultaneously compared the impacts exerted by gonadotropins and key sex steroids on primary cultures of HOSE cells with those observed in immortalized, nontumorigenic HOSE cells (39, 40) and in OCa cell lines (39). Because women are exposed to a great variety of endogenous hormones at wide concentration ranges during their lifetime, we have chosen to study the growth responses of HOSE/OCa cells to the predominant premenopausal estrogen, E_2, the major postmenopausal estrogen, E_1, the circulating androgen, T, the cellular androgen, DHT, the pregnancy hormone P4, and the gonadotropins FSH and LH at a wide dose range (10^{-11} to 10^{-6} M). Direct

Received 4/12/01; accepted 7/17/01.

The costs of publication of this article were defrayed in part by the payment of page charges. This article must therefore be hereby marked *advertisement* in accordance with 18 U.S.C. Section 1734 solely to indicate this fact.

[1] Supported by Army Ovarian Cancer Research Program Grant DAMD17-99-1-9563 (to S. C. M. and S-M. H.) and NIH Grant CA78523 (to S. C. M.). Part of this work will be used to fulfill Gregory Ulinski's Master Degree Dissertation requirement at the Worcester Polytechnic Institute (Worcester, MA).

[2] To whom requests for reprints should addressed, at Department of Surgery, University of Massachusetts Medical School, 55 Lake Avenue North, Worcester, MA 01655. Phone: (508) 856-1909; Fax: (508) 856-8699; E-mail: shuk-mei.ho@umassmed.edu.

[3] The abbreviations used are: OCa, ovarian cancer; OSE, ovarian surface epithelial; HOSE, human OSE; LH, luteinizing hormone; LH-R, LH receptor; FSH, follicle-stimulating hormone; FSH-R, FSH receptor; RT-PCR, reverse transcription-PCR; E_1, estrone; E_2, 17β-estradiol; T, testosterone; DHT, 5α-dihydrotestosterone; P4, progesterone; FBS, fetal bovine serum; MTT, 3-(4,5-dimethylthiazol-2-yl)-2,5-diphenyltetrazolium bromide; PKA, protein kinase A; AR, androgen receptor; ERT, estrogen replacement therapy.

cell counting or a surrogate cell proliferation assay was used to quantify cell growth responses, and specific hormone antagonists were used to demonstrate specificity. Semiquantitative RT-PCR was used to demonstrate expression of FSH-R and LH-R in normal HOSE cells for the first time. Our data now show that gonadotropins, estrogens, and androgens are positive regulators of HOSE and OCa cell growth, whereas P4 is a negative regulator for both cell types.

MATERIALS AND METHODS

Primary Cell Cultures and Cell Lines. Four normal primary HOSE cell cultures (HOSE 693, HOSE 770, HOSE 783, and HOSE 785), four immortalized normal HOSE cell lines (HOSE 642, HOSE 301, HOSE 306, and HOSE 12-12), and four OCa cell lines (OVCA 420, OVCA 429, OVCA 432, and OVCA 433) were used in this study. The normal HOSE cell primary cultures, HOSE 693, HOSE 770, HOSE 783, and HOSE 785, were obtained from surface scrapings of normal ovaries removed from a 32-year-old patient with adenocarcinoma of the cervix, a 42-year-old patient with moderately differentiated squamous cell carcinoma of the cervix, a 42-year-old patient with leiomyoma, and a 72-year-old patient with inflamed bladder mucosa, respectively. The immortalized normal HOSE cell lines, HOSE 642, HOSE 301, HOSE 306, and HOSE 12-12, were established by human papillomavirus E6/E7 immortalization (39) of normal HOSE cells obtained from a 46-year-old patient with normal tissue, a 47-year-old patient with endometrioid adenocarcinoma of the ovary, a 53-year-old patient with breast cancer, and 39-year-old patient with ovarian stromal hyperplasia, respectively. OCa cell lines (OVCA 420, OVCA 429, OVC A432, and OVCA 433) were established cell lines derived from freshly isolated ascites or tumor explants obtained from patients with late-stage serous ovarian adenocarcinomas according to Tsao *et al.* (39). The epithelial nature of the HOSE cell primary cultures and the HOSE cell lines was verified by immunostaining for K7, K8, K18, and K19 cytokeratins and vimentin as described previously (39). The HOSE cell primary cultures and immortalized cell lines exhibited uniform epithelial-like morphology; immunopositivity for cytokeratins K7, K8, K18, and K19; and immunonegativity for vimentin. The immortalized HOSE cell lines were shown to be nontumorigenic in nude mice and express no CA-125 (39). In addition, they responded to transforming growth factor β-induced growth inhibition (39). In contrast, the OCa cell lines (OVCA 420, OVCA 429, OVCA 432, and OVCA 433) expressed high levels of CA-125 and failed to respond to transforming growth factor β-induced growth arrest (39).

These cell lines were cultured and maintained at 37°C in a 5% CO_2 humidified atmosphere in medium 199 (Sigma Chemical Co., St. Louis, MO) and MCDB 105 (1:1; Sigma Chemical Co.) supplemented with 10% FCS (Sigma Chemical Co.), 100 units/ml penicillin (Sigma Chemical Co.), and 100 μg/ml streptomycin (Sigma Chemical Co.) under 5% CO_2. Normal and malignant cells grown in this medium after two or more passages exhibited uniform epithelium-like morphology.

Cell Proliferation Assay. Cell lines or primary cultures cultured in medium 199:MCDB 105 (1:1) were harvested when they reached 80% confluence, washed twice in PBS, and then plated into the wells of 96-well microculture plates at a density of 1000 cells/well in medium containing 10% activated charcoal (Sigma Chemical Co.)/dextran-70 (Pharmacia)-treated FBS. Forty-eight h after cell plating, the medium was replaced with the same medium containing either human FSH (Calbiochem, San Diego, CA; purity, 99%; contamination with growth factors, <1%), human LH (Calbiochem; purity, 99%; contamination with growth factors, <1%), E_2 (Sigma Chemical Co.), E_1 (Sigma Chemical Co.), DHT (Sigma Chemical Co.), T (Sigma Chemical Co.), or P4 (Sigma Chemical Co.). To study the synergistic action of FSH and E_2 on cell growth, cells were cultured with a combination of E_2 and FSH. Steroids were solubilized in absolute ethanol. The exposure concentrations ranged from 10^{-11} to 10^{-6} M for each hormone. The final concentration of ethanol in the medium was 0.1%. The control cells were exposed to ethanol vehicle without the testing hormone. The cells were treated with hormones for 5 days, with a fresh addition of hormone to ensure stable bioavailability. Because DHT was metabolized rapidly, cells were subjected to DHT treatment every 12 h. Cell proliferation was measured by a MTT cell proliferation kit (Roche Diagnostics, Indianapolis, IN). After the incubation period, 10 μl of the MTT labeling reagent (final concentration, 0.5 mg/ml) were added to each well, and plates were incubated for 4 h in a humidified atmosphere. Finally, 100 μl of solubilization solution were added to each well, and plates were incubated overnight at 37°C. Cell growth was measured based on the cellular conversion of a tetrazolium compound to a colored formazan product over a period of 18 h. At the end of the incubation period, the amount of formazan formed was measured as absorbance at 570 nm in a spectrophotometer to determine the cell number in each well. Assays were performed in triplicate to generate mean values for the control and for each treatment group. Cell number, as measured by the rate of formazan formation, in control wells with untreated cells was arbitrarily assigned a value of 1. Relative cell growth was expressed as the fold increase over control untreated cultures. Data points in all figures are group mean values ± SDs from three separate experiments.

Treatment of Normal and Malignant HOSE Cells with Hormones in the Absence and Presence of Hormone Receptor Antagonists. Primary cultures of normal HOSE cells (HOSE 693, HOSE 770, HOSE 783, and HOSE 785), immortalized normal HOSE cell lines (HOSE 642, HOSE 301, HOSE 306, and HOSE 12-12), and OCa cell lines (OVCA 420, OVCA 429, OVCA 432, and OVCA 433) were seeded at 2×10^5 cells/T-25 flask (Falcon; Becton Dickinson Labware, Bedford, MA; 25-cm^2 culture area), allowed to attach during a 24-h period, and exposed to 10^{-8} M of either FSH, LH, E_2, T, or P4 in the presence or absence of the respective receptor or signaling antagonist. This dose was selected based on the results obtained from the cell proliferation assay, which demonstrated that for all hormones tested, this dose was at the midpoint of the dose-response curve. Two doses of receptor antagonist were used to block the action of the hormone. For FSH and LH, concentrations of 10^{-5} and 10^{-4} M of the PKA-selective inhibitor H89 (*N*-[2-(*p*-bromocinnamli)ethyl]-5-isoquinolinessulfonamide; 2HCL; Calibiochem) were added 30 min before treatment with 10^{-8} M of the gonadotropins. H89 has been shown to be a specific inhibitor of PKA (K_i value, 0.048 μM) and to effectively block FSH and LH action at 10^{-4} M (41). For sex steroids, receptor-specific antagonists were used. A low (10^{-5} M) and a high (10^{-4} M) concentration of ICI 182,780 (a generous gift from Zeneca Pharmaceuticals, Macclesfield, United Kingdom), a pure estrogen receptor antagonist (42), 4-hydroxy flutamide (Schering, Kenilworth, NJ), an AR antagonist (43), or RU 38486 (Sigma Chemical Co.), a specific P4 receptor antagonist (44), were used to inhibit the action of E_2, T, or P4, respectively. The dosages of an antihormone used were based on literature reports of effective receptor antagonistic effect. The cell cultures were treated daily with hormones and hormone antagonists for a period of 5 days. After the treatment period, cell growth was determined by direct cell count on multiple aliquots of the cultures. Each experiment was carried out twice. The results are the means of two independent experiments.

RNA Isolation and Semiquantitative RT-PCR. Untreated normal and malignant HOSE cells were harvested from cell cultures when they reached approximately 70–80% confluence. Total cellular RNA was isolated using Tri reagent (Sigma Chemical Co.) according to protocols provided by the manufacturer. Multiple cautionary steps were routinely taken to ensure RNA quality and linearity of the semiquantitation method. The quality of each cellular RNA sample was checked carefully and controlled by the following steps: (*a*) measurement of absorbance at 260 and 280 nm; (*b*) running of a denaturing RNA gel capable of detecting possible RNA degradation, as judged by the integrity and intensity of the 18S and the 28S rRNA signals; and (*c*) conducting semiquantitative RT-PCR amplification of the 18S rRNA at low cycle numbers to ensure RNA quality and linearity of transcript quantification.

To investigate the relative expression levels of FSH-R and LH-R mRNA, semiquantitative RT-PCRs were performed. The oligonucleotide primers used to amplify human FSH-R and LH-R cDNA were previously published sequences (45, 46). The forward primer sequence for FSH-R amplification was 5′-GAGAGCAAGGTGACAGAGATTCC-3′ (nucleotides 97–120), and the reverse primer sequence was 5′-CCTTTGGAGAGAATGAATCTT-3 (nucleotides 417–439). For human LH-R amplification, the sense primer was 5′-CTTGGATATTTCCCACACAAA-3′ (nucleotides 676–698), and the antisense primer was 5′-TGGCATGGTTATAGTACTGGC-3′ (nucleotides 1270–1290). For amplification of human 18 S rRNA, the sense primer was 5′-TGAGGCCATGATTAAGAGGG-3′, and the antisense primer was 5′-CGCTGAGCCAGTCAGTGTAG-3′. The amplimers from cDNA of FSH-R, LH-R, and 18S ribosomal mRNA were 343, 615, and 623 bp, respectively.

An equal amount of total RNA (1–3 μg) from the cellular total RNA sample was reverse-transcribed into cDNA using the GeneAmp RNA PCR kit (Perkin-Elmer, Foster City, CA). Aliquots (1–2 μl of 50 μl) of cDNA were subjected

to hot-start PCR using AmpliTaq Gold DNA polymerase (Perkin-Elmer). The enzyme was activated by preheating the reaction mixtures at 95°C for 6 min before thermal cycling. This protocol was chosen to minimize nonspecific product amplification. Initially, to determine the conditions under which PCR amplification for FSH-R, LH-R, and 18S ribosomal mRNA was in the logarithmic phase, different amounts of total RNA were reverse transcribed, and aliquots were amplified using a different number of cycles. A linear relationship was observed between the amount of RNA and PCR products when 3 μg of total RNA were used in the reverse transcription reaction and when 35, 30, and 18 PCR amplification cycles were performed for FSH-R, LH-R, and 18S rRNA, respectively. PCR for 18S rRNA was used as a control to rule out the possibility of RNA degradation and to control the variation in mRNA concentration in the RT reaction. The PCR program was 1 min at 94°C, 1 min at 60°C (annealing temperature), and 1 min at 72°C. mRNA-specific modifications included an annealing temperature of 58°C for amplification of FSH-R cDNA and an annealing temperature of 55°C for amplification of LH-R. The PCR products were fractionated on a 2% agarose gel and visualized by ethidium bromide staining. The fluorescence images were visualized under UV transillumination, captured on 665 negative film (Polaroid Co., Cambridge, MA), and converted into digitized signals with an image scanner, and the intensities of each band, which were derived from the area under each peak, were quantified by ImageQuant (Molecular Dynamics, Sunnyvale, CA). Signal intensities of FSH-R and LH-R amplimers were normalized to those of 18S rRNA products. Message levels were expressed as the ratio of the signal intensity of the PCR product of the receptor message to that of the 18S rRNA to produce arbitrary units of relative abundance. The reproducibility of the quantitative measurements was evaluated by three independent cDNA synthesis and PCR runs from each preparation of RNA. The means of the replicated measurements were calculated and are shown in the figures.

Statistical Analyses. Statistical analysis was carried out using ANOVA, followed by Tukey's *post hoc* test. Values are presented as the mean ± SD and are considered significant at $P < 0.05$.

RESULTS

Transcripts of FSH-R and LH-R Are Expressed in Normal and Malignant HOSE Cells. The expression of FSH-R mRNA and LH-R mRNA in normal and malignant HOSE cells was investigated by semiquantitative RT-PCR. RT-PCR analyses of total cellular RNA prepared from four primary cultures of normal HOSE cells, four immortalized normal HOSE cell lines, and four OCa cell lines revealed that transcripts of FSH-R and LH-R were present in all cell cultures/lines (Fig. 1, *A* and *C*). Relative FSH-R mRNA expression levels in the four OCa cell lines were higher than those found in normal HOSE cells in primary cultures or in immortalized cell lines (Fig. 1*B*). Conversely, relative LH-R mRNA expression levels in normal HOSE cell cultures/lines were higher than those observed in OCa cell lines (Fig. 1*D*). Nonetheless, the differences in receptor expression levels between normal and malignant HOSE cell lines were not dramatic.

Because we have used four different cell lines in each group, a representative cell line from each group (primary cultures, immortalized normal HOSE cells, and OCa cells) is shown in Figs. 2–5. In addition to the representative cell lines, any cell line that showed divergence in response to hormones compared with the other cell lines in the group is shown under the respective group.

FSH and LH Are Equally Potent in Stimulating Normal and Malignant HOSE Cell Growth. The effects of a 5-day treatment with FSH or LH at a dose range between 10^{-11} and 10^{-6} M on the proliferation of normal and malignant HOSE cells were investigated. FSH and LH enhanced cell proliferation in primary cultures of normal HOSE cells (HOSE 693, HOSE 770, HOSE 783, and HOSE 785), in immortalized normal HOSE cell lines (HOSE 642, HOSE 301, HOSE 306, and HOSE 12-12), and in OCa cell lines (OVCA 420, OVCA 429, OVCA 432, and OVCA 433) compared with cell growth in the absence of hormonal stimulation. A representative cell line from primary cultures (HOSE 770), immortalized normal HOSE cells (HOSE 642), and OCa cell lines (OVCA 420) is shown in Fig. 2*A*. The hormone-induced cell growth exhibited a clear dose dependency, and both gonadotropins were found to be equally potent in stimulating cell growth in all cell cultures/lines. However, in the immortalized HOSE 12-12 cell lines, FSH might be more effective than LH in stimulating cell growth (Fig. 2*A*). Although gonadotropin significantly enhanced cell growth of all normal and cancerous HOSE cell cultures/lines, normal HOSE cells in primary cultures exhibited the best responses (8–14-fold increases), followed by those displayed in

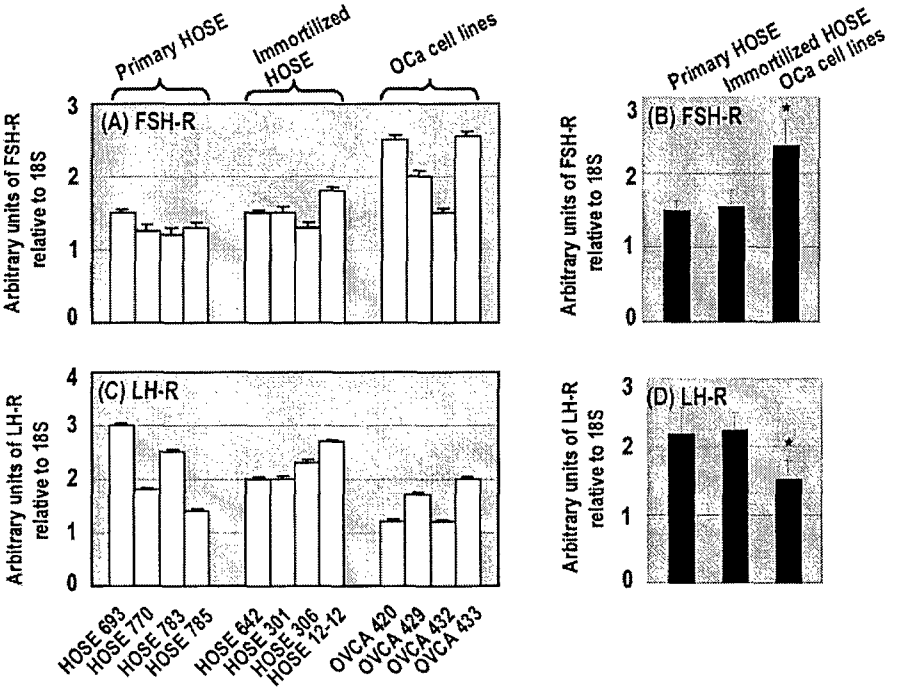

Fig. 1. Detection of mRNA for human FSH-R and human LH-R transcripts in total RNA samples from normal primary, normal immortalized, and malignant HOSE cell lines. Four normal primary (HOSE 693, HOSE 770, HOSE 783, and HOSE 785), normal immortalized (HOSE 642, HOSE 301, HOSE 306, and HOSE 12-12), and malignant OSE cell lines (OVCA 420, OVCA 429, OVCA 432, and OVCA 433) were used to isolate total RNA. Semiquantitative RT-PCRs were performed as described in "Material and Methods." *Open columns* represent the relative abundance of (*A*) FSH-R mRNA and (*C*) LH-R mRNA in individual primary HOSE cell cultures, immortalized HOSE cell lines, and OCa cell lines. Three independent RT-PCRs were performed with total RNA of primary HOSE cell cultures, immortalized HOSE cell lines, and OCa cell lines. Relative mRNA levels were expressed as arbitrary units derived from signal intensities of ethidium bromide-stained PCR products of the target cDNA normalized to those of 18S rRNA cDNA. The *open columns* and *error bars* represent the mean relative mRNA abundance ± SD ($n = 3$). The *black columns* represent group means of FSH-R (*B*) and LH-R (*D*) mRNA levels of all four primary HOSE cultures, four immortalized HOSE cell lines, and four OCa cell lines in each group. The data are shown as the means ± SD. *, statistically significant difference between mean transcript levels in OCa cell lines and those observed in primary HOSE cell cultures at $P < 0.05$.

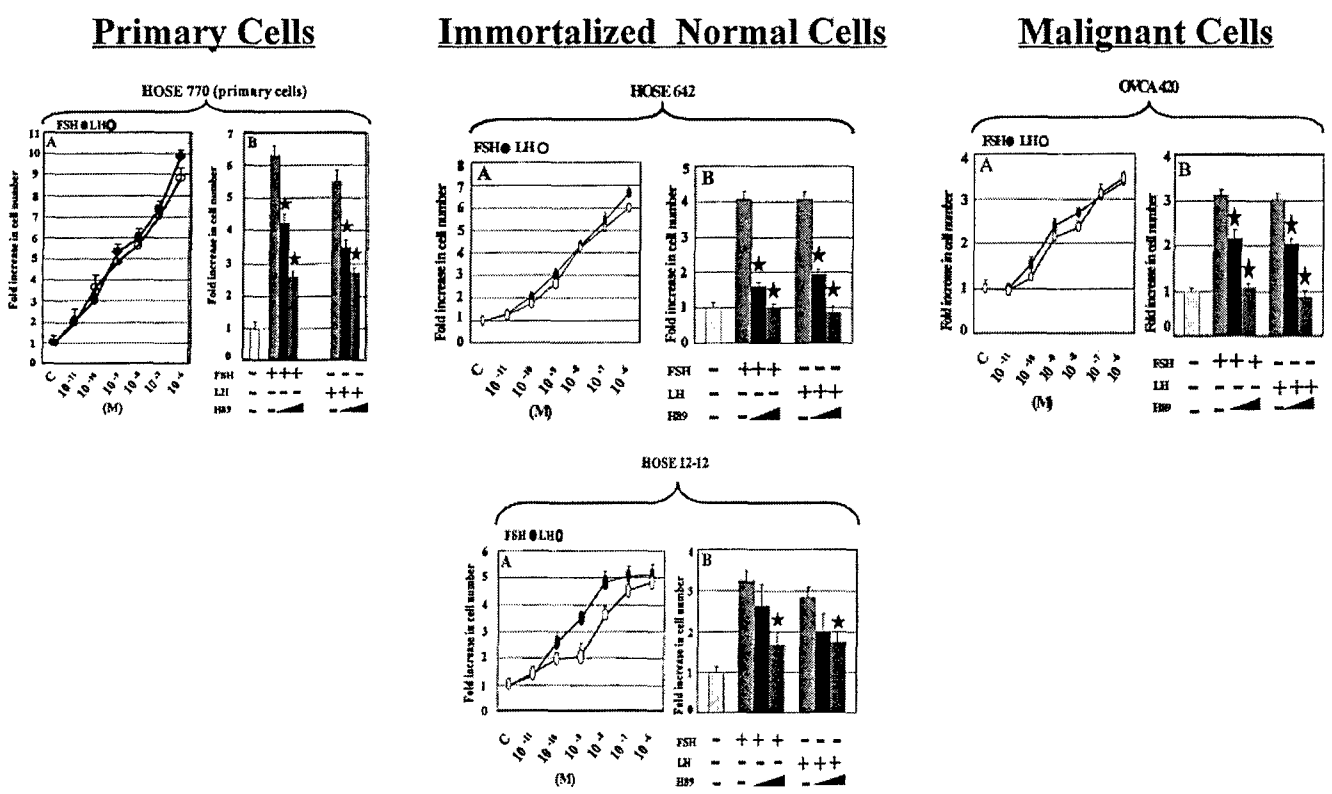

Fig. 2. Effect of FSH and LH on cell proliferation in normal primary HOSE, immortalized HOSE, and OCa cells. Representative cell lines from each group and any cell line that showed divergence from the other cell lines in a group are shown under the representative cell line. Primarily HOSE (HOSE 693, HOSE 770, HOSE 783, and HOSE 785), immortalized HOSE (HOSE 642, HOSE 301, HOSE 306, and HOSE 12-12), and malignant OCa (OVCA 420, OVCA 429, OVCA 432, and OVCA 433) cells were cultured at a density of (*A*) 1000 cells/well in a 96-well plate in medium 199:MCDB 105 supplemented with 10% FBS (heat-inactivated, charcoal-stripped FBS) and 100 units/ml penicillin-streptomycin for MTT assay. After preincubation for 48 h, the cells were treated with different concentrations (10^{-11} to 10^{-6} M) of FSH (●) or LH (○) for 5 days. The cell growth was assessed by MTT assay as described in "Materials and Methods." The absorbance of wells not exposed to hormones was arbitrarily set as 1, and FSH- and LH-treated cell growth was expressed as the fold increase compared with the control. The representative cell line from primary HOSE (HOSE 770), immortalized HOSE (HOSE 642), and malignant OCa (OVCA 420) is shown. The immortalized HOSE line (HOSE 12-12) that showed divergence from the other lines in the group is shown under the representative cell line. *B*, to confirm the specificity of FSH and LH, 2×10^5 cells/T-25 flask were cultured alone (□) or cotreated with 10^{-8} M of either FSH or LH (▨) and two doses of the PKA inhibitor H89 (10^{-5} M, ■; ▤, 10^{-4} M) for 5 days. The control cells were treated with vehicle. After 5 days, the number of cells was counted. Treatment of cells with FSH and LH induced proliferation of cells in a dose-dependent manner. Cotreatment with PKA blocker H89 abolished the response of normal HOSE cells to gonadotropins. The data are shown as the mean of two experiments with triplicate samples and represent the mean ± SD. *, $P < 0.05$.

immortalized normal HOSE cell lines (5–7-fold increases) and in OCa cell lines (3–4-fold increases; results not shown).

It is now well accepted that gonadotropins interact with their cognate receptors and activate a stimulatory G-protein that leads to an induction of cyclic AMP, followed by activation of PKA and subsequent biological responses. To ascertain whether the observed gonadotropin-stimulated cell growth is mediated via a receptor-triggered PKA signaling pathway, cell cultures/lines were treated with FSH or LH (at 10^{-8} M) for 5 days in the presence or absence of a PKA-selective antagonist, H89 (at either 10^{-5} or 10^{-4} M). Exposure of cells to H89 abolished the gonadotropin-induced cell growth enhancement in normal and malignant HOSE cell cultures/lines in a manner dependent on the dose of the PKA antagonist (Fig. 2*B*). Furthermore, H89 by itself had no effect on cell growth.

E_2 and E_1 Are Equally Effective in Stimulating Normal and Malignant HOSE Cell Growth. When increasing concentrations (10^{-11} to 10^{-6} M) of E_1 or E_2 were added to primary cultures of normal HOSE cells (HOSE 639, HOSE 783, HOSE 785, and HOSE 770; HOSE 770, representative cell line shown in Fig. 3*A*), immortalized normal HOSE cell lines (HOSE 642, HOSE 301, HOSE 306, and HOSE 12-12; HOSE 642, representative cell line shown in Fig. 3*A*), and OCa cell lines (OVCA 420, OVCA 429, OVCA 432, and OVCA 433; OVCA 420, representative cell line shown in Fig. 3*A*), a dose-dependent increase in cell growth was observed in cell cultures challenged with an estrogen. An approximately 10–14-fold increase in cell growth was noted in primary cultures of normal HOSE cells exposed to the highest concentration (10^{-6} M) of E_1 or E_2 (results not shown). In contrast, both estrogens at this dose only induced a 6-fold increase in cell growth in immortalized normal HOSE cell lines and a 3–4-fold increase in cell growth in OCa cell lines (results not shown). E_1 and E_2 were equally effective in enhancing cell proliferation in all cell lines studied, with the exception of HOSE 12-12 cells, which responded better to E_1 than to E_2 (Fig. 3*A*). Simultaneous treatment of cell cultures/lines with E_2 and FSH induced no additive effect on enhancement of cell growth (results not shown).

When normal and malignant HOSE cells were exposed to a 5-day treatment with 10^{-8} M E_2 in the presence or absence of ICI 182,780 (10^{-5} or 10^{-4} M), a marked attenuation in E_2-induced growth enhancement was observed in cultures exposed to the antiestrogen (Fig. 3*B*). ICI 182,780 is recognized as a pure antiestrogen, and it has been shown to inhibit the action of both estrogen receptor-α and estrogen receptor-β (44).

Differential Responsiveness of Normal and Malignant HOSE Cells to DHT- and T-induced Cell Growth Enhancement. Testosterone and DHT significantly stimulated cell growth in primary cultures of normal HOSE cells (HOSE 639, HOSE 783, HOSE 785, and HOSE 770), immortalized normal HOSE cell lines (HOSE 642, HOSE 301, HOSE 306, and HOSE 12-12), and malignant OCa cell lines (OVCA 420, OVCA 429, and OVCA 432, but not OVCA 433). The responses of HOSE 770, the representative cell line for primary

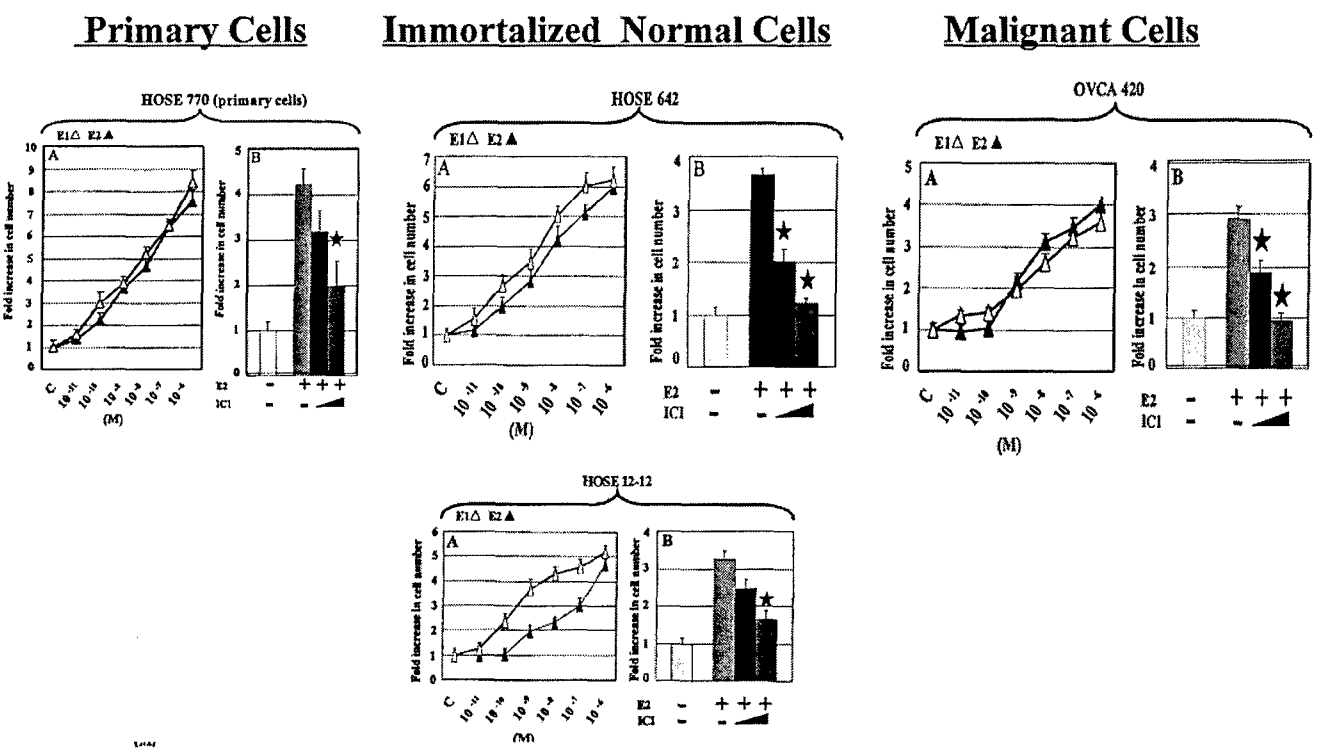

Fig. 3. Effect of E_2 and E_1 on cell proliferation in normal primary HOSE, immortalized HOSE, and malignant cells. Primarily HOSE (HOSE 693, HOSE 770, HOSE 783, and HOSE 785), immortalized HOSE (HOSE 642, HOSE 301, HOSE 306, and HOSE 12-12), and OCa (OVCA 420, OVCA 429, OVCA 432, and OVCA 433) cell lines were cultured as described in the legend of Fig. 2. After preincubation for 48 h in heat-inactivated charcoal-stripped FBS, the cells were treated with different concentrations (10^{-11} to 10^{-6} M) of E_2 (▲) or E_1 (△) for 5 days. The cell growth was assessed by MTT assay as described in "Materials and Methods." The absorbance of wells not exposed to hormones was arbitrarily set as 1, and E_2- and E_1-treated cell growth was expressed as the fold increase compared with the control. The representative cell line from primary HOSE (HOSE 770), immortalized HOSE (HOSE 642), and malignant (OVCA 420) cells is shown. The immortalized HOSE cell line (HOSE 12-12) that showed divergence from the other cell lines in the group is shown under the representative cell line. *B*, to confirm the specificity of E_2, 2×10^5 cells/T-25 flask were cultured alone (□) or cotreated with 10^{-8} M of E_2 (▨) and two doses of ICI 182,780 (10^{-5} M, ■; 10^{-4} M, ▤) for 5 days. The control cells were treated with vehicle. After 5 days, the number of cells was counted. Treatment of cells with E_2 and E_1 induced proliferation of cells in a dose-dependent manner. Cotreatment with ICI 182,780 abolished the response of normal HOSE cells to E_2. The data are shown as the mean of two experiments with triplicate samples and represent the mean ± SD. *, $P < 0.05$.

HOSE cells, HOSE 642, the representative cell line for immortalized HOSE cells, and OVCA 420, the representative cell line for malignant cells, are shown in Fig. 4*A*. Primary cell cultures of normal HOSE cells (HOSE 770, Fig. 4*A*) and immortalized normal HOSE cell lines (HOSE 642, Fig. 4*A*) were more responsive to DHT than T, whereas the OCa cell lines (Fig. 4*A*) responded equally well to both androgens. Although all of the immortalized normal HOSE cell lines were extra receptive to DHT, HOSE 306 showed a greater sensitivity to DHT (Fig. 4*A*). The OCa cell line OVCA 433 failed to respond to both T and DHT stimulation (Fig. 4*A*). The androgen-induced cell growth enhancement was found to be dose dependent (Fig. 4*A*) and reversible by cotreatment of cells with the antiandrogen 4-hydroxy flutamide (Fig. 4*B*) in all of the cell lines tested.

P4 Exerts Both Stimulatory and Inhibitory Effects on Normal and Malignant HOSE Cell Growth. The effects of P4 on cell proliferation in normal and malignant HOSE cell cultures/lines were investigated over a wide concentration range of 10^{-11} to 10^{-6} M. Results revealed that the steroid could stimulate and inhibit cell growth of normal and malignant HOSE cells depending on the dosage of exposure. All of the primary cell cultures of normal HOSE cells (HOSE 783, HOSE 785, and HOSE 770; HOSE 770 is shown as the representative cell line in Fig. 5*A*) except HOSE 693 (Fig. 5*A*) showed stimulation of cell growth when exposed to low concentrations of P4. Exposure to low concentrations (10^{-11} to 10^{-9} M) of P4 induced cell growth enhancement in two immortalized normal HOSE cell lines [HOSE 306 (Fig. 5*A*) and HOSE 301 (data not shown)], whereas the other two cell lines, HOSE 642 (shown in Fig. 5*A*) and HOSE 12-12 (data not shown), did not show any increase in cell number. OCa cell lines OVCA 432, OVCA 433, and OVCA 420 (OVCA 420 is the representative cell line shown in Fig. 5*A*) showed enhancement of cell proliferation in response to low concentrations (10^{-11} to 10^{-9} M) of P4, whereas the OCa cell line OVCA 429 failed to show proliferation of cells in response to low doses of P4 (Fig. 5*A*). However, when normal and malignant HOSE cell cultures/lines were challenged with higher doses of P4 (10^{-8} to 10^{-6} M), the steroid consistently led to growth inhibition (Fig. 5*A*, see the representative lines shown for each group). Interestingly, the lowest dose of P4 (10^{-11} M) induced the most cell growth enhancement in responsive cell cultures/lines, whereas the growth-inhibitory effect of P4 was clearly dose dependent, with the higher doses being more effective. Cotreatment of normal and malignant HOSE cells with the progestin antagonist, RU 38486, at 10^{-5} or 10^{-4} M reversed the growth-inhibitory effects of 10^{-8} M P4 in all cell lines/cultures (Fig. 5*B*). The latter finding suggests that the antiproliferative effect of P4 on all of the cell cultures/lines is mediated via the P4 receptor.

DISCUSSION

A major goal of this research was to fill a data gap regarding the lack of information on hormonal regulation of normal HOSE cell growth. Additionally, an equally important aim was to generate investigational data to explain epidemiological findings that have implicated hormones as risk factors for OCa. In this investigation, we capitalized on our unique access to normal HOSE cells as primary

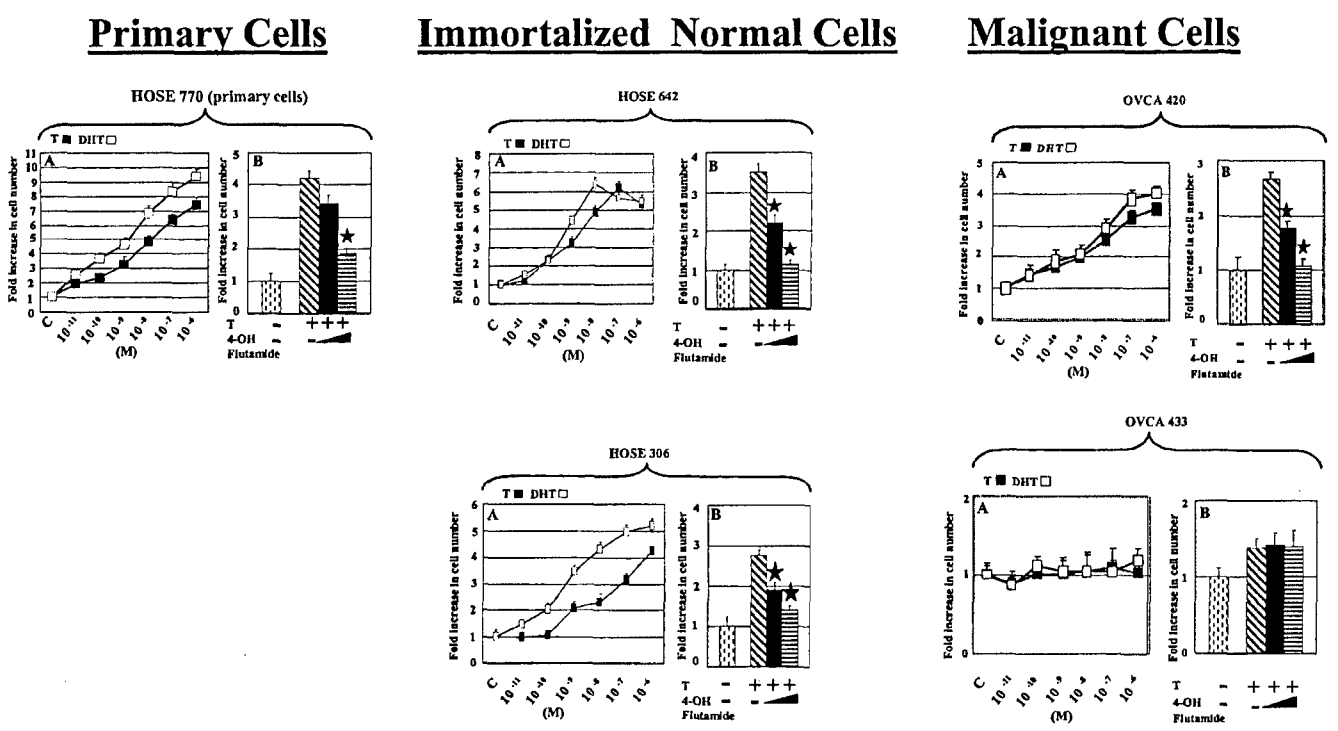

Fig. 4. Effect of T and DHT on cell proliferation in normal primary HOSE, immortalized HOSE, and malignant cells. Primarily HOSE (HOSE 693, HOSE 770, HOSE 783, and HOSE 785), immortalized HOSE (HOSE 642, HOSE 301, HOSE 306, and HOSE 12-12), and OCa (OVCA 420, OVCA 429, OVCA 432, and OVCA 433) cell lines were cultured as described in the legend of Fig. 2. After preincubation for 48 h, the cells were treated with different concentrations (10^{-11} to 10^{-6} M) of T (■) and DHT (□) for 5 days. The cell growth was assessed by MTT assay as described in "Materials and Methods." The absorbance of wells not exposed to hormones was arbitrarily set as 1, and T- and DHT-treated cell growth was expressed as the fold increase as compared with the control. The representative cell line from primary HOSE (HOSE 770), immortalized HOSE (HOSE 642), and malignant (OVCA 420) cells is shown. The immortalized HOSE cell line (HOSE 306) and the malignant cell line (OVCA 433) that showed divergence from the other lines in their respective groups are shown under the representative cell line. *B*, to confirm the specificity of T, 2×10^5 cells/T-25 flask were cultured alone (□) or cotreated with 10^{-8} M T (▨) and two doses of 4-hydroxy flutamide (10^{-5} M, ■; 10^{-4} M, ▤) for 5 days. The control cells were treated with vehicle. After 5 days, the number of cells was counted. Treatment of cells with T and DHT induced proliferation of cells in a dose-dependent manner in all of the cell lines. Cotreatment with 4-hydroxy flutamide abolished the response of normal HOSE cells to T. The data shown are the mean of two experiments with triplicate samples and represent the mean ± SD. *, $P < 0.05$.

cultures or immortalized lines to conduct a comparative study to determine cell growth responses induced by gonadotropins and key sex steroids in these cells and in their malignant counterparts. We reported here, for the first time, coexpression of LH-R and FSH-R in normal HOSE cell cultures and immortalized lines. Both gonadotropins (LH and FSH) and the two estrogens (E_1 and E_2) were equally potent in enhancing cell growth in normal and malignant HOSE cells. The cellular androgen, DHT, was more effective than the circulating androgen, T, in stimulating the growth of normal HOSE cells in primary cultures, but the two androgens were equally potent in enhancing proliferation of OCa cells. Overall, primary cultures of normal HOSE cells exhibited the greatest responses to gonadotropin-, estrogen-, or androgen-stimulated cell growth when compared with those observed in immortalized HOSE cell lines or in OCa cell lines. Importantly, P4 at low doses was a promoter, but at higher doses, it was an unvaried growth inhibitor of normal and malignant HOSE cell growth.

Indirect evidence suggests that gonadotropins may have a role in the genesis and promotion of epithelial OCa (7, 9, 16). The incidence of OCa peaks 10–20 years after menopause, when gonadotropin levels are elevated. Case studies have reported development of epithelial OCa in women undergoing fertility treatment, and an increased OCa risk has been reported in association with the use of fertility drugs in population studies (7, 8). A handful of laboratory studies have demonstrated that gonadotropins influence cell growth in some but not all OCa cell lines (23, 25, 26). In early studies (47–50), gonadotropin-binding sites were found in OCa cells. In recent studies (26, 51), transcripts of FSH-R and LH-R were detected in the great majority of ovarian tumors. In this study, we reported coexpression of FSH-R and LH-R transcripts in normal HOSE cells at levels comparable with those found in OCa cell lines. Both FSH and LH, at doses as low as 10^{-11} to 10^{-10} M, were stimulatory for normal and malignant HOSE cell growth. These doses translate to approximately 20–200 mIU/ml gonadotropin, concentrations that are well within the ranges of circulating FSH and LH reported in women. The circulating levels of FSH and LH in cycling women fluctuate between 10–25 and 18–50 mIU/ml, respectively (52). After menopause, circulating gonadotropins are elevated to levels around 66 mIU/ml for FSH and 23 mIU/ml for LH (53). In our experiments, the effects of FSH and LH on cell growth enhancement were blocked by the selective PKA inhibitor, H89, providing evidence of specificity for the gonadotropin action. When compared over a wide dose range, FSH and LH were found to be equally potent in stimulating normal and malignant HOSE cell growth. The latter finding is clearly in disagreement with a recent study (26) that found FSH and LH to have opposite effects in the growth regulation of two OCa cell lines, AO and 3AO, with FSH as the stimulator and LH as the inhibitor. Interestingly, we found normal HOSE cells in primary cultures to be more responsive to gonadotropin stimulation, producing a 10–14-fold increase in cell growth enhancement, as compared with a 3–5-fold increase in immortalized normal HOSE cell lines and OCa cell lines. This observation suggests that normal HOSE cells are hypersensitive to gonadotropin stimulation and may therefore undergo excessive cell proliferation under a postmenopausal hormonal milieu and be susceptible to malignant transformation. All in all, our findings are in accord with the theory that suggests rising levels of gonadotropins as a risk factor for OCa and are in disagreement with the hypothesis that high levels of gonadotropins are protective against OCa development (54).

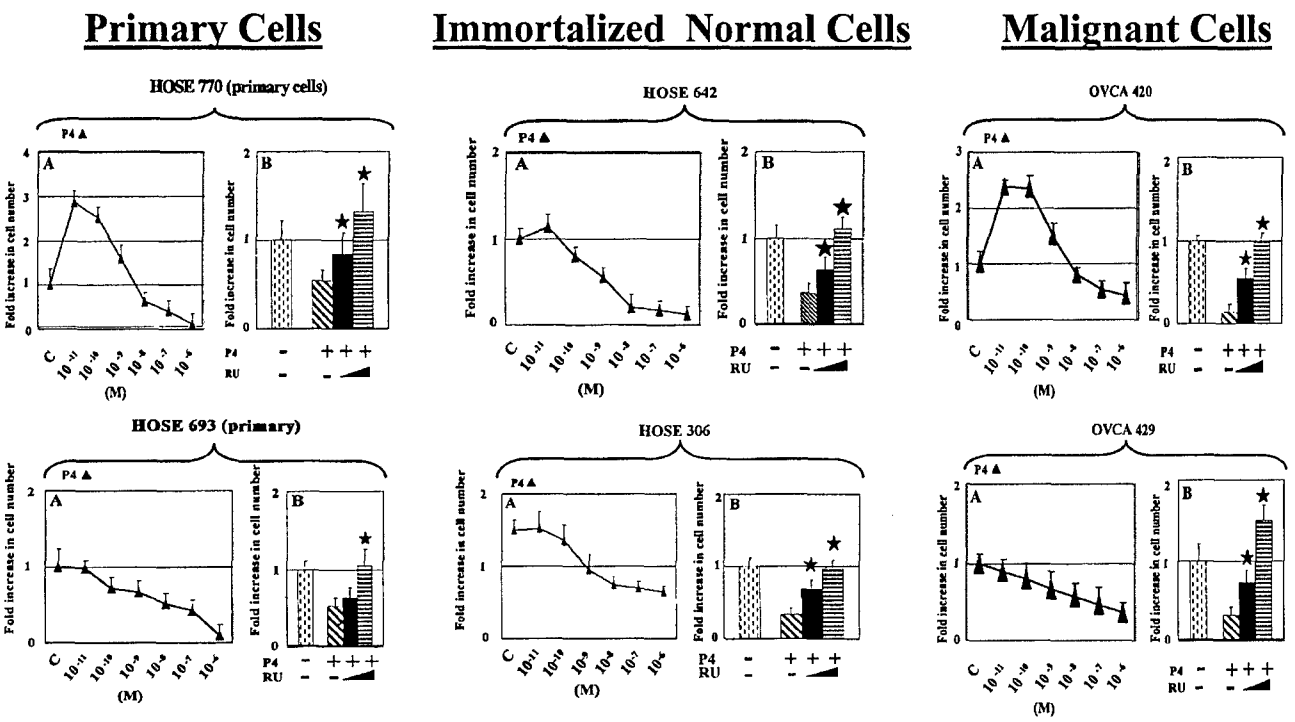

Fig. 5. Effect of P4 on cell growth in primary HOSE, immortalized normal HOSE, and malignant cell lines. Primarily HOSE (HOSE 693, HOSE 770, HOSE 783, and HOSE 785), immortalized HOSE (HOSE 642, HOSE 301, HOSE 306, and HOSE 12-12), and OCa (OVCA 420, OVCA 429, OVCA 432, and OVCA 433) cell lines were cultured as described in the legend of Fig. 2. *A*, the cells were treated with different concentrations (10^{-11} to 10^{-6} M) of P4 (▲) for 5 days. The cell growth was assessed by MTT assay as described in "Materials and Methods." The absorbance of wells not exposed to hormones was arbitrarily set as 1, and P4-treated cell growth was expressed as the fold increase/decrease as compared with the control. The representative cell line from primary HOSE (HOSE 770), immortalized HOSE (HOSE 642), and malignant (OVCA 420) cells is shown. The primary cell line (HOSE 693), immortalized HOSE cell line (HOSE 306), and malignant cell line (OVCA 433) that showed divergence from the other cell lines in their respective groups are shown under the representative line. *B*, to confirm the specificity of P4, 2×10^5 cells/T-25 flask were cultured alone (□) or cotreated with 10^{-8} M P4 (▨) and two doses of RU 38486 (10^{-5} M, ■; 10^{-4} M, ▤) for 5 days. The control cells were treated with vehicle. After 5 days, the number of cells was counted. Treatment of cells with P4 inhibited proliferation of cells in a dose-dependent manner in all cell lines tested. Cotreatment with RU 38486 abolished the response of normal HOSE cells to P4. The data are shown as the mean of two experiments with triplicate samples and represent the mean ± SD. *, $P < 0.05$.

It has become clear with data from recent large case-control studies that OCa risk is significantly increased in postmenopausal women following long-duration ERT (18, 55–61). However, the mechanisms underlying this association have not been established. Findings from our present investigation have provided the first evidence that estrogens directly promote normal HOSE cell growth, which may favor malignant transformation. Interestingly, normal HOSE cells were found to be much more responsive to estrogen stimulation than their immortalized or transformed counterparts. In addition, the major postmenopausal estrogen, E_1 (62), displayed equal potency as the premenopausal ovarian-derived circulating estrogen, E_2, in stimulating normal and malignant HOSE cell growth. Because E_1 is a weak ligand for estrogen receptors (63), the popular view maintains that this estrogen exerts little estrogenic effect on target cells. Our data therefore provide a contrary perspective that suggests the effectiveness of postmenopausal estrogen in promoting OSE cell proliferation. In premenopausal women, circulating E_2 ranges from 10–20 pg/ml during the follicular and luteal phases and peaks at 200 pg/ml during ovulation (52). These circulating E_2 levels, at 3×10^{-11} to 6×10^{-10} M, are definitely effective in stimulating normal and malignant HOSE cell growth under our culture conditions. In perimenopausal women, E_1 sulfate, which serves as a stable circulating reservoir of estrogen, reaches levels as high as 100 pg/ml or 10^{-9} M. Ovaries of postmenopausal women do not secrete estrogens, but postmenopausal women have significant levels of E_2 (9 pg/ml or 3×10^{-11} M) and E_1 (13.3–350 pg/ml or 4×10^{-11} to 1×10^{-9} M) in their circulation (64). These levels are still high enough to promote HOSE and OCa cell growth, based on the results of the current study.

Appreciable evidence implicates androgen in the pathogenesis of OCa. In premenopausal women, the circulating T levels are around 380 pg/ml or 10^{-9} M (52). Postmenopausal ovary is rich in androgen, as evidenced by T concentrations seen in ovarian veins. T (21) and DHT (37), at concentrations between 10^{-11} and 10^{-6} M, are well within the range capable of stimulating HOSE and OCa cell growth. According to the inclusion cysts theory, normal HOSE cells entrapped into inclusion cysts are predisposed to undergo neoplastic transformation, probably due to exposure to an androgen-rich stromal environment (2, 9, 10). In the present study, we observed an AR- and dose-dependent enhancement of cell growth in all normal and malignant HOSE cell cultures/lines. The cellular androgen, DHT, is apparently more potent than the circulating androgen, T, in simulating normal HOSE cell growth. However, both androgens are equally effective in stimulating OCa cell growth. The differential cellular responses to T and DHT may be related to differential activities of 5α-reductase in these cell lines (65). Our finding that OVCA 433 fails to respond to both androgens could be explained by our previous report of a complete loss of AR mRNA expression in this OCa cell line (66). In addition, we have observed loss of AR expression in several other OCa cell lines (66). Hence, although androgens may play a significant role in the early genesis of OCa, such as when the OSE is entrapped in inclusion cysts, their contribution in OCa growth regulation may be significantly reduced during tumor progression in postmenopausal women with declining androgen levels (67) and in ovarian tumors with notable loss of AR expression (63).

Perhaps the most intriguing and novel finding of this study is the inverted U-shape dose-response curves observed for many, but not all, normal HOSE cell cultures in response to P4. P4 present at low doses (10^{-11} to 10^{-9} M) was proproliferative, whereas P4 present at higher

doses (10^{-8} to 10^{-6} M) was antiproliferative to most normal and malignant HOSE cells. In premenopausal women, serum P4 levels fluctuate in the range of 2–14 ng/ml or $6–47 \times 10^{-9}$ M (52). The higher concentrations are only reached during the midluteal phase of the female cycle. Furthermore, a 10-fold increase in P4 is noted during pregnancy (68). Previous studies on the influence of P4 on OCa cell growth demonstrated a growth-inhibitory effect for the steroid (20, 36). Induction of apoptosis and p53 up-regulation were proposed as mechanisms mediating the P4-induced growth-inhibitory action on OCa cells (20). We recently obtained flow cytometry data to indicate that all HOSE and OVCA cell lines die via apoptosis after treatment with high doses of P4 (10^{-6} M).[4] It is worthwhile to note that the proproliferation effects of low-dose P4 on normal and malignant HOSE cell cultures/lines have not been reported previously. Taken together, the antiproliferative effects of P4 could explain the observed protective effect offered by pregnancy, sometimes referred to as the "pregnancy clearance effect" (19). According to this theory, pregnancy rids the OSE of early transformed cells. In this regard, our data would suggest that only high levels of P4, which are present during pregnancy, are effective in inducing massive cell death in the OSE and therefore offer a cancer prevention effect. Ironically, lower levels of P4, which are found during the luteal phase of the female cycle, are likely to be proliferative to the OSE. Thus, whereas pregnancy may offer protection against ovarian carcinogenesis, continuous ovarian cycling may increase OCa risk.

In conclusion, we have observed coexpression of FSH-R and LH-R transcripts in all normal and malignant HOSE cell cultures/lines examined. Our data have identified FSH, LH, E_1, E_2, T, DHT, and low-dose P4 as positive growth regulators for HOSE cells. Conversely, P4 at high concentrations has been shown to be a potent antiproliferative factor for HOSE cells. Collectively, these results support the notion that elevated gonadotropin levels after menopause, rising estrogen and P4 levels during the female cycle, exposure of OSE to a high androgenic environment such as that seen in the inclusion cysts, and exposure to exogenous estrogens such as that seen during ERT are probable risk factors for OCa. Conversely, high levels of P4 may offer protection against OCa development by ridding the OSE of early transformed cells, hence providing a mechanistic explanation for the phenomenon of pregnancy clearance effect. The putative protective effect of P4 also raises the issue of whether combined estrogen and progestin replacement therapy is a safer alternative than ERT with respect to OCa development.

REFERENCES

1. Holschneider, C. H., and Berek, J. S. Ovarian cancer: epidemiology, biology, and prognostic factors. Semin. Surg. Oncol., *19:* 3–10, 2000.
2. Scully, R. E. Pathology of ovarian cancer precursors. J. Cell. Biochem. Suppl., *23:* 208–218, 1995.
3. Rao, B. R., and Slotman, B. J. Endocrine factors in common epithelial ovarian cancer. Endocr. Rev., *12:* 14–26, 1991.
4. Cramer, D. W., Hutchinson, G. B., Welch, W. R., Scully, R. F., and Knapp, R. C. Factors affecting the association of oral contraceptives and ovarian cancer. N. Engl. J. Med., *307:* 1047–1051, 1982.
5. Cramer, D. W., Hutchison, B., Welch, W. R., Scully, R. E., and Ryan, K. J. Determinants of ovarian cancer risk. I. Reproductive experiences and family history. J. Natl. Cancer Inst. (Bethesda), *71:* 711–716, 1983.
6. Bandera, C. A., Cramer, D. W., Freiedman, A. J., and Sheets, E. E. Fertility therapy in the setting of a history of invasive epithelial ovarian cancer. Gynecol. Oncol., *58:* 116–119, 1995.
7. Konishi, I., Kuroda, H., and Mandai, M. Review: gonadotropins and development of ovarian cancer. Oncology (Basel), *57* (Suppl. 2)*:* 45–48, 1999.
8. Anderson, S. M., and Dimitrievich, E. Ovulation induction for infertility: is it safe or not? S. D. J. Med., *49:* 419–421, 1996.
9. Risch, H. A. Hormonal etiology of epithelial ovarian cancer, with a hypothesis concerning the role of androgens and progesterone. J. Natl. Cancer Inst. (Bethesda), *90:* 1774–1786, 1998.
10. Ghahremani, M., Foghi, A., and Dorrington, J. H. Etiology of ovarian cancer: a proposed mechanism. Med. Hypotheses, *52:* 23–26, 1999.
11. Hartge, P., Hoover, R., McGowan, L., Lesher, L., and Norris, H. J. Menopause and ovarian cancer. Am. J. Epidemiol., *127:* 990–998, 1998.
12. Hempling, R. E., Wong, C., Piver, M. S., Natarajan, N., and Mettlin, C. J. Hormone replacement therapy as a risk factor for epithelial ovarian cancer: results of a case-control study. Obstet. Gynecol., *89:* 1012–1016, 1997.
13. Hoover, R., Gray, L. A., Sr., and Fraumeni, J. F., Jr. Stilboestrol (diethylstilbestrol) and the risk of ovarian cancer. Lancet, *2:* 533–534, 1977.
14. Hildreth, N. G., Kelsey, J. L., LiVolsi, V. A., Fischer, D. B., Holford, T. R., Mostow, E. D., Schwartz, P. E., and White, C. An epidemiologic study of epithelial carcinoma of the ovary. Am. J. Epidemiol., *114:* 398–405, 1981.
15. Harris, R., Whittemore, A. S., and Itnyre, J. Characteristics relating to ovarian cancer risk: collaborative analysis of 12 US case-control studies. III. Epithelial tumors of low malignant potential in white women. Collaborative Ovarian Cancer Group. Am. J. Epidemiol., *136:* 1204–1211, 1992.
16. Riman, T., Persson, I., and Nilsson, S. Hormonal aspects of epithelial ovarian cancer: review of epidemiological evidence. Clin. Endocrinol., *49:* 695–707, 1998.
17. Tavani, A., and La, Vecchia, C. The adverse effects of hormone replacement therapy. Drugs Aging, *14:* 347–357, 1999.
18. Rodriguez, C., Patel, A. V., Calle, E. E., Jacob, E. J., and Thun, M. J. Estrogen replacement therapy and ovarian cancer mortality in a large prospective study of US women. J. Am. Med. Assoc., *285:* 1460–1465, 2001.
19. Adami, H. O., Hsieh, C. C., Lambe, M., Trichopoulos, D., Leon, D., Persson, I., Ekbom, A., and Janson, P. O. Parity, age at first childbirth, and risk of ovarian cancer. Lancet, *344:* 1250–1254, 1994.
20. Bu, S. Z., Yin, D. L., Ren, X. H., Jiang, L. Z., Wu, Z. J., Gao, Q. R., and Pei, G. Progesterone induces apoptosis and up-regulation of p53 expression in human ovarian carcinoma cell lines. Cancer (Phila.), *79:* 1944–1950, 1997.
21. Lu, J., Zhang, J., and Zeng, Y. Androgen receptors and effects of sex hormones on growth of a human ovarian carcinoma cell line. Zhonghua Fa Chan Ke Za Zhi (Chin. J. Obstet. Gynecol.), *30:* 360–362, 1995.
22. Feigelson, H. S., and Henderson, B. E. Hormonal carcinogenesis. Carcinogenesis (Lond.), *21:* 427–433, 2000.
23. Simon, W. E., Albrecht, M., Hansel, M., Dietel, M., and Holzel, F. Cell lines derived from human ovarian carcinomas: growth stimulation by gonadotropic and steroid hormones. J. Natl. Cancer Inst. (Bethesda), *70:* 839–845, 1983.
24. Wimalasena, J., Dostal, R., and Meehan, D. Gonadotropins, estradiol, and growth factors regulate epithelial ovarian cancer cell growth. Gynecol. Oncol., *46:* 345–350, 1992.
25. Kurbacher, C. M., Jager, W., Kurbacher, J. A., Bittl, A., Wildt, L., and Lang, N. Influence of human luteinizing hormone on cell growth and CA 125 secretion of primary epithelial ovarian carcinomas *in vitro*. Tumour Biol., *16:* 374–384, 1995.
26. Zheng, W., Lu, J. J., Luo, F., Zheng, Y., Feng, Y. J., Felix, J. C., Lauchlan, S. C., and Pike, M. C. Ovarian epithelial tumor growth promotion by follicle-stimulating hormone and inhibition of the effect by luteinizing hormone. Gynecol. Oncol., *76:* 80–88, 2000.
27. Feng, Y., Zhang, X., and Ge, B. Gonadotropins stimulate the proliferation of human epithelial ovarian cancer cell. Zhonghua Fu Chan Ke Za Zhi (Chin. J. Obstet. Gynecol.), *31:* 166–168, 1996.
28. Ala-Fossi, S. L., Grenman, S., Zhang, F. P., Blauer, M., Punnonen, R., and Maenpaa, J. Ovarian cancer and gonadotropins *in vitro*: new evidence in favor of independence. Anticancer Res., *19:* 4289–4295, 1999.
29. Nash, J. D., Ozols, R. F., Smyth, J. F., and Hamilton, T. C. Estrogen and anti-estrogen effects on the growth of human epithelial ovarian cancer *in vitro*. Obstet. Gynecol., *73:* 1009–1016, 1992.
30. Pavlik, E. J., Nelson, K., van Nagell, J. R., Jr., Gallion, H. S., Donaldson, E. S., DePriest, P., Meares, K., and van Nagell, J. R., III. The growth response of BG-1 ovarian carcinoma cells to estradiol, 4OH-tamoxifen, and tamoxifen: evidence for intrinsic antiestrogen activation. Gynecol. Oncol., *42:* 245–249, 1991.
31. Galtier-Dereure, F., Capony, F., Maudelonde, T., and Rochefort, H. Estradiol stimulates cell growth and secretion of procathepsin D and a 120-kilodalton protein in the human ovarian cancer cell line BG-1. J. Clin. Endocrinol. Metab., *75:* 1497–1502, 1992.
32. Wimalasena, J., Meehan, D., Dostal, R., Foster, J. S., Cameron, M., and Smith, M. Growth factors interact with estradiol and gonadotropins in the regulation of ovarian cancer cell growth and growth factor receptors. Oncol. Res., *5:* 325–337, 1993.
33. Langdon, S. P., Crew, A. J., Ritchie, A. A., Muir, M., Wakeling, A., Smyth, J. F., and Miller, W. R. Growth inhibition of oestrogen receptor-positive human ovarian carcinoma by anti-oestrogens *in vitro* and in a xenograft model. Eur. J. Cancer, *30:* 682–686, 1994.
34. Chien, C. H., Wang, F. F., and Hamilton, T. C. Transcriptional activation of c-myc proto-oncogene by estrogen in human ovarian cancer cells. Mol. Cell. Endocrinol., *99:* 11–19, 1994.
35. Baldwin, W. S., Curtis, S. W., Cauthen, C. A., Risinger, J. I., Korach, K. S., and Barrett, J. C. BG-1 ovarian cell line: an alternative model for examining estrogen-dependent growth *in vitro*. In Vitro Cell. Dev. Biol. Anim., *34:* 649–654, 1998.
36. Langdon, S. P., Gabra, H., Bartlett, J. M., Rabiaz, G. J., Hawkins, R. A., Tesdale, A. L., Ritchie, A. A., Miller, W. R., and Smyth, J. F. Functionality of the progesterone receptor in ovarian cancer and its regulation by estrogen. Clin. Cancer Res., *4:* 2245–2251, 1998.
37. Ahonen, M. H., Zhuang, Y. H., Aine, R., Ylikomi, T., and Tuohimaa, P. Androgen receptor and vitamin D receptor in human ovarian cancer: growth stimulation and inhibition by ligands. Int. J. Cancer, *86:* 40–46, 2000.

[4] V. Syed and S-M. Ho, unpublished data.

38. Thompson, M. A., and Adelson, M. D. Aging and development of ovarian epithelial carcinoma: the relevance of changes in ovarian stromal androgen production. Adv. Exp. Med. Biol., *330:* 155–165, 1993.
39. Tsao, S. W., Mok, S. C., Fey, E. G., Fletcher, J. A., Wan, T. S., Chew, E. C., Muto, M. G., Knapp, R. C., and Berkowitz, R. S. Characterization of human ovarian surface epithelial cells immortalized by human papilloma viral oncogenes (HPV-E6E7 ORFs). Exp. Cell Res., *218:* 499–507, 1995.
40. Rauh-Adelmann, C., Lau, K. M., Sabeti, N., Long, J. P., Mok, S. C., and Ho, S. M. Altered expression of BRCA1, BRCA2, and a newly identified BRCA2 exon 12 deletion variant in malignant human ovarian, prostate, and breast cancer cell lines. Mol. Carcinog., *28:* 236–246, 2000.
41. Zhou, X. L., Lei, Z. M., and Rao, C. V. Treatment of human endometrial gland epithelial cells with chorionic gonadotropin/luteinizing hormone increases the expression of the cyclooxygenase-2 gene. J. Clin. Endocrinol. Metab., *84:* 3364–3377, 1999.
42. Sharma, S. C., Clemens, J. W., Pisarska, M. D., and Richards, J. S. Expression and function of estrogen receptor subtypes in granulosa cells: regulation by estradiol and forskolin. Endocrinology, *40:* 4320–4334, 1999.
43. Simard, J., Singh, S. M., and Labrie, F. Comparison of *in vitro* effects of the pure antiandrogens OH-flutamide, Casodex, and nilutamide on androgen-sensitive parameters. Urology, *49:* 580–586, 1997.
44. Makrigiannakis, A., Coukos, G., Christofidou-Solomidou, M., Montas, S., and Coutifaris, C. Progesterone is an autocrine/paracrine regulator of human granulosa cell survival *in vitro*. Ann. N. Y. Acad. Sci., *900:* 16–25, 2000.
45. Minegishi, T., Nakamura, K., Takakura, Y., Ibuki, Y., and Igarashi, M. Cloning and sequenceing of human FSH receptor cDNA. Biochem. Biophys. Res. Commun., *175:* 1125–1130, 1991.
46. Dirnhofer, S., Berger, C., Hermann, M., Steiner, G., Madersbacher, S., and Berger, P. Coexpression of gonadotropic hormones and their corresponding FSH- and LH/CG-receptors in the human prostate. Prostate, *35:* 212–220, 1998.
47. Kammerman, S., Demopoulos, R. I., Raphael, C., and Ross, J. Gonadotropic hormone binding to human ovarian tumors. Hum. Pathol., *12:* 886–890, 1981.
48. Nakano, R., Kitayama, S., Yamoto, M., Shima, K., and Ooshima, A. Localization of gonadotropin binding sites in human ovarian neoplasms. Am. J. Obstet. Gynecol., *161:* 905–910, 1989.
49. Rajaniemi, H., Kauppila, A., Ronnberg, L., Selander, K., and Pystynen, P. LH(hCG) receptor in benign and malignant tumors of human ovary. Acta Obstet. Gynecol. Scand. Suppl., *101:* 83–86, 1981.
50. Stouffer, R. L., Grodin, M. S., Davis, J. R., and Surwit, E. A Investigation of binding sites for follicle-stimulating hormone and chorionic gonadotropin in human ovarian cancers. J. Clin. Endocrinol. Metab., *59:* 441–446, 1984.
51. Lu, J. J., Zheng, Y., Kang, X., Yuan, J. M., Lauchlan, S. C., Pike, M. C., and Zheng, W. Decreased luteinizing hormone receptor mRNA expression in human ovarian epithelial cancer Gynecol. Oncol., *79:* 158–168, 2000.
52. Ross, G. T., Vande Viele, R. L., and Frantz, A. G. The ovaries and the breasts. *In:* R. H. Williams (ed.), Textbook of Endocrinology, 6th ed., pp. 355–411. Philadelphia: W. B. Saunders Company, 1981.
53. Malacara, J. M., Fajardo, M. E., and Nava, L. E. Gonadotropins at menopause: the influence of obesity, insulin resistance, and estrogens. Steroids, *66:* 559–567, 2001.
54. Heizisouer, K. J., Alberg, A. J., Gordon, G. B., Longcope, C., Bush, T. L., Hoffman, S. C., and Comstock, G. W. Serum gonadotropins and steroid hormones and the development of ovarian cancer. J. Am. Med. Assoc., *274:* 1926–1930, 1995.
55. Polychronopoulou, A., Tzonou, A., Hsieh, C. C., Kaprinis, G., Rebelakos, A., Toupadaki, N., and Trichopoulos, D. Reproductive variables, tobacco, ethanol, coffee and somatometry as risk factors for ovarian cancer. Int. J. Cancer, *55:* 402–407, 1993.
56. Negri, E., Tzonou, A., Beral, V., Lagiou, P., Trichopoulos, D., Parazzini, F., Franceschi, S., Booth, M., and La Vecchia, C. Hormonal therapy for menopause and ovarian cancer in a collaborative re-analysis of European studies. Int. J. Cancer, *80:* 848–851, 1999.
57. Purdie, D. M., Bain, C. J., Siskind, V., Russell, P., Hacker, N. F., Ward, B. G., Quinn, M. A., and Green, A. C. Hormone replacement therapy and risk of epithelial ovarian cancer. Br. J. Cancer, *81:* 559–563, 1999.
58. Parazzini, F., La Vecchia, C., Negri, E., and Villa, A. Estrogen replacement therapy and ovarian cancer risk. Int. J. Cancer, *1:* 135–136, 1994.
59. Whittemore, A. S., Harris, R., Itnyre, J., and the Collaborative Ovarian Cancer Group. Characteristics relating to ovarian cancer risk: collaborative analysis of 12 US case-control studies. II. Invasive epithelial ovarian cancers in white women. Am. J. Epidemiol., *136:* 1184–1203, 1992.
60. Garg, P. P., Kerlikowske, K., Subak, L., and Grady, D. Hormone replacement therapy and the risk of epithelial ovarian carcinoma: a meta-analysis. Obstet. Gynecol., *92:* 472–479, 1998.
61. Risch, H. A. Estrogen replacement therapy and risk of epithelial ovarian cancer. Gynecol. Oncol., *63:* 254–257, 1996.
62. Hemsell, D. L., Grodin, J. M., Brewnner, P. F., Siiteri, P. K., and MacDonald, P. C. Plasma precursors of estrogen. II. Correlation of the extent of conversion of plasma androstenedione to estrone with age. J. Clin. Endocrinol. Metab., *38:* 476–479, 1974.
63. Sasson, S., and Notides, A. C. Estriol and estrone interaction with the estrogen receptor. I. Temperature-induced modulation of the cooperative binding of [^{3}H]estriol and [^{3}H]estrone to the estrogen receptor. J. Biol. Chem., *258:* 8113–8117, 1983.
64. Beyene, Y., and Martin, M. C. Menopausal experiences and bone density of Mayan women in Yucatan, Mexico. Am. J. Human Biol., *13:* 505–511, 2001.
65. Delos, S., Carsol, J. L., Fina, F., Raynaud, J. P., and Martin, P. M. 5α-Reductase and 17β-hydroxysteroid dehydrogenase expression in epithelial cells from hyperplastic and malignant human prostate. Int. J. Cancer, *75:* 840–846, 1998.
66. Lau, K. M., Mok, S. C., and Ho, S. M. Expression of human estrogen receptor-α and -β, progesterone receptor, and androgen receptor mRNA in normal and malignant ovarian epithelial cells. Proc. Natl. Acad. Sci. USA, *96:* 5722–5727, 1999.
67. Akamatsu, T., Chiba, H., Kamiyama, H., Hiurose, K., Saito, H., and Yanaihara, T. Menopause related changes of adrenocortical steroid production. Asia-Oceania J. Obstet. Gynaecol., *18:* 271–267, 1992.
68. Simpson, E. R., and MacDonald, P. C. Endocrinology of pregnancy. *In:* R. H. Williams (ed.), Textbook of Endocrinology, 6th ed., pp. 412–422. Philadelphia: W. B. Saunders Company, 1981.

Analytical Biochemistry **290,** 302–313 (2001)
doi:10.1006/abio.2001.5000, available online at http://www.idealibrary.com on IDEAL®

Electrospray Ionization Mass Spectrometry Analysis of Lysophospholipids in Human Ascitic Fluids: Comparison of the Lysophospholipid Contents in Malignant vs Nonmalignant Ascitic Fluids[1]

Yi-jin Xiao,* Benjamin Schwartz,† Monique Washington,† Alexander Kennedy,† Kenneth Webster,† Jerome Belinson,† and Yan Xu*,†,[2]

**Department of Cancer Biology and †Department of Gynecology and Obstetrics, Cleveland Clinic Foundation, 9500 Euclid Avenue, Cleveland, Ohio 44195*

Received August 8, 2000; published online February 15, 2001

Lysophospholipids (lyso-PLs), including various glycerol-based and sphingosine-based lysophospholipids, play important roles in many biochemical, physiological, and pathological processes. The classical methods to analyze these lipids involve gas chromatography and/or high-performance liquid chromatography, which are time-consuming, cumbersome, and sometimes inaccurate due to the incomplete separation of closely related lipid species. We now describe the quantitative analysis of lyso-PLs in ascites samples from patients with ovarian cancer using electrospray ionization spectrometry. Three new classes of lyso-PL molecules are detected: alkyl-LPA, alkenyl-LPA, and methylated lysophosphatidylethanolamine. Importantly, the following lysophospholipid species are significantly increased in ascites from patients with ovarian cancer, compared to patients with nonmalignant diseases (e.g., liver failure): LPA (including acyl-, alkyl-, and alkenyl-LPA species), lysophosphatidylinositol, and sphingosylphosphorylcholine. Lysophosphorylcholine contents are also significantly different among ascitic fluids from the two groups of patients. However, the total phosphate content in ascites samples from patients with ovarian cancer is not significantly different compared to that from patients with nonmalignant disease.

Lysophospholipids (lyso-PLs)[3] are important precursors and intermediates of phospholipid synthesis. However, the most prominent discovery in recent years is that these lipids are now recognized as important extracellular cell signaling molecules (1, 2). Among these signaling lipid molecules, lysophosphatidic acid (LPA) has been studied most extensively (2, 3). LPA is actually a group of compounds with three major subclasses. All of these subclasses contain a glycerol backbone with a long chain aliphatic acid attached to the first carbon (*sn*-1) position, a hydroxy-group at the second (*sn*-2) position, and a phosphate group at the third (*sn*-3) position. However, the different chemical linkages at the *sn*-1 position between the long-chain aliphatic acid and the glycerol result in different subclasses of LPAs (acyl-, alkyl-, and alkenyl-LPAs). In addition, within each subclass, there are different LPAs, which contain long-chain aliphatic acids with different numbers of carbons and/or double bonds. Other lysophospholipids may also have signaling properties in cellular systems. These molecules have different groups attached to the phosphate which include lysophosphatidylcholine (LPC), lysophosphatidylethanolamine (LPE), lysophosphatidylglycerol (LPG), ly-

[1] This research was supported in part by U.S. Army Grant RPG-99-062-01-CNE; Atairgin Biotechnologies. Inc. (sponsored research); Lynne Cohen Foundation (Los Angeles, CA); and a NIH Grant R21 CA84038-01 to Y.X.

[2] To whom correspondence should be addressed at Department of Cancer Biology, The Lerner Research Institute, Cleveland Clinic Foundation, 9500 Euclid Avenue, Cleveland, OH 44195. Fax: (216) 445-6269.

[3] Abbreviations used: ESI-MS, electrospray ionization mass spectrometry; LPA, lysophosphatidic acid; LPC, lysophosphatidylcholine; LPE: lysophosphatidylethanolamine; LPG, lysophosphatidylglycerol; LPI, lysophosphatidylinositol; LPS, lysophosphatidylserine; lyso-PLs, lysophopholipids; MRM, multiple reaction monitoring; MS/MS, tandem mass spectrometry; OCAF, ovarian cancer-activating factor; PAF, platelet activating factor; PE, phosphatidylethanolamine; PLD, phospholipase D; S1P, sphingosine-1-phosphate; SPC, sphingosylphosphorylcholine; TLC, thin-layer chromatography; TX100, Triton X-100.

0003-2697/01 $35.00

sophosphatidylinositol (LPI), and lysophosphatidylserine (LPS). Two lysosphingolipid molecules, sphingosine 1-phosphate (S1P) and sphingosylphosphorylcholine (SPC), are both extra- and intracellular signaling molecules (4–7).

Ovarian cancer is associated with the production of a large volume of peritoneal ascites, which frequently contains a high number of tumor cells and soluble growth factors (8–10). It represents the *in vivo* environment of the tumor cells. Another disease that tends to produce a large volume of ascites is hepatic cirrhosis. Ascitic fluids from patients with ovarian cancer, but not patients with benign diseases, such as hepatic cirrhosis, stimulate growth of ovarian cancer cells *in vitro* and *in vivo* (11). Normal ovarian epithelial cells and fresh or cultured lymphoid cells do not respond to this factor (11, 12). Identifying and understanding the mechanism of the growth-stimulating activity in ascites will provide critical information about the growth and metastatic regulation of ovarian cancer.

Previously, we purified and identified a factor from ovarian cancer ascites that is growth stimulating in ovarian cancer cells. We termed it ovarian cancer-activating factor, or OCAF. OCAF is composed of several molecular species of LPA (6, 7). We have shown that another bioactive lyso-PL, S1P, is also present in ascites from patients with ovarian cancer and modulates both growth and adhesion of ovarian cancer (13). We also found that LPA was significantly elevated in the plasma of ovarian cancer patients, compared to healthy controls. In particular, elevated plasma LPA levels were detected in patients with Stage I ovarian cancer, suggesting that LPA may represent a useful marker for the early detection of ovarian cancer (14). More recently, we have developed an electrospray mass spectrometry (ESI-MS)-based method to analyze lyso-PL molecules in ascites and found that in addition to LPA, LPI may be a valuable biomarker for detecting ovarian cancer (15).

To further investigate the biochemical, physiological, and/or pathological role of LPA and related bioactive lysolipids in ovarian cancer, we have developed the ESI-MS-based method to further analyze all lyso-PL molecules with either a glycerol or a sphingosine backbone in ascites. To determine whether any lyso-PLs could be related to ovarian cancer, quantitative analyses have been conducted in ascites samples from patients with ovarian cancer, compared with those from patients with nonmalignant diseases using the standard curves established for a variety of lyso-PLs in this study.

MATERIALS AND METHODS

Materials

LPA and other lyso-PLs were purchased from Avanti Polar Lipids (Birmingham, AL). LPI was from Sigma (St. Louis, MO). S1P was from Toronto Research Chemicals (Toronto, Ontario, Canada) and SPC was from Matreya, Inc. (Pleasant Gap, PA). Precoated silica gel 60 TLC plates were obtained from EM Science (Gibbstown, NJ). HPLC-grade methanol (MeOH), chloroform, ammonium hydroxide (AmOH), and hydrochloric acid (HCl) were purchased from Sigma (St. Louis, MO) or Fisher Scientific (Pittsburgh, PA).

Lipid Extraction

Ascites samples were centrifuged at 1660*g* (3000 rpm in a JS7.5 Beckman rotor) for 30 min. The cell-free ascites was stored at −80°C in aliquots. All extraction procedures were performed in 15-ml glass disposable centrifuge tubes (15). To extract lipids in the upper phase, 2 ml of butanol was added to the mixture of the upper and inter phases, vortexed for 1 min, and then incubated on ice for 1 h. Two milliliters of H_2O was added to separate the phases. The sample was vortexed for 1 min and centrifuged at 2000*g* for 10 min. The upper phase was transferred to a fresh glass tube and dried under N_2. The dried lipids were resuspended in 1.5 ml chloroform and centrifuged at 2000*g* for 10 min to remove the salts and insoluble materials. The lipids in chloroform were transferred to a new tube and the solvent was evaporated under nitrogen at 40°C. The dried sample was dissolved in 0.1 ml of MeOH and then diluted 10-fold, prior to MS detection. Lipids were separated and eluted from TLC plates as previously described (15).

Preparation of Standards

14:0-LPA and 17:0-LPC (purchased from Avanti in chloroform form) were used as internal standards in the negative and positive mode of detection, respectively. Standard LPAs (16:0, 18:0, and 18:1), LPI (16:0 and 18:0), and LPCs (6:0, 8:0,10:0, 12:0, 14:0, 16:0, 18:0, 20:0, 22:0, and 24:0) were obtained from Avanti and solutions were made in methanol. To obtain standard curves, different amounts (5–300 pmol) of standard LPAs, LPIs, or LPCs were mixed with the same amount (50 pmol) of internal standard 14:0-LPA or 17:0-LPC. ESI-MS was performed and the intensity ratios (standard vs internal standard) were plotted against molar ratios (standard vs internal standard). For quantitative analysis of lysolipid, 500 pmol of the internal standard was added to each ascites sample before the lipid extraction and one-fifth of each sample was used for MS detection.

Preparation of Alkyl- and Alkenyl-LPAs

Alkyl- and alkenyl-LPA were prepared through hydrolysis of the corresponding lyso-PAF (Avanti Polar Lipids) or lyso-plasmalogen phosphatidylethanolamine

(alkenyl-LPE) (Matreya, Inc.), respectively, by phospholipase D (PLD) reaction (Calbiochem, La Jolla, CA). Briefly, 1 mg of alkenyl-LPE or lyso-PAF was dispersed in 0.1 ml of 0.04 M Tris buffer, pH 8.0, containing 0.05 M $CaCl_2$ and 1% TX100. After addition of enzyme (4 units of PLD in 15 μl of 0.01 M Tris buffer, pH 8.0), the sample was mixed vigorously. The reaction vessel was sealed tightly and the contents were rotated overnight at room temperature. After the incubation period, the mixture was extracted with 1.2 ml of chloroform:methanol:HCl (5:4:0.2). The chloroform layer was evaporated under a stream of nitrogen and the residue was dissolved in 50 μl chloroform:methanol (1:2 v/v). The substrate and the product were separated on a TLC plate using a solvent system of chloroform:methanol:AmOH (65:35:5.5) and the product was eluted from the plate by 2 ml chloroform:methanol (1:2), twice, and then dried under N_2.

ESI-MS Conditions

ESI-MS and tandem mass spectrometry (MS/MS) analyses were performed using a Micromass Quattro II triple quadrupole mass spectrometer equipped with an ESI source (Micromass Inc., Beverly, MA). The samples were delivered into the ESI source using a LC system (HP1100) with an injection valve (20-μl injection loop) via 125-μm PEEK tubing. The mobile phase used for all experiments was MeOH:H_2O (1:1 v/v) and the flow rate was 50 μl/min.

The instrument settings used were the same as described previously (15). Parent scanning and MS/MS analyses were performed to detect and confirm the structures of all lyso-PLs in ascites samples. All quantitative analyses were performed in the multiple reaction monitoring (MRM) mode, since it provides better sensitivity and separation than the parent scanning does. LPA and other negatively charged lyso-PLs were analyzed in the negative mode with the monitoring ions at *m/z* 378 (parent ion)–79 (product ion) for S1P, 381–79 for 14:0-LPA, 393–79 for 16:0-alkenyl-LPA, 395–79 for 16:0-alkyl-LPA, 409–79 for 16:0-LPA, 421–79 for 18:0-alkenyl-LPA, 423–79 for 18:0-alkyl-LPA, 433–79 for 18:2-LPA, 435–79 for 18:1-LPA, 437–79 for 18:0-LPA, 571–79 for 16:0-LPI, 599–79 for 18:0-LPI, and 619–79 for 20:4-LPI. All lipids with the phosphorylcholine group (positively charged) were analyzed in the positive mode. Monitoring ions were at *m/z* 465 (parent ion)–184 (product ion) for SPC, 483–184 for lyso-PAF, 496–184 for 16:0-LPC, 510–184 for 17:0-LPC, 520–184 for 18:2-LPC, 524–184 for 18:0-LPC 544–184 for 20:4-LPC, and 568–184 for 22:6-LPC. For LPC standard curves, 356–184 for 6:0-LPC, 384–184 for 8:0-LPC, 412–184 for 10:0-LPC, 440–184 for 12:0-LPC, 468–184 for 14:0-LPC, 522–184 for 18:1-LPC, 552–184 for 20:0-LPC, 580–184 for 22:0-LPC, and 608–184 for 24:0-LPC were used. The dwell time in the MRM mode was 100 ms and other conditions were the same as those in the parent scanning as described above.

Total Phosphate Determination

To determine total phospholipid content in ascites samples, total phosphorus was determined in extracted lipids. Lipids were extracted from 0.5 ml of ascites and dried under nitrogen as described. Perchloric acid (0.5 ml, 70%) was added to the dry lipid sample in a test tube, and the lipids were digested by gentle refluxing for 20 min on a heating block at ~200°C in a fume hood. After cooling, ammonium molybdate reagent (2.5 ml; 0.5% ammonium molybdate in 1 N H_2SO_4; Fisher Scientific) was added and followed by addition of 2.5 ml of reducing reagent (0.62% sodium bisulfate, 0.37% sodium sulfite, and 0.01% 1-amino-2-naphthol-4-sulphonic acid; Labchem Inc., Pittsburgh, PA). The solution was mixed thoroughly and heated in a boiling water bath for 10 min for color development. After cooling, the absorbance of the solution was measured at 830 nm (some dilution may have been required). A blank sample was analyzed simultaneously and a standard solution of 1.0 mM sodium dihydrogen phosphate was prepared for establishing the standard curve.

Sample Collection and Statistical Analysis

Ascites samples were obtained 15 patients with ovarian cancer (median age 74.0 years; range 48–86 years) and 15 patients with benign liver diseases (median age 52 years; range 43–74 years). Informed consent was obtained from all participants. Ascites samples were centrifuged at 1660*g* for 30 min to remove cells. The cell-free ascites samples were aliquoted and stored at −80°C. Statistical analyses were performed using the Student *t* test. $P \leq 0.01$ is considered to be statistically significant.

RESULTS

Lysolipids Were Distributed in both Organic and Aqueous Phases

Using the acidified chloroform:MeOH extraction method as previously described (15), we found that most negatively charged lysolipids, including LPA, LPI, derivatives of LPE, and S1P, were exclusively extracted into the organic phase. Phosphorylcholine-containing lipids, which are positively charged under acidic conditions, including SPC, LPC, and lyso-PAF were distributed in both organic and aqueous phases. The distribution of these lipids in the aqueous phase was approximately ≥90, 70, and 45% for SPC, LPC, and lyso-PAF, respectively. We collected

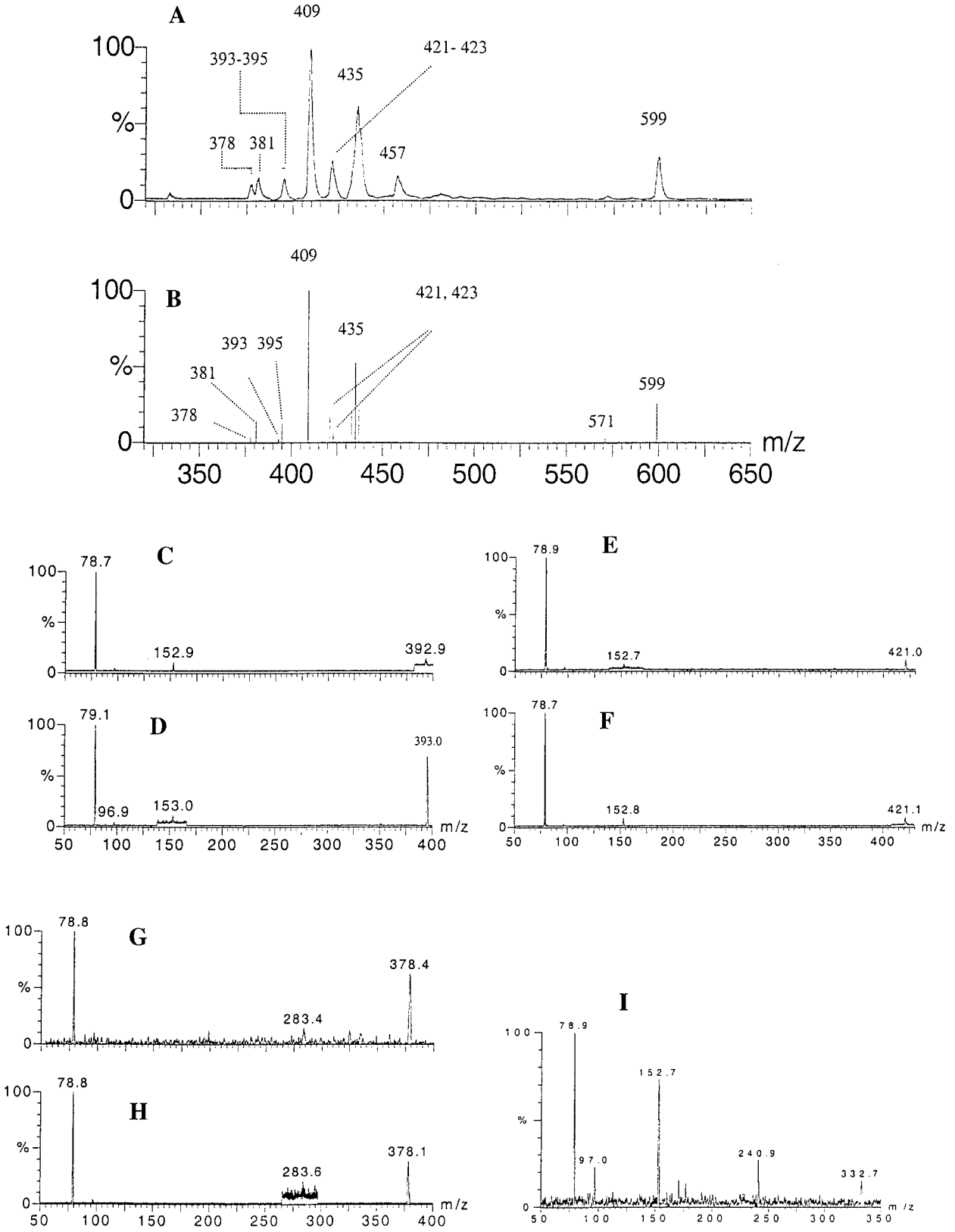

FIG. 1. Representative spectra of lyso-PLs from the "LPA band" in 0.5 ml of an ascites sample from an ovarian cancer patient. The parent of 79 scan mode in negative detection (A) or a MRM mode (B) was used. The MS/MS spectra of the ion peak at *m/z* 393 from the ascites sample (C) and the standard 16:0-alkenyl-LPA (D). The MS/MS spectra of the ion peak at *m/z* 421 from the ascites sample (E) and the standard 18:0-alkenyl-LPA (F). The MS/MS spectra of the ion at *m/z* 378 (G) and the standard S1P (H). The MS/MS spectrum of the ion peak at *m/z* 333 (I).

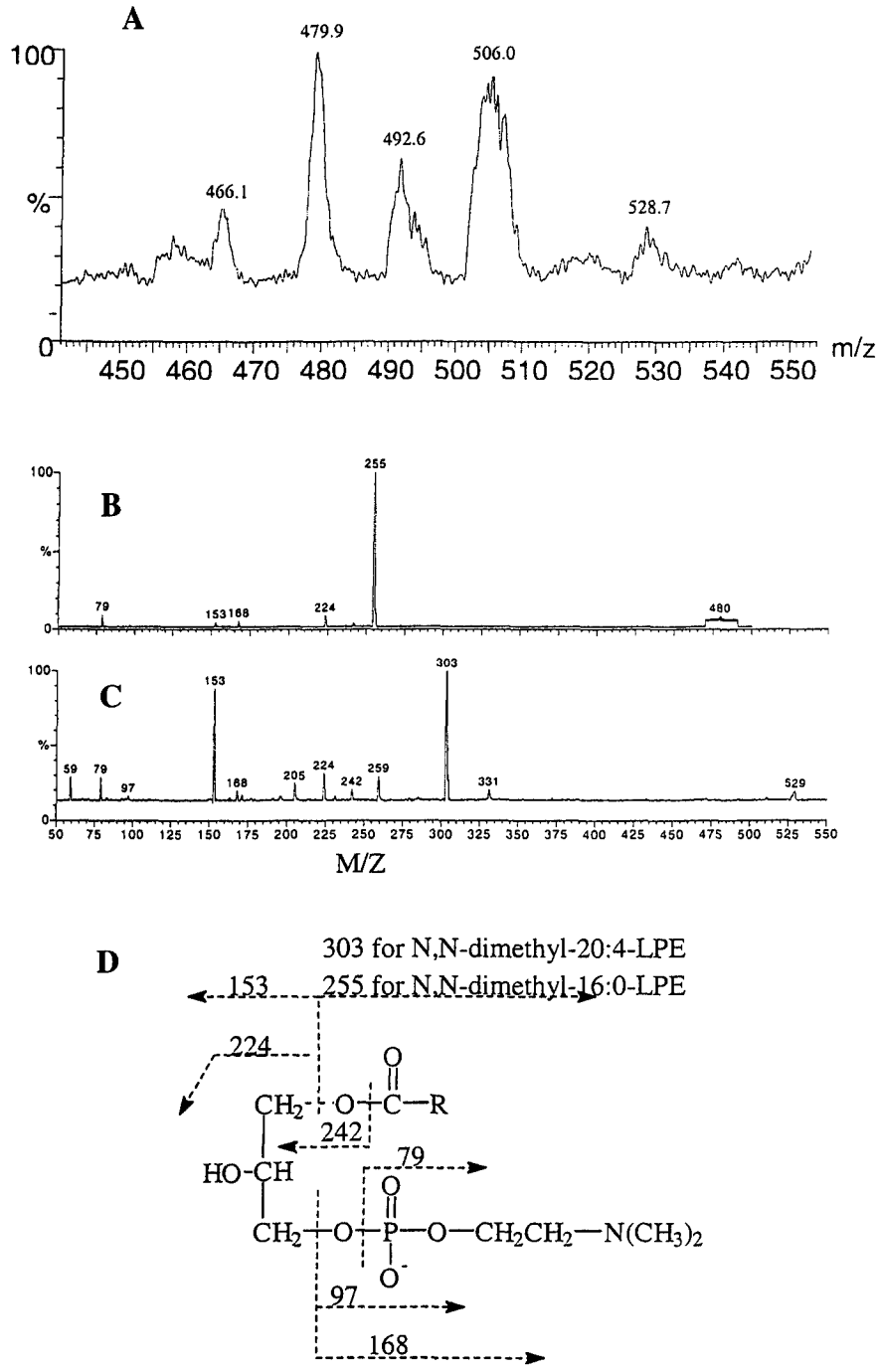

FIG. 2. Representative spectra of lyso-PLs from the "LPE band" in 0.5 ml of an ascites sample from an ovarian cancer patient. The parent of 79 scan mode in negative detection was used (A). The MS/MS spectra of the ion peak at *m/z* 480 (B) and 529 (C) from the ascites sample. The fragmentation assignment to dimethylated LPEs (D).

both aqueous and organic phases and developed a butanol reextraction method to recover the lipids in the aqueous phase (Material and Methods). The salt and insoluble materials were removed by chloroform and the purified lipids were used directly for MS analysis.

Ascites from Patients with Ovarian Cancer Contain Various Species of Acyl-, Alkyl-, and Alkenyl-LPA

In addition to acyl-LPAs detected in plasma samples (14, 15), two new species at *m/z* 393–395 and 421–423 were detected in ascites samples (Figs. 1A and 1B). MS/MS analyses in comparison with standard alkyl-

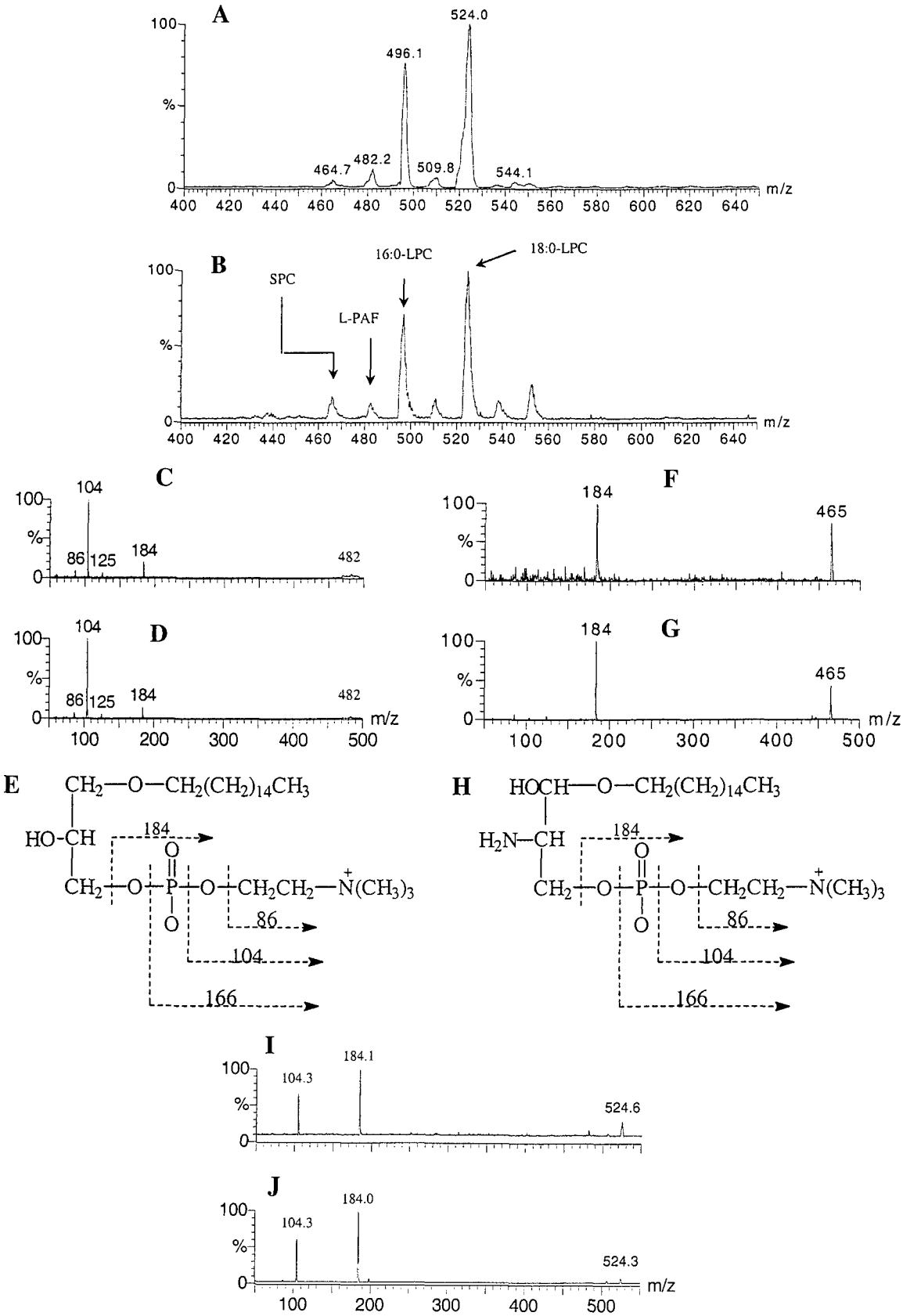

FIG. 3. Representative spectra of lyso-PLs containing phosphorylcholine from 0.5 ml of an ascites sample from an ovarian cancer patient. The parent of 184 scan mode in positive detection was used (A). Standard SPC, lyso-PAF, 16:0-LPC, and 18:0-LPC (molar ratios 0.04:0.4:19:22) (B). The assay conditions were the same for (A) and (B). The MS/MS spectra of the ion peak at *m/z* 482 from the ascites sample (C) and the standard 16:0-lyso-PAF (D). The MS/MS spectra of the ion peak at *m/z* 465 from the ascites sample (F) and the standard SPC (G). The fragmentation assignments to lyso-PAF (E) and SPC (H). The MS/MS spectra of the ion peak at *m/z* 524 from the ascites samples (I) and the standard 18:0-LPC (J).

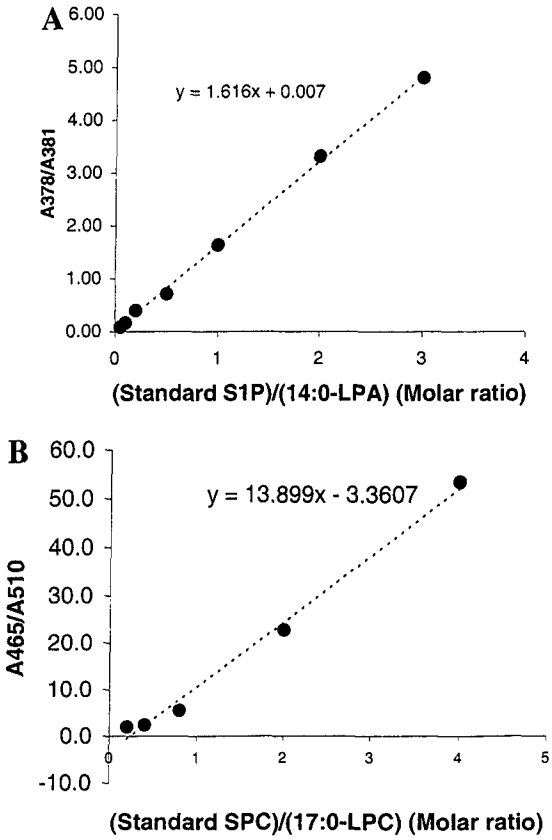

FIG. 4. Standard curves of SPC and S1P. (A). S1P standard curve: internal standard 14:0-LPA was used and the ionization ratios were determined in the parent of 79 MRM scan mode in negative detection. (B). SPC standard curve: internal standard 17:0-LPC was used and the ionization ratios were determined in the parent of 184 MRM scan mode in positive detection.

LPA identified ion peaks 395 and 423 as 16:0- and 18:0-alkyl-LPAs (data not shown). The ion peaks at 393 and 421 were identified as 16:0- and 18:0-alkenyl-LPAs by three lines of evidence: (i) the parental molecular weight; (ii) the MS/MS spectrum of ion peaks at 393 and 421, compared with 16:0- and 18:0-alkenyl-LPA produced through PLD reaction (Materials and Methods) (Figs. 1C, 1D, 1E, and 1F); and (iii) ion peaks at 393 and 421 were sensitive to HCl treatment: two ascites samples were extracted using the method as described under Materials and Methods. The lipids were then suspended in 50 μl MeOH:chloroform (2:1) and then spotted on a TLC plate. The TLC plate was placed in a TLC tank, which was saturated with HCl vapors (generated by placing 50 ml concentrated HCl in a sealed TLC tank) for 15 min. The sample spots were eluted with 2 ml of MeOH:chloroform (2:1) twice and dried under nitrogen at 40°C. As controls, the same ascites samples were extracted and spotted on a TLC plate in a similar fashion and the plate was placed in a TLC tank without the HCl vapors. These samples were subjected to MS analysis for comparison. In control samples, ion peaks at 393 and 421 were detected and they were noted to completely disappear after HCl vapor treatment (data not shown).

The ion peak at *m/z* 378 was identified as S1P (Figs. 1G and 1H). The following indicates that the ion peak at *m/z* 333 was a deacylated form of LPI (glycerolphosphoinositol): (i) the MS/MS spectrum was consistent with the assignment. In particular, the fragment ion peak at 241 is characteristic of the inositol groups (Fig. 1I); and (ii) the intensity of peak 333 increased as the amount of standard LPI was added, suggesting that glycerolphosphoinositol was not a genuine lipid species in ascites. Rather, it was generated during mass spectrometry analysis.

Other Lyso-PLs Detected in the Negative Mode

The solvent system used for TLC development (Materials and Methods) can separate different lyso-PLs as described previously (15). Standard lyso-PLs, including LPC, LPE, LPG, LPI, LPS, PAF, and lyso-PAF were applied to the TLC plates along with lipid samples extracted from ascites. The lipids at locations corresponding to various lyso-PLs were eluted and analyzed. In the negative mode, other than different subclasses of LPAs, we also detected LPIs with different fatty acid chains in ascites samples. The ion peaks at *m/z* 571, 599, and 619 were 16:0-, 18:0-, and 20:4-LPIs, respectively (15) (Fig. 1A).

We did not detect LPS (15), LPE, or LPG in the bands corresponding to standard LPS, LPE, or LPG. However, several ion peaks at *m/z* 466, 480, 493, 506, and 529 were detected in the "LPE band" and the "LPG band" (Fig. 2A). Based on their molecular weights and the MS/MS analyses shown in Figs. 2B and 2C, they appeared to be the N-methylated derivatives of LPE. For example, the ion peak at *m/z* 466 was assigned to *N*-methyl-16:0-LPE, 480 to *N,N*-dimethyl-16:0-LPE, 493 to *N*-methyl-18:1-LPE, 506 to *N,N*-dimethyl-18:1-LPE, and 529 to *N,N*-dimethyl-20:4-LPE through MS/MS analyses (Figs. 2B–2D).

SPC, Lyso-PAF, and LPC Were Present in Ascites Samples

Phosphorylcholine-containing lyso-PLs were detectable with high sensitivity in the parent of 184 scan mode with positive detection. As shown in Fig. 3A, we found that relatively low levels of SPC, lyso-PAF, and high levels of LPCs were present in ascites. The MS spectrum of the standard compounds (SPC, lyso-PAF, 16:0- and 18:0-LPC) using similar molar ratios found in ascites is shown in Fig. 3B for comparison, and the identifications of ion peaks at *m/z* 465 (SPC), 482 (lyso-PAF), 496 (16:0-LPC), and 524 (18:0-LPC) were confirmed by MS/MS analyses (Figs. 3C–3E for lyso-PAF,

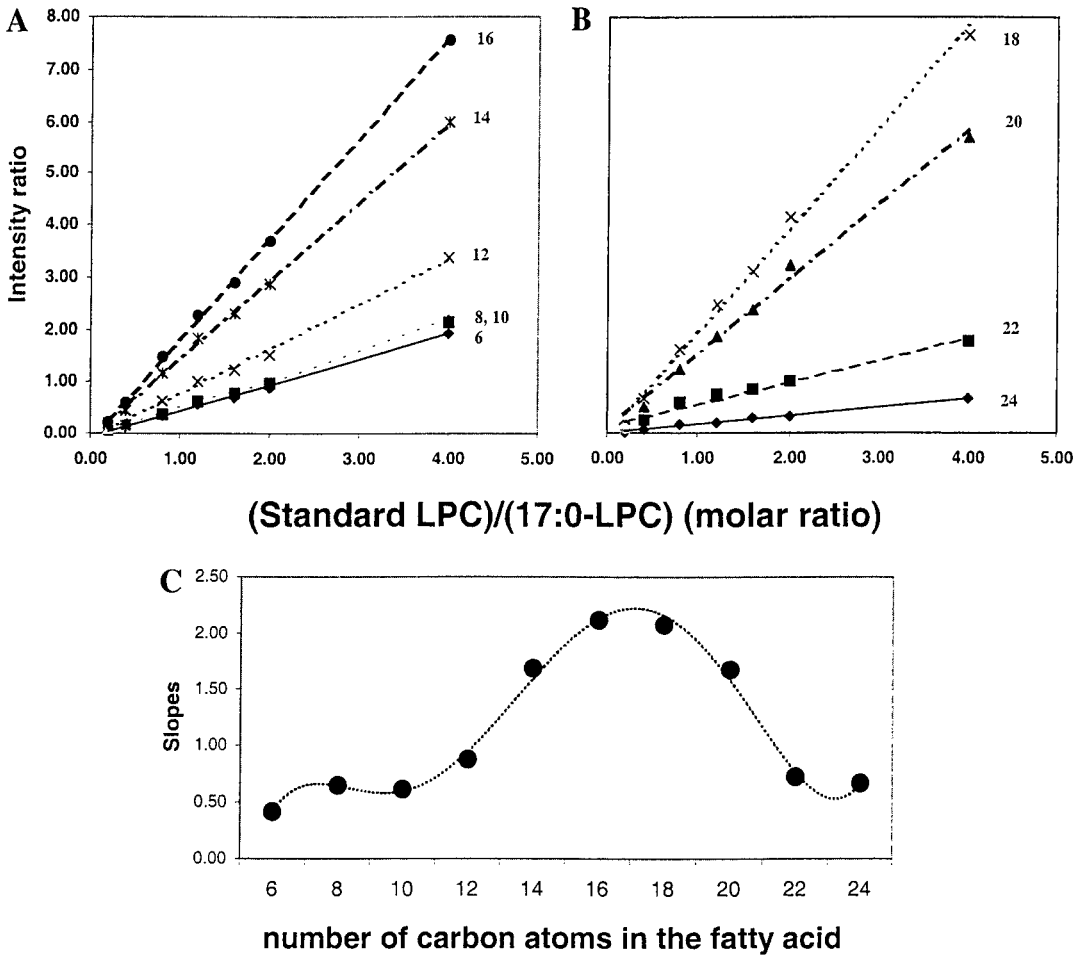

FIG. 5. Standard curves of LPCs. (A) Standard curves of 6:0-, 8:0-, 10:0-, 12:0-, 14:0-, and 16:0-LPCs. (B) 18:0-, 20:0-, 22:0-, and 24:0-LPCs. (C). The relationship between the ionization and fragmentation efficiencies (as reflected by the slopes of the standard curves in A and B) and the number of carbon atoms in the fatty acid chain in LPC.

Figs. 3F–3H for SPC, Figs. 3I and 3J for 18:0-LPC). The ion peak at *m/z* 524 could be either 16:0-PAF or 18:0-LPC. However, PAF and LPC can be separated on TLC (15) and the isolated PAF band from the TLC plate did not contain PAF (data not shown), suggesting that ascites from patients with ovarian cancer did not contain detectable amounts of PAF (<5 nM).

Quantitative Analysis of Different Lipids

The yield/recovery of extraction for S1P was 79 ± 5%; SPC, 100 ± 5%; and LPI, 80 ± 5%. Since internal standards of LPA and LPC were added to the ascites samples, the recoveries for these lipids were adjusted to the standards, and the quantities were calculated based on the standard curves.

For quantitative measurements, standard curves were established in the MRM mode. Standard curves for LPA and LPI had been established and described previously (15). Standard curves for S1P in the negative mode and SPC in the positive mode were also established as shown in Fig. 4.

To establish the standard curves for LPCs, we purchased a series of LPCs with the fatty acid chains from 6 to 24 carbons (all with even numbers of carbons; from Avanti Polar Lipids, Inc.). The standard curves for these LPCs were plotted (Figs. 5A and 5B). We found that the slopes, which reflect the ionization and fragmentation efficiencies, reached the maximum between 16 and 18 carbons and declined between 18 and 24 carbons, resulting in a bell-shaped curve (slope vs number of carbons in fatty acid chains of LPCs) (Fig. 5C).

Lyso-PLs Are Elevated in Ascites from Patients with Ovarian Cancer Compared to Patients with Nonmalignant Diseases

Accumulation of ascitic fluids are most often seen in patients with ovarian cancer or some benign liver dis-

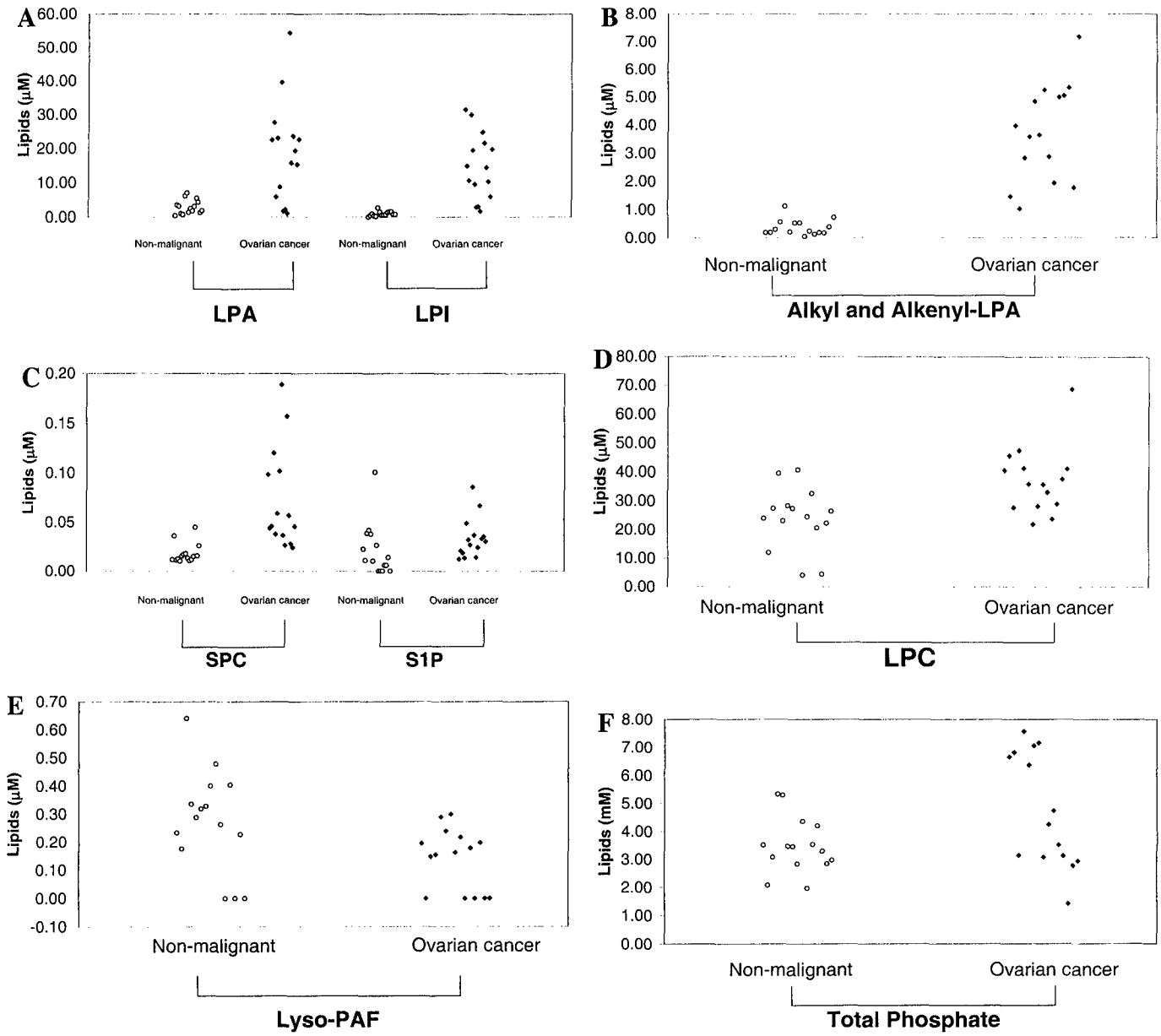

FIG. 6. The levels of various lyso-PLs in 15 pairs of ascites samples. (A) The total LPA and LPI levels; (B) the total alkyl- and alkenyl-LPAs (A-LPA) levels; (C) the SPC and S1P levels; (D) the total LPC levels; (E) the lyso-PAF levels; and (F) the total phospholipid levels in 15 pairs of ascites samples.

eases, such as hepatic cirrhosis. Importantly, ovarian cancer cells are growing in ascitic fluids so that ascites is the living environment for tumor cells. Ascitic fluids from patients with ovarian cancer, but not from patients with nonmalignant diseases, stimulate growth of ovarian tumor cells *in vitro* and *in vivo* (11, 12). To determine whether levels of bioactive lyso-PLs, which may be responsible for the different mitogenic activities, were different between these two groups of ascites samples, we quantitatively analyzed the levels of LPAs, LPIs, S1P, SPC, lyso-PAF, and LPCs in 15 pairs of ascites samples from patients with ovarian cancer or liver failure.

Quantitative analyses of lyso-PLs were performed for all ascites samples in both negative and positive modes. Figure 6 shows the data points from the 15 pairs of samples for each group of lysolipids, including total acyl-LPAs, total LPIs, total alkyl- and alkenyl-LPA, SPC, S1P, lyso-PAF, and total LPC (Figs. 6A to 6E). To determine whether patients with ovarian cancer had overall increased total phospholipids, the total phosphorus content from these samples was deter-

TABLE 1

Statistical Analysis of Lyso-PLs in 15 Pairs of Ascites Samples

	LPA (μM)	LPI (μM)	A-LPA[a] (μM)	SPC (nM)	S1P (nM)	LPC (μM)	L-PAF[b] (μM)	Total P_i (mM)
Ovarian cancer								
Mean	18.9	14.7	3.7	71.5	33.5	37.3	0.1	4.7
SD	14.7	9.7	1.7	50.8	20.5	11.6	0.1	2.0
Median	19.4	14.4	3.6	46.1	30.5	36.1	0.2	4.3
Minimum	1.1	1.7	1.0	24.3	12.5	22.1	0.0	1.4
Maximum	54.3	31.5	7.2	188.9	86.1	68.7	0.3	7.6
Nonmalignant								
Mean	2.9	0.9	0.4	17.9	21.1	23.8	0.3	3.5
SD	2.0	0.7	0.3	10.1	26.6	10.6	0.2	1.0
Median	2.4	0.7	0.2	15.0	11.1	24.5	0.3	3.5
Minimum	0.4	0.0	0.0	10.3	0.0	4.1	0.0	2.1
Maximum	7.0	2.6	1.1	44.8	100.9	40.7	0.6	5.3
P value	0.0008	0.0001	0.0000	0.0011	0.1631	0.0025	0.0227	0.0466

[a] A-LPA, total alkyl- and alkenyl LPAs.
[b] L-PAF, lyso-PAF.

mined and results are shown in Fig. 6F. The statistical analyses were conducted and the results are summarized in Table 1.

DISCUSSION

Using quantitative ESI-MS, we confirmed our previous observations analyzed by gas chromatography that high concentrations (1–54 μM) of LPAs are present in ovarian cancer ascites. However, the ESI-MS method offers several advantages when compared with the GC method: (i) ESI-MS uses soft ionization and intact molecular species are detected, which makes the identification of lipids relatively easy; (ii) structures of interesting ion peaks can be determined through the MS/MS and/or LC/MS/MS analysis; (iii) it simultaneously detects many molecular species, including lipids with different fatty acid chains; (iv) it is highly sensitive (typically in the femtomole to low picomole range); and (v) the assay can be easily adapted to an autosampler.

We have used the parent of 79 and 184 scan modes to detect the presence or absence of ion peaks corresponding to a variety of lyso-PLs in ascites sample. These modes were found to be ideal for obtaining overall information about the profiles of lyso-PLs in a particular samples. However, MRM is the best for quantitative work, since it is at least 10 times more sensitive than the parent scan modes to detect lyso-PLs with higher resolutions. The lyso-PLs with a difference mass of 2 can be resolved easily only in the MRM mode without loss of required sensitivity (Fig. 1B).

We reported previously that LPAs (14:0-, 16:0-, and 18:0-LPAs) showed increased ionization and fragmentation efficiencies (as reflected by increased slope) when the length of the fatty acid chain increases (15). Similarly, LPCs from 14:0 to 18:0 also demonstrated increased slopes, suggesting increased ionization efficiencies and fragmentation efficiencies. LPAs with longer fatty acid chains were not commercially available and the ionization efficiencies and fragmentation efficiencies for those LPAs were not detected directly. In our previous report, we predicted the trend of increased ionization efficiencies may continue for LPAs with longer fatty acid chains, such as 20:4- and 22:6-LPAs (15). Based on the results from LPCs, however, decreased slopes may also be true for LPAs with long fatty acid chains (20–24 carbons).

The most important finding of this work is that malignant ascites contain significantly higher levels of lyso-PLs, including total acyl-LPAs, total alkyl- and alkenyl-LPAs, total LPIs, SPC, and total LPCs, than nonmalignant ascites. In contrast, the differences in S1P and lyso-PAF levels between the two groups of ascites are not significant (Fig. 6 and Table 1). The elevated lyso-PL levels are not due to a generalized overproduction of phospholipids, since the total phospholipid contents in these two groups of ascites samples were not statistically different ($P = 0.05$; $P \leq 0.01$ is considered to be statistically significant). We have previously shown that LPA stimulates tumor cell proliferation (6, 7). The high levels of bioactive lipids may play important roles in tumor development and metastasis. Furthermore, these lipids are potentially useful prognostic markers for disease progression and/or novel therapeutic target(s). Total LPIs and total alkyl and alkenyl-LPAs are particularly good ($P < 0.0001$) in distinguishing malignant from nonmalignant ascites.

We detected three new classes of lysolipids in ascites, alkyl-LPAs, alkenyl-LPAs, and methylated LPEs, although the identifications of methylated LPEs remain to be confirmed by comparing their spectra to that from standard methylated LPEs, which are not commercially available currently. Synthetic alkyl-LPA has been shown to have signaling activities (16–18) and induced hypotensive activity on feline arterial blood pressure (19, 20). However, naturally occurring alkyl-LPA has only been detected in rat brains recently and induces rounding in neuroblastoma/glioma hybrid cells (21). Alkenyl-LPA was generated after corneal injury in the aqueous humor and lacrimal gland fluid of the rabbit eye (22) and may activate different receptors from those for acyl-LPA (23). Both acyl-LPA and alkenyl-LPA induce proliferation in NIH3T3 cells (24, 25). To our knowledge this is the first time that alkyl-LPA and alkenyl-LPA were detected in human body fluids. The biological function of these subclasses of LPAs remains to be determined. However, the relative elevation of these lipids in ovarian cancer ascites vs nonmalignant ascites suggests the involvement of these lipids in tumor biology.

N-Monomethylphosphatidylethanolamine (PE) and *N,N*-dimethyl-PE are present in animal tissues and they are precursors of phosphatidylcholine synthesis (26, 27). In addition, the methylation has been demonstrated to be important in transmembrane signaling. Phospholipid methylation is coupled to calcium influx and the release of arachidonic acid (28). However, to our knowledge, methylated derivatives of LPE have not been reported and their biological function(s) remains to be determined.

ACKNOWLEDGMENT

We thank Linnea Baudhuin for technical assistance and editing of the manuscript.

REFERENCES

1. Liscovitch, M., and Cantley, L. (1994) Lipid second messengers. *Cell* **77,** 329–334.
2. Moolenaar, W., Kranenburg, O., Postma, F., and Zondag, G. (1997) Lysophosphatidic acid: G-protein signalling and cellular responses. *Curr. Opin. Cell Biol.* **9,** 168–173.
3. Moolenaar, W. H. (2000) Development of our current understanding of bioactive lysophospholipids [in process citation]. *Ann. N. Y. Acad. Sci.* **905,** 1–10.
4. Meyer zu Heringdorf, D., van Koppen, C., and Jakobs, K. (1997) Molecular diversity of sphingolipid signalling. *FEBS Lett.* **410,** 34–38.
5. Spiegel, S. (1999) Sphingosine 1-phosphate: A prototype of a new class of second messengers. *J. Leukocyte Biol.* **65,** 341–344.
6. Xu, Y., Fang, X., Casey, G., and Mills, G. (1995) Lysophospholipids activate ovarian and breast cancer cells. *Biochem. J.* **309,** 933–940.
7. Xu, Y., Gaudette, D., Boynton, J., Frankel, A., Fang, X., Sharma, A., Hurteau, J., Casey, G., Goodbody, A., Mellors, A., *et al.* (1995) Characterization of an ovarian cancer activating factor in ascites from ovarian cancer patients. *Clin. Cancer Res.* **1,** 1223–1232.
8. Berchuck, A., and Carney, M. (1997) Human ovarian cancer of the surface epithelium. *Biochem. Pharmacol.* **54,** 541–544.
9. Bookman, M. A. (1998) Biological therapy of ovarian cancer: Current directions. *Semin. Oncol.* **25,** 381–396.
10. Westermann, A., Beijnen, J., Moolenaar, W., and Rodenhuis, S. (1997) Growth factors in human ovarian cancer. *Cancer Treat. Rev.* **23,** 113–131.
11. Mills, G., May, C., McGill, M., Roifman, C., and Mellors, A. (1988) A putative new growth factor in ascitic fluid from ovarian cancer patients: Identification, characterization, and mechanism of action. *Cancer Res.* **48,** 1066–1071.
12. Mills, G., May, C., Hill, M., Campbell, S., Shaw, P., and Marks, A. (1990) Ascitic fluid from human ovarian cancer patients contains growth factors necessary for intraperitoneal growth of human ovarian adenocarcinoma cells. *J. Clin. Invest.* **86,** 851–855.
13. Hong, G., Baudhuin, L. M., and Xu, Y. (1999) Sphingosine-1-phosphate modulates growth and adhesion of ovarian cancer cells. *FEBS Lett.* **460,** 513–518.
14. Xu, Y., Shen, Z., Wiper, D., Wu, M., Morton, R., Elson, P., Kennedy, A., Belinson, J., Markman, M., and Casey, G. (1998) Lysophosphatidic acid as a potential biomarker for ovarian and other gynecologic cancers. *JAMA* **280,** 719–723.
15. Xiao, Y., Chen, Y., Kennedy, A. W., Belinson, J., and Xu, Y. (2000) Evaluation of plasma lysophospholipids for diagnostic significance using electrospray ionization mass spectrometry (ESI-MS) analyses. *Ann. N. Y. Acad. Sci.* **905,** 242–259.
16. Simon, M., Chap, H., and Douste-Blazy, L. (1982) Human platelet aggregation induced by 1-alkyl-lysophosphatidic acid and its analogs: A new group of phospholipid mediators? *Biochem. Biophys. Res. Commun.* **108,** 1743–1750.
17. Svetlov, S., Siafaka-Kapadai, A., Hanahan, D., and Olson, M. (1996) Signaling responses to alkyllysophosphatidic acid: The activation of phospholipases A2 and C and protein tyrosine phosphorylation in human platelets. *Arch. Biochem. Biophys.* **336,** 59–68.
18. Tokumura, A., Okuno, M., Fukuzawa, K., Houchi, H., Tsuchiya, K., and Oka, M. (1998) Positive and negative controls by protein kinases of sodium-dependent Ca2+ efflux from cultured bovine adrenal chromaffin cells stimulated by lysophosphatidic acid. *Biochim. Biophys. Acta* **1389,** 67–75.
19. Tokumura, A., Homma, H., and Hanahan, D. J. (1985) Structural analogs of alkylacetylglycerophosphocholine inhibitory behavior on platelet activation. *J. Biol. Chem.* **260,** 12710–12714.
20. Tokumura, A., Maruyama, T., Fukuzawa, K., and Tsukatani, H. (1985) Effects of lysophosphatidic acids and their structural analogs on arterial blood pressure of cats. *Arzneimittelforschung* **35,** 287–292.
21. Sugiura, T., Nakane, S., Kishimoto, S., Waku, K., Yoshioka, Y., Tokumura, A., and Hanahan, D. (1999) Occurrence of lysophosphatidic acid and its alkyl ether-linked analog in rat brain and comparison of their biological activities toward cultured neural cells. *Biochim. Biophys. Acta* **1440,** 194–204.
22. Liliom, K., Fischer, D., Virag, T., Sun, G., Miller, D., Tseng, J., Desiderio, D., Seidel, M., Erickson, J., and Tigyi, G. (1998) Identification of a novel growth factor-like lipid, 1-*O*-*cis*-alk-1′-enyl-2-lyso-*sn*-glycero-3-phosphate (alkenyl-GP) that is present in

commercial sphingolipid preparations. *J. Biol. Chem.* **273,** 13461–13468.

23. Liliom, K., Murakami-Murofushi, K., Kobayashi, S., Murofushi, H., and Tigyi, G. (1996) *Xenopus* oocytes express multiple receptors for LPA-like lipid mediators. *Am. J. Physiol.* **270,** C772–C777.
24. Fischer, D., Liliom, K., Guo, Z., Nusser, N., T., V., Murakami-Murofushi, K., Kobayashi, S., Erickson, J., Sun, G., Miller, D., and Tigyi, G. (1998) Naturally occurring analogs of lysophosphatidic acid elicit different cellular responses through selective activation of multiple receptor subtypes. *Mol. Pharmacol.* **54,** 979–988.
25. Munzel, P., and Koschel, K. (1982) Alteration in phospholipid methylation and impairment of signal transmission in persistently paramyxovirus-infected C6 rat glioma cells. *Proc. Natl. Acad. Sci. USA* **79,** 3692–3696.
26. Samad, A., Licht, B., Stalmach, M., and Mellors, A. (1988) Metabolism of phospholipids and lysophospholipids by *Trypanosoma brucei*. *Mol. Biochem. Parasitol.* **29,** 159–169.
27. Chen, S., and Kou, A. (1982) High-performance liquid chromatography of methylated phospholipids. *J. Chromatogr. A* **232,** 237–249.
28. Hirata, F., and Axelrod, J. (1980) Phospholipid methylation and biological signal transmission. *Science* **209,** 1082–1090.

The Role and Clinical Applications of Bioactive Lysolipids in Ovarian Cancer

Yan Xu, PhD, Yi-jin Xiao, PhD, Linnea M. Baudhuin, MS, and Benjamin M. Schwartz, MD

OBJECTIVE: *To review the current understanding of the role of bioactive lysolipids in ovarian cancer and their potential clinical applications.*

METHODS: *A MEDLINE search and our own work, including some unpublished work, are the major sources of the review. The MEDLINE search terms used included lysophosphatidic acid, lysophophatidylcholine (LPC), lysophosphatidylinositol (LPI), sphingosine-1-phosphate, and sphingosylphosphorylcholine (SPC).*

RESULTS: *Elevated lysolipid levels were detected in plasma and ascites samples from patients with ovarian cancer compared with samples from healthy controls or patients with nonmalignant diseases. These lysolipids regulate growth adhesion, production of angiogenic factors, and chemotherapeutic drug resistance in ovarian cancer cells. Ovarian cancer cells were likely to be at least one of the sources for elevated lysolipid levels in the blood and ascites of patients with ovarian cancer.*

CONCLUSIONS: *Bioactive lysolipid levels might be sensitive markers for detecting gynecologic cancers, particularly ovarian cancer. The prognostic value of lysolipids in ascites is worth further investigation. Bioactive lysolipid molecules can affect both the proliferative and metastatic potentials of ovarian cancer cells; therefore, regulation of the production or degradation of these lipids and interception of the interaction between these lipids and their receptors could provide novel and useful preventative or therapeutic measures. (J Soc Gynecol Investig 2001;8:1–13)*

KEY WORDS: Ovarian cancer, bioactive lysolipids, lysophosphatidic acid, diagnosis, clinical management.

Ovarian carcinoma has the worst prognosis of any gynecologic malignancy because of difficulties in early detection, the high metastatic potential of the tumor, and the lack of highly effective treatments for the metastatic disease.[1] If the disease is detected at stage I (confined to the ovaries), the long-term survival rate is approximately 90%; however, more than 70% of women with ovarian cancer have advanced stage disease (spread to the abdominal cavity and/or other organs) at diagnosis, and the 5-year survival rate for those women remains very poor (only 20–30%).[1–3] The processes governing growth and metastasis of ovarian carcinomas have been studied in the past few decades but are still poorly understood.

In order to improve the overall outcome of ovarian cancer, significant progress in the following areas is required: development of highly sensitive and reliable methods for early detection of the disease, development of better prognostic and clinical treatment methods for patients, and further understanding of the mechanisms of growth regulation of ovarian cancer by studying growth-stimulating factors and their pathways. This third objective will provide information for potential new therapeutic targets and methods.

One of the frequent consequences of the metastasis of ovarian tumors to the peritoneal cavity is the production of large volumes of ascitic fluids. Ascites from patients with ovarian cancer typically contains a high number of tumor cells, mesothelial cells, lymphocytes, other hematopoietic cells, and soluble growth-regulating factors. These factors potentially regulate growth metastasis and chemosensitivity of the tumor cells.[4–6] Peptide factors related to ovarian cancer include epidermal growth factor (EGF), basic fibroblastic growth factor (bFGF), transforming growth factor-α (TGF-α), TGF-β, vascular endothelial growth factor (VEGF), macrophage colony-stimulating factor (CSF-1), interleukin-2 (IL-2), IL-6, IL-8, IL-10, and tumor necrosis factor-α (TNF-α).[4–6] We and others have recently found that, in addition to these peptide factors, there is a group of lipid factors involved in ovarian cancer. In this article we review the role and potential clinical applications of bioactive lysolipids in ovarian cancer.

From the Department of Cancer Biology Lerner Research Institute and the Department of Gynecology and Obstetrics Cleveland Clinic Foundation; and the Department of Chemistry, Cleveland State University, Cleveland, Ohio.

Supported in part by an United States Army Medical Research grant (DAMD17-99-1-9563) a National Institutes of Health grant R21 CA84038-01, Atairgin Technologies Inc., and the Lynne Cohen Foundation.

Address reprint requests to: Yan Xu, PhD, Department of Cancer Biology, Cleveland Clinic Foundation, 9500 Euclid Ave., Cleveland, OH 44195.

1071-3576/01/$20.00
PII S1071-3576(00)00092-7

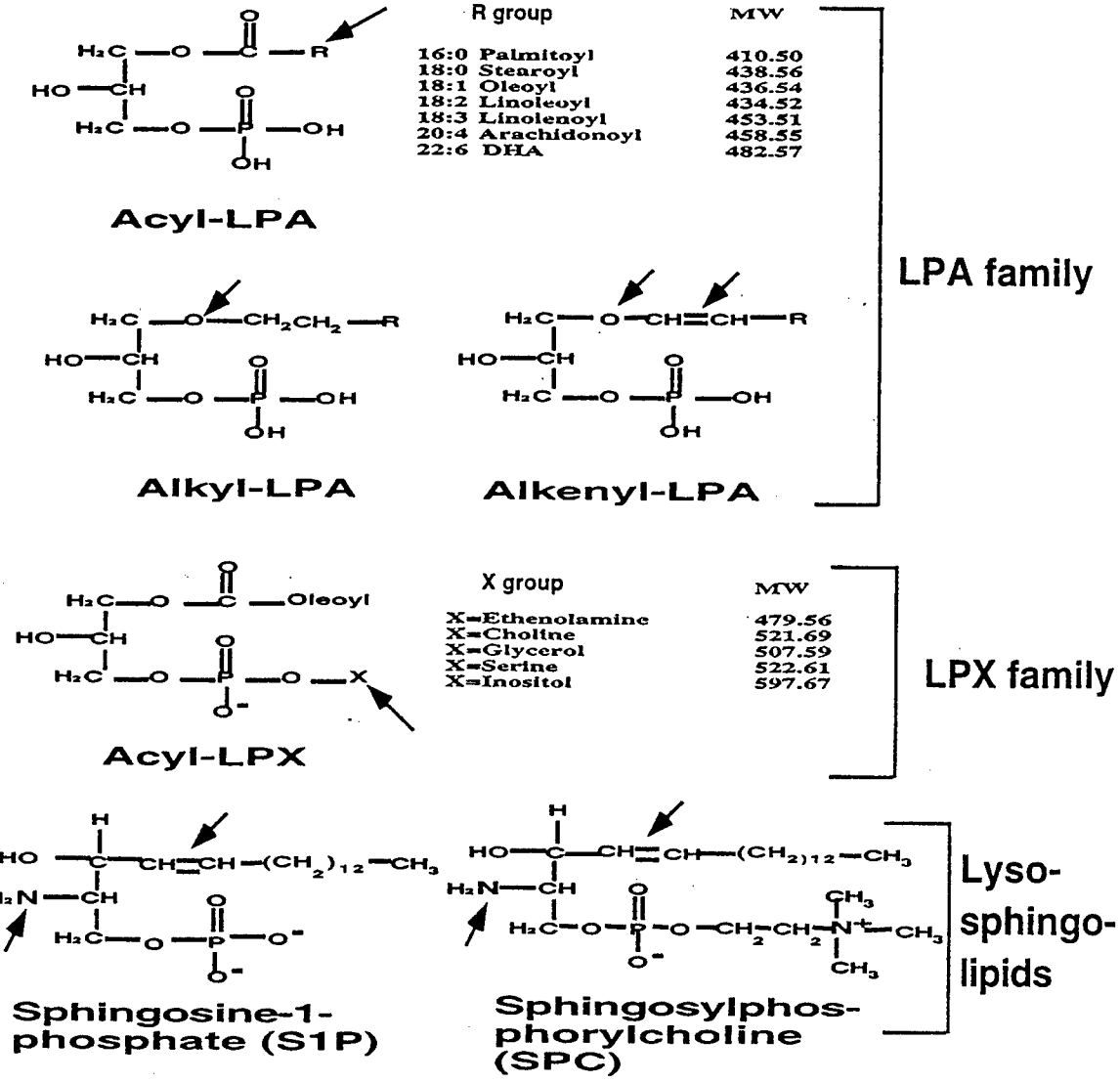

Figure 1. The structures of different lysolipids, including subclasses of lysophosphatidic acid (LPA), lysophospholipid-X (LPX), and two lysosphingolipids—sphingosine-1-phosphate (S1P) and sphingosylphosphorylcholine (SPC). *R* = the long aliphatic side chain. LPXs can also have different fatty acid chains, as indicated in acyl-LPA structure. The structures of LPXs (only oleoyl-LPXs) and their different molecular weights are shown in the figure. *Arrows* point to distinguishing structural features in each family of lysolipids.

BIOACTIVE LYSOLIPIDS

Although previously viewed primarily as structural building blocks of the cell membrane, lipids and lysolipids are now recognized as important cell-signaling molecules.[7,8] These lipids can be classified generally into two major groups, intracellular and extracellular, with some lipid molecules being both intracellular and extracellular.[9,10] Among extracellular signaling lipid molecules, lysophosphatidic acid (LPA) has been studied most extensively.[7,11] Lysophosphatidic acid consists of many different molecular species as a result of alterations in the fatty acid chain, as indicated in Figure 1. In addition, the long-chain aliphatic group (the R group in Figure 1) may link to the glycerol backbone through different chemical linkages resulting in various subclasses of LPAs (acyl-, alkyl-, and alkenyl-LPAs). Other lysophospholipids might also have signaling properties in cellular systems. These molecules have different head groups attached to the phosphate and include lysophosphatidylethanolamine (LPE), lysophosphatidylcholine (LPC), lysophosphatidylglycerol (LPG), lysophosphatidylinositol (LPI), and lysophosphatidylserine (LPS) (Figure 1). Two lysosphingolipid molecules, sphingosine-1-phosphate (S1P) and sphingosylphosphorylcholine (SPC), are both extracellular and intracellular signaling molecules.[9,10,12,13] The structures of the subclasses of LPAs, ie, acyl-LPA, alkyl-LPA, alkenyl-LPA, lysophospholipid-X (LPX), S1P, and SPC, are shown in Figure 1.

All of the lipid molecules shown in Figure 1 are phosphate-containing lysolipids (lyso-PLs) with a glycerol or sphingosine backbone. They are less hydrophobic compared with their diacyl or N-acyl partners and can be secreted extracellularly.

Table 1. The Biological Functions of Lysophosphatidic acid, Sphingosine-1-phosphate, and Sphingosylphosphorylcholine

	LPA	S1P	SPC
Cell differentiation (stimulation or inhibition)	14–16	17–19	20
Cell invasion, activation, or inhibition; cell motility	21–26	27–33	20
Chemotaxis	34, 35	27, 36–38	20
Cell morphologic and shape changes	34, 39, 40	41–43	20
Cell contraction	44–46	47	47, 48
Wound healing	49, 50	51	52
Platelet activation	53–66	43, 58, 67, 68	69
Gene regulation	70, 25, 71–73	74	74, 75
Superoxide or nitric oxide regulation	76	77–79	80
Disease related	81–87	88	89, 90

LPA = lysophosphatidic acid; S1P = sphingosine-1-phosphate; SPC = sphingosylphosphorylcholine.
Data are reference numbers.

More importantly most of them have been clearly shown to be signaling molecules.[7,10,11,13] These molecules have a broad range of biologic effects on a variety of cellular systems through numerous signaling pathways, which are summarized in Tables 1 and 2. These lipids regulate cell growth, and these growth effects are dependent on the cellular environment. In most cases, LPA promotes cell proliferation and prevents apoptosis; S1P has dual roles (both growth stimulation and inhibition); and SPC promotes cell proliferation in several nonmalignant cell types but inhibits cell growth in leukemia, breast, ovarian, and pancreatic cancer cells (Table 3). These lipids apparently have even broader biologic effects on different cell and tissue types, a phenomenon that has not been well characterized. In particular, our understanding of the role of these lipid molecules in cancer development has just begun.

OCCURRENCE OF BIOACTIVE LYSOLIPIDS IN OVARIAN CANCER

Our understanding of the potential involvement of bioactive lysolipids in ovarian cancer began when we identified LPA as an activating factor in ascites from patients with ovarian cancer.[185,186] We found that LPA isolated from ovarian cancer ascitic fluids had tumor growth-promoting activity.

Ovarian cancer is associated with the production of a large volume of peritoneal ascites. Ovarian cancer cells usually grow on the surface of the ovary, which is situated in the peritoneal cavity, or they metastasize to other organs in the peritoneal cavity. Therefore, ascites represents the in vivo environment for the tumor. To a large extent, tumor cells are growing in suspension in ascitic fluids. Ascitic fluids from patients with ovarian cancer but not from patients with benign diseases that produce large volumes of ascites, such as hepatic cirrhosis, stimulated intracellular calcium release from ovarian cancer cells in vitro. This activity was not associated with any of the peptide factors previously mentioned, thereby implicating a novel factor(s). Furthermore, normal ovarian epithelial cells and fresh or cultured lymphoid cells did not respond to that factor.[187] In addition, ascitic fluids stimulated proliferation of ovarian cancer cells in vivo in nude mice.[188] The human ovarian cancer cell line HEY grew intraperitoneally in nude mice in the presence but not absence of ascites from human ovarian cancer patients. The mice eventually developed ascites

Table 2. Receptors and Signaling Pathways of Lysophosphatidic acid, Sphingosine-1-phosphate, and Sphingosylphosphorylcholine

	LPA	S1P	SPC
Receptor	8, 29, 91–96 (Edg2, 4, 7)	8, 29, 91–98 (Edg1, 3, 5, 6, 8)	OGR1, 99
Increase intracellular calcium	8, 96	100–103	99, 104–106
Potassium channel	107	108	109, 110
Chloride efflux	111	112	112
Arachidonic acid release	113	114	115
cAMP increase or decrease	113	41, 116–120	106, 115, 121, 122
PKC activation	123	124	125, 126
PLC activation	32, 127, 128	119	129
PLA_2 activation	8, 96	. . .	130
PLD activation	131	132–136	132, 137
PI3K/Akt activation	138, 139	. . .	. . .
NF-κB activation	140	141	. . .
Ras activation	11, 96, 142, 143	96	115, 118, 144
Tyrosine phosphorylation	143, 145, 146	147	148, 149
MAP kinase activation	116, 143, 146, 150–152	153, 154	99, 155
Rho activation	32, 150	149	156, 121, 148, 157, 158

LPA = lysophosphatidic acid; S1P = sphingosine-1-phosphate; SPC = sphingosylphosphorylcholine; cAMP = cyclic adenosine monophosphate; PKC = protein kinase C; phospholipase C; phospholipase A_2; PLD = phospholipase D; PI3K = phosphatidylinositol 3-kinase; Akt = human cellular homologues of the viral oncogene *v-Akt*, also known as protein kinase B; MAP = mitogen-activated protein.
Data are reference numbers.

Table 3. Growth Effects of Lysophosphatidic acid, Sphingosine-1-phosphate, and Sphingosylphosphorylcholine

	LPA	S1P	SPC
DNA synthesis	159	160	115
Cell proliferation	159, 161–165	160, 166–169	115, 170–174
Growth inhibition	175	168, 176, 177	152, 178, 179
Apoptosis stimulation or prevention	180–182	166, 169, 183, 184	...

Abbreviations as in Table 1.
Data are reference numbers.

that contained potent growth-stimulating activity, suggesting an autocrine mechanism of growth regulation.[188] Ascites from patients with benign diseases was ineffective at tumor induction.[188]

We purified and identified this factor with growth-stimulating activity in ascites from ovarian cancer patients and termed it ovarian cancer activating factor (OCAF).[185] Ovarian cancer activating factor is not a peptide growth factor or cytokine that has been identified previously. Instead, OCAF is composed of several molecular species of LPA. Both OCAF and synthetic LPA stimulated the growth of ovarian cancer cells in vitro.[185,186] We have also reported that S1P is present in ascites from patients with ovarian cancer.[189]

More recently we developed an electrospray ionization mass spectrometry (ESI-MS)-based assay for detection and quantification of LPA and closely related lysolipids. This method can reproducibly detect various lipid species simultaneously with high sensitivity.[190] Using this method we detected alkyl-LPAs and alkenyl-LPAs for the first time in human body fluids (ascites from patients with ovarian cancer). We also detected SPC and other lysolipids in ovarian cancer ascites, which is described later in more detail. Most importantly, levels of these bioactive lysolipids were higher in blood[81,190] and ascitic fluids from patients with ovarian cancer compared with normal healthy controls or patients with nonmalignant diseases. These findings suggested that those lipid molecules are likely to be pathologically relevant to ovarian cancer.

BIOLOGICAL FUNCTIONS OF LYSOLIPIDS IN OVARIAN CANCER CELLS

The biologic functions of most markers currently used in ovarian cancer, including CA 125, are unknown. In contrast, the discovery and development of lysolipid markers began from functional studies. Considerable information pertaining to lysolipids has been collected recently to indicate that lysolipids might be involved in the initiation and development of ovarian cancer.

The Effects of Different Lysolipid Molecules on Cell Growth of Ovarian Cancer Cells

We observed distinct and sometimes opposite growth effects induced by different lysolipid molecules on ovarian cancer cells. Because ovarian tumor cells can grow either as solid tumor or as individual cells floating in ascites, we tested the cell growth effects of lysolipids on attached and detached ovarian cancer cells. We found that LPA (1–15 μM) stimulated ovarian cancer cell growth when cells were either attached or detached,[176,185] but S1P (1–15 μM) had a dual effect on ovarian cancer cell growth and survival: it induced death in cells that were in suspension but stimulated growth in cells that were attached.[189] In contrast, SPC (1–15 μM) inhibited cell growth regardless of cell attachment status.[185]

Lysophosphatidylinositol species with different fatty acid side chains are present and elevated in the blood and ascites of patients with ovarian cancer (see below for details). Lysophosphatidylinositol levels were elevated and were mitogenically active in k-Ras-transformed epithelial cells.[191] However, our preliminary studies indicated that LPI had no effect on the growth of ovarian cancer cells in vitro (unpublished results). Another lysolipid, LPS, which is not present in ascites had a limited effect on the growth of ovarian cancer cells unless high concentrations (greater than 20 μM) were used.[190]

Effects of Different Lysolipid Molecules on Cell Morphology, Mobility, Adhesion, and Invasion

Tumor metastasis remains a major cause of death for cancer patients. Several events are required for malignant cells to detach from the primary tumor site, migrate to distant sites and proliferate at these sites, including blood vessel formation (angiogenesis), cell attachment, invasion (matrix degradation and cell motility), and cell proliferation.[192,193] In relation to these metastatic events, we found that different lysolipids regulate cell morphology and cell-cell or cell-matrix adhesion differently.[189] Whereas LPA enhances cell attachment, both S1P and SPC inhibit cell adhesion to the surface of tissue culture dishes and to the following extracellular matrix (ECM) proteins: laminin, collagens I and IV, and fibronectin.[189] Sphingosine-1-phosphate also induced cell-cell aggregation in suspended cells.[189]

Lysophosphatidic acid (20 μM) was shown to upregulate urokinase plasminogen activator (uPA) production in both the SKOV3 and OVCAR3 ovarian cancer cell lines.[70] Urokinase plasminogen activator contributes to metastasis and migration because it catalyzes the conversion of plasminogen to plasmin, thus leading to degradation of the basement membrane.[70] Furthermore, in ovarian cancer cells, LPA stimulates the activation of matrix metalloproteinase 2,[194] an important extracellular matrix protease involved in tumor metastasis.

Although not directly tested in ovarian cancer cells, LPA induced tumor cell invasion in other types of tumor cells.[21,53,195,196] Conversely, S1P has a more complex effect on different cell types by being either stimulatory or inhibitory on cell motility.[27,156,196]

Taken together these results suggest that LPA and other lysolipids may regulate metastasis of ovarian tumors.

Regulation of Angiogenic Factors by Bioactive Lipids in Ovarian Cancer Cells

Angiogenesis underlies progressive tumor events such as metastasis. Interleukin-8 (IL-8) is a proinflammatory and proangiogenic factor. High expression of IL-8 mRNA has been detected in clinical specimens of late-stage ovarian carcinomas[197,198] and in malignant ascites.[199–201] It has been shown that the expression level of IL-8 directly correlates with the progression of human ovarian carcinomas implanted into the peritoneal cavity of nude mice. Furthermore, the mean survival rates of mice bearing tumors derived from human ovarian cancer cells are inversely associated with the expression of IL-8.[198]

Several factors have been shown to regulate IL-8 in ovarian cancer cells. Hypoxia, which is a common feature of solid tumors, induces IL-8 expression in the human ovarian cancer cell lines SKOV3 and HEY-8A.[202] All-trans-retinoic acid and TNF-α stimulate IL-8 release and mRNA expression in the human ovarian cancer cell line HOC-7.[203] In addition, paclitaxel, a chemotherapeutic drug for ovarian cancer, induces IL-8 transcription and secretion in a subset of human ovarian cancer cells (OVCA420 and OVCA429 but not OVCA194 or OCVA432).[204] Other physiologic and pathologic conditions might also contribute to the regulation of IL-8 expression and secretion in ovarian cancer cells.

We found that several lysolipid factors in ascites, including lysophosphatidic acid (LPA), sphingosine-1-phosphate (S1P), and sphingosylphosphorylcholine (SPC), increased mRNA levels and protein secretion of IL-8 from ovarian cancer cells in vitro. These regulations are both time-dependent and dose-dependent. Each lipid molecule regulates IL-8 through distinct signaling pathways.[205] We also found that both S1P and SPC at pathologic concentrations found in ascites (20–100 nM), were synergistic with 5–15 μM of LPA in enhancing IL-8 production from HEY cells.[205] The fact that IL-8 secretion was stimulated by pathologic concentrations of individual or combined lipids suggests that these lipids might regulate IL-8 in vivo and might be pathologically related to the development of the disease.[205]

Modulation of Chemosensitivity

Ovarian carcinomas are usually chemosensitive. After surgical debulking, systemic or intraperitoneal delivery of antineoplastic agents is the main treatment for patients with ovarian cancer.[206–208] Platinum- or paclitaxel-containing anticancer drugs are the main therapeutic agents for ovarian cancer.[209] Unfortunately most patients with stage III or IV disease are not cured by these therapies, and when cancer recurs, the patients usually develop resistance to their prior chemotherapy drugs.[210] Studying and understanding the mechanism of chemoresistance is important to overcoming this problem.

Lysophosphatidic acid increases the resistance of the HEY ovarian cancer cell line to platinum-based chemotherapeutic reagents, which are the most frequently used drugs in the treatment of ovarian cancer. This resistance appears to occur because OCAF/LPA can decrease the ability of cisplatin to induce apoptosis.[210]

Interleukin-8 has been identified as a differentially upregulated gene in the paclitaxel- and adriamycin-resistant human ovarian carcinoma cell lines SKOV3 and CAOV3, as well as in cell lines from other carcinomas. This suggests that IL-8 might have a general role in the multidrug-resistant phenotype or in the stress response of cells exposed to an antineoplastic agent.[211] Our findings that lysolipids regulate IL-8 expression and production suggest a potential link between lysolipids and drug resistance.

RECEPTORS FOR LYSOLIPIDS AND THEIR SIGNALING PATHWAYS

Receptors for Lysolipids in Ovarian Cancer

Recently, eight receptors known as endothelial differentiation gene (Edg) receptors have been identified as receptors for LPA or S1P.[212–216] Many of these receptors are expressed in ovarian cancer cells lines. For example, HEY cells express Edg1 and Edg3, which are receptors for S1P, as well as Edg2, a receptor for LPA (authors' unpublished results). Another LPA receptor, Edg4, is prominently expressed in primary cultures and established lines of ovarian cancer cells but not in nonmalignant ovarian surface epithelial cells.[217] Conversely, Edg2, another LPA receptor, might mediate LPA-independent apoptosis in ovarian cancer cells.[180] The receptors for S1P (Edg1, Edg3, Edg5, and Edg6) are also low-affinity receptors for SPC.[144,218]

Recently we identified the first highly specific and high-affinity receptor for SPC.[99] We have shown that SPC is a high-affinity ligand for an orphan ovarian cancer G-protein coupled receptor 1 (OGR1). In OGR1-transfected cells SPC binds to OGR1 with high affinity (dissociation constant = 33.3 nM) and high specificity, transiently increases intercellular calcium, activates p42/44 mitogen-activated protein (MAP) kinases, and inhibits cell proliferation. In addition SPC causes internalization of OGR1 in a structurally specific manner.[99] Ovarian cancer HEY and OCC1 cell lines both express OGR1.[99]

Activation of Signaling Pathways by Lysolipids in Ovarian Cancer

The signaling pathways of LPA, S1P, and SPC have been studied extensively in fibroblasts and other cellular systems.[8,11,13] Through their receptors, these lipids activate at least three classes of G proteins: G_i, G_q, and $G_{12/13}$. Lipid-dependent activation of the $G_{\alpha i}$ pathway is linked to the mitogenic Ras-MAPK cascade in addition to possible involvement of phosphoinositide 3-kinase (PI3K). The lipid-activated $G_{\alpha q}$ activates phospholipase C (PLC), which is linked to calcium release and protein kinase C (PKC) activation. Lipid receptors can also couple to $G_{\alpha 12/13}$, which activates Rho, a key regulator of the cytoskeleton.[8,11] The Rho pathway acti-

vates early gene transcription through the serum response factor. Works by us and others suggest that similar signaling pathways are also active in ovarian cancer cells.[185,186]

INTRACELLULAR CALCIUM ($[Ca^{2+}]_i$) RELEASE AND TYROSINE PHOSPHORYLATION. Intracellular ($[Ca^{2+}]_i$) and phosphorylated tyrosine are important signaling components that regulate numerous cellular functions. Both LPA and SPC stimulate transient increases in intracellular calcium ($[Ca^{2+}]_i$) in ovarian cancer cells.[185] Moreover SPC and LPA cross-desensitize each other in inducing an increase in $[Ca^{2+}]_i$, suggesting that the signaling pathways activated by these two lipids interact with each other at some point causing receptor downregulation.[185] We recently tested alkyl- and alkenyl-LPA and found that both stimulated transient increases in $[Ca^{2+}]_i$ in ovarian cancer cells (Y. Xu, unpublished results). Lysophosphatidic acid, SPC, and LPS induced a rapid increase in tyrosine phosphorylation of cellular proteins including p^{125FAK}, the EGF receptor, and other unidentified proteins.[185]

MITOGEN-ACTIVATED PROTEIN KINASE ACTIVATION. Mitogen-activated protein (MAP) kinases are a multiple gene family activated by many extracellular stimuli, including growth factors and ligands for G-protein coupled receptors (GPCRs) through either G_i- or $G_{q/11}$-mediated pathways.[219] Based on their dual phosphorylation motifs, there are three groups of MAP kinases: extracellular signal-regulated protein kinases (ERK1/2), stress-activated protein kinase (SAPK)/c-Jun N-terminal kinase (JNK), and p38. Mitogen-activated protein kinases mediate diverse processes ranging from stimulation of proliferation to induction of cell differentiation or apoptosis. Although p42/44 kinases are mainly involved in mitogenic signaling, they also participate in induction of cell differentiation and growth inhibition.[219–221] Lysophosphatidic acid but not SPC activates p42/44 mitogen-activated protein (MAP) kinase activation in ovarian cancer cells.[185]

CLINICAL APPLICATIONS OF LYSOLIPIDS IN OVARIAN CANCER

Diagnosis

The importance of developing better tools for the screening of asymptomatic patients for ovarian cancer cannot be understated. However, such a modality for ovarian cancer has eluded researchers to date. The presently available screening tools for ovarian cancer (ultrasound, CA 125 blood testing, and pelvic examination) are insensitive to early-stage disease and/or are highly nonspecific. Lack of sensitivity results in a decreased ability to diagnose early-stage ovarian cancer. Poor specificity means that many patients with abnormal test findings have to undergo surgical exploration to exclude the presence of malignancy. It is estimated that 5–10% of all women in the United States will have a surgical procedure for a suspected ovarian neoplasm during their lifetime, and only 13–21% of these women will have an ovarian malignancy.[222] This low percentage is because the overwhelming majority of adnexal masses are benign.[222] In some patients with concurrent medical conditions, surgical intervention could put the patient at significant risk. In addition, many younger women might have ovarian surgery with possible oophorectomy for a lesion that was benign but appeared cancerous on diagnostic evaluation. This will cause some women to be sterilized unnecessarily for fear of malignancy when cancer actually did not exist.

To determine whether OCAF or LPA is a diagnostic or prognostic biomarker for ovarian cancer and other cancers, we measured LPA levels in plasma from patients with cancer and from healthy individuals.[81] We found that the ovarian cancer patients ($n = 48$) had significantly higher ($P < .0001$) plasma LPA levels compared with the control group ($n = 48$). High plasma LPA levels were detected in nine of ten patients with stage I; 24 of 24 patients with stage II, III, or IV ovarian cancer; and 14 of 14 patients with recurrent ovarian cancer. Most patients with other gynecologic cancers (33 of 36) also had elevated LPA levels compared with controls. In contrast, high plasma LPA levels were detected in only a minority of healthy controls (5 of 48) and patients with benign gynecologic diseases (4 of 18) and in none of the patients with breast cancer (0 of 11) or leukemia (0 of 5). When compared with LPA, CA 125 data from the same group of ovarian cancer patients showed a substantially lower rate of detection, especially in stage I.[81] Furthermore, using the ESI-MS method we found that both LPA and LPI are elevated in plasma from patients with ovarian cancer compared with healthy controls, and the combination of both of these lipids might provide better sensitivity than each lipid individually in detection of the disease.[190] These results suggest that LPA and related lysophospholipids could be useful markers for the early detection of ovarian cancer. In order to critically evaluate the diagnostic significance of LPA and related lipids, large scale clinical trials are currently being conducted at Ataigin Biotechnologies, Inc. (Irvine, CA), the Cleveland Clinic Foundation, Northwestern University, MD Anderson Cancer Center, University of California at Los Angeles, University of California at Davis and Toronto General Hospital.

Prognosis and Clinical Management

Using the ESI-MS method, we compared the lysophospholipid contents of ascites samples from patients with ovarian cancer to patients with nonmalignant diseases.[223] Statistically significantly higher concentrations of bioactive lysolipids, including alkyl-LPAs, alkenyl-LPAs, LPIs, and SPC, were present in ascites or washings from patients with ovarian cancer. These lipids may represent sensitive and specific markers for differentiating between benign and malignant masses in ascites. In addition, measurement of lysolipids in ascites may be complementary to presently accepted blood tests in providing increased sensitivity or specificity for the detection of ovarian or other gynecologic cancers. Furthermore, these lipid molecules might be useful as prognostic markers for ovarian cancer, in the clinical treatment of ovarian cancer, and in the development of novel therapeutic targets.

Potential Therapeutic Applications

As described above, lysolipids are likely to be involved in ovarian cancer by regulating various aspects of tumor development, and elevated lysolipid levels in blood and ascites are associated with the disease. Therefore, controlling the levels and activities of these lysolipids could be a novel therapeutic means of treating the disease.

To control the levels of these lipids, we first need to understand how and where the elevated lysolipids are generated. Most of the available information related to LPA production is from studies in platelets; LPA is produced during blood coagulation and platelet activation. It is a normal constituent of serum but not of plasma or whole blood, where platelets are not activated.[224–226] Because we found that over 95% of patients with gynecologic cancer had elevated plasma LPA levels whereas patients with breast cancer or leukemia did not,[190] it seems unlikely that a nonspecific platelet effect could explain the association of gynecologic cancer and elevated plasma LPA. Westermann et al[4] reported that malignant effusions from ovarian cancer contain higher LPA-like activities compared with effusions from other tumors, including breast and lung cancers. These data suggest that there might be increased production of LPA associated specifically with ovarian and other gynecologic cancers.

We showed that ovarian cancer cells, but not breast or leukemia cells, can produce LPA upon stimulation with a phorbol ester, PMA, through PKC and phospholipase A_2 (PLA_2) activation in vitro.[82] These data suggest that ovarian cancer cells may be at least one of the sources for elevated levels of LPA and other bioactive lipids. However the pathologic source(s) and stimuli for the production of LPA and other lysolipids remain to be determined.

A variety of enzymes, including PLA_2, lysophospholipase D, phosphatidic acid phosphatases (PAPs), sphingomyelinase, and sphingosine kinase or lyase, are involved in the production or degradation of LPA, S1P, SPC, and other lipid molecules.[8,10,54,55,227–235] These enzymes may be abnormally regulated in association with disease initiation or progression. They either produce high levels of these lipids or decrease the degradation rate of lipids, resulting in a built-up pool of lysolipids. Although such abnormalities have not been reported in ovarian cancer, we have recently found that malignant ovarian ascitic fluids contained not only high levels of lysolipids but also enzymatic activities that produced different species of LPAs. These activities were much higher in ascites from patients with ovarian cancer compared with nonmalignant ascites (Y. Xu and Y-j. Xiao, unpubilished results). Although these data are preliminary, they are nonetheless highly intriguing and warrant further studies on the enzymatic activities present in ovarian cancer ascites.

Conversely, regulation of lipid activities through their receptor signaling pathways or their downstream effectors are alternative approaches. As described above, we have begun to understand the mechanism of lipid signaling in ovarian cancer cells, a critical step for the development of new strategies to modulate the actions of lipids.

CONCLUSION

In summary, LPA and other lysolipids are present and elevated in blood and ascites from patients with ovarian cancer compared with healthy controls or patients with nonmalignant diseases, such as liver cirrhosis or ovarian fibrothecomas. Elevated lipid concentrations might regulate tumor cell growth and metastasis in vivo. Although the concentrations of S1P or SPC present in ascites alone (20–200 nM) are not high enough to induce significant growth regulatory effects on ovarian cancer cells cultured in vitro, they are sufficient to induce early signaling events, including an increase in intracellular calcium ($[Ca^{2+}]_i$) activation of MAP kinase or cell rounding.[99] More important, these lipids may have a combinatorial effect (additive, synergistic, or inhibitory) with other lipids as we have shown in regulation of IL-8 production. These results provide the basis for further investigation, not only of the pathologic role of these lipids in cancer development but also of their potential clinical applications for cancer detection, predicting prognosis, clinical treatment, and therapeutic treatment.

REFERENCES

1. ACS Cancer Facts & Figures-2000. American Cancer Society Inc, New York, 2000.
2. Schwartz PE, Taylor KJ. Is early detection of ovarian cancer possible? Ann Med 1995;27:519–28.
3. Taylor KJ, Schwartz PE. Screening for early ovarian cancer. Radiology 1994;192:1–10.
4. Westermann AM, Beijnen JH, Moolenaar WH, Rodenhuis S. Growth factors in human ovarian cancer. Cancer Treat Rev 1997;23:113–31.
5. Berchuck A, Carney M. Human ovarian cancer of the surface epithelium. Biochem Pharmacol 1997;54:541–4.
6. Bookman MA. Biological therapy of ovarian cancer: Current directions. Semin Oncol 1998;25:381–96.
7. Liscovitch M, Cantley LC. Lipid second messengers. Cell 1994; 77:329–34.
8. Moolenaar WH. Bioactive lysophospholipids and their G protein-coupled receptors. Exp Cell Res 1999;253:230–8.
9. Van Brocklyn JR, Lee MJ, Menzeleev R, et al. Dual actions of sphingosine-1-phosphate: Extracellular through the Gi-coupled receptor Edg-1 and intracellular to regulate proliferation and survival. J Cell Biol 1998;142:229–40.
10. Spiegel S, Milstien S. Sphingolipid metabolites: Members of a new class of lipid second messengers. J Membr Biol 1995;146: 225–37.
11. Moolenaar WH, Kranenburg O, Postma FR, Zondag GC. Lysophosphatidic acid: G-protein signalling and cellular responses. Curr Opin Cell Biol 1997;9:168–73.
12. Meyer zu Heringdorf D, van Koppen CJ, Jakobs KH. Molecular diversity of sphingolipid signalling. FEBS Lett 1997;410: 34–8.
13. Spiegel S. Sphingosine 1-phosphate: a prototype of a new class of second messengers. J Leukoc Biol 1999;65:341–4.
14. Gaits F, Salles JP, Chap H. Dual effect of lysophosphatidic acid on proliferation of glomerular mesangial cells. Kidney Int 1997; 51:1022–7.
15. Gennero I, Xuereb JM, Simon MF, et al. Effects of lysophosphatidic acid on proliferation and cytosolic Ca++ of human

adult vascular smooth muscle cells in culture. Thrombosis Res 1999;94:317–26.
16. Goetzl EJ, Dolezalova H, Kong Y, Zeng L. Dual mechanisms for lysophospholipid induction of proliferation of human breast carcinoma cells. Cancer Res 1999;59:4732–7.
17. Edsall LC, Pirianov GG, Spiegel S. Involvement of sphingosine 1-phosphate in nerve growth factor-mediated neuronal survival and differentiation. J Neurosci 1997;17:6952–60.
18. Alessenko AV. The role of sphingomyelin cycle metabolites in transduction of signals of cell proliferation differentiation and death. Membr Cell Biol 2000;13:303–20.
19. Spiegel S, Cuvillier O, Edsall L, et al. Roles of sphingosine-1-phosphate in cell growth differentiation and death. Biochemistry (Mosc) 1998;63:69–73.
20. Boguslawski G, Lyons D, Harvey KA, Kovala AT, English D. Sphingosylphosphorylcholine induces endothelial cell migration and morphogenesis. Biochem Biophys Res Commun 2000;272: 603–9.
21. Imamura F, Mukai M, Ayaki M, et al. Involvement of small GTPases Rho and Rac in the invasion of rat ascites hepatoma cells. Clin Exp Metastasis 1999;17:141–8.
22. Genda T, Sakamoto M, Ichida T, et al. Cell motility mediated by rho and Rho-associated protein kinase plays a critical role in intrahepatic metastasis of human hepatocellular carcinoma. Hepatology 1999;30:1027–36.
23. Manning TJ Jr, Parker JC, Sontheimer H. Role of lysophosphatidic acid and rho in glioma cell motility. Cell Motil Cytoskeleton 2000;45:185–99.
24. Mukai M, Imamura F, Ayaki M, et al. Inhibition of tumor invasion and metastasis by a novel lysophosphatidic acid (cyclic LPA). Int J Cancer 1999;81:918–22.
25. Panetti TS, Chen H, Misenheimer TM, Getzler SB, Mosher DF. Endothelial cell mitogenesis induced by LPA: Inhibition by thrombospondin-1 and thrombospondin-2. J Lab Clin Med 1997;129:208–16.
26. Ren XD, Kiosses WB, Schwartz MA. Regulation of the small GTP-binding protein Rho by cell adhesion and the cytoskeleton. EMBO J 1999;18:578–85.
27. Wang F, Van Brocklyn JR, Edsall L, Nava VE, Spiegel S. Sphingosine-1-phosphate inhibits motility of human breast cancer cells independently of cell surface receptors. Cancer Res 1999;59:6185–91.
28. Sadahira Y, Zheng M, Ruan F, Hakomori S, Igarashi Y. Sphingosine-1-phosphate inhibits extracellular matrix protein-induced haptotactic motility but not adhesion of B16 mouse melanoma cells. FEBS Lett 1994;340:99–103.
29. An S. Molecular identification and characterization of G protein-coupled receptors for lysophosphatidic acid and sphingosine 1-phosphate. Ann N Y Acad Sci 2000;905:25–33.
30. Sadahira Y, Ruan F, Hakomori S, Igarashi Y. Sphingosine 1-phosphate a specific endogenous signaling molecule controlling cell motility and tumor cell invasiveness. Proc Natl Acad Sci U S A 1992;89:9686–90.
31. Spiegel S, Olivera A, Zhang H, Thompson EW, Su Y, Berger A. Sphingosine-1-phosphate a novel second messenger involved in cell growth regulation and signal transduction affects growth and invasiveness of human breast cancer cells. Breast Cancer Res Treat 1994;31:337–48.
32. Stam JC, Michiels F, van der Kammen RA, Moolenaar WH, Collard JG. Invasion of T-lymphoma cells: Cooperation between Rho family GTPases and lysophospholipid receptor signaling. EMBO J 1998;17:4066–74.
33. Yanai N, Matsui N, Furusawa T, Okubo T, Obinata M. Sphingosine-1-phosphate and lysophosphatidic acid trigger invasion of primitive hematopoietic cells into stromal cell layers. Blood 2000;96:139–44.
34. Jalink K, Eichholtz T, Postma FR, van Corven EJ, Moolenaar WH. Lysophosphatidic acid induces neuronal shape changes via a novel receptor-mediated signaling pathway: Similarity to thrombin action. Cell Growth Differentiation 1993;4:247–55.
35. Sakai T, Peyruchaud O, Fassler R, Mosher DF. Restoration of beta1A integrins is required for lysophosphatidic acid-induced migration of beta1-null mouse fibroblastic cells. J Biol Chem 1998;273:19378–82.
36. English D, Kovala AT, Welch Z, et al. Induction of endothelial cell chemotaxis by sphingosine 1-phosphate and stabilization of endothelial monolayer barrier function by lysophosphatidic acid potential mediators of hematopoietic angiogenesis. J Hematother Stem Cell Res 1999;8:627–34.
37. Spiegel S. Sphingosine 1-phosphate: A ligand for the EDG-1 family of G-protein-coupled receptors. Ann N Y Acad Sci 2000;905:54–60.
38. Bornfeldt KE, Graves LM, Raines EW, et al. Sphingosine-1-phosphate inhibits PDGF-induced chemotaxis of human arterial smooth muscle cells: Spatial and temporal modulation of PDGF chemotactic signal transduction. J Cell Biol 1995;130:193–206.
39. Ramakers GJA, Moolenaar WH. Regulation of astrocyte morphology by RhoA and lysophosphatidic acid. Exp Cell Res 1998;245:252–62.
40. Baker RR, Chang HY. Lysophosphatidic acid alkylglycerophosphate and alkylacetylglycerophosphate increase the neuronal nuclear acetylation of 1-acyl lysophosphatidyl choline by inhibition of lysophospholipase. Mol Cell Biochem 1999;198: 47–55.
41. Tas PW, Koschel K. Sphingosine-1-phosphate induces a Ca2+ signal in primary rat astrocytes and a Ca2+ signal and shape changes in C6 rat glioma cells. J Neurosci Res 1998;52:427–34.
42. Postma FR, Jalink K, Hengeveld T, Moolenaar WH. Sphingosine-1-phosphate rapidly induces Rho-dependent neurite retraction: Action through a specific cell surface receptor. EMBO J 1996;15:2388–92.
43. Yatomi Y, Ruan F, Hakomori S, Igarashi Y. Sphingosine-1-phosphate: A platelet-activating sphingolipid released from agonist-stimulated human platelets. Blood 1995;86:193–202.
44. Kranenburg O, Poland M, Gebbink M, Oomen L, Moolenaar WH. Dissociation of LPA-induced cytoskeletal contraction from stress fiber formation by differential localization of RhoA. J Cell Sci 1997;110:2417–27.
45. Manning TJ Jr, Rosenfeld SS, Sontheimer H. Lysophosphatidic acid stimulates actomyosin contraction in astrocytes. J Neurosci Res 1998;53:343–52.
46. Toews ML, Ustinova EE, Schultz HD. Lysophosphatidic acid enhances contractility of isolated airway smooth muscle. J Appl Physiol 1997;83:1216–22.
47. Bischoff A, Czyborra P, Fetscher C, Meyer Zu Heringdorf D, Jakobs KH, Michel MC. Sphingosine-1-phosphate and sphingosylphosphorylcholine constrict renal and mesenteric microvessels in vitro. Br J Pharmacol 2000;130:1871–7.
48. Bitar KN, Yamada H. Modulation of smooth muscle contraction by sphingosylphosphorylcholine. Am J Physiol 1995;269: G370–7.
49. Sturm A, Sudermann T, Schulte KM, Goebell H, Dignass AU. Modulation of intestinal epithelial wound healing in vitro and in vivo by lysophosphatidic acid. Gastroenterology 1999;117:368–77.
50. Pietruck F, Busch S, Virchow S, Brockmeyer N, Siffert W. Signalling properties of lysophosphatidic acid in primary human skin fibroblasts: role of pertussis toxin-sensitive GTP-binding proteins. Naunyn Schmiedebergs Arch Pharmacol 1997;355: 1–7.
51. Kupperman E, An S, Osborne N, Waldron S, Stainier DY. A sphingosine-1-phosphate receptor regulates cell migration during vertebrate heart development. Nature 2000;406:192–5.
52. Sun L, Xu L, Henry FA, Spiegel S, Nielsen TB. A new wound

healing agent—sphingosylphosphorylcholine. J Investig Dermatol 1996;106:232–7.
53. Imamura F, Shinkai K, Mukai M, et al. Rho-mediated protein tyrosine phosphorylation in lysophosphatidic-acid-induced tumor-cell invasion. Int J Cancer 1996;65:627–32.
54. Jalink K, Moolenaar WH, Van Duijn B. Lysophosphatidic acid is a chemoattractant for Dictyostelium discoideum amoebae. Proc Natl Acad Sci U S A 1993;90:1857–61.
55. Snitko Y, Yoon ET, Cho W. High specificity of human secretory class II phospholipase A2 for phosphatidic acid. Biochem J 1997;321:737–41.
56. Nugent D, Xu Y. Sphingosine-1-phosphate: Characterization of its inhibition of platelet aggregation. Platelets 2000;11:226–32.
57. Motohashi K, Shibata S, Ozaki Y, Yatomi Y, Igarashi Y. Identification of lysophospholipid receptors in human platelets: the relation of two agonists lysophosphatidic acid and sphingosine 1-phosphate. FEBS Lett 2000;468:189–93.
58. Gueguen G, Gaige B, Grevy JM, et al. Structure-activity analysis of the effects of lysophosphatidic acid on platelet aggregation. Biochemistry 1999;38:8440–50.
59. Yatomi Y, Yamamura S, Ruan F, Igarashi Y. Sphingosine 1-phosphate induces platelet activation through an extracellular action and shares a platelet surface receptor with lysophosphatidic acid. J Biol Chem 1997;272:5291–7.
60. Gerrard JM, Robinson P Narvey M, McNicol A. Increased phosphatidic acid and decreased lysophosphatidic acid in response to thrombin is associated with inhibition of platelet aggregation. Biochem Cell Biol 1993;71:432–9.
61. Fernhout BJ, Dijcks FA, Moolenaar WH, Ruigt GS. Lysophosphatidic acid induces inward currents in Xenopus laevis oocytes; evidence for an extracellular site of action. Eur J Pharmacol 1992;213:313–5.
62. Gerrard JM, Beattie LL, McCrae JM, Singhroy S. The influence of lysophosphatidic acid on platelet protein phosphorylation. Biochem Cell Biol 1987;65:642–50.
63. Simon MF, Chap H, Douste-Blazy L. Platelet aggregating activity of lysophosphatidic acids is not related to their calcium ionophore properties. FEBS Lett 1984;166:115–9.
64. MacIntyre DE, Shaw AM. Phospholipid-induced human platelet activation: effects of calcium channel blockers and calcium chelators. Thromb Res 1983;31:833–44.
65. Gerrard JM, Kindom SE, Peterson DA, White JG. Lysophosphatidic acids. II. Interaction of the effects of adenosine diphosphate and lysophosphatidic acids in dog rabbit and human platelets. Am J Pathol 1979;97:531–47.
66. Schumacher KA, Classen HG, Spath M. Platelet aggregation evoked in vitro and in vivo by phosphatidic acids and lysoderivatives: Identity with substances in aged serum (DAS). Thromb Haemost 1979;42:631–40.
67. Nugent D, Xu Y. Sphingosine-1-phosphate: characterization of its inhibition of platelet aggregation [In Process Citation]. Platelets 2000;11:226–32.
68. Simon CG Jr, Gear AR. Sphingolipid metabolism during human platelet activation. Thromb Res 1999;94:13–23.
69. Zanglis A, Lianos EA, Demopoulos CA. The biological activity of acetylated sphingosylphosphorylcholine derivatives. Int J Biochem Cell Biol 1996;28:63–74.
70. Pustilnik TB, Estrella V, Wiener JR, et al. Lysophosphatidic acid induces urokinase secretion by ovarian cancer cells. Clin Cancer Res 1999;5:3704–10.
71. Piazza GA, Ritter JL, Baracka CA. Lysophosphatidic acid induction of transforming growth factors alpha and beta: Modulation of proliferation and differentiation in cultured human keratinocytes and mouse skin. Exp Cell Res 1995;216:51–64.
72. Cunnick JM, Dorsey JF, Standley T, et al. Role of tyrosine kinase activity of epidermal growth factor receptor in the lysophosphatidic acid-stimulated mitogen-activated protein kinase pathway. J Biol Chem 1998;273:14468–75.
73. Reiser CO, Lanz T, Hofmann F, Hofer G, Rupprecht HD, Goppelt-Struebe M. Lysophosphatidic acid-mediated signal-transduction pathways involved in the induction of the early-response genes prostaglandin G/H synthase-2 and Egr-1: A critical role for the mitogen-activated protein kinase p38 and for Rho proteins. Biochem J 1998;330:1107–14.
74. Berger A, Bittman R, Schmidt RR, Spiegel S. Structural requirements of sphingosylphosphocholine and sphingosine-1-phosphate for stimulation of activator protein-1 activity. Mol Pharmacol 1996;50:451–7.
75. Imokawa G, Takagi Y, Higuchi K, Kondo H, Yada Y. Sphingosylphosphorylcholine is a potent inducer of intercellular adhesion molecule-1 expression in human keratinocytes. J Invest Dermatol 1999;112:91–6.
76. Holtsberg FW, Steiner MR, Bruce-Keller AJ, et al. Lysophosphatidic acid and apoptosis of nerve growth factor-differentiated PC12 cells. J Neurosci Res 1998;53:685–96.
77. Niwa M, Kozawa O, Matsuno H, Kanamori Y, Hara A, Uematsu T. Tumor necrosis factor-alpha-mediated signal transduction in human neutrophils: involvement of sphingomyelin metabolites in the priming effect of TNF-alpha on the fMLP-stimulated superoxide production. Life Sci 2000;66:245–56.
78. Irie F, Hirabayashi Y. Ceramide prevents motoneuronal cell death through inhibition of oxidative signal. Neurosci Res 1999;35:135–44.
79. Alemany R, Meyer zu Heringdorf D, van Koppen CJ, Jakobs KH. Formyl peptide receptor signaling in HL-60 cells through sphingosine kinase. J Biol Chem 1999;274:3994–9.
80. Mogami K, Mizukami Y, Todoroki-Ikeda N, et al. Sphingosylphosphorylcholine induces cytosolic Ca(2+) elevation in endothelial cells in situ and causes endothelium-dependent relaxation through nitric oxide production in bovine coronary artery [published erratum appears in FEBS Lett 2000 Jan 28; 466(2-3):395]. FEBS Lett 1999;457:375–80.
81. Xu Y, Shen Z, Wiper D, et al. Lysophosphatidic acid as a potential biomarker for ovarian and other gynecologic cancers. JAMA 1998;280:719–23.
82. Shen Z, Belinson J, Morton RE, Xu Y. Phorbol 12-myristate 13-acetate stimulates lysophosphatidic acid secretion from ovarian and cervical cancer cells but not from breast or leukemia cells. Gynecol Oncol 1998;71:364–8.
83. Westermann AM, Havik E, Postma FR, et al. Malignant effusions contain lysophosphatidic acid (LPA)-like activity. Ann Oncol 1998;9:437–42.
84. Inoue CN, Epstein M, Forster HG, Hotta O, Kondo Y, Iinuma K. Lysophosphatidic acid and mesangial cells: Implications for renal diseases. Clin Sci 1999;96:431–6.
85. Siess W, Zangl KJ, Essler M, et al. Lysophosphatidic acid mediates the rapid activation of platelets and endothelial cells by mildly oxidized low density lipoprotein and accumulates in human atherosclerotic lesions. Proc Natl Acad Sci U S A 1999;96:6931–6.
86. Sayas CL, Moreno-Flores MT, Avila J, Wandosell F. The neurite retraction induced by lysophosphatidic acid increases Alzheimer's disease-like tau phosphorylation. J Biol Chem 1999;274:37046–52.
87. Xu Y, Shen Z, Wiper DW, et al. Lysophosphatidic acid as a potential biomarker for ovarian and other gynecologic cancers [see comments]. JAMA 1998;280:719–23.
88. Merrill AH Jr, Schmelz EM, Dillehay DL, et al. Sphingolipids—the enignatic lipid class: biochemistry physiology and pathophysiology. Toxicol Appl Pharmacol 1997;142:208–25.
89. Berger A, Rosenthal D, Spiegel S. Sphingosylphosphocholine a signaling molecule which accumulates in Niemann-Pick disease type A stimulates DNA-binding activity of the transcription

activator protein AP-1. Proc Natl Acad Sci U S A 1995;92: 5885–9.
90. Ohno K. Niemann-Pick disease types A and B. Nippon Rinsho 1995;53:3014–8.
91. An S, Goetzl EJ, Lee H. Signaling mechanisms and molecular characteristics of G protein-coupled receptors for lysophosphatidic acid and sphingosine 1-phosphate. J Cell Biochem 1998; 30–31(Suppl):147–57.
92. Chun J. Lysophospholipid receptors: Implications for neural signaling. Crit Rev Neurobiol 1999;13:151–68.
93. Chun J, Contos JJ, Munroe D. A growing family of receptor genes for lysophosphatidic acid (LPA) and other lysophospholipids (LPs). Cell Biochem Biophys 1999;30:213–42.
94. Pyne S, Pyne NJ. Sphingosine 1-phosphate signalling in mammalian cells. Biochem J 2000;349:385–402.
95. Lynch KR, Im I. Life on the edg. Trends Pharmacol Sci 1999;20:473–5.
96. Moolenaar WH. Development of our current understanding of bioactive lysophospholipids [In Process Citation]. Ann N Y Acad Sci 2000;905:1–10.
97. Yamazaki Y, Kon J, Sato K, et al. Edg-6 as a putative sphingosine 1-phosphate receptor coupling to Ca(2+) signaling pathway. Biochem Biophys Res Commun 2000;268:583–9.
98. Im DS, Heise CE, Ancellin N, et al. Characterization of a novel sphingosine 1-phosphate receptor Edg-8. J Biol Chem 2000; 275:14281–6.
99. Xu Y, Zhu K, Hong G, et al. Sphingosylphosphorylcholine is a ligand for ovarian cancer G-protein-coupled receptor 1. Nat Cell Biol 2000;2:261–7.
100. Spiegel S, Olivera A, Carlson RO. The role of sphingosine in cell growth regulation and transmembrane signaling. Adv Lipid Res 1993;25:105–29.
101. Spiegel S. Sphingosine and sphingosine 1-phosphate in cellular proliferation: Relationship with protein kinase C and phosphatidic acid. J Lipid Mediators 1993;8:169–75.
102. Spiegel S, Olivera A, Zhang H, Thompson EW, Su Y, Berger A. Sphingosine-1-phosphate: A novel second messenger involved in cell growth regulation and signal transduction affects growth and invasiveness of human breast cancer cells. Breast Cancer Res Treatment 1994;31:337–48.
103. Ghosh TK, Bian J, Gill DL. Intracellular calcium release mediated by sphingosine derivatives generated in cells. Science 1990; 248:1653–6.
104. Catalan RE, Miguel BG, Calcerrada MC, Ruiz S, Martinez AM. Sphingolipids increase calcium concentration in isolated rat liver nuclei. Biochem Biophys Res Commun 1997;238:347–50.
105. Calcerrada MC, Miguel BG, Catalan RE, Martinez AM. Sphingosylphosphorylcholine increases calcium concentration in isolated brain nuclei. Neurosci Res 1999;33:229–32.
106. Van Koppen CJ, Meyer Zu, Heringdorf D, Zhang C, Laser KT, Jakobs KH. A distinct G(i) protein-coupled receptor for sphingosylphosphorylcholine in human leukemia HL-60 cells and human neutrophils. Mol Pharmacol 1996;49:956–61.
107. Repp H, Koschinski A, Decker K, Dreyer F. Activation of a Ca2+-dependent K+ current in mouse fibroblasts by lysophosphatidic acid requires a pertussis toxin-sensitive G protein and Ras. Naunyn Schmiedebergs Arch Pharmacol 1998;358:509–17.
108. Bunemann M, Liliom K, Brandts BK, et al. A novel membrane receptor with high affinity for lysosphingomyelin and sphingosine 1-phosphate in atrial myocytes. EMBO J 1996;15:5527–34.
109. Himmel HM, Meyer Zu Heringdorf D, Graf E, et al. Evidence for edg-3 receptor-mediated activation of I(K.ACh) by sphingosine-1-phosphate in human atrial cardiomyocytes [In Process Citation]. Mol Pharmacol 2000;58:449–54.
110. Bunemann M, Liliom K, Brandts BK, et al. A novel membrane receptor with high affinity for lysosphingomyelin and sphingosine 1-phosphate in atrial myocytes. EMBO J 1996;15:5527–34.
111. Durieux ME, Salafranca MN, Lynch KR, Moorman JR. Lysophosphatidic acid induces a pertussis toxin-sensitive Ca(2+)-activated Cl- current in Xenopus laevis oocytes. Am J Physiol 1992;263:C896–900.
112. Durieux ME, Carlisle SJ, Salafranca MN, Lynch KR. Responses to sphingosine-1-phosphate in X. laevis oocytes: Similarities with lysophosphatidic acid signaling. Am J Physiol 1993;264: C1360–4.
113. Moolenaar WH, van Corven EJ. Growth factor-like action of lysophosphatidic acid: Mitogenic signalling mediated by G proteins. Ciba Found Symp 1990;150:99–106.
114. Vasta V, Meacci E, Catarzi S, Donati C, Farnararo M, Bruni P. Sphingosine 1-phosphate induces arachidonic acid mobilization in A549 human lung adenocarcinoma cells. Biochim Biophys Acta 2000;1483:154–60.
115. Desai NN, Carlson RO, Mattie ME, et al. Signaling pathways for sphingosylphosphorylcholine-mediated mitogenesis in Swiss 3T3 fibroblasts. J Cell Biol 1993;121:1385–95.
116. An S, Goetzl EJ, Lee H. Signaling mechanisms and molecular characteristics of G protein-coupled receptors for lysophosphatidic acid and sphingosine 1-phosphate. J Cell Biochem 1998; 31(Suppl):147–57.
117. Sato K, Murata N, Kon J, et al. Downregulation of mRNA expression of Edg-3 a putative sphingosine 1-phosphate receptor coupled to Ca2+ signaling during differentiation of HL-60 leukemia cells. Biochem Biophys Res Commun 1998; 253:253–6.
118. Gonda K, Okamoto H, Takuwa N, et al. The novel sphingosine 1-phosphate receptor AGR16 is coupled via pertussis toxin-sensitive and -insensitive G-proteins to multiple signalling pathways. Biochem J 1999;337:67–75.
119. Okajima F, Tomura H, Sho K, et al. Sphingosine 1-phosphate stimulates hydrogen peroxide generation through activation of phospholipase C-Ca2+ system in FRTL-5 thyroid cells: Possible involvement of guanosine triphosphate-binding proteins in the lipid signaling. Endocrinology 1997;138:220–9.
120. Okajima F, Tomura H, Sho K, Nochi H, Tamoto K, Kondo Y. Involvement of pertussis toxin-sensitive GTP-binding proteins in sphingosine 1-phosphate-induced activation of phospholipase C-Ca2+ system in HL60 leukemia cells. FEBS Lett 1996;379: 260–4.
121. Gonda K, Okamoto H, Takuwa N, et al. The novel sphingosine 1-phosphate receptor AGR16 is coupled via pertussis toxin-sensitive and -insensitive G-proteins to multiple signalling pathways. Biochemical J 1999;337:67–75.
122. Okamoto H, Takuwa N, Gonda K, et al. EDG1 is a functional sphingosine-1-phosphate receptor that is linked via a Gi/o to multiple signaling pathways including phospholipase C activation Ca2+ mobilization Ras-mitogen-activated protein kinase activation and adenylate cyclase inhibition. J Biol Chem 1998; 273:27104–10.
123. Sando JJ, Chertihin OI. Activation of protein kinase C by lysophosphatidic acid: Dependence on composition of phospholipid vesicles. Biochem J 1996;317:583–8.
124. Buehrer BM, Bardes ES, Bell RM. Protein kinase C-dependent regulation of human erythroleukemia (HEL) cell sphingosine kinase activity. Biochim Biophys Acta 1996;1303:233–42.
125. Orlati S, Hrelia S, Rugolo M. Pertussis toxin- and PMA-insensitive calcium mobilization by sphingosine in CFPAC-1 cells: evidence for a phosphatidic acid-dependent mechanism. Biochim Biophys Acta 1997;1358:93–102.
126. Seufferlein T, Rozengurt E. Sphingosylphosphorylcholine activation of mitogen-activated protein kinase in Swiss 3T3 cells

requires protein kinase C and a pertussis toxin-sensitive G protein. J Biol Chem 1995;270:24334–42.
127. Suzuki Y, Ozawa Y, Murakami K, Miyazaki H. Lysophosphatidic acid inhibits epidermal-growth-factor-induced Stat1 signaling in human epidermoid carcinoma A431 cells. Biochem Biophys Res Commun 1997;240:856–61.
128. Ohata H, Aizawa H, Momose K. Lysophosphatidic acid sensitizes mechanical stress-induced Ca2+ response via activation of phospholipase C and tyrosine kinase in cultured smooth muscle cells. Life Sci 1997;60:1287–95.
129. Okajima F, Kondo Y. Pertussis toxin inhibits phospholipase C activation and Ca2+ mobilization by sphingosylphosphorylcholine and galactosylsphingosine in HL60 leukemia cells. Implications of GTP-binding protein-coupled receptors for lysosphingolipids. J Biol Chem 1995;270:26332–40.
130. Spangelo BL, Jarvis WD. Lysophosphatidylcholine stimulates interleukin-6 release from rat anterior pituitary cells in vitro. Endocrinology 1996;137:4419–26.
131. van der Bend RL, de Widt J, van Corven EJ, Moolenaar WH, van Blitterswijk WJ. The biologically active phospholipid lysophosphatidic acid induces phosphatidylcholine breakdown in fibroblasts via activation of phospholipase D. Comparison with the response to endothelin. Biochem J 1992;285:235–40.
132. Orlati S, Porcelli AM, Hrelia S, Van Brocklyn JR, Spiegel S, Rugolo M. Sphingosine-1-phosphate activates phospholipase D in human airway epithelial cells via a G protein-coupled receptor. Arch Biochem Biophys 2000;375:69–77.
133. Banno Y, Fujita H, Ono Y, et al. Differential phospholipase D activation by bradykinin and sphingosine 1-phosphate in NIH 3T3 fibroblasts overexpressing gelsolin. J Biol Chem 1999;274: 27385–91.
134. Meacci E, Vasta V, Donati C, Farnararo M, Bruni P. Receptor-mediated activation of phospholipase D by sphingosine 1-phosphate in skeletal muscle C2C12 cells. A role for protein kinase C. FEBS Lett 1999;457:184–8.
135. Meacci E, Donati C, Cencetti F, Romiti E, Farnararo M, Bruni P. Receptor-activated phospholipase D is present in caveolin-3-enriched light membranes of C2C12 myotubes. FEBS Lett 2000;473:10–4.
136. Natarajan V, Jayaram HN, Scribner WM, Garcia JG. Activation of endothelial cell phospholipase D by sphingosine and sphingosine-1-phosphate. Am J Respir Cell Mol Biol 1994; 11:221–9.
137. Dygas A, Sidorko M, Bobeszko M, Baranska J. Exogenous sphingosine 1-phosphate and sphingosylphosphorylcholine do not stimulate phospholipase D in C6 glioma cells. Acta Biochim Polonica 1999;46:99–106.
138. Takeda H, Matozaki T, Takada T, et al. PI 3-kinase gamma and protein kinase C-zeta mediate RAS-independent activation of MAP kinase by a Gi protein-coupled receptor. EMBO J 1999; 18:386–95.
139. Roche S, Downward J, Raynal P, Courtneidge SA. A function for phosphatidylinositol 3-kinase beta (p85alpha-p110beta) in fibroblasts during mitogenesis: Requirement for insulin- and lysophosphatidic acid-mediated signal transduction. Mol Cell Biol 1998;18:7119–29.
140. Shahrestanifar M, Fan X, Manning DR. Lysophosphatidic acid activates NF-kappaB in fibroblasts. A requirement for multiple inputs. J Biol Chem 1999;274:3828–33.
141. Shatrov VA, Lehmann V, Chouaib S. Sphingosine-1-phosphate mobilizes intracellular calcium and activates transcription factor NF-kappa B in U937 cells. Biochem Biophys Res Commun 1997;234:121–4.
142. Moolenaar WH. Lysophosphatidic acid signalling. Curr Opin Cell Biol 1995;7:203–10.
143. van Corven EJ, Hordijk PL, Medema RH, Bos JL, Moolenaar WH. Pertussis toxin-sensitive activation of p21ras by G protein-coupled receptor agonists in fibroblasts. Proc Natl Acad Sci U S A 1993;90:1257–61.
144. Okamoto H, Takuwa N, Yatomi Y, Gonda K, Shigematsu H, Takuwa Y. EDG3 is a functional receptor specific for sphingosine 1-phosphate and sphingosylphosphorylcholine with signaling characteristics distinct from EDG1 and AGR16. Biochem Biophys Res Commun 1999;260:203–8.
145. Luttrell LM, Daaka Y, Della Rocca GJ, Lefkowitz RJ. G protein-coupled receptors mediate two functionally distinct pathways of tyrosine phosphorylation in rat 1a fibroblasts. Shc phosphorylation and receptor endocytosis correlate with activation of Erk kinases. J Biol Chem 1997;272:31648–56.
146. Jalink K, Eichholtz T, Postma FR, van Corven E, Moolenaar WH. Lysophosphatidic acid induces neuronal shape changes via a novel receptor-mediated signaling pathway: similarity to thrombin action. Cell Growth Differ 1993;4:247–55.
147. Lee OH, Lee DJ, Kim YM, et al. Sphingosine 1-phosphate stimulates tyrosine phosphorylation of focal adhesion kinase and chemotactic motility of endothelial cells via the G(i) protein-linked phospholipase C pathway. Biochem Biophys Res Commun 2000;268:47–53.
148. Seufferlein T, Rozengurt E. Sphingosylphosphorylcholine rapidly induces tyrosine phosphorylation of p125FAK and paxillin rearrangement of the actin cytoskeleton and focal contact assembly. Requirement of p21rho in the signaling pathway. J Biol Chem 1995;270:24343–51.
149. Wang F, Nobes CD, Hall A, Spiegel S. Sphingosine 1-phosphate stimulates rho-mediated tyrosine phosphorylation of focal adhesion kinase and paxillin in Swiss 3T3 fibroblasts. Biochem J 1997;324:481–8.
150. Ramakers G JA, Moolenaar WH. Regulation of astrocyte morphology by RhoA and lysophosphatidic acid. Exp Cell Res 1998;245:252–62.
151. Buist A, Tertoolen LG, den Hertog J. Potentiation of G-protein-coupled receptor-induced MAP kinase activation by exogenous EGF receptors in SK-N-MC neuroepithelioma cells. Biochem Biophys Res Commun 1998;251:6–10.
152. Xu Y, Fang XJ, Casey G, Mills GB. Lysophospholipids activate ovarian and breast cancer cells. Biochem J 1995;309:933–40.
153. Conway AM, Pyne NJ, Pyne S. Sphingosine 1-phosphate activation of MAP kinase—involvement of PI 3-kinase and protein kinase C. Biochem Soc Trans 1997;25:S585.
154. Guo C, Zheng C, Martin-Padura I, Bian ZC, Guan JL. Differential stimulation of proline-rich tyrosine kinase 2 and mitogen-activated protein kinase by sphingosine 1-phosphate. Eur J Biochem 1998;257:403–8.
155. Chin TY, Chueh SH. Sphingosylphosphorylcholine stimulates mitogen-activated protein kinase via a Ca2+-dependent pathway. Am J Physiol 1998;275:C1255–63.
156. Rumenapp U, Lummen G, Virchow S, Hanske J, Meyer ZU, Heringdorf D, Jakobs KH. Sphingolipid receptor signaling and function in human bladder carcinoma cells: Inhibition of LPA- but enhancement of thrombin-stimulated cell motility. Naunyn-Schmiedebergs Arch Pharmacol 2000;361:1–11.
157. Koval M, Pagano RE. Lipid recycling between the plasma membrane and intracellular compartments: transport and metabolism of fluorescent sphingomyelin analogues in cultured fibroblasts. J Cell Biol 1989;108:2169–81.
158. Wolf DE, Winiski AP, Ting AE, Bocian KM, Pagano RE. Determination of the transbilayer distribution of fluorescent lipid analogues by nonradiative fluorescence resonance energy transfer. Biochemistry 1992;31:2865–73.
159. Moolenaar WH. Development of our current understanding of bioactive lysophospholipids. Ann N Y Acad Sci 2000;905:1–10.
160. Desai NN, Zhang H, Olivera A, Mattie ME, Spiegel S. Sphingosine-1-phosphate a metabolite of sphingosine increases phos-

phatidic acid levels by phospholipase D activation J Biol Chem 1992;267:23122–8.
161. van Corven EJ, van Rijswijk A, Jalink K, van der Bend RL, van Blitterswijk WJ, Moolenaar WH. Mitogenic action of lysophosphatidic acid and phosphatidic acid on fibroblasts. Dependence on acyl-chain length and inhibition by suramin. Biochem J 1992;281:163–9.
162. Ikeda H, Yatomi Y, Yanase M, et al. Effects of lysophosphatidic acid on proliferation of stellate cells and hepatocytes in culture. Biochem Biophys Res Commun 1998;248:436–40.
163. Keller JN, Steiner MR, Holtsberg FW, Mattson MP, Steiner SM. Lysophosphatidic acid-induced proliferation-related signals in astrocytes. J Neurochem 1997;69:1073–84.
164. Levine JS, Koh JS, Triaca V, Lieberthal W. Lysophosphatidic acid: A novel growth and survival factor for renal proximal tubular cells. Am J Physiol 1997;273:F575–85.
165. Liliom K, Fischer DJ, Virag T, et al. Identification of a novel growth factor-like lipid 1-O-cis-alk-1′-enyl-2-lyso-sn-glycero-3-phosphate (alkenyl-GP) that is present in commercial sphingolipid preparations. J Biol Chem 1998;273:13461–8.
166. An S, Zheng Y, Bleu T. Sphingosine 1-phosphate-induced cell proliferation survival and related signaling events mediated by G protein-coupled receptors Edg3 and Edg5. J Biol Chem 2000; 275:288–96.
167. Carpio LC, Stephan E, Kamer A, Dziak R. Sphingolipids stimulate cell growth via MAP kinase activation in osteoblastic cells. Prostaglandins Leukotrienes Essential Fatty Acids 1999;61: 267–73.
168. Spiegel S. Sphingosine and sphingosine 1-phosphate in cellular proliferation: relationship with protein kinase C and phosphatidic acid. J Lipid Mediat 1993;8:169–75.
169. Spiegel S, Cuvillier O, Edsall LC, et al. Sphingosine-1-phosphate in cell growth and cell death. Ann N Y Acad Sci 1998; 845:11–8.
170. Berger A, Cultaro CM, Segal S, Spiegel S. The potent lipid mitogen sphingosylphosphocholine activates the DNA binding activity of upstream stimulating factor (USF) a basic helix-loop-helix-zipper protein. Biochim Biophys Acta 1998;1390:225–36.
171. Chin TY, Chueh SH. Sphingosylphosphorylcholine stimulates mitogen-activated protein kinase via a Ca2+-dependent pathway. Am J Physiol 1998;275:C1255–63.
172. Desai NN, Spiegel S. Sphingosylphosphorylcholine is a remarkably potent mitogen for a variety of cell lines. Biochem Biophys Res Commun 1991;181:361–6.
173. Sekiguchi K, Yokoyama T, Kurabayashi M, Okajima F, Nagai R. Sphingosylphosphorylcholine induces a hypertrophic growth response through the mitogen-activated protein kinase signaling cascade in rat neonatal cardiac myocytes. Circ Res 1999;85:1000–8.
174. Tokura Y, Wakita H, Seo N, Furukawa F, Nishimura K, Takigawa M. Modulation of T-lymphocyte proliferation by exogenous natural ceramides and sphingosylphosphorylcholine. J Investig Dermatol Symp Proc 1999;4:184–9.
175. Imagawa W, Bandyopadhyay GK, Nandi S. Analysis of the proliferative response to lysophosphatidic acid in primary cultures of mammary epithelium: Differences between normal and tumor cells. Exp Cell Res 1995;216:178–86.
176. Hong G, Baudhuin LM, Xu Y. Sphingosine-1-phosphate modulates growth and adhesion of ovarian cancer cells. FEBS Lett 1999;460:513–8.
177. Goetzl EJ, Dolezalova H, Kong Y, Zeng L. Dual mechanisms for lysophospholipid induction of proliferation of human breast carcinoma cells. Cancer Res 1999;59:4732–7.
178. Xu Y, Zhu K, Hong G, et al. Sphingosylphosphorylcholine is a ligand for ovarian cancer G-protein-coupled receptor 1. Nat Cell Biol 2000;2:261–7.
179. Yamada T, Okajima F, Ohwada S, Kondo Y. Growth inhibition of human pancreatic cancer cells by sphingosylphosphorylcholine and influence of culture conditions. Cell Mol Life Sci 1997;53:435–41.
180. Furui T, LaPushin R, Mao M, et al. Overexpression of edg-2/vzg-1 induces apoptosis and anoikis in ovarian cancer cells in a lysophosphatidic acid-independent manner. Clin Cancer Res 1999;5:4308–18.
181. Goetzl EJ, Kong Y, Mei B. Lysophosphatidic acid and sphingosine 1-phosphate protection of T cells from apoptosis in association with suppression of Bax. J Immunol 1999; 162:2049–56.
182. Holtsberg FW, Steiner MR, Keller JN, Mark RJ, Mattson MP, Steiner SM. Lysophosphatidic acid induces necrosis and apoptosis in hippocampal neurons. J Neurochem 1998;70:66–76.
183. Cuvillier O, Pirianov G, Kleuser B, et al. Suppression of ceramide-mediated programmed cell death by sphingosine-1-phosphate. Nature 1996;381:800–3.
184. Cuvillier O, Rosenthal DS, Smulson ME, Spiegel S. Sphingosine 1-phosphate inhibits activation of caspases that cleave poly(ADP-ribose) polymerase and lamins during Fas- and ceramide- mediated apoptosis in Jurkat T lymphocytes. J Biol Chem 1998;273:2910–6.
185. Xu Y, Fang X, Casey G, Mills G. Lysophospholipids activate ovarian and breast cancer cells. Biochem J 1995;309:933–40.
186. Xu Y, Gaudette D, Boynton J, et al. Characterization of an ovarian cancer activating factor in ascites from ovarian cancer patients. Clin Cancer Res 1995;1:1223–32.
187. Mills G, May C, McGill M, Roifman C, Mellors A. A putative new growth factor in ascitic fluid from ovarian cancer patients: Identification characterization and mechanism of action. Cancer Res 1988;48:1066–71.
188. Mills GB, May C, Hill M, Campbell S, Shaw P, Marks A. Ascitic fluid from human ovarian cancer patients contains growth factors necessary for intraperitoneal growth of human ovarian adenocarcinoma cells. J Clin Investig 1990;86:851–5.
189. Hong G, Baudhuin LM, Xu Y. Sphingosine-1-phosphate modulates growth and adhesion of ovarian cancer cells. FEBS Lett 1999;460:513–8.
190. Xiao Y, Chen Y, Kennedy AW, Belinson J, Xu Y. Evaluation of plasma lysophospholipids for diagnostic significance using electrospray ionization mass spectrometry (ESI-MS) analyses. Ann N Y Acad Sci 2000;905:242–59.
191. Falasca M, Corda D. Elevated levels and mitogenic activity of lysophosphatidylinositol in k-ras-transformed epithelial cells. Eur J Biochem 1994;221:383–9.
192. Meyer T, Hart IR. Mechanisms of tumour metastasis. Eur J Cancer 1998;34:214–21.
193. Joseph-Silverstein J, Silverstein RL. Cell adhesion molecules: An overview. Cancer Investig 1998;16:176–82.
194. Fishman D, Yung Y, Stack S. Lysophosphatidic acid stimulation of matrix metalloproteinase-2 activation. In: Proceedings of the American Association of Cancer Research, 2000: 131.
195. Imamura F, Horai T, Mukai M, Shinkai K, Sawada M, Akedo H. Induction of in vitro tumor cell invasion of cellular monolayers by lysophosphatidic acid or phospholipase D. Biochem Biophys Res Commun 1993;193:497–503.
196. Stam JC, Michiels F, van der Kammen RA, Moolenaar WH, Collard JG. Invasion of T-lymphoma cells: Cooperation between Rho family GTPases and lysophospholipid receptor signaling. EMBO J 1998;17:4066–74.
197. Merogi AJ, Marrogi AJ, Ramesh R, Robinson WR, Fermin CD, Freeman SM. Tumor-host interaction: analysis of cytokines growth factors and tumor-infiltrating lymphocytes in ovarian carcinomas. Hum Pathol 1997;28:321–31.
198. Yoneda J, Kuniyasu H, Crispens MA, Price JE, Bucana CD, Fidler IJ. Expression of angiogenesis-related genes and progres-

sion of human ovarian carcinomas in nude mice. J Natl Cancer Inst 1998;90:447–54.
199. Radke J, Schmidt D, Bohme M, Schmidt U, Weise W, Morenz J. Zytokinspiegel im malignen Aszites und peripheren Blut von Patientinnen mit fortgeschrittenem Ovarialkarzinom. Geburtshilfe Frauenheilkd 1996;56:83–7.
200. Gawrychowski K, Skopinska-Rozewska E, Barcz E, et al. Angiogenic activity and interleukin-8 content of human ovarian cancer ascites. Eur J Gynaecol Oncol 1998;19:262–4.
201. Ivarsson K, Runesson E, Sundfeldt K, et al. The chemotactic cytokine interleukin-8—a cyst fluid marker for malignant epithelial ovarian cancer? Gynecol Oncol 1998;71:420–3.
202. Xu L, Xie K, Mukaida N, Matsushima K, Fidler IJ. Hypoxia-induced elevation in interleukin-8 expression by human ovarian carcinoma cells. Cancer Res 1999;59:5822–9.
203. Harant H, Lindley I, Uthman A, et al. Regulation of interleukin-8 gene expression by all-trans retinoic acid. Biochem Biophys Rese Commun 1995;210:898–906.
204. Lee LF, Schuerer-Maly CC, Lofquist AK, et al. Taxol-dependent transcriptional activation of IL-8 expression in a subset of human ovarian cancer. Cancer Res 1996;56:1303–8.
205. Schwartz B, Morrison B, Wu W, Xu Y. Regulation of interleukin-8 production and gene expression in human ovarian cancer cells by lysophospholipids. In: Proceedings of the American Association of Cancer Research, 2000:585.
206. Markman M. Systemic therapy for gynecologic cancer. Curr Opin Oncol 1992;4:939–45.
207. Markman M. Intraperitoneal therapy of ovarian cancer. Oncologist 1996;1:18–21.
208. Markman M. Intraperitoneal therapy of ovarian cancer. Semin Oncol 1998;25:356–60.
209. Ozols R, Bookman M. Carboplatin and paclitexal combination chemotherapy. In: Sharp F, Blackett T, Leake R, Berek J, eds. Ovarian cancer 4. Vol. 4. London: Chapman and Hall Medical, 1996:165–73.
210. Hamilton T, Johnson S, Godwin A, et al. Drug resistance in ovarian cancer and potential for its reversal. In: Ovarian cancer 3. Vol. 3. London: Chapman and Hall Medical, 1995:203–13.
211. Duan Z, Feller AJ, Penson RT, Chabner BA, Seiden MV. Discovery of differentially expressed genes associated with paclitaxel resistance using cDNA array technology: Analysis of interleukin (IL) 6, IL-8 and monocyte chemotactic protein 1 in the paclitaxel-resistant phenotype. Clin Cancer Res 1999;5: 3445–53.
212. Hecht JH, Weiner JA, Post SR, Chun J. Ventricular zone gene-1 (vzg-1) encodes a lysophosphatidic acid receptor expressed in neurogenic regions of the developing cerebral cortex. J Cell Biol 1996;135:1071–83.
213. Lee MJ, Thangada S, Liu H, Thompson BD, Hla T. Lysophosphatidic acid stimulates the G-protein-coupled receptor EDG-1 as a low affinity agonist. J Biol Chem 1998;273:22105–12.
214. Bandoh K, Aoki J, Hosono H, et al. Molecular cloning and characterization of a novel human G-protein-coupled receptor EDG7 for lysophosphatidic acid. J Biol Chem 1999;274:27776–85.
215. Goetzl EJ, An S. Diversity of cellular receptors and functions for the lysophospholipid growth factors lysophosphatidic acid and sphingosine 1-phosphate FASEB J 1998;12:1589–98.
216. Lynch KR, Im I. Life on the edg. Trends Pharmacol Sci 1999;20:473–5.
217. Goetzl EJ, Dolezalova H, Kong Y, et al. Distinctive expression and functions of the type 4 endothelial differentiation gene-encoded G protein-coupled receptor for lysophosphatidic acid in ovarian cancer. Cancer Res 1999;59:5370–5.
218. Yamazaki Y, Kon J, Sato K, et al. Edg-6 as a putative sphingosine 1-phosphate receptor coupling to Ca(2+) signaling pathway. Biochem Biophys Res Commun 2000;268:583–9.
219. Bogoyevitch MA, Clerk A, Sugden PH. Activation of the mitogen-activated protein kinase cascade by pertussis toxin-sensitive and -insensitive pathways in cultured ventricular cardiomyocytes. Biochem J 1995;309:437–43.
220. Casillas AM, Amaral K, Chegini-Farahani S, Nel AE. Okadaic acid activates p42 mitogen-activated protein kinase (MAP kinase;ERK-2) in B-lymphocytes but inhibits rather than augments cellular proliferation: Contrast with phorbol 12-myristate 13-acetate. Biochem J 1993;290:545–50.
221. Zhu L, Yu X, Akatsuka Y, Cooper JA, Anasetti C. Role of mitogen-activated protein kinases in activation-induced apoptosis of T cells. Immunology 1999;97:26–35.
222. DiSaia P, Creasman W. Clinical gynecologic oncology. 5th ed. St. Louis, Missouri: Mosby-Year Book Inc, 1993.
223. Xu Y, Xiao Y, Baudhuin L. Ascitic fluids from ovarian cancer patients contain significantly higher levels of lysophospholipids compared with ascites from patients with non-malignant diseases. In: Proceedings of the American Association of Cancer Ressearch, 2000:860.
224. Watson SP, McConnell RT, Lapetina EG. Decanoyl lysophosphatidic acid induces platelet aggregation through an extracellular action. Evidence against a second messenger role for lysophosphatidic acid. Biochem J 1985;232:61–6.
225. Tigyi G, Henschen A, Miledi R. A factor that activates oscillatory chloride currents in Xenopus oocytes copurifies with a subfraction of serum albumin. J Biol Chem 1991;266:20602–9.
226. Tigyi G, Miledi R. Lysophosphatidates bound to serum albumin activate membrane currents in Xenopus oocytes and neurite retraction in PC12 pheochromocytoma cells. J Biol Chem 1992;267:21360–7.
227. Roberts R, Sciorra VA, Morris AJ. Human type 2 phosphatidic acid phosphohydrolases. Substrate specificity of the type 2a 2b and 2c enzymes and cell surface activity of the 2a isoform. J Biol Chem 1998;273:22059–67.
228. Hooks SB, Ragan SP, Lynch KR. Identification of a novel human phosphatidic acid phosphatase type 2 isoform. FEBS Lett 1998;427:188–92.
229. Ulrix W, Swinnen JV, Heyns W, Verhoeven G. Identification of the phosphatidic acid phosphatase type 2a isozyme as an androgen-regulated gene in the human prostatic adenocarcinoma cell line LNCaP. J Biol Chem 1998;273:4660–5.
230. Kai M, Wada I, Imai S, Sakane F, Kanoh H. Cloning and characterization of two human isozymes of Mg2+-independent phosphatidic acid phosphatase. J Biol Chem 1997;272:24572–8.
231. Fourcade O, Simon MF, Viode C, et al. Secretory phospholipase A2 generates the novel lipid mediator lysophosphatidic acid in membrane microvesicles shed from activated cells. Cell 1995;80:919–27.
232. Cho W, Han SK, Lee BI, Snitko Y, Dua R. Purification and assay of mammalian group I and group IIa secretory phospholipase A2. Methods Mol Biol 1999;109:31–8.
233. Snitko Y, Koduri RS, Han SK, et al. Mapping the interfacial binding surface of human secretory group IIa phospholipase A2. Biochemistry 1997;36:14325–33.
234. Kim Y, Lichtenbergova L, Snitko Y, Cho W. A phospholipase A2 kinetic and binding assay using phospholipid-coated hydrophobic beads. Anal Biochem 1997;250:109–16.
235. van Dijk MC, Postma F, Hilkmann H, Jalink K, van Blitterswijk WJ, Moolenaar WH. Exogenous phospholipase D generates lysophosphatidic acid and activates Ras Rho and Ca2+ signaling pathways. Curr Biol 1998;8:386–92.

Science

Lysophosphatidylcholine as a Ligand for the Immunoregulatory Receptor G2A

Janusz H. S. Kabarowski,[1]* Kui Zhu,[2]* Lu Q. Le,[1] Owen N. Witte,[1,3]† and Yan Xu[2,4]†

27 July 2001, Volume 293, pp. 702–705

Lysophosphatidylcholine as a Ligand for the Immunoregulatory Receptor G2A

Janusz H. S. Kabarowski,[1]* Kui Zhu,[2]* Lu Q. Le,[1]
Owen N. Witte,[1,3]† Yan Xu[2,4]†

Although the biological actions of the cell membrane and serum lipid lysophosphatidylcholine (LPC) in atherosclerosis and systemic autoimmune disease are well recognized, LPC has not been linked to a specific cell-surface receptor. We show that LPC is a high-affinity ligand for G2A, a lymphocyte-expressed G protein–coupled receptor whose genetic ablation results in the development of autoimmunity. Activation of G2A by LPC increased intracellular calcium concentration, induced receptor internalization, activated ERK mitogen-activated protein kinase, and modified migratory responses of Jurkat T lymphocytes. This finding implicates a role for LPC-G2A interaction in the etiology of inflammatory autoimmune disease and atherosclerosis.

Lysophospholipids regulate a variety of biological processes including cell proliferation, tumor cell invasiveness, and inflammation (*1*, *2*). LPC, produced by the action of Phospholipase A_2 (PLA_2) on phosphatidylcholine, promotes inflammatory effects, including increased expression of endothelial cell adhesion molecules and growth factors (*3*, *4*), monocyte chemotaxis (*5*), and macrophage activation (*6*). As a component of oxidized low density lipoprotein (oxLDL), LPC plays an etiological role in atherosclerosis (*7*) and is implicated in the pathogenesis of the autoimmune disease systemic lupus erythematosus (SLE) (*8*). Despite physiologically high concentrations in body fluids (up to 100 μM) (*9*), extracellular actions of LPC through G protein–coupled receptors (GPCRs) are indicated (*10*, *11*). Although LPC action through a platelet activating factor (PAF) receptor(s) has been suggested (*10*, *11*), a specific LPC receptor has yet to be identified. OGR1 is a high-affinity receptor for sphingosylphosphorylcholine (SPC), a lysophospholipid structurally similar to LPC (*12*). OGR1 is closely related to G2A (*13*), TDAG8 (*14*), and GPR4 (*15*). G2A is a transcriptionally regulated GPCR expressed predominantly in lymphocytes, and its expression in response to stress stimuli and prolonged mitogenic signals suggests that it may negatively regulate lymphocyte growth (*13*). Genetic ablation of G2A function in mice further indicates a role for G2A in the homeostatic regulation of lymphocyte pools and autoimmunity (*16*).

To determine if G2A is a lysophospholipid receptor, we assessed signaling responses in cells ectopically expressing G2A (*17*). Human breast epithelial MCF10A cells were used because they do not express G2A or OGR1, and do not respond to SPC (*12*). Intracellular calcium concentration ($[Ca^{2+}]_i$) was determined in MCF10A cells that were transfected with plasmids encoding green fluorescent protein–tagged G2A (G2A.GFP) (*18*) or GFP (*19*). LPC and SPC (0.1 μM) treatment induced transient $[Ca^{2+}]_i$ increases in G2A.GFP expressing cells only. Responses to lysophosphatidic acid (LPA) (1 μM), PAF (0.1 μM), and adenosine triphosphate (ATP) (20 μM) were not affected by G2A expression (Fig. 1A). Dose-dependent increases in $[Ca^{2+}]_i$ were observed in G2A.GFP-expressing cells [LPC, median effective concentration (EC_{50}) ~0.1 μM; SPC, EC_{50} ~0.4 μM] (Fig. 1B). Pretreatment of G2A.GFP-expressing cells with the PAF receptor antagonist BN 52021 (200 μM) blocked $[Ca^{2+}]_i$ elevation induced by PAF, but not that induced by LPC (1 μM), SPC (1 μM), LPA (1 μM), or ATP (20 μM) (Fig. 1C), indicating that LPC and SPC did not act through a PAF receptor. The pretreatment of G2A.GFP-expressing cells with LPC (1 μM) or SPC (10 μM) induced desensitization to subsequent stimulation with either agonist (1 μM) (Fig. 1D).

When G2A.GFP-expressing cells were pretreated with pertussis toxin (PTX, 100 ng/ml), an inhibitor of $G\alpha_i$, transient $[Ca^{2+}]_i$ increases induced by LPA (1 μM), LPC (0.1 to 5 μM), and SPC (1 to 5 μM) were inhibited (Fig. 1E). Calcium transients elicited by PAF (0.1 μM) or ATP (20 μM) were not affected. Pretreatment of

[1]Department of Microbiology, Immunology, and Molecular Genetics; [2]Department of Cancer Biology, Lerner Research Institute, 9500 Euclid Avenue, Cleveland, OH 44195, USA. [3]Howard Hughes Medical Institute, University of California Los Angeles, Los Angeles, CA 90095–1662, USA. [4]Department of Gynecology and Obstetrics, Cleveland Clinic Foundation, 9500 Euclid Avenue, Cleveland, OH 44195, USA.

*These authors contributed equally to this work.
†To whom correspondence should be addressed. E-mail: owenw@microbio.ucla.edu (O.N.W.); xuy@ccf.org (Y.X.)

G2A.GFP-expressing cells with phorbol 12-myristate 13-acetate (PMA), an activator of protein kinase C (PKC), abolished transient $[Ca^{2+}]_i$ increases induced by LPA, LPC, and SPC (up to 10 μM), but did not affect those induced by PAF (0.1 μM) and ATP (20 μM) (Fig. 1F). This suggests that PKC affects LPC and SPC signaling pathways by inducing G2A desensitization and/or inhibition of $G\alpha_i$. Several putative consensus PKC phosphorylation sites are present in G2A (*13*).

To determine binding affinities of LPC and SPC toward G2A, we performed radioligand binding assays (*12*, *20*). [^{3}H]LPC and [^{3}H]SPC bound to homogenates of human embryonic kidney (HEK) 293 cells expressing G2A.GFP (HEK 293 G2A.GFP) in a time-dependent manner and reached equilibrium after 60 min of incubation at 4°C (Fig. 2, A and B). Binding of [^{3}H]LPC and [^{3}H]SPC to HEK 293 G2A.GFP homogenates were saturable, and Scatchard analysis indicated a dissociation constant (K_d) of 65 nM for LPC and 230 nM for SPC (Fig. 2, C and D). The maximum binding capacities for LPC and SPC were about 1500 fmol/10^5 cells and 1840 fmol/10^5 cells, respectively. Competition analyses revealed that only SPC and various LPC species, but not 14:0 LPC, LPA, sphingosine-1-phosphate (S1P), lysophosphatidylinositol (LPI), sphingomyelin (SM), PAF, or lyso-PAF, competed for binding (Fig. 2, E and F).

GPCRs are internalized in response to ligand stimulation. In serum-starved HEK 293 G2A.GFP cells, G2A.GFP is expressed predominantly at the plasma membrane. LPC (0.1 μM), as well as SPC (1 μM), induced internalization of G2A.GFP in more than 90% of cells (*21*, *22*). Neither PAF, LPA, nor S1P induced receptor internalization.

ERK mitogen-activated protein (MAP) kinase activity is stimulated by SPC after transfection of otherwise unresponsive cell lines with OGR1 (*12*). Similarly, LPC does not stimulate ERK MAP kinase activation in a number of cell lines (*23*) (Fig. 3). G2A expression conferred responsiveness to these lysophospholipids in terms of ERK MAP kinase activation in Chinese hamster ovary (CHO) cells (*24*). A dose-dependent increase in ERK MAP kinase activity was observed in response to LPC and SPC (Fig. 3A), and activation was inhibited by PTX pretreatment, indicating the involvement of a $G\alpha_i$ family G protein (Fig. 3B).

LPC is thought to have chemoattractant properties toward T lymphocytes (*25*). Cellular transmigration of Jurkat T cells expressing GFP or G2A.GFP (both populations were 20% GFP-positive) through a polycarbonate membrane tissue-culture chamber toward the ligand was assessed over a 1-hour period (*26*). Although LPC suppressed transmigration of the GFP-positive fraction of Jurkat GFP populations, LPC (10 μM) stimulated transmigration of Jurkat G2A.GFP cells by four times that of Jurkat cells expressing GFP only (Fig. 4). SPC did not stimulate transmigration of Jurkat G2A.GFP cells (*27*), and the possible physiological functions of an SPC-G2A interaction have yet to be determined.

Different LPC species may have different affinities for G2A (Fig. 2, E and F); 14:0 LPC is not able to compete [^{3}H]–16:0 LPC binding, whereas 16:0 LPC, 18:0 LPC, and 18:1 LPC are potent competitors. Consistently, 14:0 LPC is unable to stimulate $[Ca^{2+}]_i$ increases in G2A expressing MCF10A cells (*27*). G2A also binds SPC with low affinity. The physiological significance of this promiscuity remains to be

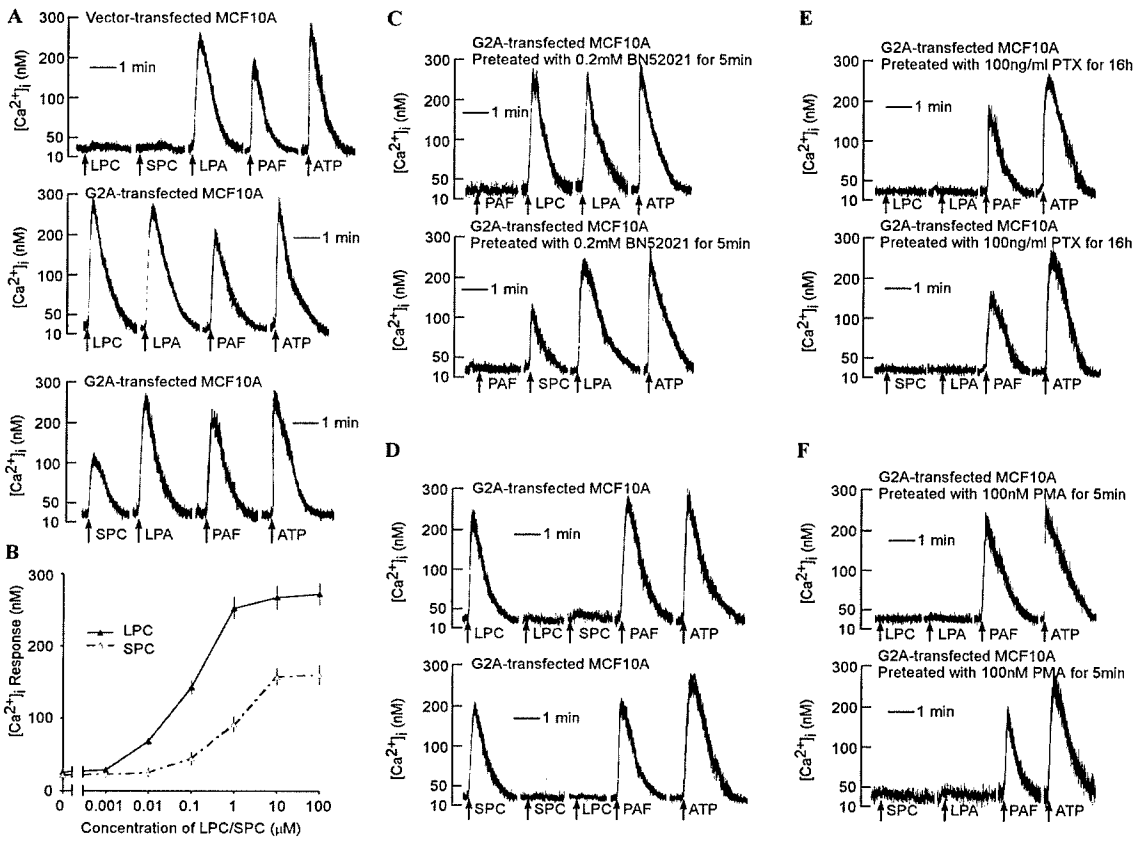

Fig. 1. LPC and SPC induce transient $[Ca^{2+}]_i$ increases in G2A-transfected MCF10A cells. (**A**) (Upper panel) Calcium responses of pEXV3 GFP (vector)-transfected MCF10A cells to 16:0 LPC (1 μM), SPC (1 μM), LPA (1 μM), PAF (0.1 μM), and ATP (20 μM). (Middle panel) Calcium responses of G2A-transfected MCF10A cells to 16:0 LPC (1 μM), LPA (1 μM), PAF (0.1 μM) and ATP (20 μM). (Lower panel) Calcium responses of G2A-transfected MCF10A cells to SPC (1 μM), LPA (1 μM), PAF (0.1 M), and ATP (20 μM). (**B**) 16:0 LPC and SPC dose responses in G2A-transfected MCF10A cells. (**C**) (Upper panel) The effect of PAF receptor inhibitor [BN52021 (Biomol, Plymouth Meeting, Pennsylvania)] on $[Ca_{2+}]_i$ increases induced by PAF (0.1 μM), 16:0 LPC (1 μM), LPA (1 μM), and ATP (20 μM). (Lower panel) The effect of BN52021 on $[Ca^{2+}]_i$ increases induced by PAF (0.1 μM), SPC (1 μM), LPA (1 μM), and ATP (20 μM). (**D**) Pretreatment of G2A-transfected MCF10A cells with 16:0 LPC (1 μM) (upper panel) or SPC (10 μM) (lower panel) induces desensitization to subsequent stimulation with 16:0 LPC or SPC (1 μM). (**E**) PTX (100 ng/ml, 16 hours) inhibits G2A-dependent $[Ca^{2+}]_i$ increases induced by 16:0 LPC (1 μM) (upper panel), SPC (1 μM) (lower panel), and LPA (1 μM) (both panels). (**F**) PMA pretreatment (100 nM, 5 min) inhibits G2A-dependent $[Ca^{2+}]_i$ increases induced by 16:0 LPC (1 μM) (upper panel), SPC (1 μM) (lower panel), and LPA (1 μM) (both panels). Data are representative of three independent experiments.

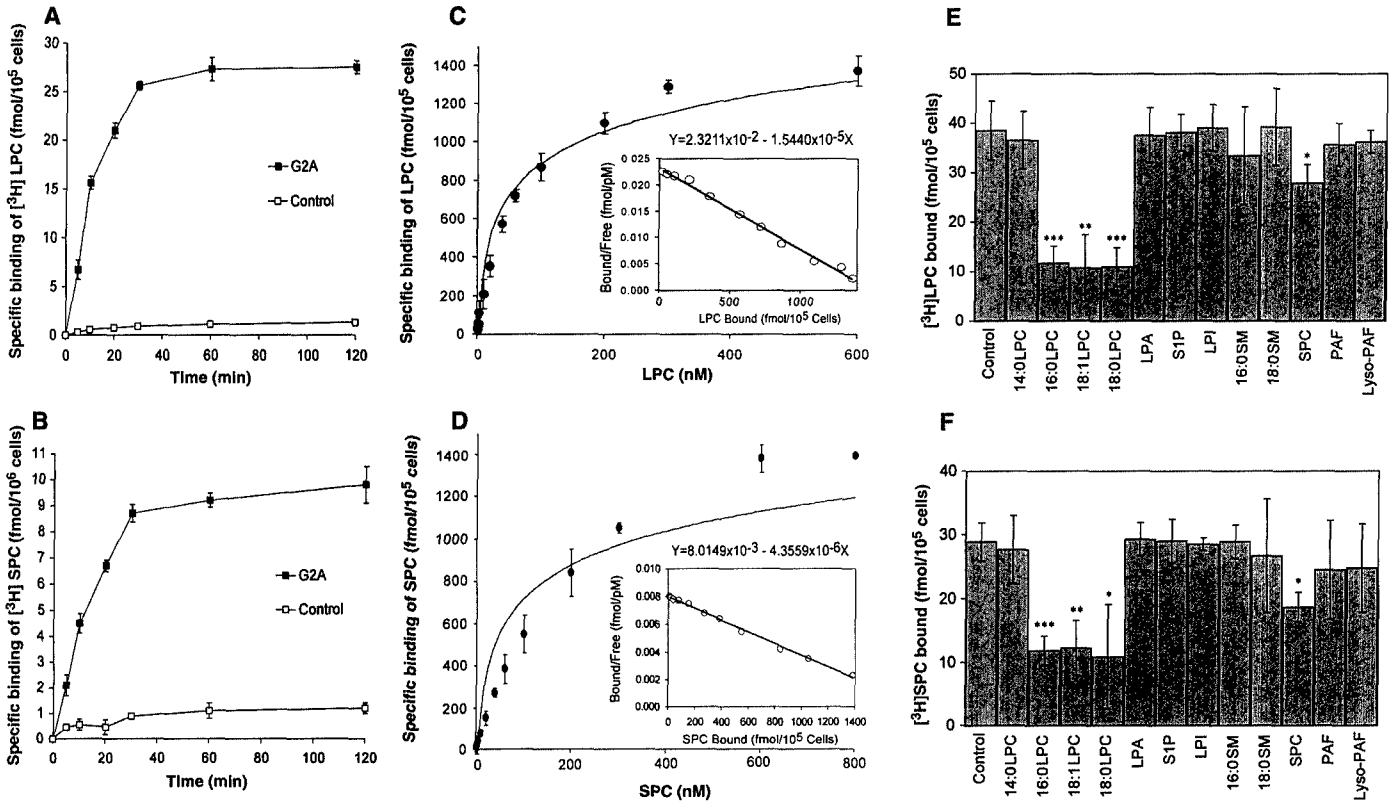

Fig. 2. LPC and SPC bind to G2A. (**A** and **B**) Time dependence of [^{3}H]LPC and [^{3}H]SPC binding. Cell homogenates from HEK 293 GFP or HEK 293 G2A.GFP cells (>90% GFP-positive) were incubated with [^{3}H]–16:0 LPC (1 nM) or [^{3}H]SPC (1 nM) for the indicated times. Specific binding is presented. (**C** and **D**) Saturation isotherms of [^{3}H]LPC and [^{3}H]SPC binding to HEK293 G2A.GFP cells. Cell homogenates were incubated with the indicated concentrations of [^{3}H]–16:0 LPC or [^{3}H]SPC and specific binding was measured. (Insets) Scatchard analyses of [^{3}H]–16:0 LPC and [^{3}H]SPC binding. (**E** and **F**) Structural specificity of [^{3}H]–16:0 LPC and [^{3}H]SPC binding to G2A. HEK 293 G2A.GFP homogenates were incubated with [^{3}H]–16:0 LPC (1 nM) or [^{3}H]SPC (1 nM) in the presence or absence of unlabeled lipids (100 nM). Total binding is presented. Data are means ± SD representing three independent experiments. $*P < 0.05$; $**P < 0.01$; $***P < 0.001$, compared to control (Student's t test).

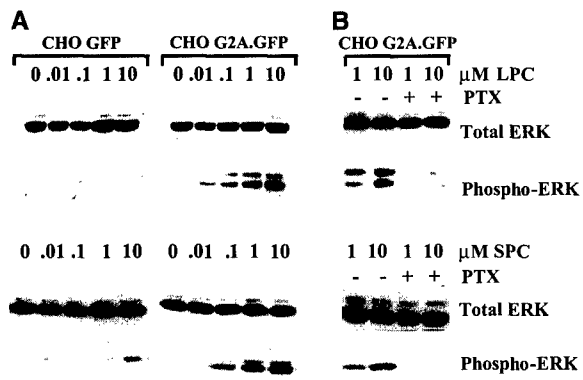

Fig. 3. LPC and SPC activate ERK MAP kinase in G2A-expressing CHO cells. (**A**) Serum-starved CHO GFP and CHO G2A.GFP cells were stimulated with the indicated concentrations of agonist for 10 min. Total lysates were Western blotted with antibodies against ERK MAP kinase or phospho-ERK MAP kinase. (**B**) Pretreatment of CHO G2A.GFP cells with PTX (100 ng/ml, 16 hours) inhibits ERK MAP kinase activation induced by LPC and SPC.

defined. A related receptor, TDAG8, responds to the glycolipid psychosine (*28*), suggesting the possibility that this GPCR subfamily (OGR1, G2A, TDAG8, and GPR4) responds to a structurally diverse set of lipids.

G2A may be a hitherto unrecognized etiological factor in the chronic inflammatory diseases SLE and atherosclerosis. The receptor may play a role as a sensor of LPC levels at sites of inflammation to limit expansion of tissue-infiltrating cells and progression to overt autoimmune disease. An immunosuppressive action of LPC on T cell proliferation has been reported (*11*), and T cells from G2A-deficient mice exhibit hyperproliferative responses to antigen receptor stimulation in vitro (*16*). LPC may also influence homing and/or localization of lymphocytes through G2A to modulate T-dependent immune responses and atherogenesis. The effects of the physiologically high concentrations of LPC in body fluids and serum, as well as possible functional redundancy with G2A receptor analogs, may determine the suitability of these GPCRs in the treatment of disease.

References and Notes

1. S. Spiegel, S. Milstien, *J. Membr. Biol.* **146**, 225 (1995).
2. W. H. Moolenaar, *Exp. Cell Res.* **253**, 230 (1999).
3. N. Kume, M. I. Cybulsky, M.A. Gimbrone Jr., *J. Clin. Invest.* **90**, 1138 (1992).
4. N. Kume, M. A. Gimborne Jr., *J. Clin. Invest.* **93**, 907 (1994).
5. Q. Jing *et al.*, *Circ. Res.* **84**, 52 (2000).
6. N. Yamamoto, S. Homma, I. Millman, *J. Immunol.* **147**, 273 (1991).
7. A. J. Lusis, *Nature* **407**, 233 (2000).
8. J. S. Koh, Z. Wang, J.S. Levine, *J. Immunol.* **165**, 4190 (2000).
9. M. Okita, D. C. Gaudette, G. B. Mills, B. J. Holub, *Int. J. Cancer* **71**, 31 (1997).
10. Y. H. Huang, L. Schafer-Elinder, R. Wu, H. E. Claesson, J. Frostegard, *Clin. Exp. Immunol.* **116**, 326 (1999).
11. A. Amberger *et al.*, *Cell Stress Chaperones* **2**, 94 (1997).
12. Y. Xu *et al.*, *Nature Cell Biol.* **2**, 261 (2000).
13. Z. Weng *et al.*, *Proc. Natl. Acad. Sci. U.S.A.* **95**, 12334 (1998).
14. J. W. Choi, S. Y. Lee, Y. Choi, *Cell Immunol.* **168**, 78 (1996).
15. M. Heiber *et al.*, *DNA Cell Biol.* **14**, 25 (1995).
16. L. Q. Le *et al.*, *Immunity* **14**, 561 (2001).
17. MCF10A, HEK 293, and CHO cells do not express G2A as determined by reverse transcriptase polymerase chain reaction (*29*).

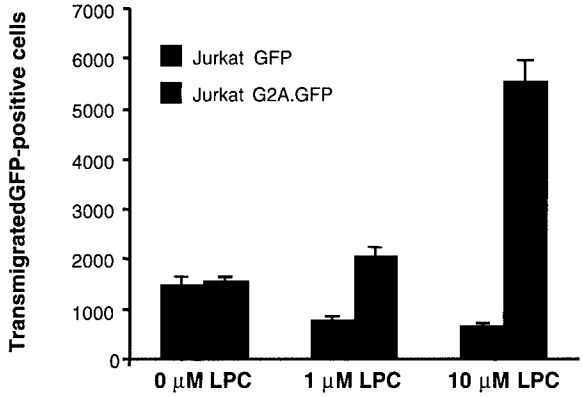

Fig. 4. LPC stimulates migration in G2A-expressing Jurkat T cells. A total of 10^5 Jurkat GFP or Jurkat G2A.GFP cells (both populations 20% GFP-positive) were allowed to transmigrate through 5-μm pore-size membranes toward the indicated concentrations of LPC for 1 hour. GFP-positive fractions (%) and cell numbers of transmigrated populations were measured by flow cytometry. Results are presented as numbers of transmigrated GFP-positive cells. Assays were performed in triplicate and results shown are representative of three independent experiments.

18. J. H. S. Kabarowski *et al.*, *Proc. Natl. Acad. Sci. U.S.A.* **97**, 12109 (2000).
19. Calcium assays were performed as described (*12*). MCF10A cells were loaded with Fura-2/AM (Molecular Probes) and $[Ca^{2+}]_i$ increases were measured in single transfected (GFP-positive) cells with a dual-wavelength spectrofluorometer (RFK-6002, Photon Technology, Brunswick, NJ) coupled to an inverted fluorescence microscope (Olympus, IX-70, Lake Success, NY).
20. HEK 293 GFP or HEK 293 G2A.GFP cells were serum-starved for 20 hours and collected in phosphate-buffered saline (PBS)/EDTA. Pelleted cells were stored at −80°C until use. Frozen cells were homogenized in "binding buffer" (10^6 cells/ml) (*13*). Assays were performed in 96-well plates in triplicate with 100-μl cell homogenate. [^{3}H]–16:0 LPC or [^{3}H]SPC were added to cell homogenates in 50 μl of binding buffer in the presence or absence of cold 16:0 LPC or SPC, or other competitors. Plates were incubated at 4°C for 2 hours, or for the indicated times. Cell-bound [^{3}H]LPC or [^{3}H]SPC was collected onto a filter (Printed Filtermat A, Wallac, Gaithersburg, MD) with an automated cell harvester (Harvester 96, Tomtec, Orange, CT). Specific binding was calculated by subtraction of nonspecific binding (in the presence of 100-fold excess unlabeled lipid) from total binding. [^{3}H]–18:0 LPC and [^{3}H]SPC were from Amersham Pharmacia Biotech (Buckinghamshire, England) (102 Ci/mmol, 1 mCi/ml for [^{3}H]–18:0 LPC, and 68 Ci/mmol, 1 mCi/ml for [^{3}H]SPC). [^{3}H] 16:0–LPC (60 Ci/mmol) was from American Radiolabelled Chemicals (St Louis, MO). LPCs (14:0, 16:0, 18:0, and 18:1), LPI, LPA, C16-PAF, and C16-lysoPAF were from Avanti Polar Lipids, (Alabaster, AL). Sphingomyelins (16:0 and 18:0), S1P, and SPC were from Toronto Research Chemicals (Toronto, ON) or Matreya (Pleasant Gap, PA).
21. Supplementary Web material is available on *Science* Online at www.sciencemag.org/cgi/content/full/293/5530/702/DC1.
22. HEK 293 G2A.GFP cells seeded onto glass cover slips were serum-starved for 18 hours before treatment with agonists for 2 hours. Cover slips were washed with PBS and fixed with PBS–4% paraformaldehyde. Subcellular localization of G2A.GFP was visualized under a confocal fluorescence microscope with an oil immersion lens (magnification, ×60).
23. X. Fang *et al.*, *J. Biol. Chem.* **272**, 13683 (1997).
24. CHO GFP or CHO G2A.GFP cells were serum-starved for 18 hours before treatment with agonist for 10 min at 37°C. Western blotting was performed to detect total ERK MAP kinase with a polyclonal antibody to ERK2, and activated p44/42 ERK MAP kinase with a specific antibody to phospho-ERK (Santa Cruz Biotechnology).
25. H. F. McMurray, S. Parthasarathy, D. Steinberg, *J. Clin. Invest.* **92**, 1004 (1993).
26. Although G2A is expressed in Jurkat cells, our experimental strategy was based on the hypothesis that increased expression in a physiologically relevant cell type may elicit a biological response. For transmigration assays, Jurkat GFP and Jurkat G2A.GFP cells were derived by retroviral infection and assayed 48 hours later. GFP-positive fractions of Jurkat GFP and Jurkat G2A.GFP populations were adjusted to 20% by the addition of appropriate numbers of parental Jurkat cells. Cells were washed three times in RPMI containing 0.25% bovine serum albumin (BSA) and finally resuspended in RPMI–0.25% BSA at 2×10^6 cells/ml. One hundred microliters of this cell suspension (10^5 cells) was applied to the upper chamber of a 6.5-mm diameter transwell cell culture insert comprising a 5-μm pore-size polycarbonate membrane (Corning Costar Corporation, Cambridge, MA) and containing 600 μl RPMI–0.25% BSA with or without agonist in the lower chamber. After incubation at 37°C for 1 hour, transmigrated cells were collected and analyzed by flow cytometry for GFP expression and cell number.
27. J. H. S. Kabarowski *et al.*, data not shown.
28. D.-S. Im, C. E. Heise, T. Nguyen, B. F. O'Dowd, K. R. Lynch, *J. Cell. Biol.* **153**, 429 (2001).
29. L. M. Baudhuin, Y. Xu, unpublished data.

30. Supported by U.S. Army grant RPG-99-062-01-CNE and NIH grant 1 R21 CA84038-01 (Y.X.) and NIH grant CA76204 (O.N.W.). O.N.W. is an Investigator of the Howard Hughes Medical Institute. J.H.S.K. is a fellow of the Leukemia and Lymphoma Society of America. L.Q.L. is supported by National Research Service Award T32 CA09056. We thank H. Bourne, B. Williams, J. Lusis, L. Birnbaumer, M. Simon, S. Smale, L. Zipursky, and D. Fruman for critical review of the manuscript. This paper is dedicated to the memory of our dear friend and colleague Matthew I. Wahl, M.D., Ph.D.

20 April 2001; accepted 1 June 2001

JBC Papers in Press. Published on September 4, 2001 as Manuscript M008057200

SPHINGOSYLPHOSPHORYLCHOLINE AND LYSOPHOSPHATIDYLCHOLINE ARE LIGANDS FOR THE G PROTEIN COUPLED RECEPTOR GPR4*

Kui Zhu‡, Linnea M. Baudhuin‡¶, Guiying Hong‡, Freager S. Williams†, Kelly L. Cristina‡, Janusz H.S. Kabarowski#, Owen N. Witte# and Yan Xu‡† ,

‡Department of Cancer Biology, †Department of Gynecology and Obstetrics, Cleveland Clinic Foundation, 9500 Euclid Ave., Cleveland OH 44195. ¶Department of Chemistry, Cleveland State University, 24th and Euclid Ave, Cleveland OH 44115. #Department of Microbiology, Immunology and Molecular Genetics, Howard Hughes Medical Institute, University of California, Los Angeles, Los Angeles, CA 90095-1662.

* This work was supported in part by the American Cancer Society Grant RPG-99-062-01-CNE, the US Army grant DAMD 17-99-1-9563, the NIH grant R21 CA84038-01 to YX and NIH Grant CA76204 to ONW. JHSK is a fellow of the Leukemia and Lymphoma Society of America.

To whom correspondence should be addressed. Phone (216) 444-1168; fax: (216) 445-6269; E-mail: xuy@ccf.org

Running title: GPR4 as a receptor for SPC and LPC

SUMMARY

Sphingosylphosphorylcholine (SPC[1]) and lysophosphatidylcholine (LPC) are bioactive lipid molecules involved in numerous biological processes. We have recently identified ovarian cancer G protein coupled receptor 1 (OGR1) as a specific and high affinity receptor for SPC, and G2A as a receptor with high-affinity for LPC, but low affinity for SPC. Among G protein coupled receptors (GPCRs), GPR4 shares highest sequence homology with OGR1 (51%). In this work, we have identified GPR4 as not only another high affinity receptor for SPC, but also a receptor for LPC, albeit of lower affinity. Both SPC and LPC induce increases in intracellular calcium concentration in GPR4-, but not vector-transfected, MCF10A cells. These effects are insensitive to treatment with BN52021, WEB-2170 and WEB-2086 [specific platelet activating factor (PAF) receptor antagonists], suggesting that they are not mediated through an endogenous PAF receptor. SPC and LPC bind to GPR4 in GPR4-transfected CHO cells with Kd/SPC=36 nM, and Kd/LPC=159 nM, respectively. Competitive binding is elicited only by SPC and LPC. Both SPC and LPC activate GPR4-dependent activation of serum response element (SRE) reporter and receptor internalization. Swiss 3T3 cells expressing GPR4 respond to both SPC and LPC, but not sphingosine-1-phosphate (S1P), PAF, psychosine (Psy), glucosyl-β1'1-

[1] The abbreviations used are: ERK: extracellular signal-regulated kinase; CHO, Chinese hamster ovary; Glu-Sph, Glucosyl-β1'1-sphingosine; Gal-Cer, galactosyl-β1'1-ceramide; Lac-Cer: lactosyl-β1'1-ceramide; LPA, lysophosphatidic acid; LPC, lysophosphatidylcholine; GPCR, G protein coupled receptor; OGR1, ovarian cancer G protein coupled receptor 1; ox-LDL: oxidized low-density lipoprotein; PAF, platelet activating factor; Psy, psychosine; S1P, sphingosine-1-phosphate; SM, sphingomyelin; SRE, serum response element; SPC, sphingosylphosphorylcholine; SLE, systemic lupus erythematosus; TDAG8, T cell death-associated gene 8.

sphingosine (Glu-Sph), galactosyl--β1'1-ceramide (Gal-Cer), or lactosyl-β1'1-ceramide (Lac-Cer) to activate extracellular signal-regulated kinase (ERK) MAP kinase in a concentration- and time-dependent manner. SPC and LPC stimulate DNA synthesis in GPR4-expressing Swiss 3T3 cells. Both ERK activation and DNA synthesis stimulated by SPC and LPC are pertussis toxin (PTX)-sensitive, suggesting the involvement of a Gi-heterotrimeric G protein. In addition, GPR4 expression confers chemotactic responses to both SPC and LPC in Swiss 3T3 cells. Taken together, our data indicate that GPR4 is a receptor with high affinity to SPC and low affinity to LPC, and that multiple cellular functions can be transduced via this receptor.

INTRODUCTION

SPC is a bioactive lipid molecule involved in numerous biological processes, where it acts as a signaling molecule (1). We have recently identified a GPCR, OGR1, as the first specific high affinity receptor for SPC (2). OGR1 shares homology with several other GPCRs, including GPR4, G2A, T cell death associated GPCR8 (TDAG8), and the PAF receptor (3-10). We have postulated that these receptors belong to a subfamily and their ligands may be lysolipids containing the phosphorylcholine moiety shared by SPC and PAF (2). Other than SPC and PAF, there are two naturally occurring phosphorylcholine-containing lysolipids: LPC and lyso-PAF. LPC is an important lipid mediator involved in many cellular processes. In particular, LPC is believed to play an important role in atherosclerosis and inflammatory diseases by altering various functions of a variety of cell types, including endothelial cells, smooth muscle cells, monocytes, macrophages and T cells (11-13). However, the reported signaling mechanisms of LPC are variable and the initial interaction of LPC with cell membranes is poorly understood. We have recently identified G2A as the first receptor for LPC (14). G2A is also a low-affinity receptor for SPC.

In the present study, we sought to identify the ligand(s) for GPR4. We tested SPC, LPC, PAF, lyso-PAF and psychosine [Psy; a recently identified glycosphingolipid ligand of TDAG8 (15)] as potential ligands for GPR4. GPR4 exhibits the highest homology with OGR1 (51% identity and 64% similarity in amino acid sequence) (2). Similarly to OGR1, GPR4 responded to SPC, but also responded to LPC, mediating an increase in intracellular calcium concentration, SRE activation, receptor internalization, ERK activation, and stimulation of cell migration. LPC bound to GPR4, albeit with lower affinity compared to SPC, and competed with SPC for specific binding to GPR4. GPR4 did not bind or respond to PAF, lyso-PAF, Psy, Glu-Sph, Gal-Cer, or Lac-Cer. Our results indicate that SPC is a high-affinity and LPC is a lower-affinity ligand for GPR4, and its activation by SPC and LPC mediates biological functions.

EXPERIMENTAL PROCEDURES

Materials-LPCs (14:0, 16:0, 18:0, and 18:1), lysophosphatidylinositol (LPI; from liver, 80% 18:0), 18:1-LPA, 16:0-PAF, 16:0-lysoPAF, psychosine, glucosyl-β1'1-sphingosine, galactosyl-1'1-C8-ceramide, and lactosyl-β1'1-C8-ceramide were from Avanti Polar Lipids, Inc. (Alabaster, AL). Sphingomyelin (SM; bovine brain, mainly 18:0), C6-ceramide, sphingosine-1-phosphate (S1P) and SPC were from Toronto Research Chemicals (Toronto, ON) or Matreya, Inc. (Pleasant Gap, PA). D-erythro- and L-threo-SPC were from Matreya, Inc. (Pleasant Gap, PA). pcDNA1-C3 (encoding the C3-exoenzyme), was a kind gift from Dr. A. Wolfman, Cleveland Clinic Foundation. The PAF receptor antagonist, BN52021, was from Biomol (Plymouth Meeting, PA). WEB-2170 and WEB-2086 were from Boehringer Ingelheim (Ridgefield, CT). [^{3}H]SPC or [^{3}H]18:0-LPC were custom synthesized by Amersham Pharmacia Biotech, Buckinghamshire, England (68 Ci/mmol, 1 mCi/ml for [^{3}H]SPC and 102 Ci/mmol, 1 mCi/ml for [^{3}H]18:0-LPC). [^{3}H]16:0-LPC (60 Ci/mmol) was purchased from American Radiolabeled Chemicals, Inc. (St Louis, MO).

Cell culture—MCF10A cells (passage 34) were purchased from the Barbara Ann Karmanos Cancer Institute (Detroit, MI) and cultured as recommended by the provider. Experiments were performed using MCF10A cells from passage 40-46. Other cells were obtained from ATCC and were cultured either in RPMI1640 with 10% FBS or DMEM with 5% FBS (CHO and Swiss 3T3 cells).

Human RNA Master Blot Probed with GPR4—Human RNA Master Blot (Clontech, Palo Alto, CA) was probed with radiolabeled full-length GPR4. Briefly, the full-length GPR4 was gel purified and 25 ng was used for the synthesis of a StripAble DNA α-^{32}P-labeled probe (Ambion, Austin, TX), as per the manufacturer's instructions. The radiolabeled probe (20 ng, 20 X 10^6 CPM) was hybridized to the Master Blot in ExpressHyb hybridization solution (Clontech) overnight with continuous agitation at 65°C. The following day, the Master Blot was washed following the manufacturer's instructions and exposed to a Phospho Screen (Molecular Dynamics, Sunnyvale, CA).

Real-time Quantitative PCR of GPR4—Total RNA was extracted from cells using the SV Total RNA Isolation System (Promega, Madison, WI). One to five micrograms of total RNA were reverse transcribed using Superscript II RT (Gibco BRL, Rockville, MD). Eight nanograms of derived cDNA were used as a template for real-time quantitative SYBR Green I PCR. Primers for human GPR4 (Genbank accession number U21051) were 5'-TAATGCTAGCGGCAACCACACGTGGGAG and 5'-TCCAGTTGTCGTGGTGCAG, yielding a 230 bp product. Glyceraldehyde-3-phosphate dehydrogenase (GAPDH) was amplified in a separate tube as a housekeeping gene with primers 5'-GAAGGTGAAGGTCGGAGT and 5'-GAAGATGGTGATGGGATTTC, yielding a 226 bp product. Primers for mouse GPR4 were 5'-CTACCTGGCTGTGGCTCAT and 5'-CAAAGACGCGGTATAGATTCA, yielding a 222 bp product. Mouse GAPDH was amplified with primers 5'-TGATGGGTGTGAACCAAGACA and 5'-CCAGTGGATCAGGGATGAT. All SYBR Green I core reagents, including AmpliTaq Gold DNA polymerase, were from PE Applied Biosystems

(Foster City, CA). The thermal cycling conditions were 95°C for 10 minutes, followed by 40 cycles of 95°C, 15 seconds and 60°C, 1 minute. PCR reactions and product detection were carried out in an ABI Prism 7700 Sequence Detection System (PE Applied Biosystems). The amplified product was detected by measurement of SYBR Green I, which was added to the initial reaction mixture. The threshold cycle (C_T) values obtained through the experiments indicate the fractional cycle numbers at which the amount of amplified target reach a fixed threshold. The C_T values of both target and internal reference (GAPDH) were measured from the same samples, and the expression of the target gene relative to that of GAPDH was calculated using the comparative C_T method. This method normalizes the expression levels and allows calculation of the relative efficiency of the target and reference amplification.

Cloning—A GPR4 PCR fragment (nucleotides #1175-1535) (4) was obtained by PCR amplification using cDNA from HEY ovarian cancer cells as the template. This PCR fragment was used to screen a human genomic library (Clontech, Palo Alto, CA) to obtain the full-length clone of GPR4. GPR4 was subsequently cloned into mammalian expression vectors using PCR amplifications with the high fidelity Advantage cDNA polymerase (Clontech). The PCR reactions were conducted for fewer than 20 cycles and the sequence of the products was confirmed by sequencing. The primers: 5'-CAGGAATTCTCGGCAACCACACGTGGGAGG, and 5'-CGCTCTAGAGCCACTCGGGGTTCATTGTG were used to generate full length GPR4, which was digested with EcoR I and Xba I and cloned into the pBs3HA vector (pBluescript II KS^+ vector with three HA-tags inserted; a kind gift from Dr. J. DiDonato, Cleveland Clinic Foundation). The resulting 3HA-GPR4 was subsequently cloned into the mammalian expression vector pIRES-hygro (Clontech) to generate pIREShyg-GPR4, using primer 5'-CAGATGCATAAACGCTCAACTTTGG and the T7 primer (inserted into the Nsi I and Not I sites of pIRES-hygro). pGPR4-GFP was generated using the T3 primer and 5'-GTCGGTACCTGTGCTGGCGGCAGCATC (stop codon was deleted and the resulting GPR4 was

cloned into Hind III and Kpn I sites of pEGFP-N1; Clontech). pSRE-Luc was purchased from Stratagene (La Jolla, CA). MCF10A cells were transiently transfected with pGPR4-GFP and used for calcium assays. CHO cells were transfected with pIREShyg-GPR4 (LipofectAMINE reagent; Life Technologies, Rockville, MD) and stable clones were selected with 200 μg/ml hygromycin in DMEM/F12 plus 5% FBS. HEK293 cells were transfected with pGPR4-GFP and stable clones were selected with 400 μg/ml G418 in RPMI 1640 plus 10%FBS. Swiss 3T3 cells expressing GPR4 were derived by infection with retroviruses encoding receptor (MSCV GPR4 ires-GFP) followed by FACS sorting of GFP positive cells (16).

Calcium assays—Measurement of $[Ca^{2+}]_i$, was performed as described previously (2). Briefly, pGPR4-GFP-transfected MCF10A cells were grown in specialized glass-bottom dishes (Bioptech, Inc., Butler, PA) and loaded with fura-2 in HEPES buffered saline. Using a dual-wavelength spectrofluorometer (RFK-6002, Photon Technology Int'l, So. Brunswick, NJ) coupled to an inverted fluorescence microscope (Olympus, IX-70, Lake Success, NY), GFP-positive cells were identified using an excitation wavelength of 488 nm, a dichroic 505 nm long-pass filter and an emitter filter at bandpass of 535 nm (Chroma Technology, Brattleboro, VT). Measurements of $[Ca^{2+}]_i$ were performed on individual GPR4-GFP positive cells at excitation wavelengths of 340 and 380 nm and an emission wavelength of 510 nm. Conversion of the 340/380-ratio value into $[Ca^{2+}]_i$ in nM was estimated by comparing the cellular fluorescence ratio with ratios acquired using fura-2 (free acid) in buffers containing known Ca^{2+} concentrations. $[Ca^{2+}]_i$ was then calculated as described by Grynkiewicz *et al.* (17). All calcium assays were performed in the presence of 1 mM EGTA in the assay buffers. Therefore, intracellular calcium release, not calcium influx, was analyzed.

Internalization—pGPR4-GFP stably expressing HEK293 cells were cultured in 6 cm tissue culture dishes in RPMI1640 with 10% FBS. After 16-24 h serum starvation, cells were treated with different lipids

at 37°C for 2 h. Cells were washed with cold PBS and fixed with 4% paraformaldehyde in PBS. The subcellular localization of GPR4-GFP protein was visualized under a Leica TV confocal fluorescence microscope with a 63x oil immersion lens (Wetzler, Heidelberg, Germany). The excitation and emission wavelengths were 488 nm and 515-540 nm, respectively.

Binding assays—CHO cells were chosen for GPR4 binding assays, since HEK293 cells express relatively high levels of endogenous GPR4. CHO cells stably transfected with empty vector or GPR4 were serum starved for 20 h, then collected after exposure to 2 mM EDTA in PBS. The pelleted cells were stored at -80°C until use. Binding assays were performed essentially as described previously (2), except binding was performed at 4°C. Briefly, frozen cells (10^6 cells/ml) were homogenized in a binding buffer (2). Assays were performed in 96-well plates in triplicate with 100µl cell homogenate (equivalent to 10^5 cells/well). Different amounts of [^{3}H] SPC or [^{3}H] 16:0-LPC were added to the cell homogenates in 50 µl of binding buffer, in the presence or absence of cold SPC or 16:0-LPC, or other competitors. The plates were incubated at 4°C for 120 min, unless otherwise indicated. Cell-bound [^{3}H] SPC or [^{3}H] LPC was collected onto a filter (Printed Filtermat A, Wallac, Gaithersburg, MD) using an automated cell harvester (HARVESTER 96, Tomtec, Orange, CT). Specific binding was calculated by subtraction of nonspecific binding (binding detected in the presence of 100-fold excess unlabeled SPC or 16:0-LPC) from the total binding.

Reporter (SRE) assays—The SRE reporter system (pSRE-Luc) was a gift from Dr. Songzhu An (UCSF), or purchased from Stratagene (La Jolla, CA). Both systems gave identical results. HEK293 and HEK293-GPR4 cells were cultured in RPMI1640 with 10%FBS in 10 cm dishes to ~85% confluence. To the cells in each dish, pSRE-Luc (10 µg) was transfected in the presence of 60 µl LipofectAMINE reagent. Cells were seeded in 96-well plates 16 h after transfection, incubated for another 24 h in RPMI1640 with 10% FBS, and starved in serum-free medium for 16 h. SPC (dissolved in PBS to 10 mM) and other lipids

(LPCs were dissolved in 70% ethanol. Other lipids were dissolved in PBS, 70-95% ethanol, or 100% MeOH) were diluted in serum free RPMI 1640 and added to the cells, followed by a 10 h incubation. Luciferase activity was measured in Microlite™ 1 plates (DYNEX Technologies, Inc., Virginia) using 60 µl of cell lysate and 20 µl luciferase substrate. PTX (100 ng/ml) was added during the 16 h serum starvation period and pcDNA1-C3 (encoding the C3-exoenzyme, 2 µg) was co-transfected with pSRE-Luc (10 µg).

ERK activation assays—Swiss 3T3 cells were infected with MSCV GPR4-ires-GFP or MSCV ires.GFP, and subsequently cells sorted by FACS for positive expression of GFP as described previously (16). Cells were plated in 6-well plates in DMEM containing 5% FBS, serum-starved overnight, and then treated lipids in DMEM for the indicated times. Cells were lysed on ice in RIPA buffer containing 50 mM Tris-HCl, pH 7.5, 1% Nonidet P-40, 0.5% deoxycholate, 0.1% SDS, 150 mM NaCl, 2mM EGTA, 25 mM sodium fluoride, 1 mM sodium orthovanadate, and 1 x protease inhibitors (Sigma P8340). Lysates containing equal amounts of protein were separated on 10% SDS-polyacrylamide gels and transferred onto nitrocellulose membranes. Antibodies against phosphorylated ERK1/2 (Cell Signaling Technologies; Beverly, MA) were used to probe the membrane and the ECL system (Amersham) was used for detection. To normalize the amounts of protein loaded in each lane, membranes were stripped and re-probed with antibodies against total ERK (Cell Signaling Technologies). In some experiments, cells were pretreated with 100 ng/ml PTX for 12 -16 h prior to SPC and LPC stimulation.

DNA synthesis assay—The effect of SPC and LPC on DNA synthesis was measured using [^{3}H] thymidine incorporation. Briefly, GPR4-ires-GFP- and GFP-Swiss 3T3 cells were plated in 96-well plates, serum-starved for 24 h, and treated with SPC, LPC, or other lipids in serum-free DMEM for 24 h. Cells were incubated with 0.75 µCi/ml [^{3}H] thymidine in serum-free DMEM for the last 18 h. Cells were harvested onto filter papers presoaked in 1% polyethylenimine using the automated cell harvester

HARVEST 96. Incorporated [^{3}H] thymidine was counted in a 1450 Microbeta Trilux Liquid Scintillation and Luminescence Counter (Perkin-Elmer-Wallac, Inc.)

Cell Migration Assay—Chemotaxis was measured in a modified Boyden chamber assay. Briefly, different lipids were added to the lower chambers. GPR4-ires-GFP- and GFP-Swiss 3T3 cells were serum starved for 4 h, trypsinized, and seeded in the upper chambers of Boyden-transwell plates (Corning Inc., Corning, NY). The chambers were incubated for 6 to 8 h. The number of cells that migrated to the lower face of the membrane was counted in 4 random fields. Data are represented as the average ± SD of three independent experiments. For the chemokinetic assay, the same concentrations of lipids were added to both the upper and lower chambers. For Rho inhibition studies, C3-exoenxyme was transiently transfected into Swiss 3T3 cells and cell migration assays were performed 48 hours later.

RESULTS

Human RNA Master Blot Probed with GPR4—GPR4 has been shown to be expressed in many human tissues (18). For a wider analysis of GPR4 expression in human tissues, we probed the Human RNA Master Blot (Clontech) containing RNAs from 50 different human tissues with the full length human GPR4 clone labeled with [^{32}P]dCTP (Experimental Procedures). GPR4 showed the highest expression in ovary, liver, lung, kidney, lymph node, and sub-thalamic nucleus (Fig. 1). Other areas of the brain had a lower expression of GPR4, as did the aorta, placenta, bone marrow, skeletal muscle, spinal cord, prostate, small intestine, and some fetal tissues. GPR4 was also expressed at a detectable level in appendix, trachea, testis, spleen, thymus, pituitary gland, adrenal gland, thyroid gland, and heart, but not in other tissues including some areas of the brain, colon, bladder, uterus, stomach, pancreas, salivary gland, mammary gland, peripheral blood leukocytes, fetal brain, and fetal heart (Fig. 1) .

Both SPC and 16:0-LPC induced transient increases in intracellular calcium concentration ($[Ca^{2+}]_i$) in GPR4-transfected MCF10A cells—We have shown that OGR1 is a high-affinity receptor for SPC (2). To test whether GPR4, which shares 51% sequence homology with OGR1, is also a receptor for SPC, MCF10A cells were transiently transfected with pGPR4-GFP. MCF10A cells were chosen since these cells do not respond to either SPC or 16:0-LPC in calcium assays and they express very low levels of endogenous GPR4 among many human cell lines tested (Fig. 2).

The GFP receptor fusion was used to identify positively transfected cells, and single-cell calcium assays were performed as described in our previous studies (2). SPC (1 μM) stimulated an increase in $[Ca^{2+}]_i$ in GPR4-, but not vector-transfected MCF10A cells (Fig. 3A, 1st and the 2nd panels), suggesting that GPR4 is a receptor for SPC. This is further confirmed by the stereo selectivity of GPR4 favoring D-erythro-SPC (the bioactive form of SPC) vs. L-threo-SPC (Fig. 3A, 3rd panel). Interestingly, unlike OGR1, which is specific for SPC as its ligand (2), GPR4-transfected cells were stimulated to produce increased $[Ca^{2+}]_i$ by an additional phosphorylcholine-containing lysolipid, 16:0-LPC (Fig. 3A, 4th panel). To assess the affinities and potencies of SPC and 16:0-LPC, concentrations of each were varied and calcium mobilization was measured (Fig. 3B). SPC appeared to have a higher efficiency (EC_{50}=105 nM) than LPC (EC_{50}=1.1 μM), although the $[Ca^{2+}]_i$ responses to LPC in GPR4-transfected cells were higher than those of SPC at greater concentrations of LPC (up to 10 μM) (Fig. 3B).

LPC has been shown to activate cellular responses in a PAF receptor-dependent manner (19-21). However, LPC and SPC were not able to induce an increase in calcium through the endogenous PAF receptor in parental cells (Fig. 3A, upper panel). Therefore, it is unlikely that the increase in calcium induced by LPC was mediated by a PAF receptor. Nevertheless, to confirm that LPC and/or SPC did not activate the endogenous PAF receptor in GPR4-transfected cells, three specific PAF receptor antagonists,

BN52021, WEB-2170, and WEB-2086, were used. Both BN52021 (200 μM) and WEB-2086 (2 μM) completely abolished the calcium signal induced by PAF (100 nM) (Fig. 3C and 3D). However, the cellular calcium response to LPC or SPC was not affected, indicating that calcium increases induced by SPC and LPC were not mediated through an endogenous PAF receptor. Another PAF antagonist, WEB-2170 (2 μM), also completely blocked the action of PAF, but did not affect the increase in calcium induced by either LPC or SPC (data not shown). In addition, LPC and SPC showed not only homologous, but also heterologous, desensitization to each other (Fig. 3E), suggesting that these two lipids activated the same receptor.

To determine which G protein is involved in the increased $[Ca^{2+}]_i$ response to SPC and LPC in GPR4-transfected cells, the sensitivity of this activity to PTX was tested. The increase in $[Ca^{2+}]_i$ response to both SPC and LPC, as well as to stimulation of endogenous LPA receptor(s), but not PAF or ATP receptors, was completely abolished by PTX (100 ng/ml, 16 h pretreatment) (Fig. 3F), suggesting the involvement of a G_i pathway.

In plasma, LPC is mainly present in albumin- and lipoprotein-bound forms (22). To determine whether BSA-bound SPC and LPC are able to induce increases in $[Ca^{2+}]_i$, we pre-incubated SPC (1 μM) and LPC (1 μM) with a molar excess of BSA [0.5% fatty acid-free BSA (Sigma)], for a lipid:BSA molar ratio of approximately 1:75. At this molar ratio, BSA blocked more than 50% and 95% of the increases in $[Ca^{2+}]_i$ induced by SPC and LPC, respectively (Fig. 3G). These results suggest that albumin-bound LPC may not be able to activate this receptor, and support the concept of multiple LPC compartmentalization (e.g. bound and free) (23).

Recently, Im *et al* have identified Psy as a ligand for TDAG8. TDAG8 shares approximately 38% homology with OGR1, GPR4 and G2A (15). To determine whether Psy is a ligand for GPR4, and to

delineate the structural specificity of ligands for GPR4, we tested the effect of Psy, Glu-Sph, Gal-Cer, and Lac-Cer to increase $[Ca^{2+}]_i$ in MCF10A cells. We found that at 1 μM, Psy, Glu-Sph, and Lac-Cer did not stimulate increases in $[Ca^{2+}]_i$ in either MCF10A parental or GPR4-expressing cells (Fig. 3H). Gal-Cer (1μM) induced the same level of increased $[Ca^{2+}]_i$, in both parental and GPR4-expressing MCF10A cells (Fig. 3H). These data suggest that these glycosphingolipids are unlikely to be ligands of GPR4.

SPC and LPC bind to GPR4—To characterize the binding of SPC and LPC to GPR4, we conducted radioligand binding assays, using a method similar to that developed for OGR1 as described previously (2). Cell homogenates were used for binding assays. Binding was conducted at 4°C for 120 min or as indicated. [^{3}H] SPC and [^{3}H] 16:0-LPC specifically bound to cell homogenates from GPR4-transfected CHO cells in a time-dependent manner and reached equilibrium after 60 min incubation at 4°C (Fig. 4A and 4B). Both CHO cells and CHO cells transfected with empty vector displayed low background binding of SPC and LPC (Fig. 4A and 4B). SPC and 16:0-LPC bindings were saturable and Scatchard analyses indicated dissociation constants (K_d) of 36 nM for SPC and 159 nM for LPC. The maximum binding capacities for SPC and 16:0-LPC were 996 fmole/10^5 cells for SPC and 1,528 fmole/10^5 cells for 16:0-LPC (Fig. 4C and 4D). SPC ($p<0.001$) and various LPC species (16:0, 18:0 and 18:1; p values 0.001-0.01), but not LPA (18:1), LPI (18:0), S1P, SM (18:0), 16:0-PAF or 16:0-lyso-PAF (p values >0.05), successfully competed for binding (Fig. 4E and 4F). Binding assays using [^{3}H] 18:0-LPC gave similar results (data not shown). We also tested the four glycosphingolipids, Psy, Glu-Sph, Gal-Cer, and Lac-Cer, for their ability to compete for the binding of [^{3}H] SPC and [^{3}H] 16:0-LPC to GPR4. None of these glycosphingolipids competed successfully (Data not shown). Thus, GPR4 was able to specifically bind both SPC and LPC (16:0, 18:0 and 18:1), with a higher affinity for SPC than LPC.

Internalization of GPR4 induced by SPC and LPC—G protein coupled receptors undergo agonist-dependent desensitization and internalization (24-26). When HEK293 cells were transfected with

the pEGFP-N1 vector, GFP protein was expressed in the cytosol of the cells (2). The GPR4-GFP fusion protein, on the other hand, was expressed only on the plasma membrane (Fig. 5A). One micromolar concentrations of SPC and 16:0-LPC, but not 16:0-PAF, induced internalization of GPR4 at 37°C (Fig. 5B, C and F). The PAF receptor-specific antagonist BN52021 did not block the internalization of GPR4 induced by either SPC or 16:0-LPC (Fig. 5D and E). Similarly, WEB-2170 and WEB-2086 did not affect the internalization of GPR4 induced by either SPC or 16:0-LPC (data not shown).

LPC and SPC activated the SRE reporter system in HEK293 cells—The serum-response element (SRE) reporter system is a sensitive assay for receptors of lipid factors (27,28). Using the luciferase assay, vector-transfected HEK293 cells transfected with the SRE reporter system responded to SPC (1 μM), but not 16:0-LPC, with less than1.5-fold activation (Fig. 6A). Activation was increased 3.1- and 4-fold, respectively, in response to 16:0-LPC (1 μM) and SPC (1 μM) in GPR4-transfected HEK293 cells that were also transfected with the SRE reported system (Fig. 6B). These increases were statistically significant ($p<0.001$) when compared to the responses in vector-transfected cells (Fig. 6A). In contrast, although LPA and S1P induced significant transcriptional activation of SRE in vector-transfected HEK293 cells, this activation was not altered by GPR4 transfection. In addition, we tested other phosphorylcholine-containing lipids, including 16:0-PAF, 16:0-lyso-PAF and 18:0-SM, and found that none of them induced significant transcriptional activation of SRE (Fig. 6A).

The SRE transcriptional activity in response to SPC, but not LPC, in parental HEK293 cells (Fig. 6A and 6B), can be explained by the endogenous expression of GPR4 in HEK 293 cells and the relatively lower affinity of GPR4 for LPC compared to SPC. GPR4 transfection enhanced the activation of SRE reporter by both SPC and LPC (Fig. 6A and 6B). EC_{50} values for the activation of SRE were 63 nM for SPC and 160 nM for 16:0-LPC. The differences in EC_{50} values obtained using SRE activation from those

using the calcium assay (105 nM and 1.1 μM for SPC and LPC, respectively) are possibly derived from different coupling efficiencies of distinct signaling pathways and/or different cellular environments.

To determine which G protein and other signaling intermediates might be involved in the activation of SRE by SPC and 16:0-LPC, we pretreated cells with PTX (100 ng/ml) for 16 h, or co-transfected the specific Rho inhibitor, C3-exoenzyme (1.5 μg pcDNA3-C3), with the reporter system. Both PTX and C3-exoenzyme partially inhibited SRE-reporter activation (Fig. 6C). When the two inhibitors were added together, SRE-reporter activation in response to either SPC or 16:0-LPC was almost completely blocked, suggesting that G_i and Rho signaling pathways were involved in SRE activation through GPR4.

SPC and LPC activated ERK MAP kinase in a GPR4-dependent manner—MAP kinases are key signaling intermediates of DNA synthesis and cell proliferation. To determine whether GPR4 mediates ERK MAP kinase activation in response to SPC and LPC, we conducted Western blot analyses of GPR4-ires-GFP-Swiss 3T3 and GFP-Swiss 3T3 cells treated with SPC, 16:0-LPC, and a number of other lipids. The parental and GFP infected Swiss 3T3 cells showed a basal level of ERK activation, as detected by anti-phospho-ERK antibody (Fig. 7A). SPC (100 nM) increased this level of activation (Fig. 7A). In GPR4-ires-GFP-infected Swiss 3T3 cells, both SPC (100 nM) and LPC (100 nM) enhanced ERK activation, and SPC was more potent than LPC (Fig. 7A). A number of other lipids, including S1P, Lac-Cer and PAF, also activated ERK in Swiss 3T3 cells, but activation was independent of GPR4 expression (Fig. 7A).

Lipid stock solutions, dissolved in ethanol or MeOH, were greater than 10 mM. Since the highest final concentration of lipids used in this study was 10 μM, the solvent content was less than 0.1% in any experiment. We routinely performed solvent controls and found that at final solvent concentrations of less than 0.1%, 70-100% ethanol and 100% methanol did not alter any parameters tested.

The higher potency of SPC over LPC was further reflected in the concentration- and time-dependent ERK activation (Fig. 7B and 7C). ERK activation induced by SPC compared to that by LPC was evident at a lower concentration (approximately 10 nM vs. 100 nM), at earlier time points (1 min vs. 5 min), and was maintained for a longer time. These results strengthen the notion that both SPC and LPC are ligands for GPR4, but SPC has a higher affinity than LPC for GPR4.

In GPR4-infected Swiss 3T3 cells, SPC-induced ERK activation was sensitive to PTX, suggesting involvement of G_i signaling (Fig. 7D). This is in contrast to our previous studies where SPC induced ERK activation via a PTX-insensitive pathway in OGR1-transfected HEK293 cells (2). To determine whether this difference was due to receptor subtype or different cell lines used, we tested the PTX-sensitivity of SPC-induced ERK activation in OGR1-infected Swiss 3T3 cells. Our results showed that in Swiss 3T3 cells, SPC-induced ERK activation via OGR1 was PTX-insensitive (Fig. 7D). Thus, although GPR4 and OGR1 are highly homologous, the same high-affinity ligand (SPC) induces activation of ERK through a different G protein pathway for each receptor.

SPC stimulated DNA synthesis in GPR4-infected Swiss 3T3 cells—To determine whether SPC and LPC affect DNA synthesis in a GPR4-dependent fashion, we measured [^{3}H] thymidine incorporation into GPR4-ires-GFP-Swiss 3T3 and GFP-Swiss 3T3 cells. SPC stimulated DNA synthesis in both parental and GFP-infected cells (approximately 6.3-fold increase with 3 μM SPC). These results are qualitatively consistent with observations by Desai *et al* (29). This stimulation was further enhanced by the expression of GPR4 (1.8- to 2-fold increase over GFP-infected Swiss 3T3 cells; Fig. 8A). In both GFP- and GPR4-GFP expressing cells, DNA synthesis stimulated by SPC was inhibited by PTX (Fig. 8A), suggesting G_i signaling was required for this activity. GFP-expressing cells did not respond significantly to 16:0-LPC, whereas [^{3}H] thymidine incorporation increased 1.6-fold in GPR4-infected Swiss 3T3 cells in

response to 3 μM 16:0-LPC (Fig. 8B). Higher concentration of lipids did not further increase [^{3}H] thymidine incorporation stimulated by SPC or LPC (data not shown).

SPC and LPC induced cell migration in a GPR4-dependent manner—As a major component of oxidized low-density lipoprotein (ox-LDL), LPC has been proposed to play a role in atherosclerotic lesion development (30,31). One of the roles of LPC potentially related to atherosclerosis is as a chemoattractant for monocytes, T lymphocytes, and smooth muscle cells (32-34). We used Swiss 3T3 cells infected with GFP or GPR4-ires-GFP as a model system to compare the effects of SPC and 16:0-LPC on cell migration. GPR4 overexpression in Swiss 3T3 fibroblasts increased cell migration in response to SPC (100 nM; lower chamber only) and 16:0-LPC (100 nM; lower chamber only) 2.0-fold and 1.7-fold, respectively, over that observed in GFP-Swiss 3T3 cells (Fig. 9A). Other lipids (18:1-LPA, S1P, or 16:0-PAF) did not alter cell migration in GPR4- vs. vector-transfected cells (Fig. 9A). Cell migration stimulated by both SPC and LPC was inhibited by C3-exoenzyme expression, suggesting that Rho is involved in this process.

Concentration response studies (Fig. 9B) indicate that SPC and LPC were effective at inducing cell migration in the 1-100 nM concentration range. To determine whether this effect was chemotactic or chemokinetic, we measured cells that migrated from the upper to the lower chambers in Boyden chamber assays, conducted with lipids (at 100 nM) in both upper and lower chambers. SPC or 16:0-LPC did not significantly change cell motility when compared to controls (without lipid in either chamber) in either GFP or GFP-GPR4 expressing Swiss 3T3 cells (Fig. 9C). S1P slightly inhibited, PAF slightly enhanced, and LPA did not show a significant effect on cell migration in treated vs. untreated GFP or GFP-GPR4 expressing cells (Fig. 9C). These results suggest that the effect of SPC and 16:0-LPC on cell migration was chemotactic, not chemokinetic, and that the chemotactic effect was mediated through GPR4.

DISCUSSION

GPR4 shares ~50% homology with OGR1. We therefore speculated that these two receptors may have overlapping ligand specificity. Indeed, the results presented here show that GPR4 is a second high-affinity receptor for SPC. OGR1 and GPR4 may play both overlapping and distinct physiological and pathological roles. We have shown that OGR1 and GPR4 bind SPC with similar affinities (33 nM and 36 nM, respectively) and both receptors mediate SPC-induced increases in intracellular calcium and ERK activation. However, GPR4- and OGR1-mediated ERK activation is PTX-sensitive and –insensitive, respectively (Fig. 7A), suggesting that GPR4 and OGR1 couple to different G proteins to activate ERK. More importantly, these differential couplings appear to lead to differential effects on cell proliferation. On the other hand, while OGR1 mediates PTX-insensitive growth inhibition by SPC in a number of cells tested (2), GPR4 mediates PTX-sensitive DNA synthesis by SPC in Swiss 3T3 cells. Together, these data suggested that the endogenous receptor(s) for SPC in Swiss 3T3 cells was GPR4-like, rather than OGR1-like, since parental Swiss 3T3 cells respond to SPC to activate ERK and increase DNA synthesis through a PTX-sensitive pathway (Fig. 8A). The expression of GPR4 in these cells has been confirmed by quantitative PCR analysis (Fig. 2).

GPR4 and OGR1 have different tissue distributions, which may be related to their physiological and pathological roles. Both OGR1 and GPR4 are highly expressed in the lung. However, OGR1 is expressed at high levels in the placenta, spleen, testis, small intestine and peripheral leukocytes (8,18), whereas GPR4 is not expressed, or is expressed at relatively low levels, in these tissues. While GPR4 is expressed at high levels, in the liver, kidney, and ovary (Fig. 1), OGR1 is not expressed in these tissues (8,18). The physiological and pathological roles of these receptors remain to be further investigated.

Another significant finding from this study is the identification of GPR4 as the second G protein coupled receptor for LPC [the first LPC receptor, G2A, was recently described (14)]. GPR4 binds to

LPC (in addition to SPC), but not PAF or lyso-PAF, to mediate an increase in intracellular calcium, receptor internalization, SRE activation, MAP kinase activation, DNA synthesis, and cell migration. Although effects of LPC on transmembrane signal transduction have been widely reported, a specific receptor recognizing LPC had not been identified previously (32). LPC lyses cells at high concentrations (>30μM) (35) and many of the cellular effects previously reported for LPC were observed at high concentrations. Therefore, it is possible that some of the LPC effects *in vivo* are not receptor mediated. On the other hand, evidence has been accumulating to support the notion that, at low concentrations, LPC acts through membrane receptors: a) at relatively low concentrations (less than 10 μM), LPC exerts cell-specific effects; b) LPC increases intracellular Ca^{2+} concentration in association with production of inositolphosphates; and c) these actions of LPC are markedly inhibited by treatment of the cells with PTX and U73122 (36). Some LPC effects are believed to be mediated through the PAF receptor in various cell types, reflected by their partial sensitivity to PAF receptor antagonists (WEB-2170, WEB-2086, and CV-6209) (21,22,37,38). We have shown in the present study, however, that intracellular calcium increase and receptor internalization induced by LPC are dependent on the expression of GPR4 and are insensitive to the PAF receptor antagonists, BN52021, WEB-2071 and WEB-2086. These results clearly show that LPC does not activate these signaling pathways through PAF receptors. We have identified G2A as the first LPC receptor (14). The expression of G2A is restricted to lymphoid tissues (39), while GPR4 is more ubiquitously expressed (Fig. 1). This, together with the different affinities of these two receptors for LPC, may reflect distinct physiological functions for G2A and GPR4.

Physiological concentrations of LPC in body fluids, including blood and ascites, are very high (5-180 μM), when compared to other signaling lipid molecules, such as LPA, S1P and SPC (22, 36,40,41 and our unpublished results). All receptors would be saturated, down regulated, and/or desensitized at these concentrations of LPC if it were all in a form available to its receptors. However, different

concentrations of LPC present in various cellular and tissue systems (i.e. different LPC compartments) may regulate cellular functions differentially (23). LPC in plasma is present mainly in albumin- and lipoprotein-bound forms (22). These forms may be active in some non-receptor-mediated functions of LPC, such as delivery of fatty acids and choline (22), but may be in a form unavailable for receptor activation. It has been shown that some of the effects of LPC are decreased in the presence of albumin (42). Thus, the functionally available concentration of LPC *in vivo,* and the activation of LPC receptors may be controlled by the lower concentrations of free LPC. Although this issue remains to be further addressed, our results shown in Fig. 3G appear to support this notion. The presence of a 75-fold molar excess of BSA greatly diminished the ability of LPC to elicit an increase in $[Ca^{2+}]_i$ through the GPR4 receptor. Perhaps physiologically relevant concentrations of LPC *in vivo* that pertain to LPC's interactions with GPR4 will be better understood when estimates of unbound LPC concentrations in specific tissues can be reliably made. *In vivo* the molar ratio of albumin (approximately 3-5% in plasma) to LPC can theoretically be from 3- to100-fold in plasma. In extravascular sites where albumin concentration is less than in plasma, the ratio of albumin to LPC can be lower.

TDAG8, which shares approximately 38% homology with OGR1 and GPR4, has recently been shown to be a Psy receptor (15). Treatment of cultured cells expressing this receptor with Psy or structurally related glycosphingolipids results in the formation of globoid, multinuclear cells (15). We have tested the effect of Psy and related glycosphingolipids in calcium mobilization, competition of ligand binding, and MAP kinase activation assays and found no evidence that these lipids interact with GPR4. The questions of whether Psy is also a ligand for GPR4 and whether TDAG8 is a lysophospholipid receptor require further investigation.

It appears that ligands of GPR4 induced cell shape changes (Fig. 5), suggesting that SPC and LPC may affect the cellular cytoskeleton. Both LPA and S1P are able to affect cytoskeleton through Rho

(43,44). SPC and LPC are also able to activate Rho, as evidenced by C3-exoenzyme sensitivity of SRE reporter activity (Fig. 6) and cell migration (Fig. 9) induced by SPC/LPC. It remains to be determined whether the cell shape change induced by SPC/LPC is a Rho-mediated effect and which cellular proteins are involved in these processes.

Different cell lines (MCF10A, HEK293, CHO, and Swiss 3T3 cells) were used in our studies. As shown in Fig. 2, MCF10A cells expressed the lowest level of endogenous GPR4 among cell lines tested. This cell line does not respond to either SPC or LPC in calcium assays (2). Therefore, calcium assays described here were performed in these cells. Because the transfection efficiency of MCF10A cells is very low (2), we were unable to establish stably expressing lines for conducting other assays. Despite their relatively high level of GPR4 expression, HEK293 cells were chosen for the internalization and SRE reporter assays, mainly because they are human in origin, and also yielded a high transfection efficiency (Fig. 1). The internalization assays utilized transfected receptor-GFP fusion proteins and the transcriptional responses in SRE reporter assays were compared to those in parental or vector-transfected cells. Therefore, the effects of the exogenous GPR4 receptor were readily separable from those of the endogenous receptor(s). CHO cells were chosen for binding assays, because they exhibit low responses to SPC and LPC in calcium assays and are readily transfected. We detected SPC- and LPC-induced MAP kinase activation through GPR4 in Swiss 3T3, but not HEK293 and CHO cells (Fig. 7 and data not shown). Hence, Swiss 3T3 cells were chosen for MAP kinase activation and mitogenic studies. It is well known that receptor mediated signaling transduction is dependent on multiple cellular factors. The molecular basis for the differential activation of GPR4 in different cells remains to be further explored.

In summary, our results indicate that SPC is a high-affinity, and LPC a lower-affinity, ligand for GPR4. This conclusion is directly derived from the results of ligand binding assays (K_d values of 36 vs. 159 nM for SPC and 16:0-LPC, respectively). This is also supported by results from assays of different

signaling pathways activated by SPC and LPC, including increases in calcium, transcriptional activation of SRE, ERK activation, and stimulation of DNA synthesis and cell migration. In recent decades, many reports have described a significant elevation of LPC levels in cells and tissues in different diseases (32, 41, 45). Numerous lines of evidence suggest that LPC, which is a major lipid component of ox-LDL, and which accumulates in atherosclerotic lesions (11), plays pathological roles in the development of atherosclerosis and other chronic inflammatory diseases (11,12). LPC also plays other important biological roles. For example, LPC functions as a fatty acid and choline carrier and delivers fatty acids more specifically to brain than other tissues (22). The identification of GPR4 as a receptor for LPC and SPC solidifies the assignment of a new lysophospholipid receptor subfamily (OGR1, GPR4, and G2A). Further studies should address possible functional redundancy amongst these receptors and add important information to our understanding of inflammatory diseases.

Acknowledgement—We thank Dr. Bryan Williams and Dr. Guy Chisolm for their critical reading of this manuscript.

REFERENCES

1 Spiegel, S. and Milstien, S. (1995) *J Membr Biol* **146**, 225-237

2 Xu, Y., Zhu, K., Hong, G., Wu, W., Baudhuin, L. M., Xiao, Y. and Damron, D. S. (2000) *Nat Cell Biol* **2**, 261-267

3 Heiber, M., Docherty, J. M., Shah, G., Nguyen, T., Cheng, R., Heng, H. H., Marchese, A., Tsui, L. C., Shi, X. and George, S. R. (1995) *DNA & Cell Biology* **14**, 25-35

4 Mahadevan, M. S., Baird, S., Bailly, J. E., Shutler, G. G., Sabourin, L. A., Tsilfidis, C., Neville, C. E., Narang, M. and Korneluk, R. G. (1995) *Genomics* **30**, 84-88

5 Choi, J., Lee, S. and Choi, Y. (1996) *Cell Immunol* **168**, 78-84

6 Kyaw, H., Zeng, Z., Su, K., Fan, P., Shell, B., Carter, K. and Li, Y. (1998) *DNA Cell Biol.* **17**, 493-500

7 Weng, Z., Fluckiger, A. C., Nisitani, S., Wahl, M. I., Le, L. Q., Hunter, C. A., Fernal, A. A., Le Beau, M. M. and Witte, O. N. (1998) *Proc Natl Acad Sci U S A* **95**, 12334-12339.

8 Xu, Y. and Casey, G. (1996) *Genomics* **35**, 397-402

9. Kyaw, H., Zeng, Z., Su, K., Fan, P., Shell, B. K., Carter, K. C., and Li, Y. (1998) *DNA Cell Biol.* **17,** 493-500.

10. Choi, J. W., Lee, S. Y., and Choi, Y. (1996) *Cell Immunol.* **168,**:78-84.

11 Chisolm III, G. and Penn, M. (1996) Oxidized lipoproteins and atherosclerosis, Lippincott-Raven Publishers, Philadelphia

12 Yokota, T. and Hansson, G. (1995) *J Intern Med* **238**, 479-489

13 Murugesan, G. and Fox, P. L. (1996) *Journal of Clinical Investigation* **97**, 2736-2744

14 Kabarowski JHS, Zhu K, Le LQ, Witte ON, **Xu Y.** (2001). *Science* **293,** 702-705

15 *Im* DS, Heise CE, Nguyen T, O'Dowd BF, Lynch KR. (2001) *J Cell Biol.* **153,** 429-3413

16 Kabarowski, JHS, Feramisco, J. D., Le, L. Q., Gu, J. L., Luoh, S. W., Simon, M. I., and Witte, O. N. (2000) *Proc Natl Acad Sci U S A.* **97,** 12109-12114.

17 Grynkiewicz, G., Poenie, M. and Tsien, R. Y. (1985) *J Biol Chem* **260**, 3440-3450

18 An, S., Tsai, C. and Goetzl, E. J. (1995) *FEBS Letters* **375**, 121-124

19 Ogita, T., Tanaka, Y., Nakaoka, T, Matsuoka, R., Kira, Y., Nakamura, M., Shimizu, T. and Fujita, T. (1997) *Am J Physiol* **272**, H17-24.

20 Gomez-Munoz, A., O'Brien, L., Hundal, R. and Steinbrecher, U. P. (1999) *Journal of Lipid Research* **40**, 988-993

21 Huang, Y. H., Schafer-Elinder, L., Wu, R., Claesson, H. E. and Frostegard, J. (1999) *Clinical & Experimental Immunology* **116**, 326-331

22 Croset, M., Brossard, N., Polette, A. and Lagarde, M. (2000) *Biochem J* **345**, 61-67.

23 Carson, M. J.and Lo, D. (2001) *Science* **293**, 618-619.

24 Mukherjee, S., Ghosh, R. N. and Maxfield, F. R. (1997) *Physiol Rev* **77**, 759-803

25 Bohm, S. K., Grady, E. F. and Bunnett, N. W. (1997) *Biochem J* **322**, 1-18

26 Ferguson, S. S., Barak, L. S., Zhang, J. and Caron, M. G. (1996) *Canadian Journal of Physiology & Pharmacology* **74**, 1095-1110

27 An, S., Bleu, T., Hallmark, O. G. and Goetzl, E. J. (1998) *J Biol Chem* **273**, 7906-7910

28 An, S., Bleu, T. and Zheng, Y. (1999) *Mol Pharmacol* **55**, 787-794

29 Desai, N. N., Carlson, R. O., Mattie, M. E., Olivera, A., Buckley, N. E., Seki, T., Brooker, G. and Spiegel, S. (1993) *J Cell Biol* **121**, 1385-1395

30 Lusis, A. J. (2000) Nature **407**, 233-41.

31 Chisolm, G. M., 3rd and Chai, Y. (2000) *Free Radic Biol Med* **28**, 1697-1707.

32 Prokazova, N. V., Zvezdina, N. D. and Korotaeva, A. A. (1998) *Biochemistry (Moscow)* **63**, 31-37

33 Kohno, M., Yokokawa, K., Yasunari, K., Minami, M., Kano, H., Hanehira, T. and Yoshikawa, J. (1998) *Circulation* **98**, 353-359.

34 McMurray, H. F., Parthasarathy, S., and Steinberg, D. (1993), *J Clin Invest*. **92,** 1004-1008

35 Jalink, K., van Corven, E. J. and Moolenaar, W. H. (1990) *J Biol Chem* **265**, 12232-12239

36 Okajima, F., Sato, K., Tomura, H., Kuwabara, A., Nochi, H., Tamoto, K., Kondo, Y., Tokumitsu, Y. and Ui, M. (1998) *Biochemical Journal* **336**, 491-500

37 Hirayama, T., Ogawa, Y., Tobise, K. and Kikuchi, K. (1998) *Hypertension Research* **21**, 137-145

38 Ogita, T., Tanaka, Y., Nakaoka, T., Matsuoka, R., Kira, Y., Nakamura, M., Shimizu, T. and Fujita, T. (1997) *American Journal of Physiology* **272**, H17-24

39. Weng, Z., Fluckiger, A. C., Nisitani, S., Wahl, M. I., Le, L. Q., Hunter, C. A., Fernal, A. A., Le Beau, M. M., and Witte, O. N. (1998) *Proc Natl Acad Sci U S A,* **95**, 12334-12339

40 Sasagawa, T., Suzuki, K., Shiota, T., Kondo, T. and Okita, M. (1998*) Journal of Nutritional Science & Vitaminology* **44**, 809-818

41 Okita, M., Gaudette, D. C., Mills, G. B. and Holub, B. J. (1997) *Int J Cancer* **71**, 31-34

42 Mochizuki M, Zigler JS Jr, Russell P, Gery I. (1982-1983) *Curr Eye Res.* **2,** 621-624.

43 Goetzl, E. J. & An, S. (1998) *FASEB J* **12**, 1589-1598.

44 Moolenaar, W. H. (1999) *Exp Cell Res* **253**, 230-238.

45 Murphy, A. A., Santanam, N., Morales, A. J. and Parthasarathy, S. (1998) *J Clin Endocrinol Metab* **83**, 2110-2113

FIGURE LEGENDS

Fig 1. **GPR4 expression in different human tissues.** The human RNA Master Blot (Clontech) was probed with ^{32}P-labeled GPR4 (Experimental Procedures).

Fig. 2. **Expression of GPR4 in human cell lines.** Real-time Quantitative PCR was utilized to determine relative expression levels of GPR4 expressed in cells, as described in "Materials and Methods". All PCR reactions were performed in triplicate. The comparative C_T method was used to calculate the relative expression levels of GPR4 in different cell lines as described in Experimental procedures. HEY, OCC1, NIH:Ovca3. SKOV3, Ovca429, Ovca432, and Ovca433 are ovarian cancer cells. MCF7 is a breast cancer cell line. MCF10A is an immortalized breast cell line. HeLa is a cervical cell line. All cell lines shown, except Swiss 3T3, are human cell lines.

Fig. 3. **SPC- and LPC- induce transient increases in $[Ca^{2+}]_i$ in GPR4-transfected MCF10A cells.** ***A,*** upper panel: the effect of SPC (1 μM), 16:0-LPC (1 μM), 18:1-LPA (1μM), 16:0-PAF (0.1 μM), and ATP (20 μM) on $[Ca^{2+}]_i$ in pEGFP-N1-transfected MCF10A cells. The 2nd to the 4th panels: MCF10A cells were transiently transfected with pGPR4-GFP, and treated with SPC, L- and D-SPC, LPC, LPA, PAF, or ATP. ***B,*** SPC and 16:0-LPC concentration response curves in pEGFP-GPR4-transfected MCF10A cells. ***C,*** The effect of BN52021 on increased $[Ca^{2+}]_i$ induced by agonists. ***D,*** The effect of WEB-2086 on increased $[Ca^{2+}]_i$ induced by agonists. ***E,*** Homologous and heterologous desensitization of GPR4 by SPC and 16:0-LPC. ***F,*** The sensitivity of SPC- and 16:0-LPC-induced calcium increases to PTX pretreatment. ***G,*** The effect of BSA (0.5%) on the ability of SPC and LPC to induce an increase in $[Ca^{2+}]_i$. SPC (1μM) and LPC(1μM) were incubated with 0.5% fatty acid-free BSA for 30 min at room

temperature and the mixtures were used to stimulate MCF10A cells transfected with pGPR4-GFP. ***H,*** Gal-Cer (1 μM)-stimulated increase in $[Ca^{2+}]_i$ in parental and pGPR4-GFP expressing MCF10A cells. All calcium measurements were performed in EGTA-containing, calcium-free buffer. The data are representative of at least five independent experiments.

Fig. 4. **Binding of SPC and 16:0-LPC to GPR4.** ***A*** **and** ***B,*** **Time** dependence of specific [^{3}H] SPC and [^{3}H] LPC binding. Cell homogenates (100 μL, equivalent to 10^5 cells) from vector- or GPR4 stably-transfected CHO cells were incubated with [^{3}H] SPC (1 nM) or [^{3}H] 16:0-LPC (1 nM) for the indicated times. Specific binding is shown. ***C*** **and** ***D***, Saturation isotherm of specific binding of [^{3}H]SPC and [^{3}H]16:0-LPC to GPR4-transfected CHO cells. Cell homogenates (100 μL) were incubated with the indicated concentrations of [^{3}H] SPC or [^{3}H] 16:0-LPC in the presence or absence of unlabeled SPC (100-fold excess) or unlabeled 16:0-LPC (100-fold excess). Specific binding is presented. ***E*** **and** ***F,*** Structural specificity of binding of [^{3}H] SPC and [^{3}H]16:0-LPC to GPR4. GPR4-transfected CHO cells were incubated with [^{3}H] SPC (1 nM), or [^{3}H]16:0-LPC (1 nM) in the presence or absence of 100 nM of different unlabeled lipids. Total binding is presented. All binding experiments were performed in triplicate in 96-well plates. Data are means ± SD from three independent experiments. *, $p < 0.05$; **, $p < 0.01$; ***, $p < 0.001$; as compared to the control (Student's *t* test).

Fig. 5. **Internalization of GPR4 induced by SPC and LPC.** ***A***, HEK293 cells stably expressing pGPR4-GFP. ***B***, pGPR4-GFP stably expressing cells was treated with SPC (1 μM) at 37°C for 2h. ***C***, pGPR4-GFP-expressing cells were treated with 16:0-LPC (1 μM) at 37°C for 2 h. ***D*** and ***E***, as in *B*, and *C*, except cells were pretreated with BN52021 (200 μM) for 5 min. ***F***, pGPR4-GFP-expressing cells were

treated with PAF (1 μM). All experiments were repeated at least three times. Representative data are shown.

Fig. 6. **SPC and LPC activate SRE in a GPR4-dependent manner.** ***A***, The SRE-luciferase responses to different lipids in vector- and GPR4-transfected HEK293 cells. 18:1-LPA, 16:0-LPC, SPC, S1P, 18:0-SM, 16:0-PAF, and 16:0-lyso-PAF (1 μM of each) were used. The experiments were conducted as described in Experimental Procedures and Methods. ***B***, Concentration-dependent SRE-luciferase activity induced by SPC and 16:0-LPC in vector- and GPR4-transfected cells. ***C***, Inhibition of SPC- and 16:0-LPC-induced SRE activity by PTX and C3 exoenzyme. All experiments were performed in quadruplicate and were repeated at least three times. Representative data are shown. Cont.: control; *, $p < 0.05$; **, $p < 0.001$; as compared to the control. #, $p<0.001$ when compared to SPC- or 16:0-LPC-induced activity in vector-transfected cells. The Student's *t* test was performed using the GraphPad Instat software (San Diego, CA). $p < 0.05$ was considered to be statistically significant.

Fig. 7. **Activation of ERK MAP kinase by SPC and LPC in GFP-, and GPR4-ires-GFP-expressing Swiss 3T3 cells.** ERK MAP kinase assays were performed as described in Experimental Procedures. ***A***, Structural specificity of lipid-induced ERK activation via GPR4 in Swiss 3T3 cells. Cells were treated with 1 μM Psy, Gal-Sph, Lac-Cer), sphingosine-1-phosphate (S1P), 16:0-LPC, SPC and 16:0-PAF for 5 min. ***B***, Concentration-dependence of ERK activation stimulated by SPC and 16:0-LPC. Cells were treated with 1, 10, 100 and 1000 nM of 16:0-LPC or SPC for 5 min. ***C***, Time-dependence of ERK activation stimulated by SPC and 16:0-LPC. Cells were treated with SPC (100 nM) or LPC (100 nM) for the indicated time. ***D***, GPR4-ires-GFP-, and OGR1-ires-GFP-Swiss 3T3 cells were untreated or treated with

16:0-LPC (100 nM) or SPC (100 nM) for 5 min in the absence or presence of PTX (100 ng/ml, 16 h pre-treatment.

Fig. 8. **DNA synthesis stimulated by SPC and 16:0-LPC in GPR4-overexpressing cells.** DNA synthesis was measured by [^{3}H] thymidine incorporation as described in Experimental Procedures in both GFP- and GPR4-ires-GFP-Swiss 3T3 cells. PTX was added to selected groups at 100 ng/ml for 16 h prior to lipid treatment. The data shown represent the means ± SD from three independent experiments.

Fig. 9. **SPC and LPC stimulate cell migration in GPR4-overexpressing Swiss 3T3 cells.** Cell migration was measured in a modified Boyden chamber assay as described in Experimental Procedures. The cell numbers on the lower faces of the membranes were determined and are presented as the means ± SD of three independent experiments. **, $p < 0.01$; ***, $p < 0.001$, compared to the control. Student's *t* test was performed using the GraphPad Instat software (San Diego, CA). $p < 0.05$ was considered to be statistically significant.

whole brain	amyg-dala	caudate nucleus	cere-bellum	cerebral cortex	frontal lobe	hippo-campus	medulla oblongata
occipital lobe	putamen	substan-tial nigra	temporal lobe	thala-mus	sub-thalamic nucleus	spinal cord	
heart	aorta	skeletal muscle	colon	bladder	uterus	prostate	stomach
testis	ovary	pan-creas	pituitary gland	adrenal gland	thyroid gland	salivary gland	mam-mary gland
kidney	liver	small intestine	spleen	thymus	peri-pheral leukocyte	lymph node	bone marrow
appendix	lung	trachea	placenta				
fetal brain	fetal heart	fetal kidney	fetal liver	fetal spleen	fetal thymus	fetal lung	
yeast total RNA 100 ng	yeast tRNA 100 ng	*E. coli* rRNA 100 ng	*E. coli* DNA 100 ng	Poly r(A) 100ng	human $C_o t1$ DNA 100ng	human DNA 100ng	human DNA 500ng

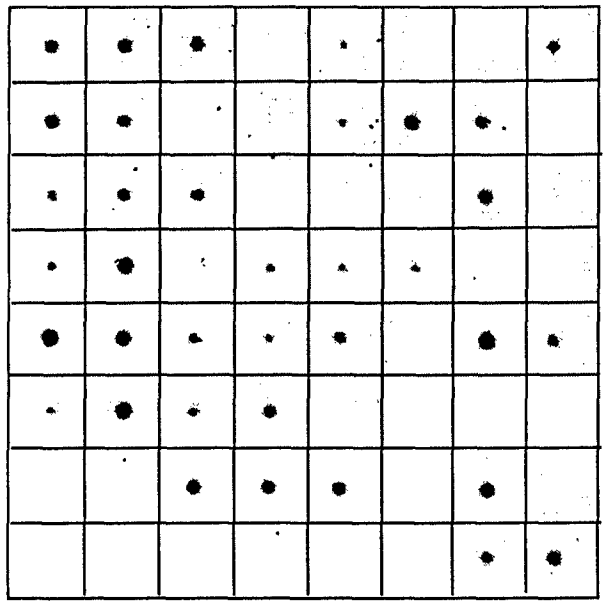

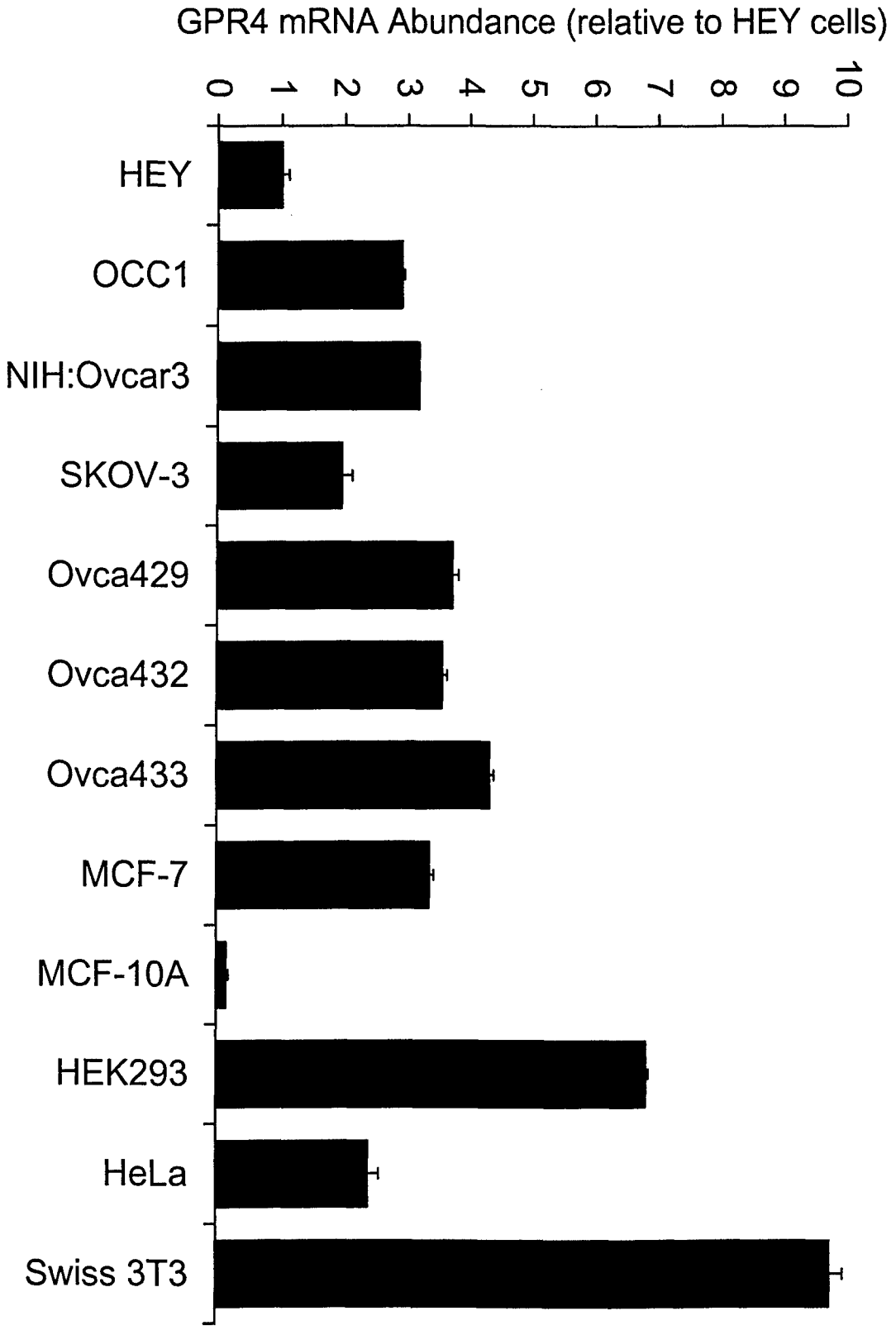
GPR4 mRNA Abundance (relative to HEY cells)
0
1
2
3
4
5
6
7
8
6
10
HEY
OCC1
NIH:Ovcar3
SKOV-3
Ovca429
Ovca432
Ovca433
MCF-7
MCF-10A
HEK293
HeLa
Swiss 3T3

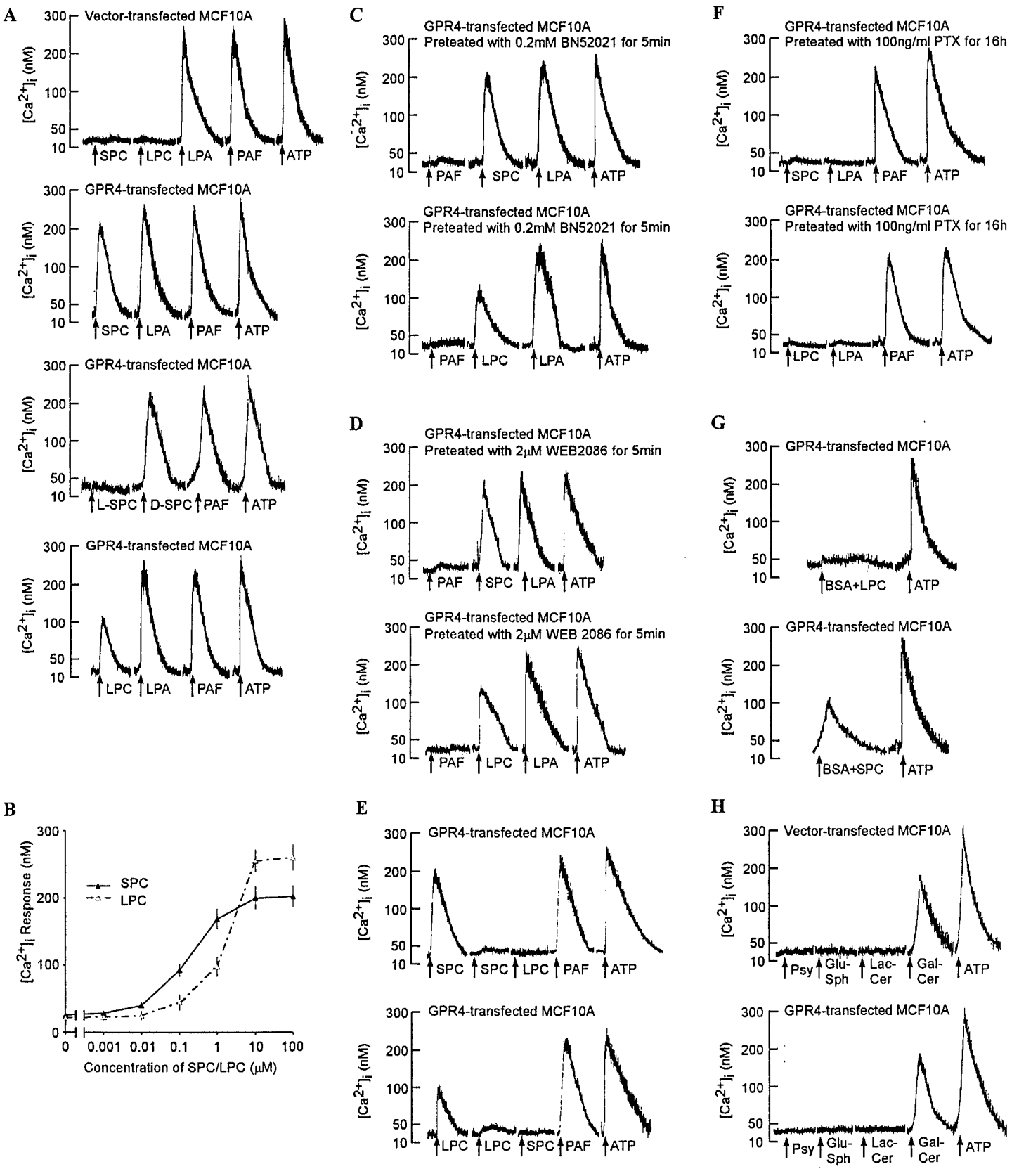
A
Vector-transfected MCF10A
SPC LPC LPA PAF ATP
GPR4-transfected MCF10A
SPC LPA PAF ATP
GPR4-transfected MCF10A
L-SPC D-SPC PAF ATP
GPR4-transfected MCF10A
LPC LPA PAF ATP
B
SPC
LPC
Concentration of SPC/LPC (μM)
C
GPR4-transfected MCF10A
Preteated with 0.2mM BN52021 for 5min
PAF SPC LPA ATP
GPR4-transfected MCF10A
Preteated with 0.2mM BN52021 for 5min
PAF LPC LPA ATP
D
GPR4-transfected MCF10A
Preteated with 2μM WEB2086 for 5min
PAF SPC LPA ATP
GPR4-transfected MCF10A
Preteated with 2μM WEB 2086 for 5min
PAF LPC LPA ATP
E
GPR4-transfected MCF10A
SPC SPC LPC PAF ATP
GPR4-transfected MCF10A
LPC LPC SPC PAF ATP
F
GPR4-transfected MCF10A
Preteated with 100ng/ml PTX for 16h
SPC LPA PAF ATP
GPR4-transfected MCF10A
Preteated with 100ng/ml PTX for 16h
LPC LPA PAF ATP
G
GPR4-transfected MCF10A
BSA+LPC ATP
GPR4-transfected MCF10A
BSA+SPC ATP
H
Vector-transfected MCF10A
Psy Glu-Sph Lac-Cer Gal-Cer ATP
GPR4-transfected MCF10A
Psy Glu-Sph Lac-Cer Gal-Cer ATP

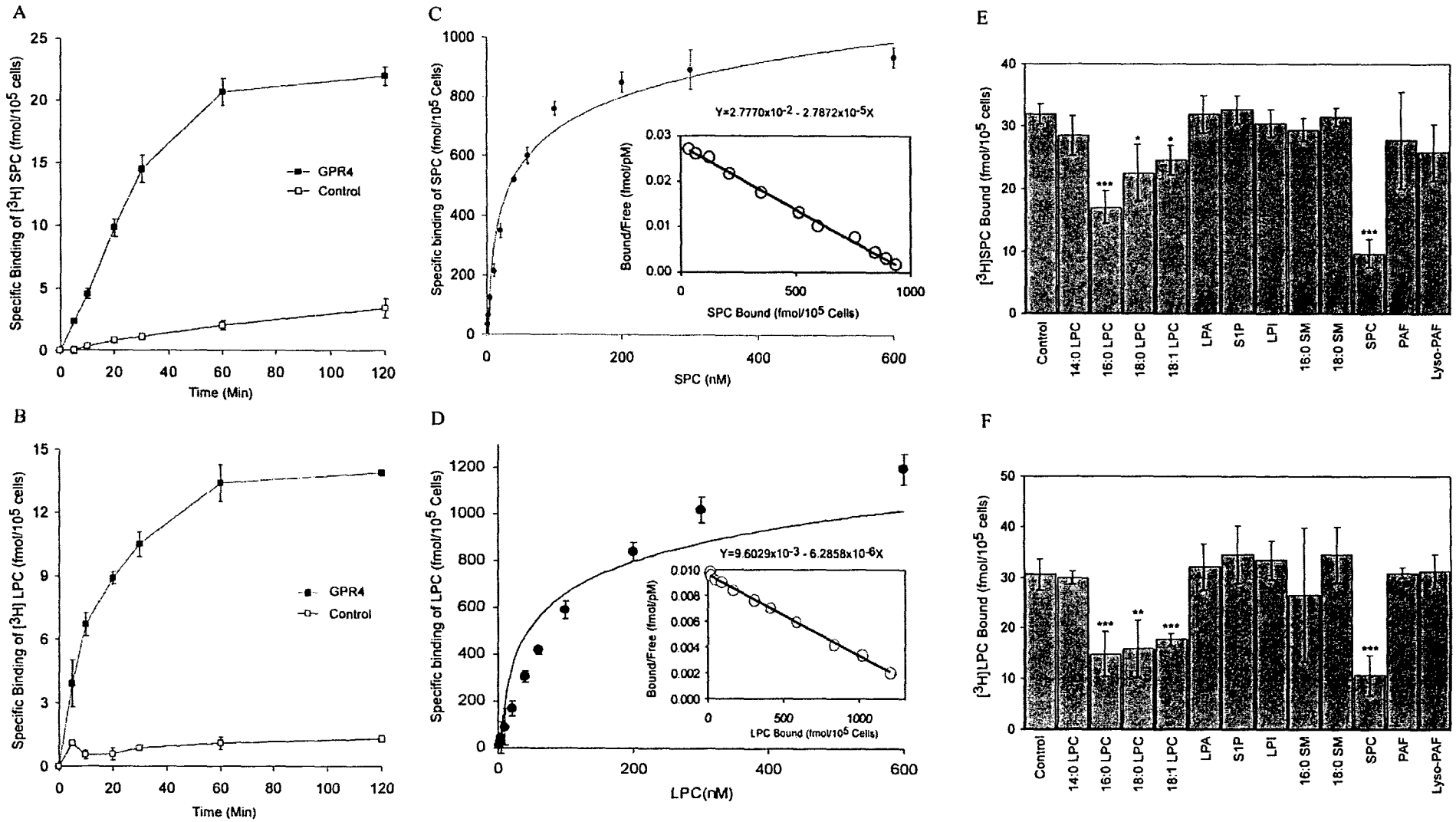
A
Specific Binding of [3H] SPC (fmol/10^5 cells)
Time (Min)
GPR4
Control
B
Specific Binding of [3H] LPC (fmol/10^5 cells)
Time (Min)
GPR4
Control
C
Specific binding of SPC (fmol/10^5 Cells)
SPC (nM)
Y=2.7770x10^-2 - 2.7872x10^-5X
Bound/Free (fmol/pM)
SPC Bound (fmol/10^5 Cells)
D
Specific binding of LPC (fmol/10^5 Cells)
LPC(nM)
Y=9.6029x10^-3 - 6.2858x10^-6X
Bound/Free (fmol/pM)
LPC Bound (fmol/10^5 Cells)
E
[3H]SPC Bound (fmol/10^5 cells)
Control
14:0 LPC
16:0 LPC
18:0 LPC
18:1 LPC
LPA
S1P
LPI
16:0 SM
18:0 SM
SPC
PAF
Lyso-PAF
F
[3H]LPC Bound (fmol/10^5 cells)
Control
14:0 LPC
16:0 LPC
18:0 LPC
18:1 LPC
LPA
S1P
LPI
16:0 SM
18:0 SM
SPC
PAF
Lyso-PAF

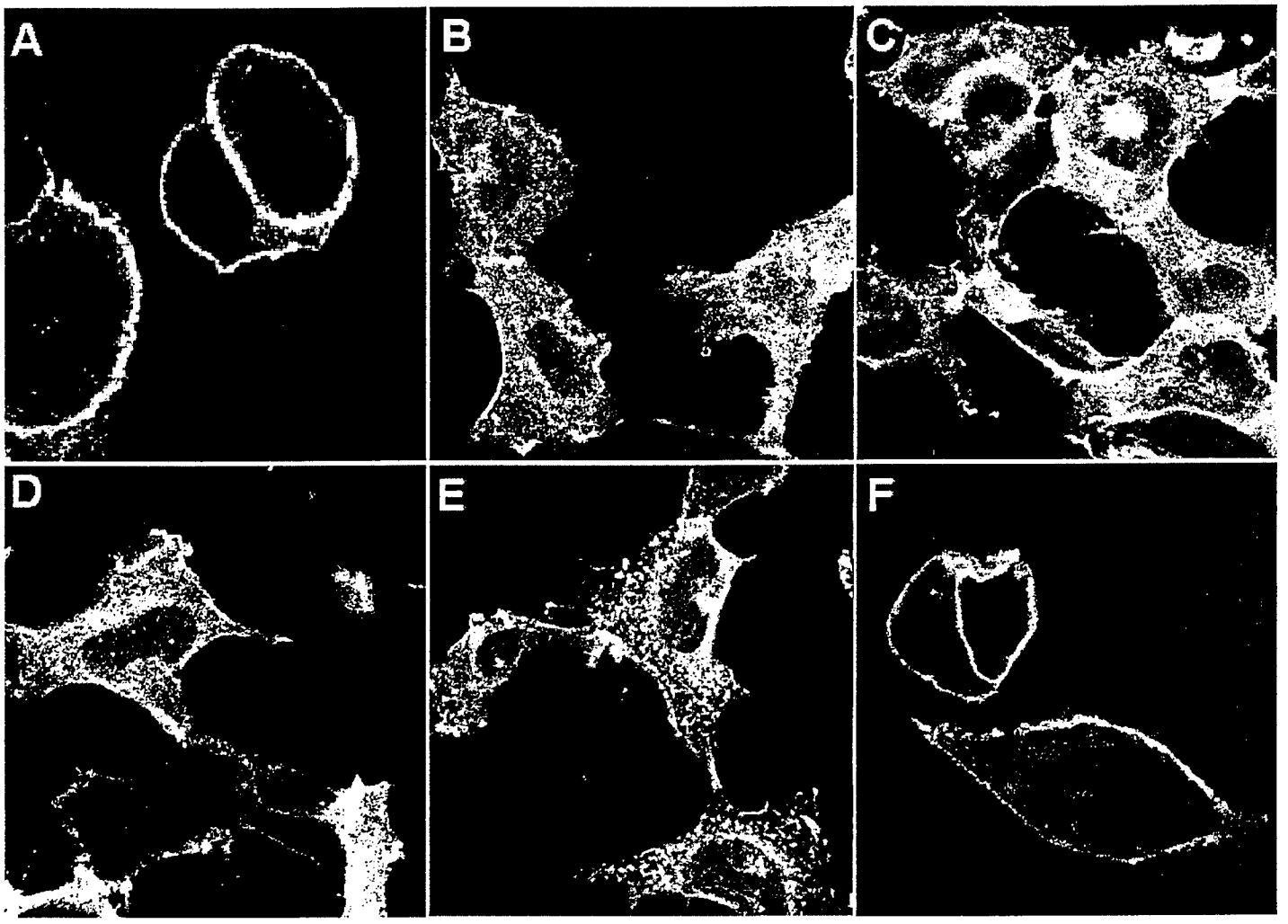
A
B
C
D
E
F

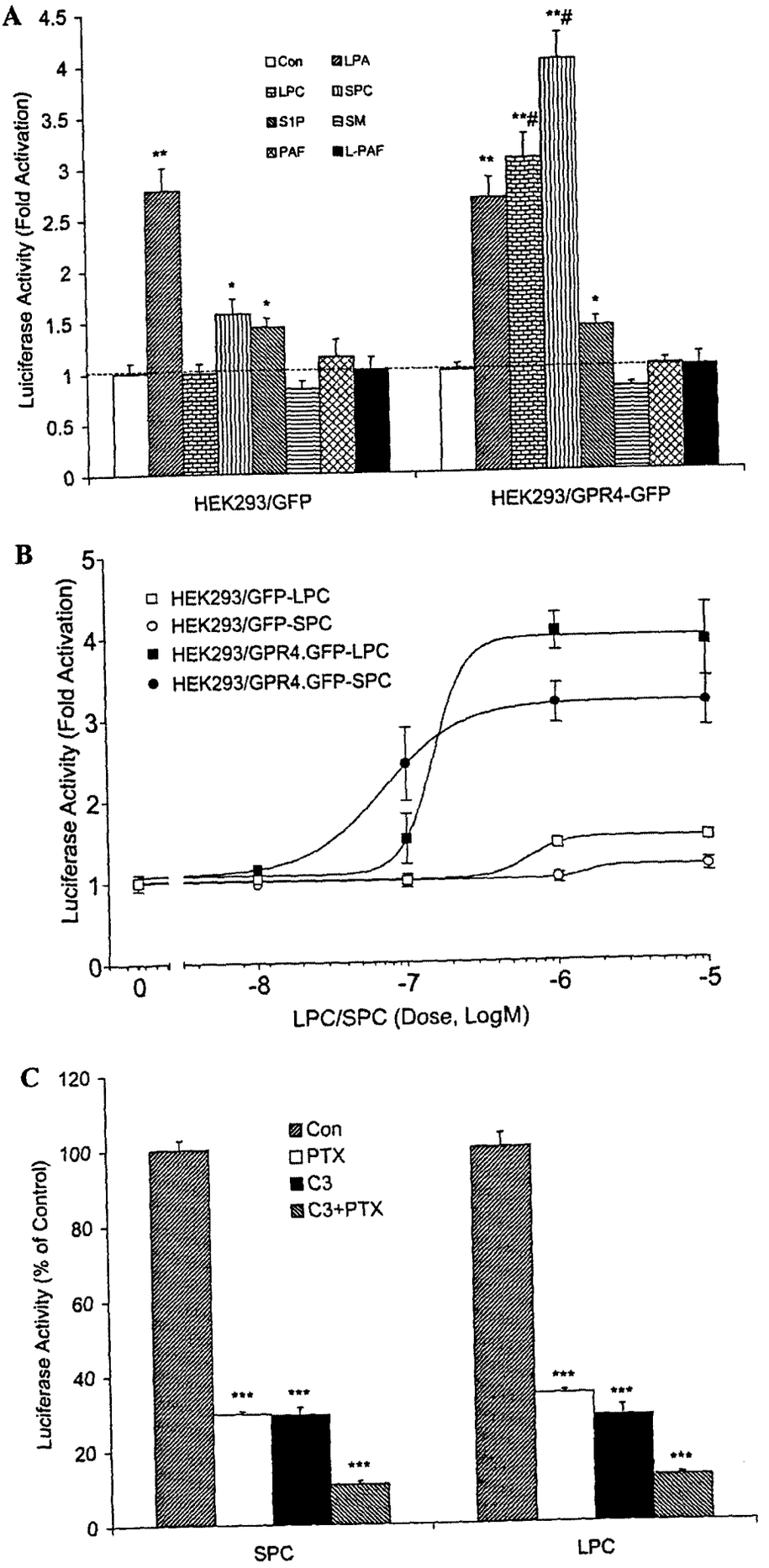
A
Luciferase Activity (Fold Activation)
Con
LPA
LPC
SPC
S1P
SM
PAF
L-PAF
HEK293/GFP
HEK293/GPR4-GFP
B
Luciferase Activity (Fold Activation)
HEK293/GFP-LPC
HEK293/GFP-SPC
HEK293/GPR4.GFP-LPC
HEK293/GPR4.GFP-SPC
LPC/SPC (Dose, LogM)
C
Luciferase Activity (% of Control)
Con
PTX
C3
C3+PTX
SPC
LPC

A

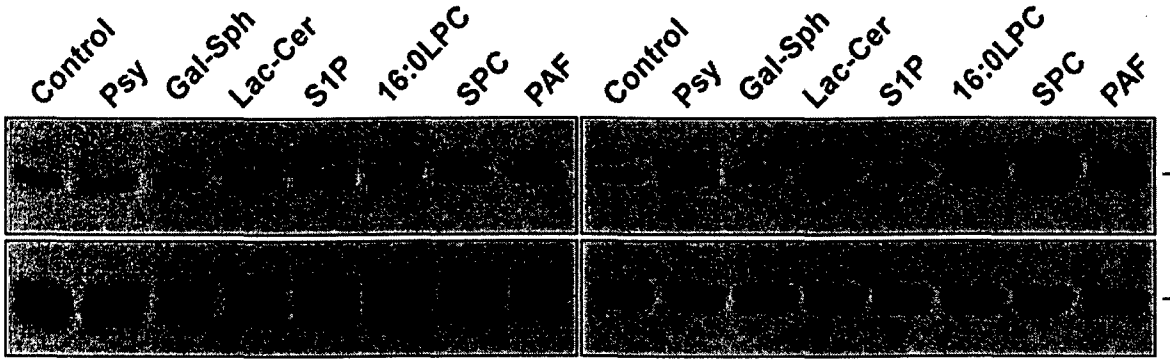

Swiss 3T3 GFP Swiss 3T3 GPR4 ires GFP

B

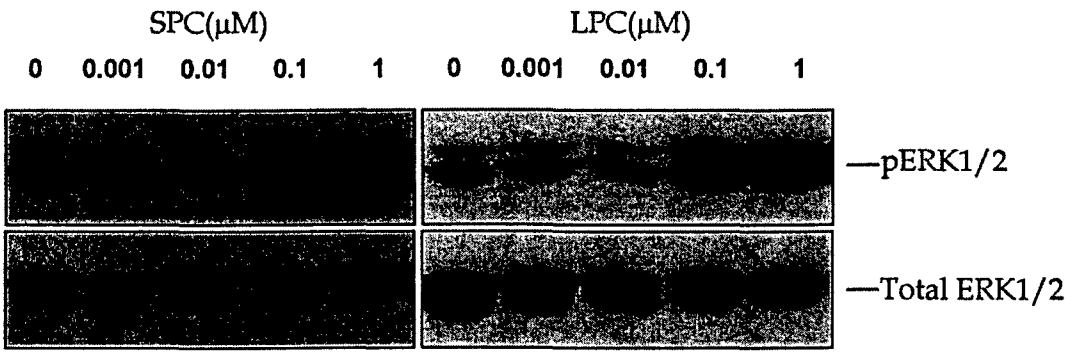

C

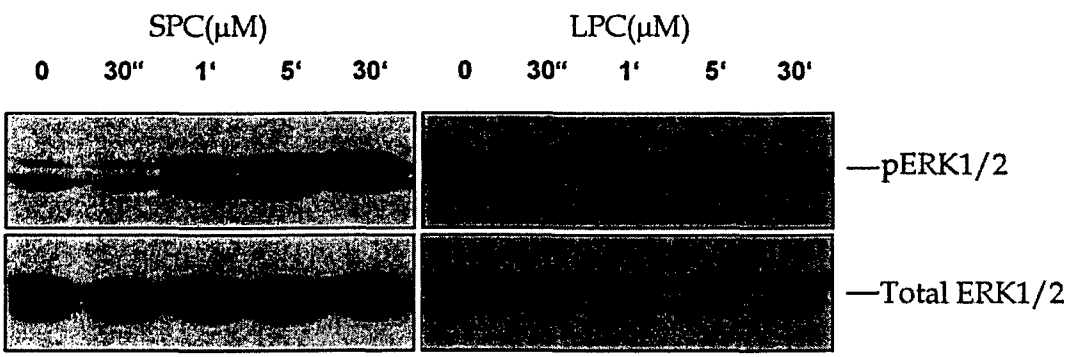

D

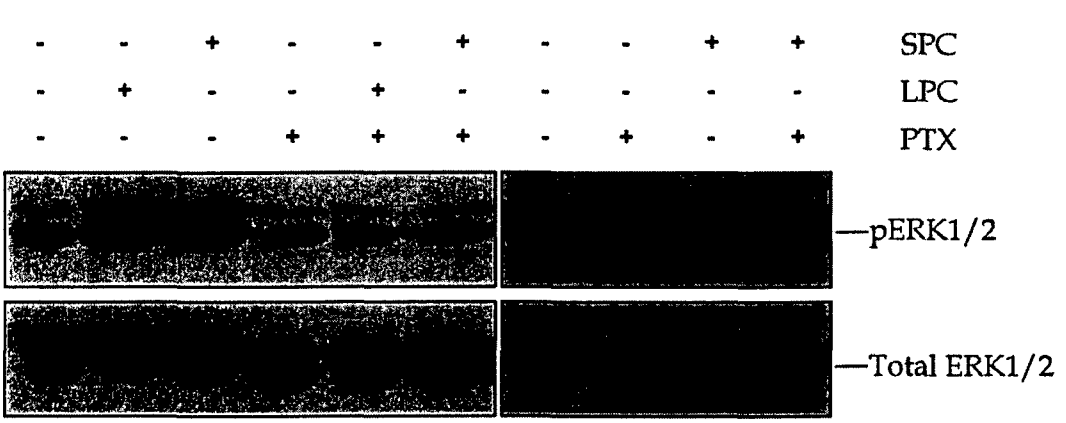

Swiss 3T3 GPR4 ires GFP Swiss 3T3 OGR1 ires GFP

The Role of Ether-linked Lysophosphatidic Acids in Ovarian Cancer Cells[1]

Jun Lu, Yi-jin Xiao, Linnea M. Baudhuin, Guiying Hong, and Yan Xu[2]

Department of Cancer Biology, Lerner Research Institute, Cleveland Clinic Foundation, 9500 Euclid Ave., Cleveland, OH 44195 [J. L., Y-J. X., L. M. B., G. H., and Y. X.]; Department of Gynecology and Obstetrics, Cleveland Clinic Foundation, 9500 Euclid Ave., Cleveland, OH 44195 [Y. X.]; Department of Chemistry, Cleveland State University, 24th and Euclid Ave., Cleveland, OH 44115 [L. M. B., Y. X.]

Running Title: Ether-linked LPAs in ovarian cancer cells

Key Words: Akt, MAP kinase, alkyl-lysophosphatidic acid (alkyl-LPA), alkenyl-LPA, and ovarian cancer

---

[1] This work is supported in part by American Cancer Society Grant RPG-99-062-01-CNE, US Army Medical Research grant DAMD17-99-1-9563, and NIH grant R21 CA84038-01 (to Y.X.)

[2] To whom requests for reprints should be addressed, at Department of Cancer Biology, Cleveland Clinic Foundation, 9500 Euclid Ave., Cleveland, OH 44195. Phone: (216) 444-1168; Fax (216) 445-6269; E-mail: xuy@ccf.org

Abstract

Naturally occurring alkyl- and alkenyl-lysophosphatidic acids (al-LPAs[3]) are detected and elevated in ovarian cancer ascites, compared with ascites from non-malignant diseases. We describe here that these ether-linked LPAs may play an important role in ovarian cancer development. They are elevated and stable in ovarian cancer ascites, which represents an *in vivo* environment for ovarian cancer cells. They stimulated DNA synthesis and proliferation of ovarian cancer cells. In addition, they induced cell migration and the secretion of a pro-angiogenic factor, interleukin-8 (IL-8), in ovarian cancer cells. The latter two processes are potentially related to tumor metastasis and angiogenesis, respectively. Al-LPAs induced diverse signaling pathways in ovarian cancer cells. Their mitogenic activity depended on the activation of the $G_{i/o}$ protein, phosphatidylinositol-3 kinase (PI3K), and mitogen-activated protein (MAP) kinase kinase (MEK), but not p38 MAP kinase. The S473 phosphorylation of Akt by these lipids required activation of the $G_{i/o}$ protein, PI3K, MEK, p38 MAP kinase, and Rho. On the other hand, cell migration induced by al-LPAs depended on activities of the $G_{i/o}$ protein, PI3K, and Rho, but not MEK.

---

[3] The abbreviations used are: Akt, protein kinase B; al-LPAs, alkyl- and alkenyl-lysophosphatidic acids; Edg, endothelial differentiation genes; ECL, enhanced chemiluminescence; ELISA, enzyme-linked immunosorbent assay; ERK, extracellular mitogen-regulated kinase; ESI-MS, electrospray ionization mass spectormetry; FBS, fetal bovine serum; GPCR, G protein-coupled receptor; IL-8, interleukin-8; LPA, lysophosphatidic acid; MAP kinase, mitogen-activated protein kinase; MEK or MKK, MAP kinase kinase; MS/MS, tandem mass spectrometry; MRM, multiple reaction monitoring; MTT, 3-(4,5-dimethylthiazol-2-yl)-2,5-diphenyltetrazolium bromide; OCAF, ovarian cancer activating factor; PI3K, phosphatidylinositol 3-kinase; PLC, phospholipase C; PLD, phospholipase D; PKC, protein kinase C; PTX, pertussis toxin; S1P, sphingosine-1-phosphate; TLC, thin layer chromatography.

INTRODUCTION

Lysophosphatidic acid (LPA) is a bioactive lysolipid that is involved in a broad range of biological processes in a variety of cellular systems (1, 2). LPA induces cell proliferation or differentiation, prevents apoptosis induced by stress or stimuli, induces platelet aggregation and smooth muscle contraction, and stimulates cell morphologic changes, cell adhesion, and cell migration (1-5). LPA has been shown to be involved in angiogenesis, wound healing, and inflammatory processes (6-15). LPA exerts many of its effects by binding to G protein-coupled receptors (GPCRs), resulting in a cascade of intracellular signaling activations (2, 16). Three endothelial differentiation genes (Edg2, 4 and 7) have been identified as receptors for LPA (17) (7, 18, 19). LPA stimulates G_i-mediated extracellular mitogen-regulated kinase (ERK) and PI3K/Akt activation, G_q-mediated phospholipase C (PLC) and protein kinase C (PKC) activation, and $G_{12/13}$-mediated Rho activation (1, 2).

We have previously identified a growth-stimulating factor, ovarian cancer activating factor (OCAF), in ascites from patients with ovarian cancer. OCAF is composed of various species of LPAs (with different fatty acid side chains) (20). OCAF and synthetic 18:1-acyl-LPA stimulate growth of ovarian, breast and Jurkat cells (21, 22). Acyl-LPA (18:1) also regulates other cellular activities. It enhances cell adhesion/attachment (23), stimulates interleukin-8 (IL-8) production from ovarian cancer cells (24), and synergizes with other agents, such as thrombin agonists, noradrenaline, ADP and arachidonic acid, to induce strong platelet aggregation (5). LPA has been shown to decrease cis-diamminedichloroplatinum-induced cell death (25), prevent cell apoptosis (26), and induce urokinase secretion (27) and vascular endothelial growth factor expression in human ovarian cancer cells (15). In addition, we have shown that acyl-LPAs are

elevated in plasma from patients with ovarian cancer and may represent a useful marker for the early detection of ovarian cancer (28).

There are three subclasses of LPA: acyl-, alkyl-, and alkenyl-LPAs. The latter two subclasses of LPAs (al-LPAs) differ from acyl-LPA in that the fatty acid chain is linked to the glycerol backbone through an ether or a vinyl, rather than an ester bond in acyl-LPAs. The majority of research work on LPA has been performed on acyl-LPAs (19, 29), although the effect of synthetic alkyl-LPA on platelet aggregation was reported decades ago (30). Most alkyl-LPA work was performed using synthetic alkyl-LPA (30, 31), and the naturally occurring al-LPAs have only been reported in recent years (12, 32-34).

We have recently developed an electrospray mass spectrometry (ESI-MS)-based method to analyze lysolipids in body fluids (35) and found that, in addition to acyl-LPAs, ascites from patients with ovarian cancer contain elevated alkyl- and alkenyl-LPAs (al-LPAs; including 16:0-/18:0-alkyl-LPA and 16:0/18:0-alkenyl-LPA), when compared with ascites from patients with benign diseases and endometrial cancer (35). These results implicate that al-LPAs may have potential pathophysiological roles in ovarian cancer.

In the present study, we describe that al-LPAs were more stable than acyl-LPAs in ascites. These lipids stimulated DNA synthesis and proliferation of ovarian cancer cells through G_i-, PI3K- and MEK-dependent pathways. Al-LPAs and acyl-LPAs induced migration of ovarian cancer cells through collagen I-coated membranes and this activity required the activation of G_i, and was partially dependent on PI3K activity. In addition, al-LPAs stimulated IL-8 production. Similar to acyl-LPAs as we reported recently (36), al-LPAs activated Akt kinase and induced a Rho-, PI3K-, and MEK-dependent S473 phosphorylation of Akt.

MATERIALS AND METHODS

Chemicals. LPAs (16:0, 18:0, and 18:1), lyso-platelet activating factor (lyso-PAF) and other lysophospholipids were purchased from Avanti Polar Lipids (Birmingham, AL). Lyso-plasmalogen phosphatidylethanolamine (alkenyl-LPE) was obtained from Matreya, Inc. (Pleasant Cap, PA). LY294002, PD98059, and SB203580 were obtained from Biomol (Plymouth Meeting, PA). Wortmannin was obtained from Sigma (St. Louis, MO). Pertussis toxin (PTX) was purchased from Life Technologies, Inc. (Rockville, MD). Pre-coated silica gel 60 TLC plates were obtained from EM Science (Gibbstown, NJ). HPLC grade methanol (MeOH), chloroform, ammonium hydroxide, and hydrochloric acid (HCl) were purchased from Sigma (St. Louis, MO) or Fisher Scientific (Pittsburgh, PA). [^{3}H]thymidine was from NEN Life Science Products, Inc. (Boston, MA). Anti-phospho-S473-Akt, anti-Akt, anti-phospho-ERK, and anti-ERK were obtained from Cell Signaling Technology (Beverly, MA). Anti-MEK2 and anti-p38 were from StressGen (Victoria, BC, Canada).

Cell lines and cell culture. HEY and SKOV3 cells were from Dr. G. Mills (M.D. Anderson) and ATCC, respectively, and maintained in RPMI 1640 medium containing 10% fetal bovine serum (FBS) at 37°C with 5% CO_2. All cells were cultured in serum-free media for 18-24 h prior to lipid treatment except in the cell migration experiments. For transient transfections, cells were plated into 35-mm dishes and transfected with DNA using LipofectAMINE (Life Technologies, Inc.) and Transfection Booster Reagents (Gene Therapy Systems, San Diego, CA) according to the manufacturers' instructions. Dominant negative MEK was from Dr. D. Templeton, Case Western University. Kinase inactive p38 was from Dr. Bryan R.G. Williams, Cleveland Clinic Foundation. The C3-exoenzyme construct was provided by Dr. Alan Wolfman,

Cleveland Clinic Foundation. Dominant negative Akt was from Dr. Kumliang Guom, University of Michigan.

Nonradioactive immunoprecipitation Akt kinase assay. The Akt kinase assay was performed with the Nonradioactive Akt Kinase Assay Kit (Cell Signaling Technology, Beverly, MA) according to the manufacturer's instructions. All reagents were provided with the kit. Briefly, cells were treated with al-LPAs, rinsed with ice-cold phosphate-buffered saline, and then lysed in cell lysis buffer. Immunoprecipitation was carried out using immobilized Akt 1G1 monoclonal antibody. The immunoprecipitate was then incubated with GSK-3 fusion protein and ATP in kinase buffer. Western analysis was used to determine the extent of GSK-3 phosphorylation by active Akt using a phospho-GSK-3 α/β (Ser21/9) antibody.

Extraction and quantitation of alkyl- and alkenyl-LPAs from ascites. Extraction of alkyl- and alkenyl-LPAs from ascites was performed as described previously (35, 37). The stability of different LPA species was tested. Briefly, ascites samples were stored at 4°C for different time periods and lipids in ascites were extracted with chloroform and methanol in the presence of HCl. The chloroform phase was dried and lipids were separated on thin layer chromatographic (TLC) plates. Different LPA species were eluted from TLC plates with a mixture of methanol and chloroform (2:1). ESI-MS and tandem mass spectrometry (MS/MS) analyses for the quantitation of alkyl- and alkenyl-LPAs were performed using a Micromass Quattro II Triple Quadrupole Mass Spectrometer. All quantitative analyses were performed in the multiple reaction monitoring (MRM) mode as described previously (35).

Preparation of alkyl- and alkenyl-LPAs. Alkyl- and alkenyl-LPAs were prepared through hydrolysis of the corresponding lyso-PAF or lyso-plasmalogen phosphatidylethanolamine (alkenyl-LPE), respectively, by phospholipase D (PLD) (Calbiochem,

La Jolla CA). Briefly, 1 mg of alkenyl-LPE or lyso-PAF was dispersed in 0.1 mL of 0.04 M Tris buffer, pH 8.0, containing 0.05 M $CaCl_2$ and 1% Triton-X100. After addition of the enzyme (4 units of PLD in 15 μL of 0.01M Tris-HCl, pH 8.0), the sample was mixed vigorously. The reaction vessel was sealed tightly and the contents were rotated overnight at room temperature. After the incubation period, the mixture was extracted with 1.2 mL of chloroform:MeOH:HCl (5:4:0.2). The chloroform layer was evaporated under a stream of nitrogen and the residue was dissolved in 50 μL chloroform:methanol (1:2 v/v). The substrate and the product were separated on a TLC plate using a solvent system of chloroform:MeOH:NH_4OH (65:35:5.5) and the product was eluted from the plate by extracting with 2 mL of chloroform:methanol (1:2) twice and then dried under N_2. The lipid product was identified and quantified by ESI-MS and then dissolved in methanol to make a 1 mM solution.

DNA synthesis and MTT assays. HEY cells were plated in 96-well plates, serum-starved for 16-24 h, and treated for 24 h with different concentrations of al-LPAs in F12/DMEM (1:1) medium supplemented with 0.1% fatty acid-free BSA, insulin, transferrin and selenium. For the DNA synthesis assays, the cells were incubated with 0.15 μCi/well [^{3}H]thymidine for the last 18 h. Cells were harvested onto filter papers presoaked in 1% polyethyleneimine using an automated cell harvester, HARVEST 96 (Perkin-Elmer-Wallac, Inc.). Incorporated [^{3}H]thymidine was counted in a 1450 Microbeta Trilux Liquid Scintillation and Luminescence Counter (Perkin-Elmer-Wallac, Inc.). For cell proliferation, 3-(4,5-dimethylthiazol-2-yl)-2,5-diphenyltetrazolium bromide (MTT) dye reduction assays were used. Twenty μL of MTT solution (5 mg/mL) was added to each well and incubated at 37°C for the last 6 h of lipid treatment. The reduced MTT crystals were dissolved in 100 μL/well of a mixture of DMSO and

95% ethanol (1:1, v/v). The color developed was read by a plate reader (SpectraMax 340, Molecular Devices Corp, Sunnyvale, CA) at 595-655 nm.

Western blotting. HEY cells were plated in 6-well plates in RPMI1640 with 10% FBS, serum-starved overnight, and then treated with or without al-LPAs in serum-free media for the indicated times. Cells were lysed on ice with Laemmli buffer containing 5% mercaptoethanol. The lysates were separated with 12% SDS-polyacrylamide gels and transferred onto PVDF membranes (Bio-Rad Laboratories, Hercules, CA). Antibodies against S473 phosphorylated Akt or phosphorylated ERK1/2 were used to probe the membrane and the ECL system (Amersham Pharmacia Biotech Inc., Piscataway, NJ) was used for detection. To normalize the amounts of protein loaded in each lane, the membranes were stripped and re-probed with antibodies against total Akt or ERK.

Cell migration assays. Chemotaxis was performed in a mini-Boyden chamber (Neuro Probe, Inc., Cabin John, MD) using Nucleopore polycarbonate filters (8 μm pore size) coated with a type-I collagen solution (100 μg/mL) (Vitrogen100, Collagen Corporation, Fremont, CA). Different concentrations of LPAs were added to the lower chamber. Checkerboard assays were performed as described by Okamoto *et al.* (38). HEY cells were starved for 3 h, trypsinized and resuspended at a concentration of 2.5×10^5 cells/mL in serum-free medium. The cell suspension (50 μL) was then placed in the upper chamber. After 4 h at 37°C, the cells that attached to the filters were fixed in 100% methanol and stained with Hematoxylin solution (Richard-Allan Scientific, Kalamazoo, MI). Cells that migrated to the lower phase of the membrane were counted under the microscope.

IL-8 ELISA assays. Cells were grown in 96-well plates, starved overnight, and treated with lipids for 6 h. The supernatants were collected and stored at -80°C. The IL-8 concentration

was measured using a quantitative sandwich enzyme-linked immunosorbent assay (ELISA) (R&D Systems, Minneapolis, MN) according to the manufacturer's protocol with minor modifications as described previously (24). All analyses were carried out in triplicate. Optical densities were determined using a SpectraMax 340 plate reader (Molecular Devices, Sunnyvale, CA) at 650-490 nm.

RESULTS

Al-LPAs were more stable than acyl-LPAs in ascites from patients with ovarian cancer. We have previously compared the lysolipid content in 15 pairs of ascites samples from patients with ovarian cancer and non-malignant diseases, and reported that al-LPAs were elevated in ovarian cancer ascites (35). Four al-LPA species were detected in ascites samples: 16:0- and 18:0-alkyl LPAs, and 16:0- and 18:0-alkenyl-LPAs. The distribution of different al-LPA and acyl-LPA species in 15 ovarian cancer and 15 non-malignant ascites samples is shown in Table I. Al-LPA species in ascites account for approximately 12% of total LPAs (both al- and acyl-LPAs). We observed that al-LPAs were more stable in ascites stored at 4°C under sterile conditions (Fig. 1*A*). The average half-lives of acyl-LPAs and al-LPAs in ascites stored at 4°C were approximately 12 months and more than 2 years, respectively (results obtained from 5 ascites samples; Fig. 1*B*).

Al-LPAs stimulated DNA synthesis and growth of HEY ovarian cancer cells. To determine the potential pathophysiological role of al-LPAs in ovarian cancer cells, we first examined the effects of al-LPAs on DNA synthesis and proliferation in HEY ovarian cancer cells. Alkyl-LPA (16:0) and 16:0/18:0-alkenyl-LPA (the ratio of 16:0 to 18:0 was approximately

1:1) were synthesized as described in Materials and Methods. Figure 2 shows the spectra of synthesized 16:0-/18:0-alkenyl- and 16:0-alkyl-LPAs. Each preparation contained a small amount of impurities, which were mainly derived from 16:0- and 18:0-acyl-LPAs. The relatively low amount (<10% and <5% in the alkyl-LPA and the alkenyl-LPA preparations, respectively) of these impurities did not affect the activities tested in this study. Starved HEY cells were incubated with different concentrations of lipids (0.1-5.0 μM; within the concentration range detected in ascites from patients with ovarian cancer) for 24 h. The effects of lipids on DNA synthesis was assessed by addition of [^{3}H]thymidine (0.15 μCi/well) and the effect of lipids on cell proliferation was measured by MTT dye reduction. Physiological concentrations of 16:0-alkyl-LPA (1-5 μM) and 16:0/18:0-alkenyl-LPA (1-5 μM) increased [^{3}H]thymidine incorporation and MTT dye reduction to approximately 2-fold (Fig. 3*A* and 3*B*).

Al-LPAs activated ERK and Akt. We have shown in our recent studies that acyl-LPA induces ERK, p38, and Akt activation in HEY cells (36). We sought to examine the activation of ERK and Akt induced by al-LPAs. Both alkyl- and alkenyl-LPAs activated Akt as assessed by an Akt kinase assay (Fig. 4*A*). Western blot analyses of phosphorylated ERK and Akt (S473) were performed after HEY cells were treated with alkyl- or alkenyl-LPAs. Both alkyl- and alkenyl-LPAs (2 μM) induced a concentration- and time-dependent activation of ERK and a transient increase in the S473 phosphorylation of Akt (Fig. 4*B*, *C*). The optimal concentrations were 5 μM and 1 μM for al-LPAs to activate ERK and Akt, respectively (Fig. 4*B*). Concentrations higher than 5 μM were not tested, since they are out of the physiological concentration ranges of al-LPAs detected in ovarian cancer ascites (Table I). The optimal times for induction of ERK and Akt phosphorylation by alkyl-LPA were 1-5 min and 30 min, respectively. Alkenyl-LPA induced maximal phosphorylation of both ERK and Akt at 30 min

(Fig. 4*C*). Similarly, al-LPAs also induced ERK and Akt phosphorylation in another ovarian cancer cell line, SKOV3 (Fig. 4*D*).

Pertussis toxin (PTX, a $G_{i/o}$ inhibitor; 100 ng/mL) partially, and two specific inhibitors of PI3K, LY294002 (10 μM) and wortmannin (100 nM), completely inhibited the activation of ERK and Akt induced by al-LPAs, suggesting that a PTX-insensitive G protein and PI3K are involved in phosphorylation of ERK and Akt (Fig. 5*A*, *B*).

Acyl-LPA-induced Akt activation is dependent on the activities of both MEK and p38, which is both ovarian cancer cell line- and stimulus-specific (36). In addition to our work, this MEK-dependent Akt activation/phosphorylation has been shown very recently in ultraviolet B- and serotonin-induced Akt activation (39, 40). To investigate whether al-LPAs activated the same signaling pathways as acyl-LPAs in HEY cells, we tested the effects of a panel of pharmacological and genetic inhibitory reagents on the Akt phosphorylation induced by al-LPAs. Similar to acyl-LPAs, Akt phosphorylation at S473 was sensitive to both PD98059 and SB203580 (the specific inhibitors for MEK1/2 and p38, respectively) (Fig. 5*C*), suggesting that MEK, and potentially its downstream effector ERK, and p38 were required for Akt phosphorylation at S473 by al-LPAs. This was further confirmed by transfecting HEY cells with dominant negative forms of MEK and p38 (MEK/2A and p38/AGF) (Fig. 5*D*). We have developed an efficient transfection method in HEY cells (36). Using both LipofectAMINE and Transfection Booster Reagents #3 (from Gene Therapy System, Inc., San Diego), the transfection efficiency was increased from 15±4% to 77±6%, as we reported previously (36). Both these dominant negative forms of MAP kinases blocked Akt activation induced by al-LPAs, indicating that both MEK and p38 activities are required for al-LPA-induced S473 phosphorylation of Akt in HEY cells.

We have shown that acyl-LPA, but not a structurally similar lipid, sphingosine-1-phosphate (S1P), induces Akt phosphorylation via a Rho-dependent pathways (36). We tested whether al-LPAs also require Rho for induction of S473 phosphorylation of Akt. Transient transfection of C3-exoenzyme, which blocks Rho activity, completely abolished al-LPA-induced S473 phosphorylation (Fig. 5*E*). Together, these results suggest that al-LPAs stimulate the same or similar signaling pathways in HEY cells as acyl-LPAs, and they may activate the same or similar receptors.

Activation of MEK/ERK, but not Akt, was required for promoting DNA synthesis by al-LPAs in HEY cells. To explore the potential signaling pathways involved in al-LPA induced DNA synthesis, we tested the effect of PTX, LY294002, wortmannin, PD98059, and SB203580 on [^{3}H]thymidine incorporation induced by alkyl- and alkenyl-LPAs (Fig. 6*A*). PTX inhibited approximately 70% and 45% of [^{3}H]thymidine incorporation triggered by alkyl-LPA and alkenyl-LPA, respectively, suggesting that both PTX-sensitive and insensitive G proteins are involved in this activity. LY294002 (10 μM), wortmannin (100 nM), and PD98059 (30 μM) completely blocked the al-LPA-stimulated DNA synthesis, suggesting that the activity of PI3K and MEK is essential for the process. In contrast, p38 activity was not required for DNA synthesis induced by al-LPAs, since [^{3}H]thymidine incorporation was insensitive to the treatment of SB203580. This was further confirmed by transfection with MEK/2A and p38/AGF (Fig.6*B*). Expression of MEK/2A completely inhibited al-LPA-induced DNA synthesis (Fig. 6*B*). In contrast, expression of p38/AGF did not affect the DNA synthesis induced by al-LPAs (Fig. 6*B*), indicating that p38 was not required for DNA synthesis induced by al-LPAs. Since S473 phosphorylation of Akt required p38 activation (Fig. 5*D*), and p38 was not required for the DNA synthesis stimulated by al-LPAs, we predict that Akt activation was not required for al-LPA-

induced DNA synthesis. To test this, we transfected the dominant negative (dn) form of Akt into HEY cells and found that dn-Akt did not affect [^{3}H]thymidine incorporation induced by al-LPAs as we predicted (Fig. 6*B*). These data suggest that al-LPA-induced MEK activation can lead to a p38- and Akt-independent stimulation of DNA synthesis in HEY cells.

Al-LPAs promoted ovarian cancer cell migration through collagen I-coated membranes. Cell migration is critically important for tumor metastasis. Acyl-LPA has been shown to induce cell migration of a number of cell types (fibroblasts, monocytes, T-lymphoma, hepatoma, and endothelial cells) (41-49). To test the effect of LPAs on ovarian cancer cell migration, we conducted Boyden chamber analyses. We found that both alkyl- and alkenyl-LPAs triggered cell migration through collagen I in a concentration-dependent manner and alkenyl-LPA was more potent than alkyl-LPA (Fig. 7*A*). To determine whether the enhanced cell migration was due to chemokinesis (random motility) or chemotaxis (directional motility), checkerboard analyses were performed essentially as described by Okamoto *et al.* (38). The number of cells that migrated to the lower phase of the membrane was reduced significantly as the concentration gradient of al-LPAs decreased (Table II), indicating that al-LPAs mainly stimulated chemotaxis.

We then compared the relative potencies of major LPA species present in ascites in stimulation of cell migration. We found that 16:0-acyl, 18:0-acyl, 18:1-acyl, 16:0-alkyl and 16:0/18:0-alkenyl LPAs all stimulated migration of HEY ovarian cancer cells through collagen I-coated membranes (Fig. 7*B*). At 1 μM concentration, the relative potencies of these LPA species were 18:1-acyl-LPA>16:0/18:0-alkeny-LPA>16:0-alkyl-LPA>16:0-acyl-LPA>18:0-acyl-LPA (Fig. 7*B*). The cell migration induced by al-LPAs was sensitive to PTX pretreatment and C3 exoenzyme transfection, and partially blocked by LY294002 (Fig. 7*C*). Interestingly,

transfection of MEK/2A, which completely blocked al-LPA-induced Akt phosphorylation (Fig. 5*D* above), did not significantly affect cell migration induced by al-LPAs, suggesting that a different downstream signaling molecule(s) of G_i, Rho, and/or PI3-K (other than MEK) was responsible for cell migration induced by al-LPAs.

Al-LPAs triggered IL-8 secretion from HEY cells. We have recently shown that 18:1-acyl-LPA induces increased IL-8 at both mRNA and protein levels in ovarian cancer cells, but not in immortalized ovarian epithelial cells (24). To determine whether al-LPAs also induce this activity, we examined IL-8 secretion from HEY cells using an ELISA assay as previously described (24). Al-LPAs induced IL-8 secretion from ovarian cancer cells with similar or higher potencies than that of 16:0- or 18:0-acyl-LPAs (Fig. 8).

DISCUSSION

We have previously reported that acyl-LPAs are growth stimulating factors for ovarian cancer and other tumor cells, which are present in ascites from patients with ovarian cancer (21, 22). The major acyl-LPA species (approximately 50% of all acyl-LPAs) in ovarian cancer ascites is 16:0-acyl-LPA (20). However, it is not a potent growth stimulator of ovarian cancer cells (21, 22). LPA species with unsaturated fatty acids, such as 18:1- and 18:2-acyl LPAs are more potent mitogens for ovarian cancer cells (20). We have recently detected elevated levels of al-LPAs in ovarian cancer ascites.

In this work, we show several lines of evidence to suggest that al-LPAs may play an important pathological role in ovarian cancer development. First, al-LPAs stimulated cell growth and DNA synthesis of HEY ovarian cancer cells (Fig. 3). Secondly, al-LPAs induced Akt

activation (Fig. 4A), which may be related to cell survival and chemoresistance. Thirdly, al-LPAs induced cell migration (Fig. 7A), which is one of the critical steps in tumor cell invasion and metastasis. Finally, al-LPAs stimulated the production of IL-8 with similar or higher potencies than 16:0- and 18:0-acyl-LPAs (Fig. 8). In particular, physiological concentrations of al-LPAs were used in this study and our results support the notion that these lipids may play important pathological roles in ovarian cancer development, although the role of al-LPAs *in vivo* remains to be further investigated.

Ovarian tumor cells inherently possess a strong metastatic potential to the peritoneum, which is the major cause of death in ovarian cancer patients (50). Preferential adhesion of ovarian epithelial carcinoma cells to migrate through collagen I (vs. collagen IV, fibronectin, laminin and vitronectin), has been demonstrated, and the ovarian carcinoma micro-environment is rich in collagen I (50). We show here that different LPA species promote cell migration through collagen I-coated membranes and this activity is potentially important in ovarian cancer pathology.

IL-8 is a pro-inflammatory and pro-angiogenic factor and may be involved in ovarian tumor development (51, 52). Angiogenesis is a critical factor of tumor development, which induces the transition from a limited to a rapid tumor growth via neovascularization (53). High expression of IL-8 mRNA has been detected in clinical specimens of late-stage ovarian carcinomas (54, 55). Ascites/cyst fluid and/or plasma of patients with ovarian cancer contain significantly higher levels of IL-8, compared to patients with benign gynecological disorders (56, 57). We have shown that al-LPAs are elevated in malignant ascites (35). Our results shown here suggest that al-LPAs present in ascites may regulate IL-8 production *in vivo*.

The results shown here suggest that the biological activities and/or signaling properties of LPA species are not only dependent on the composition of the fatty acid side chain, but also the chemical linkage between the aliphatic chain and the glycerol backbone. While 16:0- and 18:0-acyl-LPAs are not effective in growth stimulation in ovarian cancer cells (20), 16:0-alkyl- and 16:0/18:0-alkenyl-LPAs stimulated growth and DNA synthesis of HEY ovarian cancer cells. In addition, 16:0- and 18:0-al-LPAs were more potent than 16:0- and 18:0-acyl-LPAs in stimulating cell migration and IL-8 production. Interestingly, various synthetic ether-linked lysophosphatidylcholine compounds inhibit growth of many malignant cells, and clinical trials evaluating their antineoplastic potential have been conducted (58, 59). More recently, synthetic alkyl-LPA derivatives have been tested for their anti-proliferative activities (59). Together with the observations present here, these data suggest that a free phosphate group at the sn-3 position is important for the mitogenic activity of lysolipid(s).

Acyl-LPAs containing unsaturated fatty acids, such as 18:1- and 18:2-acyl-LPAs are more potent in stimulation of growth (20), IL-8 secretion, and cell migration. These data suggest that 18:1- and 18:2-acyl LPAs, which compose approximately 17% (Table I) of total acyl-LPAs in ascites (20, 35) and al-LPAs, which compose approximately 12% of all LPA species, may account for the major portion of biological activities of LPAs in ovarian cancer ascites. The pathophysiological importance of al-LPAs is further supported by our observation that these LPA species are more stable than acyl-LPAs at 4°C (Fig. 1). The instability of LPAs at 4°C may reflect LPA-degrading reactions by endogenous enzymes (at a slower reaction when compared to physiological conditions at 37°C). However, since the ascites samples were stored under sterile conditions, exogenous LPA-degrading enzymes from bacteria and/or other sources were unlikely. The two major pathways to degrade LPA are deacylation by lyso-phospholipase A_1 (PLA_1) and

de-phosphorylation by phosphatases (LPPs) (60, 61). While dephosphorylation of al-LPAs and acyl-LPAs by LPPs may be similarly effective, ether-linked al-LPAs are not degradable by PLA_1, which may account for the relative higher stability of al-LPAs.

We show here that different biological effects induced by al-LPAs require different signaling pathways. PI3K activity is required for cell proliferation, cell migration, and Akt activation/phosphorylation. MEK is required for cell proliferation and S473 phosphorylation of Akt, but not for cell migration. S473 phosphorylation of Akt, but not cell proliferation, is dependent on p38 MAP kinase activity. These data suggest that MEK activation can lead to a p38-dependent Akt phosphorylation, and a p38-independent stimulation of DNA synthesis. These signaling properties provide important information on strategies to antagonize the cellular effects of al-LPAs.

The work here shows that al-LPAs appear to stimulate the same or similar signaling pathways as acyl-LPAs, although they differ in concentration and time point for optimal simulations. In particular, we have shown recently that acyl-LPA stimulated a rather unique Rho- and MEK-dependent Akt phosphorylation. This signaling pathway is not shared by many other stimuli that we have tested, including S1P, thrombin, endothelin-1, PDGF, insulin, and EGF (36 and unpublished data). These data suggest that the effects of al-LPAs may be mediated by acyl-LPA receptors (Edgs). In fact, both Edg4 and Edg7 have been shown to respond to alkyl- and/or alkenyl-LPAs (62-64). We have found that HEY cells express Edg2, 4 and 7 and SKOV3 cells express Edg2 and 4 (36 and unpublished data). Since subtype-selective receptor antagonists are not yet available, the direct assignment of the endogenous receptors mediating the effects induced by al-LPAs in HEY cells remains to be determined.

REFERENCES

1. Moolenaar, W. H. Bioactive lysophospholipids and their G protein-coupled receptors, Experimental Cell Research. *253:* 230-8, 1999.

2. Moolenaar, W. H., Kranenburg, O., Postma, F. R., and Zondag, G. C. Lysophosphatidic acid: G-protein signalling and cellular responses, Current Opinion in Cell Biology. *9:* 168-73, 1997.

3. Liscovitch, M. and Cantley, L. C. Lipid second messengers, Cell. *77:* 329-34, 1994.

4. Xu, Y., Xiao, Y., Baudhuin, L. M., and Schwartz, B. M. The role and clinical applications of bioactive lysolipids in ovarian cancer., J. Soc. Gyn. Invest. *In press:*, 2001.

5. Nugent, D., Belinson, J., and Xu, Y. The synergistic interactions of oleoyl-lysophosphatidic acid in platelet aggregation, Med Sci Res. *27:* 435-441, 1999.

6. An, S., Goetzl, E. J., and Lee, H. Signaling mechanisms and molecular characteristics of G protein-coupled receptors for lysophosphatidic acid and sphingosine 1-phosphate, J Cell Biochem Suppl. *31:* 147-57, 1998.

7. Contos, J. J., Ishii, I., and Chun, J. Lysophosphatidic acid receptors, Mol Pharmacol. *58:* 1188-96., 2000.

8. Eichholtz, T., Jalink, K., Fahrenfort, I., and Moolenaar, W. H. The bioactive phospholipid lysophosphatidic acid is released from activated platelets, Biochem J. *291:* 677-80, 1993.

9. Palmetshofer, A., Robson, S. C., and Nehls, V. Lysophosphatidic acid activates nuclear factor kappa B and induces proinflammatory gene expression in endothelial cells, Thromb Haemost. *82:* 1532-7, 1999.

10. Weinstein, J. R., Lau, A. L., Brass, L. F., and Cunningham, D. D. Injury-related factors and conditions down-regulate the thrombin receptor (PAR-1) in a human neuronal cell line, J Neurochem. *71:* 1034-50, 1998.

11. Lee, H., Goetzl, E. J., and An, S. Lysophosphatidic acid and sphingosine 1-phosphate stimulate endothelial cell wound healing [In Process Citation], Am J Physiol Cell Physiol. *278:* C612-8, 2000.

12. Liliom, K., Guan, Z., Tseng, J. L., Desiderio, D. M., Tigyi, G., and Watsky, M. A. Growth factor-like phospholipids generated after corneal injury, Am J Physiol. *274:* C1065-74, 1998.

13. Sullivan, L. M., Honemann, C. W., Arledge, J. A., and Durieux, M. E. Synergistic inhibition of lysophosphatidic acid signaling by charged and uncharged local anesthetics, Anesth Analg. *88:* 1117-24, 1999.

14. Watsky, M. A., Griffith, M., Wang, D. A., and Tigyi, G. J. Phospholipid growth factors and corneal wound healing, Ann N Y Acad Sci. *905:* 142-58, 2000.

15. Hu, Y. L., Tee, M. K., Goetzl, E. J., Auersperg, N., Mills, G. B., Ferrara, N., and Jaffe, R. B. Lysophosphatidic acid induction of vascular endothelial growth factor expression in human ovarian cancer cells, J Natl Cancer Inst. *93:* 762-7., 2001.

16. Goetzl, E. J. and An, S. Diversity of cellular receptors and functions for the lysophospholipid growth factors lysophosphatidic acid and sphingosine 1-phosphate, FASEB Journal. *12:* 1589-98, 1998.

17. An, S., Bleu, T., Hallmark, O. G., and Goetzl, E. J. Characterization of a novel subtype of human G protein-coupled receptor for lysophosphatidic acid, Journal of Biological Chemistry. *273:* 7906-10, 1998.

18. Lynch, K. R. and Im, I. Life on the edg, Trends Pharmacol Sci. *20:* 473-5, 1999.

19. Moolenaar, W. H. Bioactive lysophospholipids and their G protein-coupled receptors, Exp Cell Res. *253:* 230-8, 1999.

20. Xu, Y., Gaudette, D., Boynton, J., Frankel, A., Fang, X., Sharma, A., Hurteau, J., Casey, G., Goodbody, A., Mellors, A., and al., e. Characterization of an ovarian cancer activating factor in ascites from ovarian cancer patients, Clin Cancer Res. *1:* 1223-32, 1995.

21. Xu, Y., Fang, X., Casey, G., and Mills, G. Lysophospholipids activate ovarian and breast cancer cells, Biochem J. *309:* 933-40, 1995.

22. Xu, Y., Casey, G., and Mills, G. Effect of lysophospholipids on signaling in the human Jurkat T cell line, J Cell Physiol. *163:* 441-50, 1995.

23. Hong, G., Baudhuin, L. M., and Xu, Y. Sphingosine-1-phosphate modulates growth and adhesion of ovarian cancer cells, FEBS Lett. *460:* 513-8, 1999.

24. Schwartz, B. M., Hong, G., Morrison, B. H., Wu, W., Baudhuin, L. M., Xiao, Y. J., Mok, S. C., and Xu, Y. Lysophospholipids increase interleukin-8 expression in ovarian cancer cells, Gynecol Oncol. *81:* 291-300., 2001.

25. Frankel, A. and Mills, G. B. Peptide and lipid growth factors decrease cis-diamminedichloroplatinum- induced cell death in human ovarian cancer cells, Clin Cancer Res. *2:* 1307-13., 1996.

26. Fang, X., Yu, S., Lapushin, R., Lu, Y., Furui, T., Penn, L. Z., Stokoe, D., Erickson, J. R., Bast Jr, R. C., and Mills, G. B. Lysophosphatidic acid prevents apoptosis in fibroblasts via Gi-protein- mediated activation of mitogen-activated protein kinase, Biochem J. *352:* 135-143, 2000.

27. Pustilnik, T. B., Estrella, V., Wiener, J. R., Mao, M., Eder, A., Watt, M. A., Bast, R. C., Jr., and Mills, G. B. Lysophosphatidic acid induces urokinase secretion by ovarian cancer cells, Clin Cancer Res. *5:* 3704-10, 1999.

28. Xu, Y., Shen, Z., Wiper, D., Wu, M., Morton, R., Elson, P., Kennedy, A., Belinson, J., Markman, M., and Casey, G. Lysophosphatidic acid as a potential biomarker for ovarian and other gynecologic cancers, JAMA. *280:* 719-23, 1998.

29. Moolenaar, W. H. Lysophosphatidic acid signalling, Curr Opin Cell Biol. *7:* 203-10, 1995.

30. Simon, M. F., Chap, H., and Douste-Blazy, L. Human platelet aggregation induced by 1-alkyl-lysophosphatidic acid and its analogs: a new group of phospholipid mediators?, Biochem Biophys Res Commun. *108:* 1743-50, 1982.

31. Svetlov, S. I., Siafaka-Kapadai, A., Hanahan, D. J., and Olson, M. S. Signaling responses to alkyllysophosphatidic acid: the activation of phospholipases A2 and C and protein tyrosine phosphorylation in human platelets, Arch Biochem Biophys. *336:* 59-68, 1996.

32. Liliom, K., Fischer, D. J., Virag, T., Sun, G., Miller, D. D., Tseng, J. L., Desiderio, D. M., Seidel, M. C., Erickson, J. R., and Tigyi, G. Identification of a novel growth factor-like lipid, 1-O-cis-alk-1'-enyl- 2-lyso-sn-glycero-3-phosphate (alkenyl-GP) that is present in commercial sphingolipid preparations, J Biol Chem. *273:* 13461-8, 1998.

33. Fischer, D. J., Liliom, K., Guo, Z., Nusser, N., Virag, T., Murakami-Murofushi, K., Kobayashi, S., Erickson, J. R., Sun, G., Miller, D. D., and Tigyi, G. Naturally occurring analogs of lysophosphatidic acid elicit different cellular responses through selective activation of multiple receptor subtypes, Mol Pharmacol. *54:* 979-88, 1998.

34. Sugiura, T., Nakane, S., Kishimoto, S., Waku, K., Yoshioka, Y., Tokumura, A., and Hanahan, D. J. Occurrence of lysophosphatidic acid and its alkyl ether-linked analog in rat brain and comparison of their biological activities toward cultured neural cells, Biochim Biophys Acta. *1440:* 194-204, 1999.

35. Xiao, Y. J., Schwartz, B., Washington, M., Kennedy, A., Webster, K., Belinson, J., and Xu, Y. Electrospray ionization mass spectrometry analysis of lysophospholipids in human ascitic fluids: comparison of the lysophospholipid contents in malignant vs nonmalignant ascitic fluids, Anal Biochem. *290:* 302-13., 2001.

36. Baudhuin, L., Lu, J., and Xu, Y. Activation of Akt by LPA and S1P is depedent on the activities of both MEK and p38 MAP kinase in ovarian cancer cells, submitted.

37. Xiao, Y., Y., C., AW., K., J., B., and Y., X. Evaluation of plasma lysophospholipids for diagnostic significance using electrospray ionization mass spectrometry (ESI-MS) analyses, Ann N Y Acad Sci. *905:* 242-59, 2000.

38. Okamoto, H., Yatomi, Y., Ohmori, T., Satoh, K., Matsumoto, Y., and Ozaki, Y. Sphingosine 1-phosphate stimulates G(i)- and rho-mediated vascular endothelial cell spreading and migration [In Process Citation], Thromb Res. *99:* 259-65, 2000.

39. Nomura, M., Kaji, A., Ma, W. Y., Zhong, S., Liu, G., Bowden, G. T., Miyamoto Ki, K., and Dong, Z. Mitogen- and stress-activated protein kinase-1 mediates activation of Akt by ultraviolet B irradiation, J Biol Chem. *11:* 11, 2001.

40. Hsu, E. H., Lochan, A. C., and Cowen, D. S. Activation of akt1 by human 5-hydroxytryptamine (serotonin)(1b) receptors is sensitive to inhibitors of mek, J Pharmacol Exp Ther. *298:* 825-32., 2001.

41. Pietruck, F., Busch, S., Virchow, S., Brockmeyer, N., and Siffert, W. Signalling properties of lysophosphatidic acid in primary human skin fibroblasts: role of pertussis toxin-sensitive GTP-binding proteins, Naunyn Schmiedebergs Arch Pharmacol. *355:* 1-7, 1997.

42. Sakai, T., de la Pena, J. M., and Mosher, D. F. Synergism among lysophosphatidic acid, beta1A integrins, and epidermal growth factor or platelet-derived growth factor in mediation of cell migration, J Biol Chem. *274:* 15480-6, 1999.

43. Panetti, T. S., Nowlen, J., and Mosher, D. F. Sphingosine-1-phosphate and lysophosphatidic acid stimulate endothelial cell migration, Arterioscler Thromb Vasc Biol. *20:* 1013-9, 2000.

44. Nobes, C. D. and Hall, A. Rho GTPases control polarity, protrusion, and adhesion during cell movement, J Cell Biol. *144:* 1235-44., 1999.

45. Imamura, F., Mukai, M., Ayaki, M., Takemura, K., Horai, T., Shinkai, K., Nakamura, H., and Akedo, H. Involvement of small GTPases Rho and Rac in the invasion of rat ascites hepatoma cells, Clin Exp Metastasis. *17:* 141-8., 1999.

46. Zhou, D., Luini, W., Bernasconi, S., Diomede, L., Salmona, M., Mantovani, A., and Sozzani, S. Phosphatidic acid and lysophosphatidic acid induce haptotactic migration of human monocytes, J Biol Chem. *270:* 25549-56, 1995.

47. Stam, J. C., Michiels, F., van der Kammen, R. A., Moolenaar, W. H., and Collard, J. G. Invasion of T-lymphoma cells: cooperation between Rho family GTPases and lysophospholipid receptor signaling, Embo J. *17:* 4066-74, 1998.

48. Anand-Apte, B., Zetter, B. R., Viswanathan, A., Qiu, R. G., Chen, J., Ruggieri, R., and Symons, M. Platelet-derived growth factor and fibronectin-stimulated migration are

differentially regulated by the Rac and extracellular signal-regulated kinase pathways, J Biol Chem. *272:* 30688-92., 1997.

49. Kundra, V., Anand-Apte, B., Feig, L. A., and Zetter, B. R. The chemotactic response to PDGF-BB: evidence of a role for Ras, J Cell Biol. *130:* 725-31., 1995.

50. Moser, T. L., Pizzo, S. V., Bafetti, L. M., Fishman, D. A., and Stack, M. S. Evidence for preferential adhesion of ovarian epithelial carcinoma cells to type I collagen mediated by the alpha2beta1 integrin, Int J Cancer. *67:* 695-701., 1996.

51. Harada, A., Mukaida, N., and Matsushima, K. Interleukin 8 as a novel target for intervention therapy in acute inflammatory diseases, Molecular Medicine Today. *2:* 482-9, 1996.

52. Koch, A. E., Polverini, P. J., Kunkel, S. L., Harlow, L. A., DiPietro, L. A., Elner, V. M., Elner, S. G., and Strieter, R. M. Interleukin-8 as a macrophage-derived mediator of angiogenesis [see comments], Science. *258:* 1798-801, 1992.

53. Folkman, J. Diagnostic and therapeutic applications of angiogenesis research, C R Acad Sci III. *316:* 909-18., 1993.

54. Merogi, A. J., Marrogi, A. J., Ramesh, R., Robinson, W. R., Fermin, C. D., and Freeman, S. M. Tumor-host interaction: analysis of cytokines, growth factors, and tumor-infiltrating lymphocytes in ovarian carcinomas, Human Pathology. *28:* 321-31, 1997.

55. Yoneda, J., Kuniyasu, H., Crispens, M. A., Price, J. E., Bucana, C. D., and Fidler, I. J. Expression of angiogenesis-related genes and progression of human ovarian carcinomas in nude mice, Journal of the National Cancer Institute. *90:* 447-54, 1998.

56. Gawrychowski, K., Skopinska-Rozewska, E., Barcz, E., Sommer, E., Szaniawska, B., Roszkowska-Purska, K., Janik, P., and Zielinski, J. Angiogenic activity and interleukin-8

content of human ovarian cancer ascites, European Journal of Gynaecological Oncology. *19:* 262-4, 1998.

57. Ivarsson, K., Runesson, E., Sundfeldt, K., Haeger, M., Hedin, L., Janson, P. O., and Brannstrom, M. The chemotactic cytokine interleukin-8--a cyst fluid marker for malignant epithelial ovarian cancer?, Gynecologic Oncology. *71:* 420-3, 1998.

58. Goto, I., Hozumi, M., and Honma, Y. Selective effect of O-alkyl lysophospholipids on the growth of a human lung giant cell carcinoma cell line, Anticancer Res. *14:* 357-62., 1994.

59. Ashagbley, A., Samadder, P., Bittman, R., Erukulla, R. K., Byun, H. S., and Arthur, G. Synthesis of ether-linked analogues of lysophosphatidate and their effect on the proliferation of human epithelial cancer cells in vitro, Anticancer Res. *16:* 1813-8., 1996.

60. Dillon, D. A., Chen, X., Zeimetz, G. M., Wu, W. I., Waggoner, D. W., Dewald, J., Brindley, D. N., and Carman, G. M. Mammalian Mg2+-independent phosphatidate phosphatase (PAP2) displays diacylglycerol pyrophosphate phosphatase activity, J Biol Chem. *272:* 10361-6., 1997.

61. Pilquil, C., Singh, I., Zhang, Q., Ling, Z., Buri, K., Stromberg, L. M., Dewald, J., and Brindley, D. N. Lipid phosphate phosphatase-1 dephosphorylates exogenous lysophosphatidate and thereby attenuates its effects on cell signalling, Prostaglandins. *64:* 83-92., 2001.

62. Aoki, J., Bandoh, K., and Inoue, K. A novel human G-protein-coupled receptor, EDG7, for lysophosphatidic acid with unsaturated fatty-acid moiety [In Process Citation], Ann N Y Acad Sci. *905:* 263-6, 2000.

63. Bandoh, K., Aoki, J., Hosono, H., Kobayashi, S., Kobayashi, T., Murakami-Murofushi, K., Tsujimoto, M., Arai, H., and Inoue, K. Molecular cloning and characterization of a novel human G-protein- coupled receptor, EDG7, for lysophosphatidic acid, J Biol Chem. *274:* 27776-85, 1999.

64. An, S., Bleu, T., Zheng, Y., and Goetzl, E. J. Recombinant human G protein-coupled lysophosphatidic acid receptors mediate intracellular calcium mobilization, Molecular Pharmacology. *54:* 881-8, 1998.

FIGURE LEGENDS

Fig 1. Al-LPAs in ascites from ovarian cancer patients are more stable than acyl-LPAs. Al-LPAs and acyl-LPAs from ascites samples were extracted and analyzed as described in Materials and Methods. Five ascites samples from patients with ovarian cancer were stored at 4°C under sterile conditions. LPAs from 0.5 mL of ascites were analyzed at the time intervals as indicated. *A*, ESI-MS spectra of LPAs from a representative ovarian cancer ascites samples analyzed at 0, 6, 12 and 18 months. *B*, the stability of LPAs in 5 ovarian cancer ascites samples.

Fig. 2. The spectra of synthetic alkyl- and alkenyl-LPAs. Al-LPAs were synthesized and analyzed as described in Materials and Methods. Al-LPAs were resuspended in methanol and 20 μL of al-LPAs containing 50 pmol of 14:0-acyl-LPA (internal standard) was used for MS analyses.

Fig 3. Al-LPAs stimulated DNA synthesis in HEY cells. *A*, DNA synthesis was measured by using [^{3}H]thymidine incorporation as described in Materials and Methods. Cells were treated with al-LPAs (1-5 μM) for 24 h. *B*, MTT dye reduction was used to measure cell proliferation. Cells were treated with al-LPAs (1-5 μM) for 24 h. MTT solution was added and incubated at 37°C for the last 6 h of lipid treatment.

Figure 4. Al-LPAs activated ERK MAP kinases and Akt in HEY and SKOV3 ovarian cancer cells. *A*, the kinase activity of Akt was performed with the Nonradioactive Akt Kinase Assay Kit according to the manufacture's instructions. Starved HEY cells were treated with 2 μM al-LPAs

for 30 min. *B*, concentration-dependent Akt (30 min) and ERK (5 min) phosphorylation by al-LPAs. HEY cells were serum-starved for 18-24 h before stimulation with lipids. *C*, the time courses of ERK and Akt phosphorylation stimulated by alkyl-LPA (2 μM) or alkenyl-LPA (2 μM) for the indicated times in HEY cells. *D*, ERK and Akt phosphorylation induced by al-LPAs in SKOV3 cells. Starved SKOV3 cells were treated with 2 μM al-LPAs for the indicated times.

Fig. 5. Al-LPAs induced phosphorylation of ERK and Akt was dependent on G_i, PI3K, MEK and p38. *A*, Akt and ERK phosphorylation induced by al-LPAs was PTX-sensitive. HEY cells were pre-treated with PTX (100 ng/mL) for 16 h prior to stimulation with lipids (2 μM) for detection of p-Akt (30 min stimulation) or p-p42/44 ERK (5 min stimulation). *B*, al-LPA-induced Akt and ERK phosphorylation was inhibited by PI3K inhibitors. Starved HEY cells were pre-treated with 10 μM LY 294002 or 0.1 μM wortmannin for 30 min prior to stimulation with lipids (2 μM; 30 min for p-Akt and 5 min for p-ERK). *C*, S473 phosphorylation of Akt induced by al-LPAs was dependent on both MEK and p38 MAP kinases. Starved HEY cells were pre-treated with 30 μM PD98059 or 10 μM SB203580 for 30 min followed by stimulation with lipid (2 μM; 30 min for p-Akt and 5 min for p-ERK). *D*, HEY cells were transiently transfected with control vector, dominant negative MEK (MEK/2A), or kinase dead p38 (p38/AGF), and then treated with 2 μM al-LPAs for 30 min. *E*, S473 phosphorylation of Akt induced by al-LPAs was dependent on Rho activity. HEY cells were transiently transfected with control vector, C3-exoenzyme (C3), and then treated with 2 μM al-LPAs for 30 min.

Fig. 6. Al-LPA-mediated proliferation was PTX-sensitive and dependent on PI3K and ERK activation, but not p38 MAP kinase. *A*, HEY cells were treated with alkyl-, alkenyl-LPAs, or

solvent (Ctrl) and [^{3}H]thymidine incorporation was conducted as described in Materials and Methods. PTX (100 ng/mL) was added to the culture 16 h prior to lipid (5 μM) stimulation. HEY cells were stimulated with alkyl-LPA or alkenyl-LPA (5 μM) in the presence of 30 μM PD 98059 (PD), 10 μM LY294002 (LY), 0.1 μM wortmanin (WT), or 10 μM SB 203580 (SB). The data shown here represent the mean ± SD of three independent experiments. *B*, HEY cells were transiently transfected with control vector, dominant negative MEK (MEK/2A), kinase dead p38 (p38/AGF), or dominant negative Akt (AKT/DN). After the starvation, the cells were incubated with 5 μM al-LPAs for 24 h. Results are plotted as mean ± SD of three independent experiments. *** $p<0.001$, ** $p<0.01$, * $p<0.05$ (Student's *t* test).

Figure 7. Al-LPA stimulated HEY cell migration. *A*, cell mobility was measured in a modified Boyden chamber assay as described in Materials and Methods. Alkyl- or alkenyl-LPA (0 - 5 μM) was added to the lower chamber. Cells migrated to the lower phase of the membrane were counted after starved cells were seeded in the upper chamber for 4 h. *B*, the relative potencies of different LPA species in stimulating cell migration. Different LPA species (1 μM) were added to the lower chamber of the migration chamber, and starved cells were added to the upper chamber. Migration was allowed for 4 h at 37°C. *C*, al-LPA-stimulated migration was PTX- and Rho-sensitive and PI3K-dependent. HEY cells were pretreated with PTX (100 ng/mL) for 16 h or transiently transfected with C3-exoenzyme (C3, a Rho inhibitor) or dominant negative MEK (MEK/2A). HEY cells in the absence (Control) or presence of LY294002 (10 μM, LY), as well as PTX pretreated cells or transfected cells were loaded into the upper chambers and the lipids (1 μM) were added to the lower chamber. The migration was conducted for 4 h. The cell number on the

lower face of the membrane was counted. The results are presented as the mean ± SD of three independent experiments. *** $p<0.001$ (Student's *t* test).

Figure 8. Stimulation of IL-8 secretion by LPAs in HEY cells. Cells were starved from serum for 18-24 h and treated for 6 h with varying doses of LPAs. The supernatants were then removed and stored in a freezer at -80°C until ELISA (Materials and Methods) was performed.

Table I Statistical Analysis of LPAs in 15 pairs of Ascites Samples from Patients with Ovarian Cancer or Non-malignant Diseases[a]

		Alkyl-LPA (μM)		Alkenyl-LPA (μM)		Total al-LPAs	Acyl-LPA(μM)						Total acyl-LPAs	Total LPAs
		16:0	18:0	16:0	18:0	(μM)	16:0	18:2	18:1	18:0	20:4	22:6	(μM)	(μM)
Ovarian Cancer	min.	0.3540	0.1046	0.0943	0.4688	1.0217	0.1498	0.2708	0.2973	0.3465	0.2198	0.1064	1.9994	3.0211
	max.	3.8929	1.2483	0.6663	2.3318	7.1772	37.1935	3.7894	8.0704	11.1937	6.7902	2.5948	63.7062	69.0424
	mean	1.4800	0.6371	0.2906	1.3036	3.7113	13.1215	1.6590	3.4871	4.7761	2.4634	0.9257	26.4329	30.1442
	median	1.2620	0.6577	0.2651	1.2278	3.6384	12.5786	0.8795	2.5284	4.1882	2.0456	0.8293	25.5248	28.4011
Benign Diseases	min.	0.0000	0.0000	0.0000	0.0164	0.0423	0.2779	0.0000	0.0392	0.0735	0.0000	0.0000	0.3966	0.4389
	max.	0.4450	0.2541	0.0585	0.4081	1.1072	7.8070	1.5854	2.5443	1.8295	1.2583	0.3686	14.9973	15.7150
	mean	0.1430	0.0997	0.0082	0.1072	0.3580	1.8975	0.4775	0.5401	0.3774	0.4181	0.1557	3.8662	4.2243
	median	0.0928	0.0820	0.0000	0.0602	0.2287	1.3920	0.3660	0.3540	0.2300	0.2907	0.1111	2.6937	2.9665

[a]Sample collection, lipid extraction and analyses were performed as described previously (35).

Table II. Checkerboard analysis of HEY cells[a]

	Alkyl-LPA, upper chamber (μM)			
	0	0.1	1	5
Alkyl-LPA, lower chamber (μM)				
0	68±15	72±13	65±13	55±13
0.1	280±50	167±29	88±10	77±15
1	408±36	367±115	210±30	87±12
5	659±112	587±55	343±21	120±12

	Alkenyl-LPA, upper chamber (μM)			
	0	0.1	1	5
Alkenyl -LPA, lower chamber (μM)				
0	78±13	77±8	67±6	82±8
0.1	230±26	150±26	118±28	118±28
1	493±51	293±40	207±15	132±28
5	827±122	550±30	270±72	112±38

[a]Different concentrations of alkyl-LPA or alkenyl-LPA were added to the upper and/or lower chamber, and HEY cells in the upper chamber were allowed to migrate for 4 h at 37°C.

Figure 1A

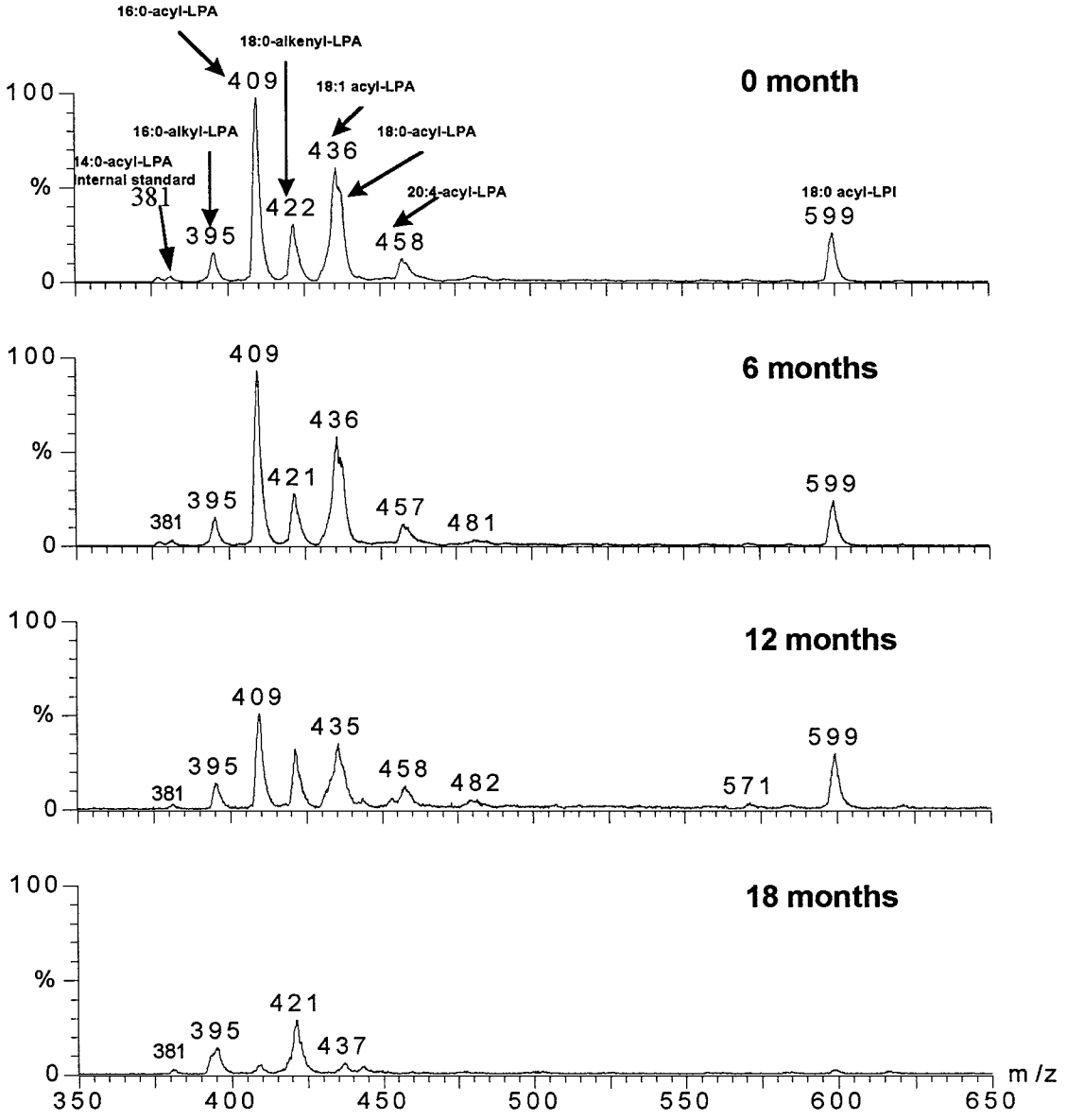
16:0-acyl-LPA
18:0-alkenyl-LPA
18:1 acyl-LPA
16:0-alkyl-LPA
18:0-acyl-LPA
14:0-acyl-LPA
internal standard
20:4-acyl-LPA
18:0 acyl-LPI
0 month
6 months
12 months
18 months
100
%
0
409
436
422
395
381
458
599
421
457
481
435
482
571
437
m/z
350
400
450
500
550
600
650

Figure 1B

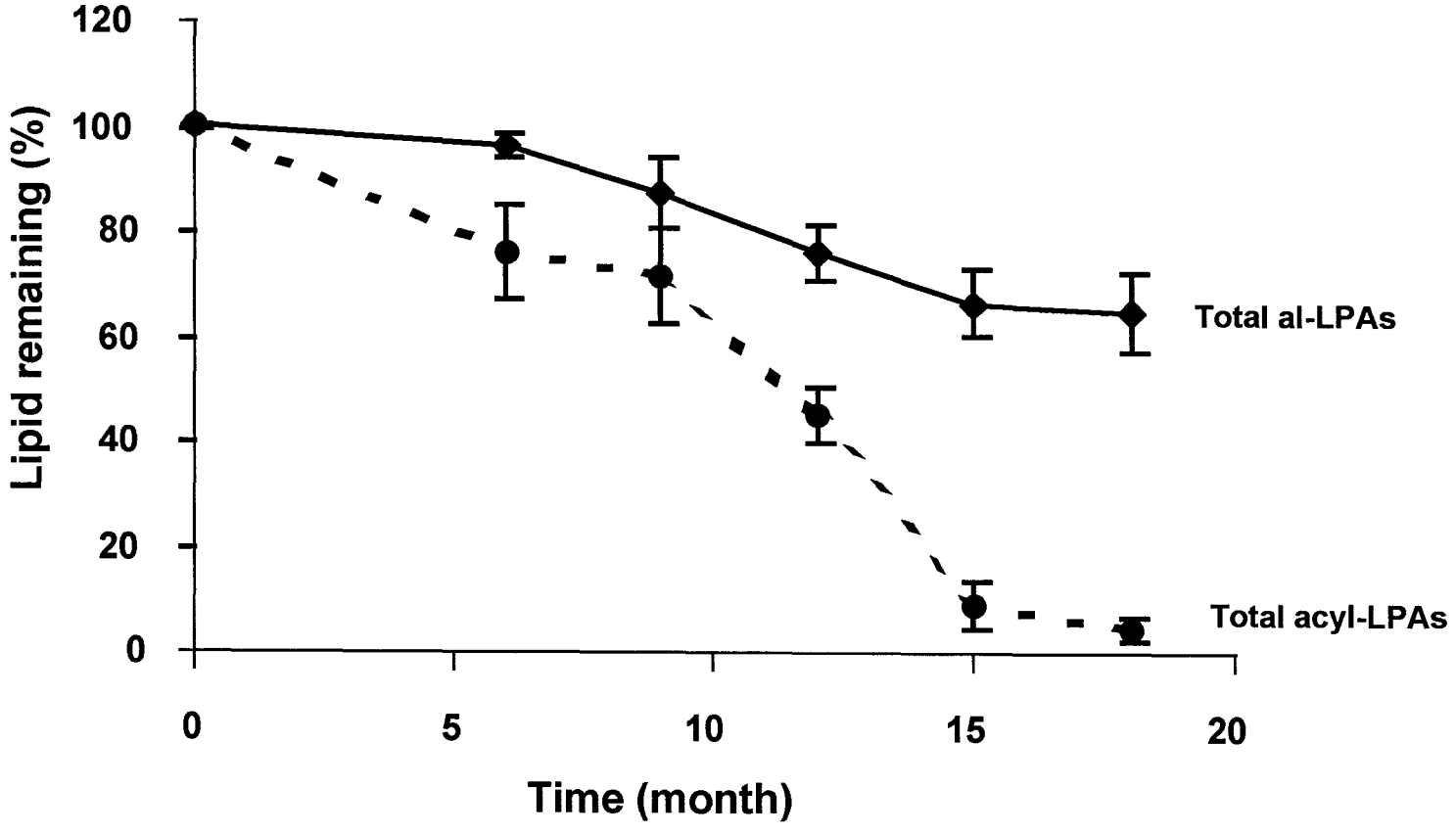
120
100
80
60
40
20
0
Lipid remaining (%)
0
5
10
15
20
Time (month)
Total al-LPAs
Total acyl-LPAs

Figure 2

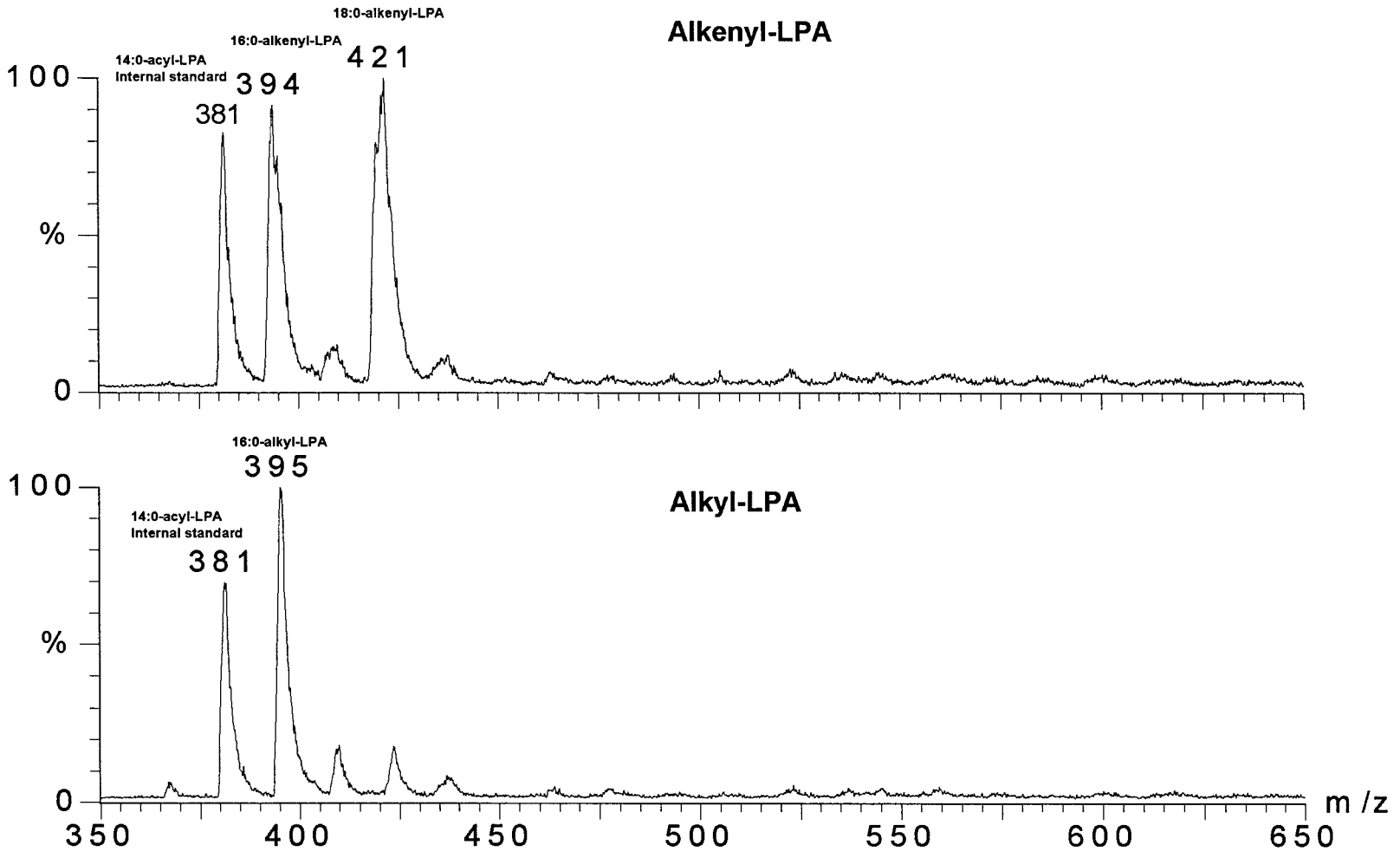
Alkenyl-LPA
18:0-alkenyl-LPA
16:0-alkenyl-LPA
14:0-acyl-LPA
Internal standard
421
394
381
100
%
0
Alkyl-LPA
16:0-alkyl-LPA
395
14:0-acyl-LPA
Internal standard
381
100
%
0
350
400
450
500
550
600
650
m/z

Figure 3A

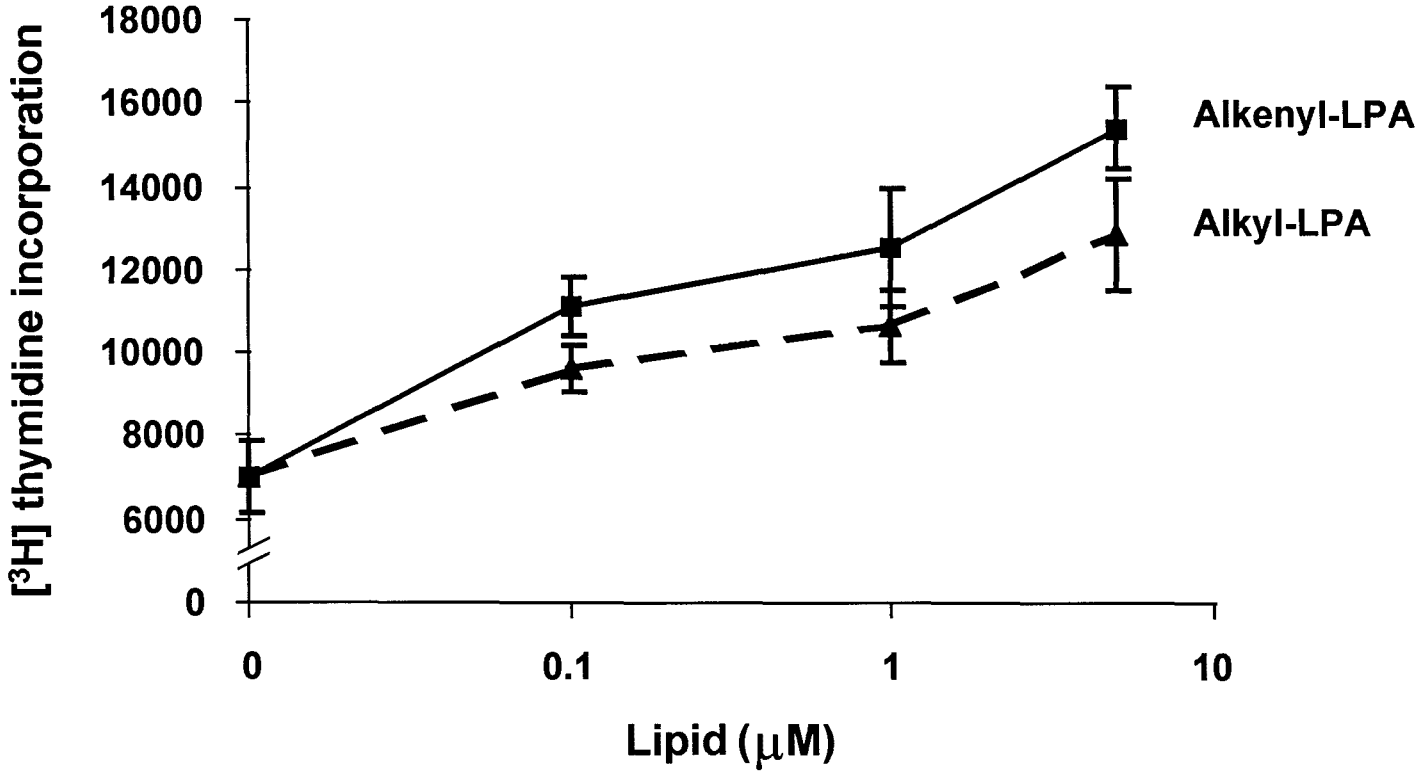
[3H] thymidine incorporation
18000
16000
14000
12000
10000
8000
6000
0
0
0.1
1
10
Lipid (μM)
Alkenyl-LPA
Alkyl-LPA

Figure 3B

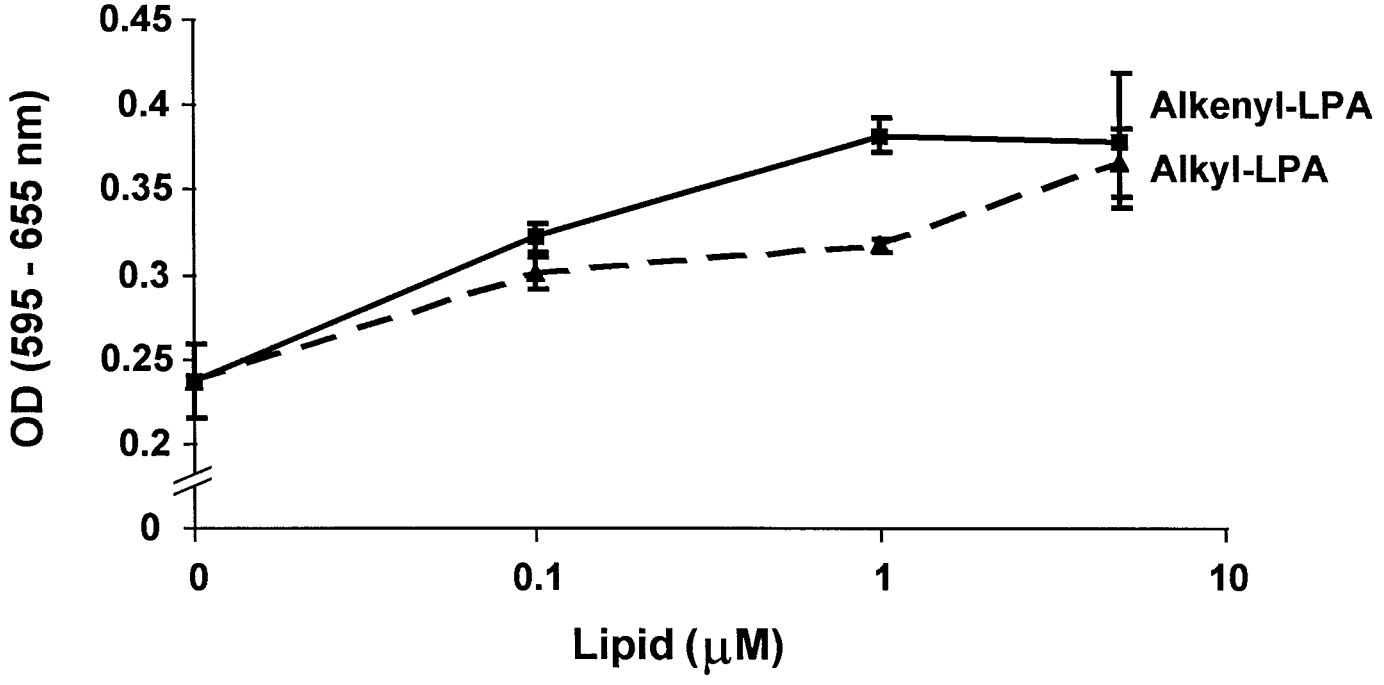
0.45
0.4
0.35
0.3
0.25
0.2
0
OD (595 - 655 nm)
0
0.1
1
10
Lipid (μM)
Alkenyl-LPA
Alkyl-LPA

Figure 4A

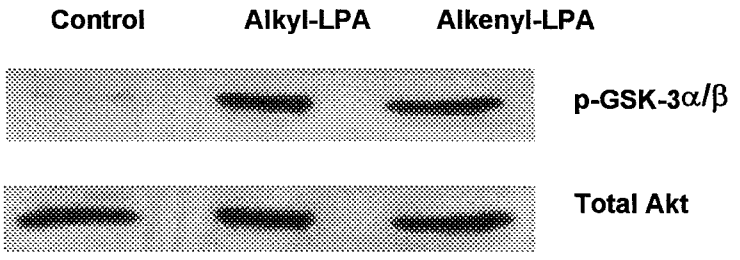

Figure 4B

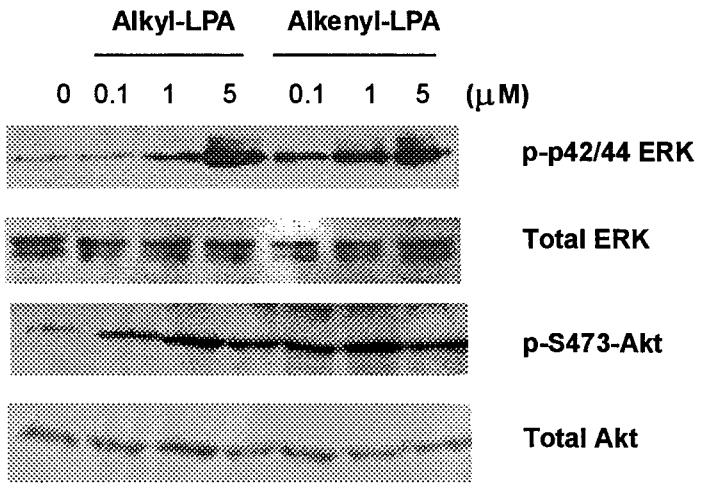

Figure 4C

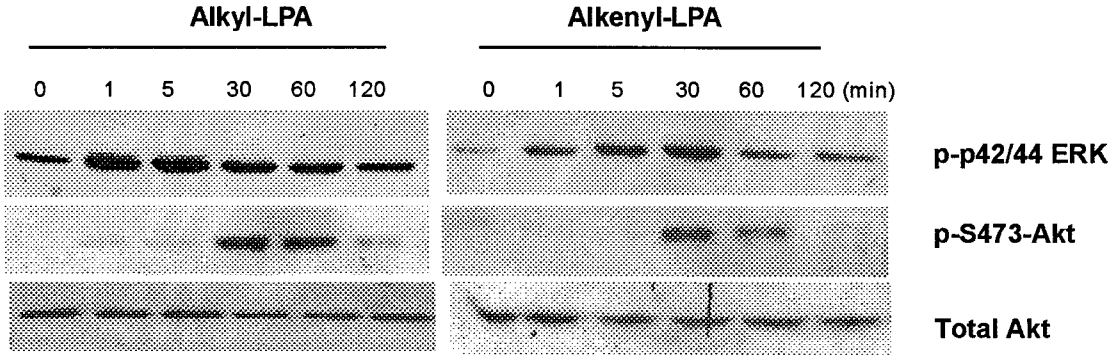

Figure 4D

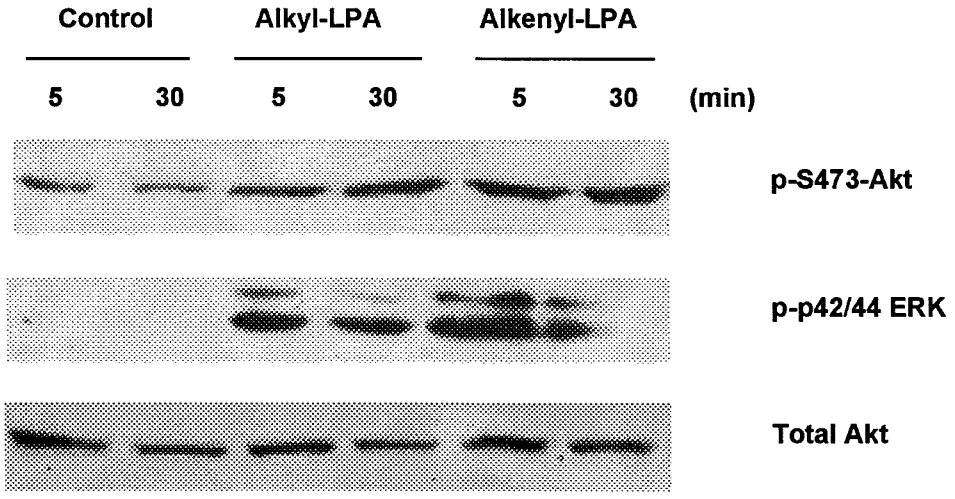
Control
Alkyl-LPA
Alkenyl-LPA
5
30
5
30
5
30
(min)
p-S473-Akt
p-p42/44 ERK
Total Akt

Figure 5A

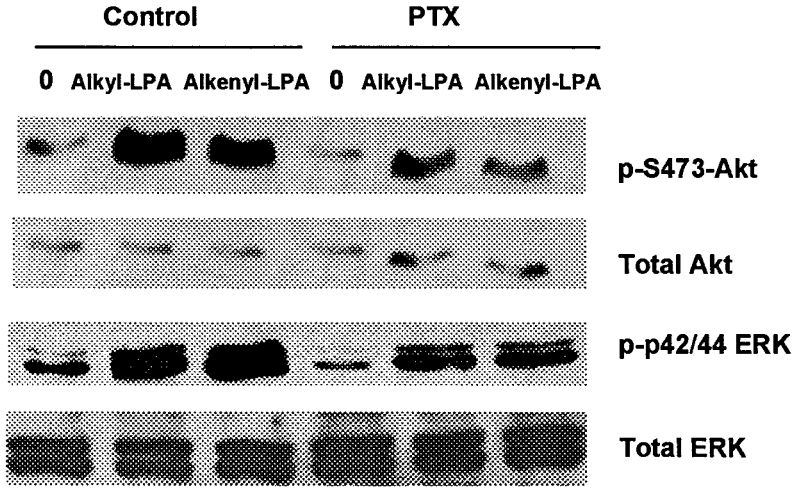

Figure 5B

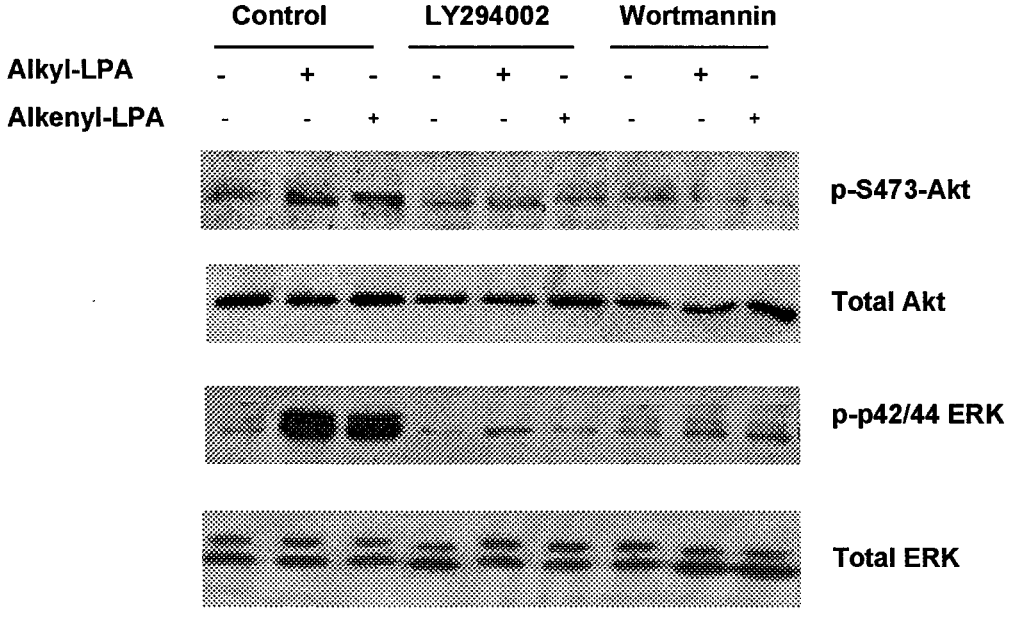

Figure 5C

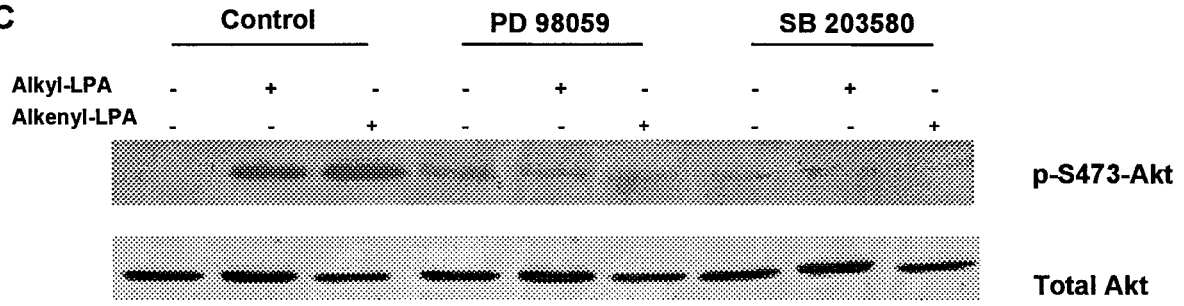

Figure 5D

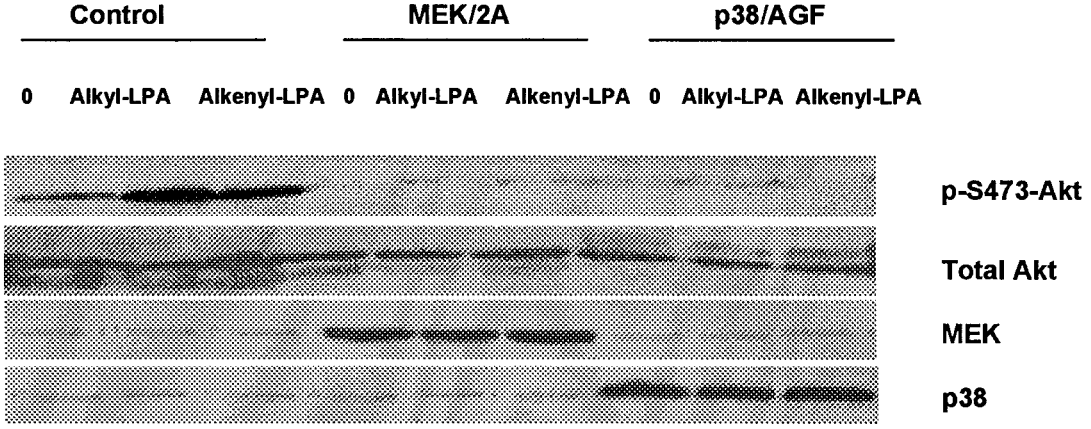

Figure 5E

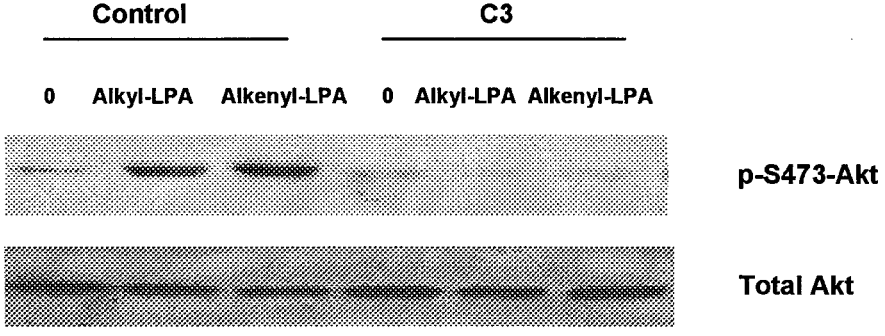

Figure 6A

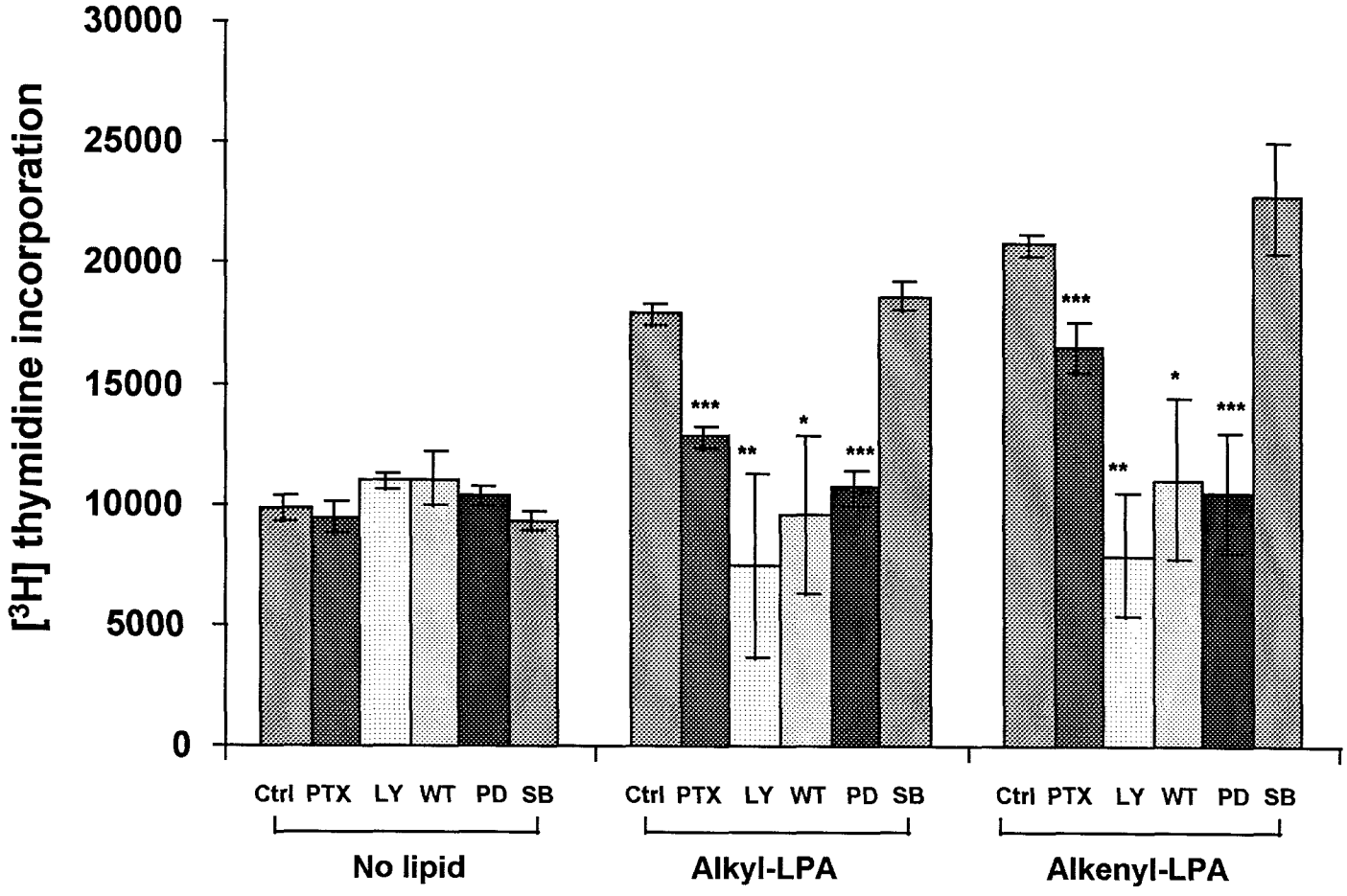
[3H] thymidine incorporation
30000
25000
20000
15000
10000
5000
0
Ctrl PTX LY WT PD SB
No lipid
Alkyl-LPA
Alkenyl-LPA
***
**
*

Figure 6B

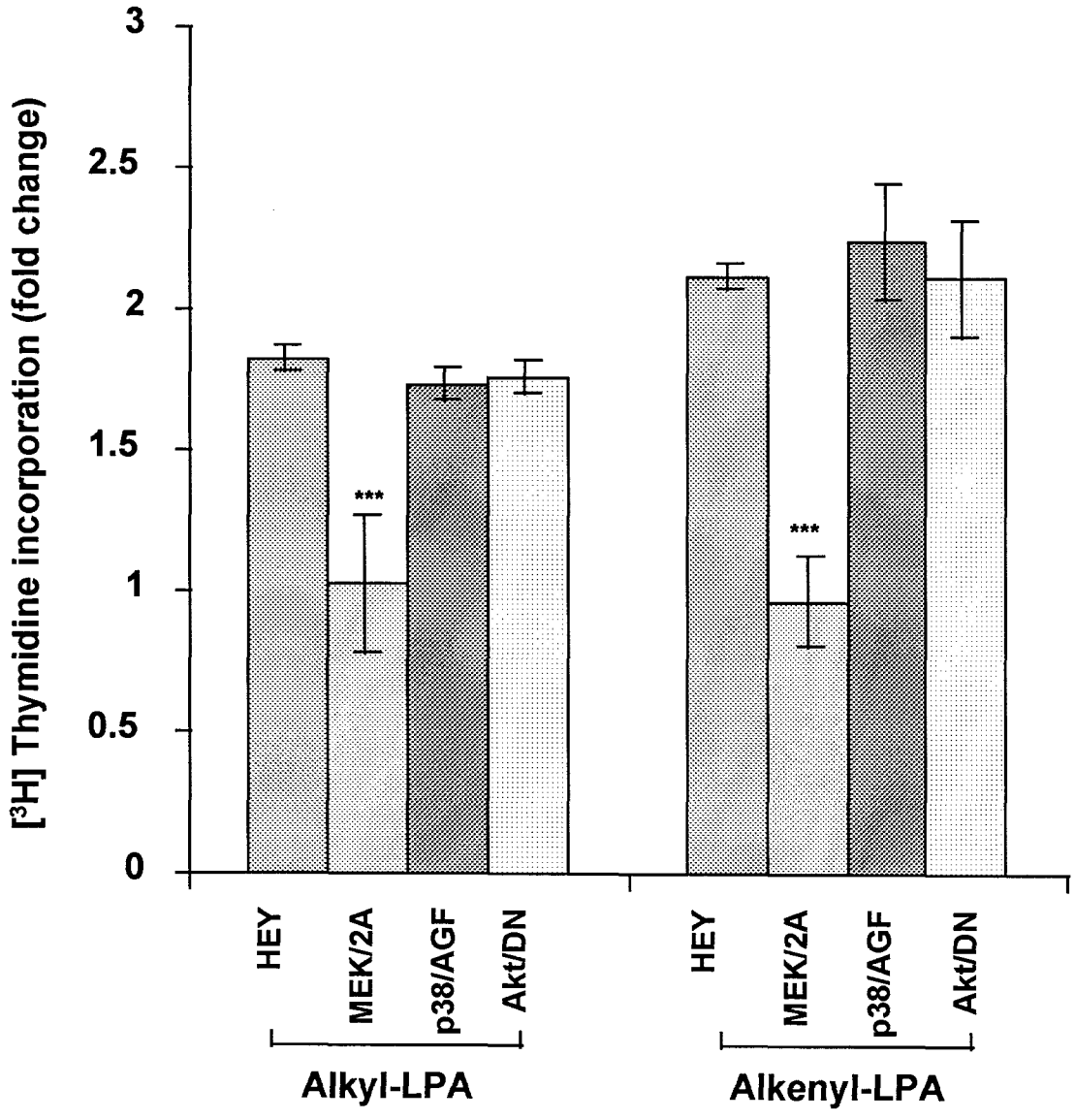
[3H] Thymidine incorporation (fold change)
3
2.5
2
1.5
1
0.5
0
***
***
HEY
MEK/2A
p38/AGF
Akt/DN
HEY
MEK/2A
p38/AGF
Akt/DN
Alkyl-LPA
Alkenyl-LPA

Figure 7A

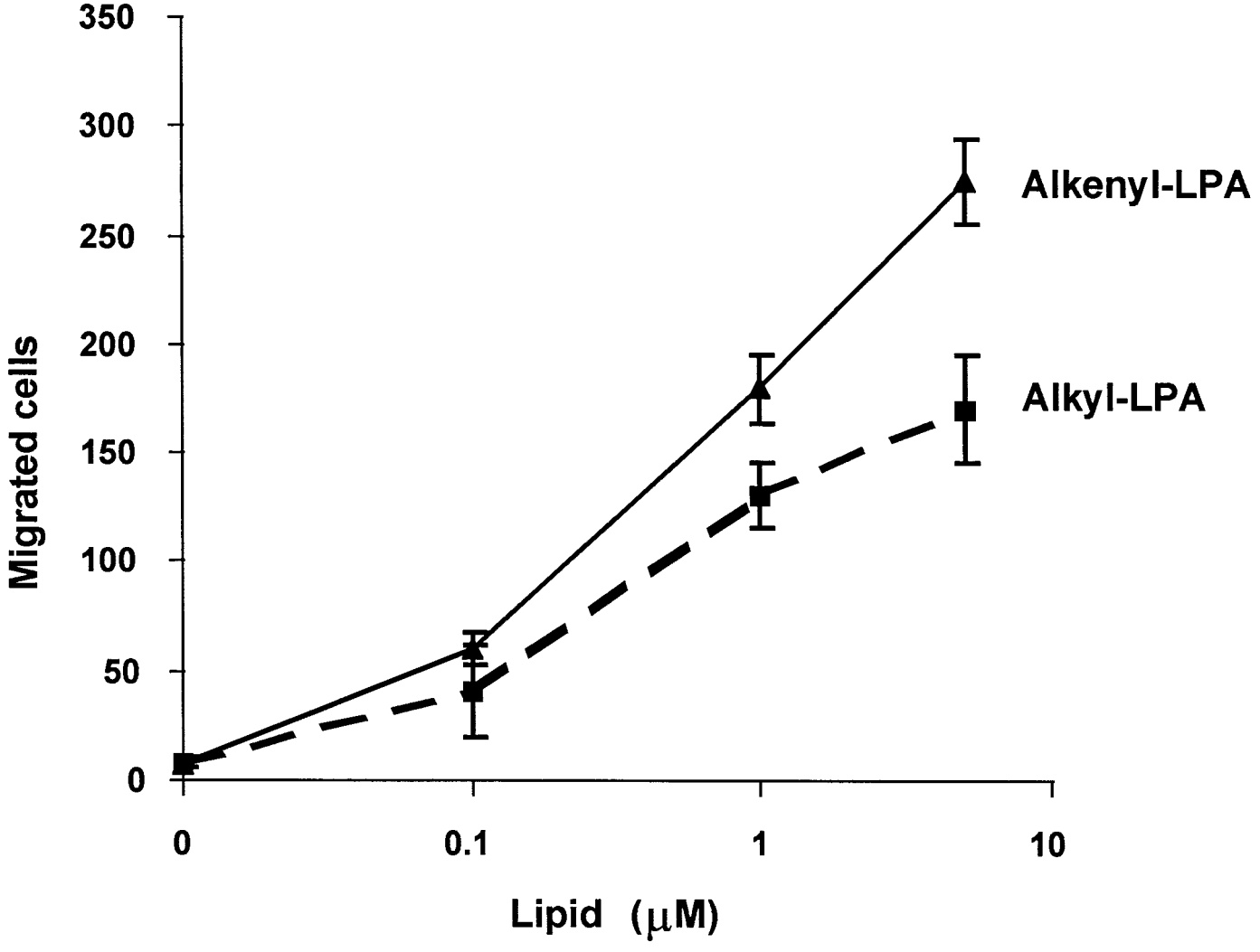
350
300
250
200
150
100
50
0
Migrated cells
0
0.1
1
10
Lipid (μM)
Alkenyl-LPA
Alkyl-LPA

Figure 7B

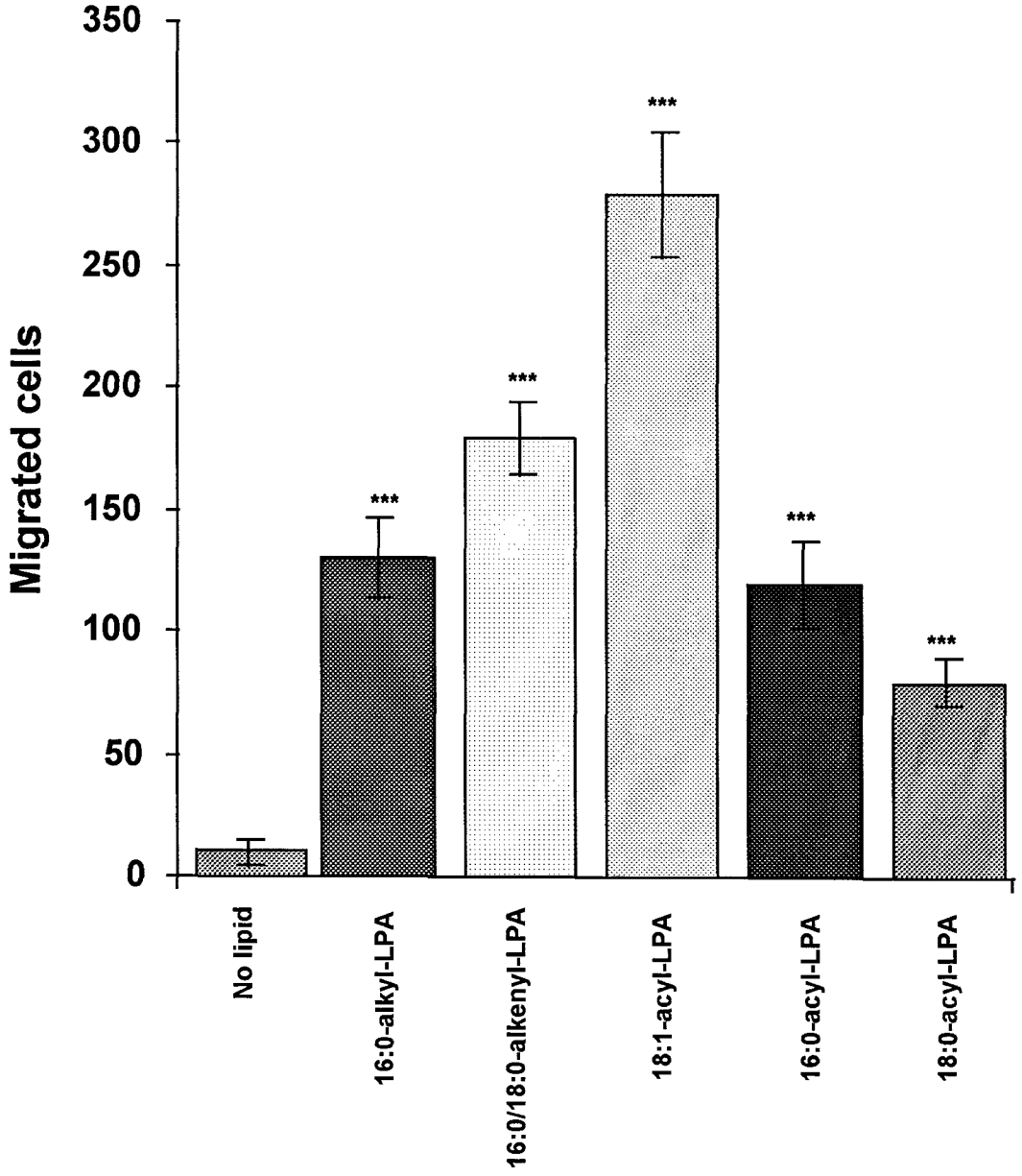
Migrated cells
350
300
250
200
150
100
50
0
***
***
***
***
***
No lipid
16:0-alkyl-LPA
16:0/18:0-alkenyl-LPA
18:1-acyl-LPA
16:0-acyl-LPA
18:0-acyl-LPA

Figure 7C

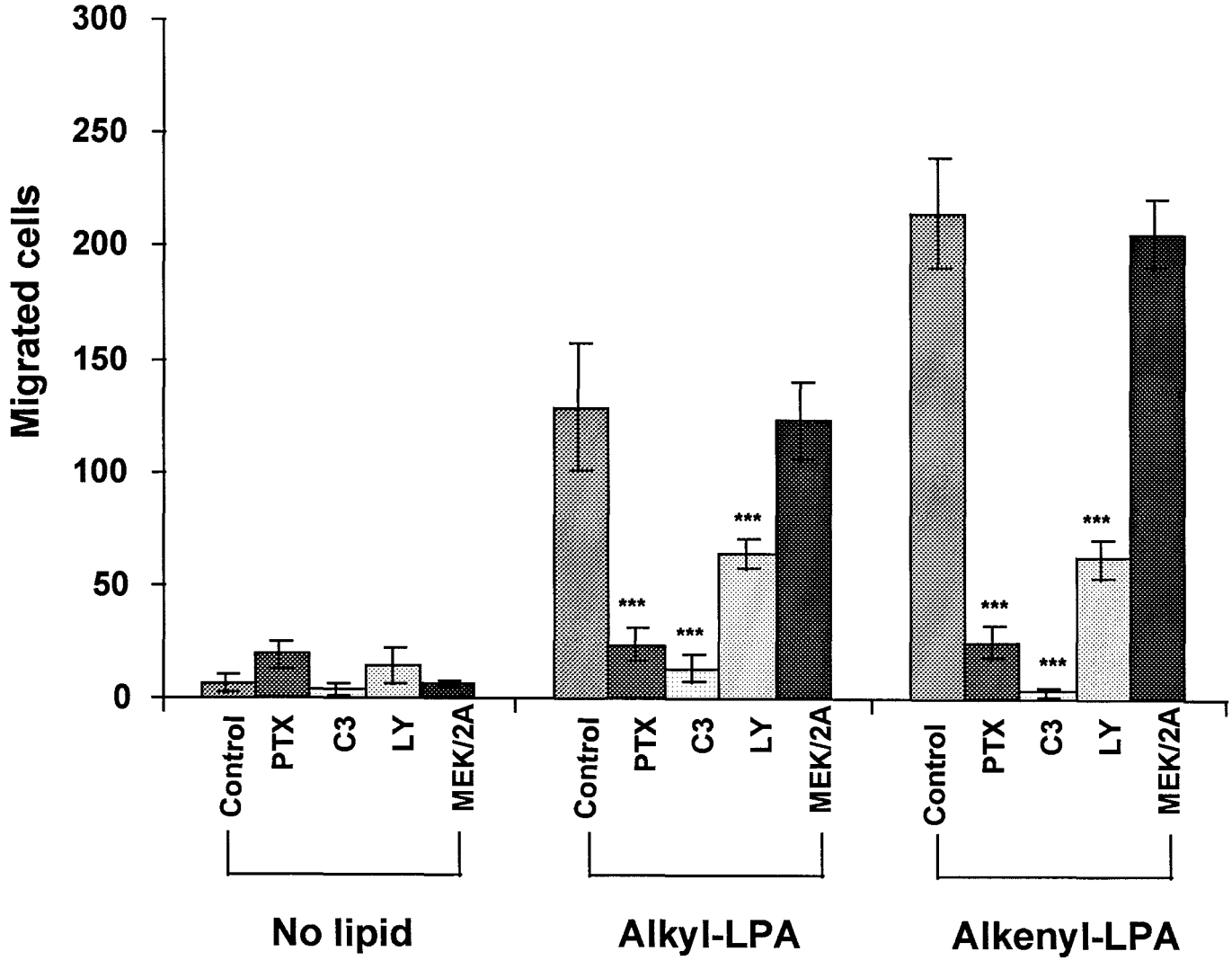
Migrated cells
300
250
200
150
100
50
0
***
Control
PTX
C3
LY
MEK/2A
No lipid
Alkyl-LPA
Alkenyl-LPA

Figure 8

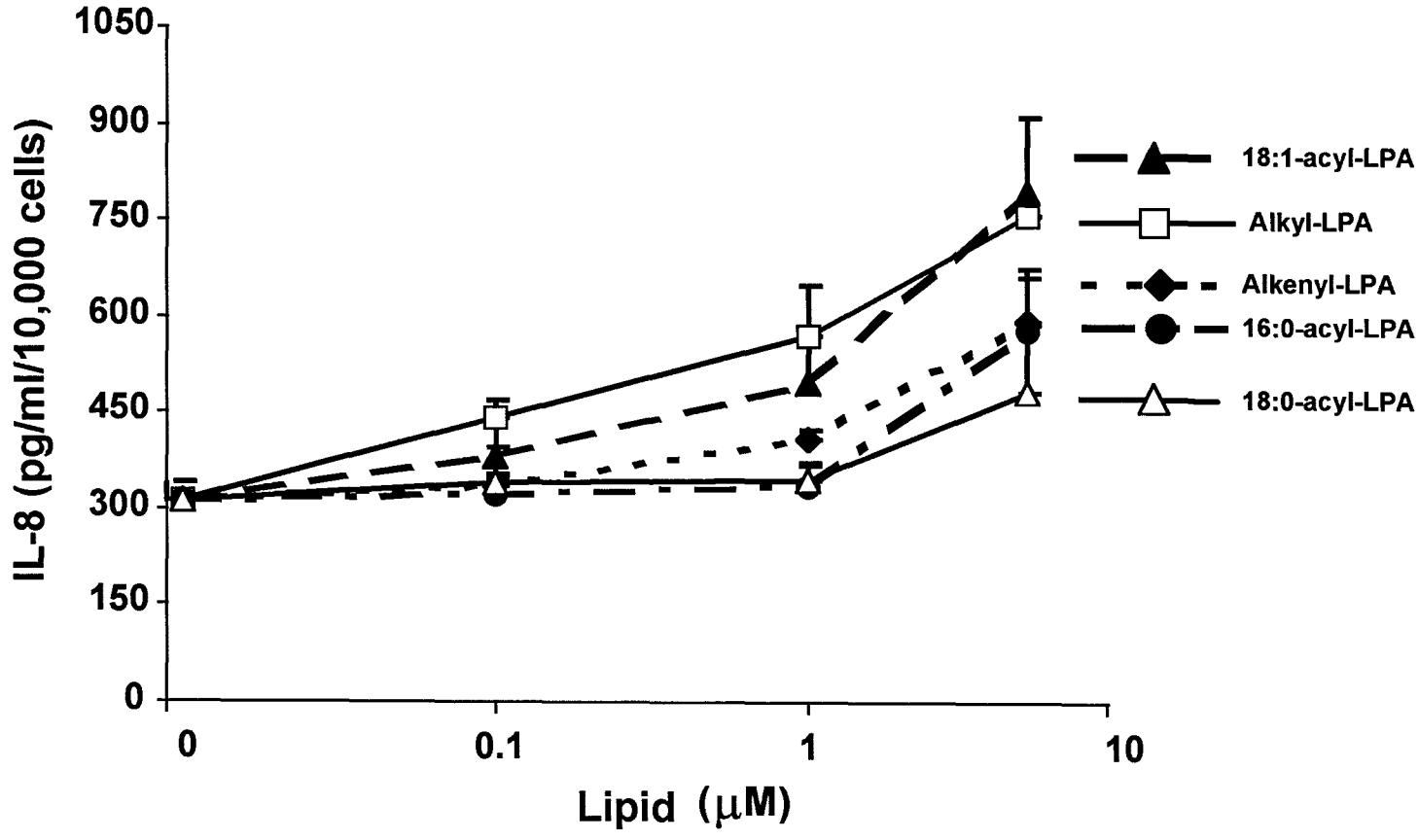
1050
900
750
600
450
300
150
0
IL-8 (pg/ml/10,000 cells)
0
0.1
1
10
Lipid (μM)
18:1-acyl-LPA
Alkyl-LPA
Alkenyl-LPA
16:0-acyl-LPA
18:0-acyl-LPA

THE
FASEB JOURNAL
A MULTIDISCIPLINARY RESOURCE FOR THE LIFE SCIENCES

Experimental Biology 2001®
Orlando, Florida
March 31–April 4, 2001

ABSTRACTS
PART I

Abstracts 2.1–537.42

Official Publication of the Federation of American Societies for Experimental Biology
Volume 15, Number 4, March 7, 2001

190.17

Modulation of nitric oxide synthase and cyclooxygenase 2 by CpG DNA in murine macrophages

Dipak K. Ghosh, Mary Misukonis, Molly Mast, Charles Reigh, David Pisetsky, Joe Brice Weinberg: Duke university &VA Medical center, Medicine/Hem-oncology, 508 fulton street, Durham, NC 27705

Bacterial and synthetic DNA can act an immune stimulators and induce inflammation in vivo. The purpose of this study was to determine the abilities of various phosporothioated, cytosine guanosine-containing DNAs ("CpG-DNA") to activate mouse macrophages for nitric oxide (NO) and prostaglandin E2 (PGE2) production and inducible NO synthase (NOS2) and cyclooxygenase (COX2) expression. As little as 0.3 ug/ml CpG-DNA increased NO and PGE2 production-in a dose- and time-dependent fashion. An oligonucleotide containing 2 CpG sequences ("SAK2") was generally the most potent. NO and PGE2 production was noted by 4 to 8 hours after initiation of cultures with CpG-DNA, with kinetics of NO production for CpG-DNA being comparable to that induced by LPS/IFN-gamma. LPS, IFN-gamma,, or LPS/IFN-gamma did not induce PGE2 production. J774 cells treated with CpG-DNA had enhanced expression of NOS2 and COX2 protein as determined by immunoblot, with the relative potencies of the DNAs corresponding to that noted for induc-tion of NO and PGE2 production, as well as that for induction of IL-6, IL-12, and TNF. Extracts from CpG-DNA-treated cells converted L-arginine to L-citrulline, and this was inhibited by the NOS inhibitor NMMA. The COX2-specific inhibitor NS398 completely inhibited CpG-DNA-induced PGE2 production, but had no effect on NO production. The NOS inhibitors NMMA, 1400W, and L-NIL effectively blocked NO production, but increased production of PGE2 in a dose-dependent fashion. Thus, CpG-DNA activates mouse macrophages for expression of NOS2 and COX2 and production of the pro-inflammatory mediators NO and PGE2.

190.18

The Presentation of Nitric Oxide is Critical in Promoting Monocyte Cell Survival or Apoptosis

Yijie Wang, Andrea Doseff, Pete Mustillo, Philip Nowicki, Clay B. Marsh: The Ohio State University and Dorothy M. Davis Heart and Lung Research Institute, 473 West 12th Ave., Columbus, OH 43210

Monocytes undergo spontaneous apoptosis through activation of caspase-3, a critical cysteine protease involved in the death pathway (J Immunol. 163:1755-62). It has been shown that nitric oxide can inhibit both apoptosis and activation of caspase-3 by S-nitrosylating the active cysteine residue in caspase-3. (J. Biol. Chem. 272:31138-48). Paradoxically, nitric oxide has also been identified as an inducer of apoptosis (Am J Physiol. 277(3 Pt 2):H1189-99). In this context, we hypothesized that the presentation of nitric oxide may determine whether nitric oxide acted as a pro- or anti-apoptotic molecule in human peripheral blood monocytes by either suppressing tyrosine phosphorylation events or inhibiting caspase-3 activity. This hypothesis was tested by the nitrosothiol donor S-nitrosoglutathione (GS-NO), which S-nitrosylates cysteine residues by donating a nitrosyl group to the thiol residue or "NONOates" (1-substituted diazen-1-ium-1, 2-diolates) DEA/NO and PAPA/NO which release nitrogen monoxide and can target tyrosine residues. Monocytes were incubated over a 24-hour period with the nitric oxide donors and measured for their ability to produce NO by using a Seiver 280 chemiluminescence analyzer. Apoptosis was detected in monocytes by DNA fragmentation analysis and measured for caspase-3-like protease activity by measuring the release of AFC from the tetra-fluoro-substrate DEVD-AFC. Despite producing equivalent amounts of NO, GS-NO promoted monocyte survival and suppressed caspase-3-like activity while the NONOates did not. Moreover, NONOates blocked monocyte survival in M-CSF-treated cells and activated caspase-3 like activity, while GSNO did not. Therefore, we provide evidence that the presentation of NO to monocytes can influence pro- or anti-apoptotic effects of NO. Grant support: 1RO1 HL63800. MO1RR00034 ALA Johnie Walker Murphy Career Development Award, Kelly Clark Fund

190.19

Active endothelial nitric oxide synthase is localized at cell-cell contacts

Roland Govers, Lonneke Bevers, Petra de Bree, Elly van Donselaar, Ton J Rabelink, Jan-Willem Slot: UMC Utrecht, Heidelberglaan 100, Utrecht, 3584 CX Netherlands

The enzyme endothelial nitric oxide synthase (eNOS) generates nitric oxide (NO) which is essential for vascular function. Previously, studies have demonstrated that eNOS is localized in the cytosol, Golgi complex and caveolae. By using immunofluorescence and immuno-electron microscopy techniques on a murine microvascular endothelial cell line we show that plasma membrane-resident eNOS is predominantly localized at cell-cell contacts. eNOS is localized at these contacts in detergent-insoluble membrane rafts, while Golgi-localized eNOS is detergent-soluble. The presence of eNOS at the contact sites is important for its activity, since non-confluent endothelial cell layers hardly express eNOS at the plasma membrane and generate less NO than confluent monolayers. Confluent endothelial cells release more than twice the amount of nitrite in the medium compared to non-confluent cells under basal conditions and upon stimulation with calcium ionophore or acetylcholine. This difference in NO production is not due to a change in the total cellular eNOS content, since the amount of eNOS in the cell is not increased when endothelial cell cultures reach confluence. Furthermore, in confluent monolayers the Golgi-disrupting fungal metabolite brefeldin A causes a redistribution of eNOS from the Golgi complex into the cytosol, without affecting its localization at the plasma membrane or its activity. Since cytosolic eNOS is inactive it demonstrates that active eNOS is localized at cell-cell contacts. These findings are highly relevant for the role of NO in vascular physiology. Since NO is essential for increases in endothelial permeability (induced by e.g. leukocyte adhesion, hypoxia, thrombin, VEGF and histamine) our data imply that the presence of eNOS at cell-cell contacts is required for local increases of NO at these sites, resulting in a dynamic and precise regulation of the permeability of the endothelial lining of the vessel wall.

PHOSPHOLIPIDS (191.1-191.2)

191.1

Alkyl and Alkenyl Lysophosphotidic Acid Are Elevated in Peritoneal Washings of Patients with Early and Late Stage Ovarian Cancer

Yi Jin Xiao, Li Song, Benjamin Schwartz, Monique Washington, Alexander Kennedy, Kenneth Webster, Jerome Belinson, Yan Xu: Cleveland Clinic Foundation, 9500 Euclid Ave., Cleveland, OH 44195

We have shown recently that in addition to ester-linked lysophosphatidic acid (LPA), ether-linked LPA species, including alkyl- and alkenyl LPAs (Al-LPAs) are also present in ascitic fluids. In particular, Al-LPAs are elevated in malignant ascites from patients with ovarian cancer, compared with ascites from patients with non-malignant diseases (liver failure or benign gynecological diseases). In this study, we evaluated the levels of various lysolipids in peritoneal washings of patients with ovarian cancer (OvCA), who did not produce ascites, compared with those patients with benign/borderline (BB) and endometrial cancer (EC) lesions. Subjects had an adnexal mass or EC prior to surgery. At laparotomy, 100 ml of saline was placed into the peritoneal cavity. 20 ml was then used for analysis. Lysolipids were extracted, separated on a thin-layer chromatography plate, and directly analyzed for LPAs, Al-LPAs, lysophosphatidylinositol (LPI), and sphingosine-1-phosphate (S1P) using an electrospray ionization mass spectrometry-based method. Statistical analysis was performed with Kruska-Wallis and Wilcoxon tests. Of 26 patients enrolled, 6 had OvCA (4 with Stage IA & 2 with Stage IIIC), 10 had EC (Stage IA or IB), 8 had benign neoplasms, and 2 had borderline ovarian neoplasms. Pair-wise tests demonstrated that Al-LPA levels were elevated in OvCA vs. BB ($p=0.026$), and OvCA vs. EC ($p=0.015$). With 35 nM as a cut-off point, 4 of 4 stage I OvCA (100%) were detected as well as 1 borderline tumor. All EC & benign subjects had normal levels. On the other hand, S1P, LPI, and acyl-LPA levels were not significantly elevated. These results suggest that Al-LPAs are potential useful markers for clinic management of OvCA. We are currently exploring the clinical implications of these findings

191.2

Association of Mg^{2+}-ATPase, Flippase and Scramblase Activities in Human Erythrocytes

David Daleke, Rajeswari Pichika, Michel Julien: Indiana University, Bloomington, Indiana 47405

Transbilayer phospholipid asymmetry in the erythrocyte membrane is regulated in part by two lipid transporters: an inwardly-directed, ATP-dependent aminophospholipid transporter (a flippase) and a Ca^{2+}-activated non-specific transporter (a scramblase) that catalyzes the energy-independent, bi-directional movement of lipids across the membrane. A Mg^{2+}-ATPase that may play a role in flippase activity has been purified from detergent-solubilized human erythrocyte membranes. Polyclonal antisera obtained from mice immunized with this ATPase inhibits the purified Mg^{2+}-ATPase in detergent-phospholipid micelles and both flippase and scramblase activities in intact erythrocyte membranes. Immunoglobulins purified from the anti-Mg^{2+}-ATPase antisera also inhibit the activities of these enzymes. In addition, monoclonal hybridomas generated from mice immunized with the purified Mg^{2+}-ATPase yield subsets of antibodies that inhibit 1) both ATPase and the flippase activity, 2) only one or the other of these activities, or 3) neither enzyme. The epitopes recognized by the inhibitory antibodies are cytofacial; anti-Mg^{2+}-ATPase antisera inhibits the activity of the cytofacially-exposed fraction of the Mg^{2+}-ATPase reconstituted into proteoliposomes. When added to erythrocyte ghosts prior to resealing, the antisera and the purified antibodies inhibit both phosphatidylserine transport and scramblase activity. However, when added to intact erythrocytes or to previously resealed ghosts, the antisera have no effect, indicating that the anti-transporter antibodies recognize epitopes on the cytosolic face of the membrane. These data suggest that the Mg^{2+}-ATPase is associated with aminophospholipid flippase activity and that the scramblase and flippase might be closely linked.

FASEB Experimental Biology 2001 Meeting, Orlando, Florida March 31-April 4, 2001

Identification of the first two high affinity receptors for Sphingosylphosphorylcholine (SPC) and the first receptor for Lysophosphatidylcholine (LPC)

Kui Zhu‡, Linnea M. Baudhuin‡¶, Guiying Hong‡, Freager S. Williams, Kelly L. Cristina, Janusz H.S. Kabarowski#, Owen N. Witte# and Yan Xu‡†*,
‡Department of Cancer Biology, †Department of Gynecology and Obstetrics, Cleveland Clinic Foundation, 9500 Euclid Ave., Cleveland OH 44195. ¶Department of Chemistry, Cleveland State University, 24th and Euclid Ave, Cleveland OH 44115. #Department of Microbiology, Immunology and Molecular Genetics, Howard Hughes Medical Institute, University of California, Los Angeles, Los Angeles, CA 90095-1662.

Sphingosylphosphorylcholine (SPC) and lysophosphatidylcholine (LPC) are bioactive lipid molecules sharing structural similarity and involved in numerous biological processes. We have recently identified ovarian cancer G protein coupled receptor 1 (OGR1) as a specific and high affinity receptor for SPC (Xu, Zhu et al, Natuare Cell Biol. 2, 261, 2000). Among G protein coupled receptors (GPCRs), GPR4 shares highest sequence homology (51%) with OGR1. In this work, we have identified GPR4 as not only a high affinity receptor for SPC, but also a receptor for LPC with a relative low affinity. Both SPC (EC_{50}=105 nM) and LPC (EC_{50}=1.1 μM) induce increases in intracellular calcium in GPR4-, but not vector-transfected, MCF10A cells. These effects are insensitive to the treatment of BN52021 (a specific PAF receptor antagonist), suggesting that they are not mediated through an endogenous PAF receptor. HEK293 cells transfected with GPR4 respond to SPC and, to a lesser extent, LPC, in serum responsive element (SRE) reporter assays. SPC binds to GPR4 in GPR4-transfected CHO cells with high affinity (K_d=35.9 nM), with competitive binding elicited by only SPC and LPC. In GPR4-transfected HEK293 cells, both SPC and LPC, but not platelet activating factor (PAF), lyso-PAF, lysophosphatidic acid (LPA) or sphingosine-1-phosphate (S1P), induce internalization of the receptor (receptor-GFP fusion). SPC regulates diverse cellular functions, include both cell proliferation and growth inhibition, smooth muscle contraction and wound healing. LPC plays an important role in atherosclerosis and inflammatory diseases by affecting various aspects of a variety of cell types involved in these diseases. However, the signaling mechanisms of LPC have not been studied extensively. The identification of GPR4 as the first LPC receptor and further studies on the role of GPR4 and its related genes in the development of atherogenesis and other inflammatory diseases will add important information to our understanding of these diseases.

* To whom correspondence should be addressed. Phone (216) 444-1168; fax: (216) 445-6269; E-mail: xuy@ccf.org

FASEB Summer Research Conference-Lysophospholipids and Related Bioactive Lipids in Biology & Diseases. Tucson, AZ (6/10/01).

Roles of Ether-linked Lysophosphatidic Acid in Ovarian Cancer Cells

Jun Lu*, Yi-Jin Xiao*, and Yan Xu*#

*Department of Cancer Biology, Lerner Research Institute, Cleveland Clinic Foundation, 9500 Euclid Ave., Cleveland, OH 44195, USA

#Department of Gynecology and Obstetrics, Cleveland Clinic Foundation, 9500 Euclid Ave., Cleveland, OH 44195, USA

ABSTRACT

Lysophosphatidic acid (LPA) is involved in many biological processes, including cell survival, growth, migration and differentiation. We have recently reported that ether-linked LPAs (alkyl- and alkenyl-LPAs) are present at elevated levels in ascites from patients with ovarian cancer, when compared with ascites from patients with non-malignant diseases. Since ascitic fluid in cancer patients represents an *in vivo* environment for ovarian cancer cells, the presence of large amounts of alkyl- and alkenyl-LPAs suggests that they play a potential pathological role in the development of ovarian cancer. In the present study, we found that alkyl- and alkenyl-LPAs were more stable than acyl-LPAs in ascites. These lipids stimulated DNA synthesis and proliferation of ovarian cancer cells through G_i, phosphatidylinositol-3 kinase (PI3-K). and ERK-dependent pathways. They also induced migration of ovarian cancer cells through the collagen I-coated membrane. This activity required the activation of Rho and was partially dependent on Akt activation. In addition, alkyl- and alkenyl-LPAs stimulated interleukin-8 (IL-8) production. Together, these results implicated that both alkyl- and alkenyl-LPAs may play important pathological and physiological roles in ovarian cancer growth and metastasis.

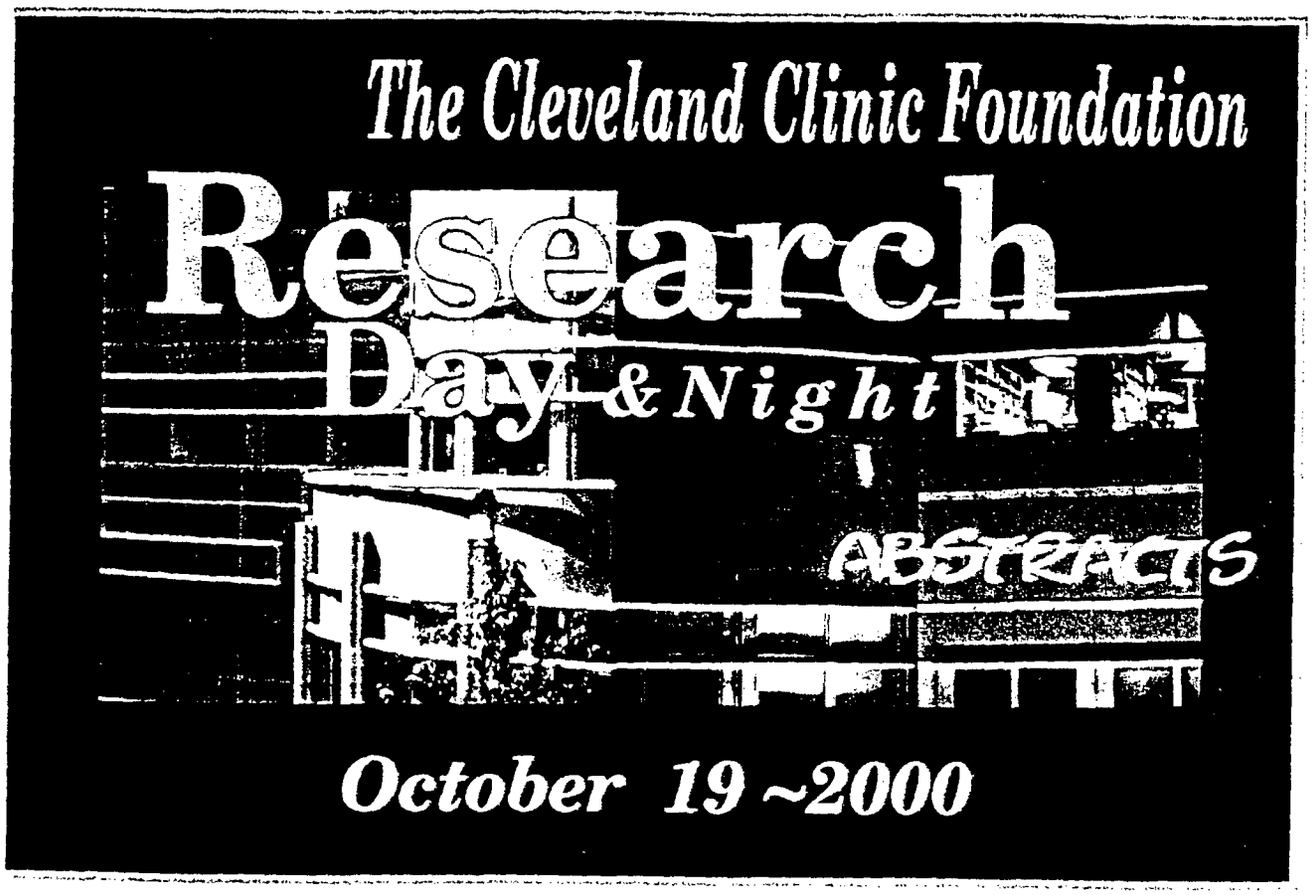
The Cleveland Clinic Foundation
Research
Day & Night
ABSTRACTS
October 19 ~2000

Sphingosylphosphorylcholine is a ligand for ovarian cancer G-protein-coupled receptor 1

Yan Xu, Kui Zhu, Guiying Hong, Weihua Wu, Linnea M. Baudhuin, Yijin Xiao and Derek S. Damron

Sphingosylphosphorycholine (SPC) is a bioactive lipid that acts as an intracellular and extracellular signalling molecule in numerous biological processes. Many of the cellular actions of SPC are believed to be mediated by the activation of unidentified G-protein-coupled receptors. Here we show that SPC is a high-affinity ligand for an orphan receptor, ovarian cancer G-protein-coupled receptor 1 (OGR1). In OGR1-transfected cells, SPC binds to OGR1 with high affinity (K_d=33.3nM) and high specificity and transiently increases intracellular calcium. The specific binding of SPC to OGR1 also activates p42/44 mitogen-activates protein kinases (MAP kinases) and inhibits cell proliferation. In addition, SPC causes internalization of OGR1 in a structually specific manner. Based on our results, we show for the first time the identification of a high-affinity and specific receptor for SPC.

Up-regulation and Activation of Akt2 by Bioactive Lysolipids in Ovarian Cancer

Linnea M. Baudhuin[1,3] and Yan Xu[1,2,3]

[1]Department of Cancer Biology, Cleveland Clinic Foundation, 9500 Euclid Avenue, Cleveland, OH, 44195; [2]Department of Gynecology and Obstetrics, Cleveland Clinic Foundation, 9500 Euclid Avenue, Cleveland, OH, 44195; [3]Department of Chemistry, Cleveland State University, 24th and Euclid Avenue, Cleveland, OH, 44115

The structurally related bioactive lysolipids, lysophosphatidic acid (LPA), sphingosine-1-phosphate (S1P), and sphingosylphosphorylcholine (SPC) have been shown to affect the growth and invasiveness of ovarian cancer cells. All three of these lipids have been detected in the ascitic fluid and/or plasma of patients with ovarian cancer. Akt2 (PKBβ, RAC-PKβ) is an oncogene that regulates specific apoptotic proteins and is amplified with high frequency in ovarian, breast, and pancreatic carcinomas. With the aid of GeneChip analyses, we show that S1P regulates increased mRNA expression of Akt2 in the HEY ovarian cancer cell line. Using quantitative RealTime RT-PCR, we confirm that S1P, and additionally LPA and SPC, regulate increases in Akt2 mRNA expression in ovarian cancer cells in a time- and dose-dependent manner. Furthermore, by detection of serine 473 phosphorylated Akt2, we show that LPA, S1P, and SPC activate Akt2 in HEY cells. With the use of specific inhibitors, we further demonstrate that this activation of Akt2 is dependent on G_i, phosphatidylinositol 3-kinase (PI3-K), and phospholipase C (PLC).

Overexpression of the OGR1 in HEK293 Cells Inhibite Cell Growth, Migration and Spreading

Guiying Hong, Linnea Baudhuin, and Yan Xu

Cancer Biology Department

We recently described the identification of the ligand (sphingosylphosphorylcholine, SPC) for an orphan G protein coupled receptor, OGR1 (Xu et al., Nature Cell Biology, 2, 2000, 261-267). To explore the potential cellular functions of OGR1 and its ligand, we established an OGR1-induible system (the ecdysone-indusible system, Invitrogen) in HEK293 cells. We found that overexpression of OGR1, even in the absence of its ligand, had profound effect on cell growth, spreading and migration, and the ligand (SPC) further enhance these effects. Induction of OGR1 induced inhibitions of cell growth (10-57%), cell spreading on tissue culture dishes (20-60%), and cell migration through FN in Boyden Chambers (decreased for 4-fold) in a OGR1 expression level-dependent manner. The mechanisms of these inhibitions are under investigation. Our preliminary results suggest that AKT2, integrins and FAK may be involved.

Activation of RNase L by 2',5'-Oligoadenylates Regulates MAP Kinases: Implications for IFN- and Viral-Mediated Apoptosis

Geqiang Li and Robert H. Silverman
Department of Cancer Biology,
Lerner Research Institute

RNase L is a uniquely-regulated endoribonuclease that functions in the anti-viral and apoptotic activities of type I IFNs. IFN treatment of mammalian cells induces a family of 2-5A synthetases that produce 2'-to-5' linked oligoadenylates (2-5A) in response to viral double stranded RNA (dsRNA). The inactive, monomeric form of RNase L is converted to its active, dimeric form after binding to 2-5A leading to degradation of cellular and viral RNA. Recently, we reported that stimulation of c-Jun NH2-terminal kinase (JNK) and its upstream activator kinase, MKK4, by dsRNA were both deficient in RNase $L^{-/-}$ cells (Iordanov, M. et al. *Mol. Cell. Biol.* 20, 617, 2000). We have now extended these findings by directly implicating RNase L in the activation of JNK1 and JNK2. Transfection of human ovarian carcinoma cells (HeyIB) with 2-5A [ppp(A2'p)$_n$A, n = 2 to 6] caused activation of RNase L resulting in characteristic rRNA cleavage products. In the presence of 2-5A and the protein synthesis inhibitor, cycloheximide (CHI), there was also a potent activation of JNK1 and JNK2. In contrast, the dimeric form of 2-5A (pppA2'p5'A) failed to activate RNase L and failed to activate JNKs in the presence or absence of CHI. In addition, stimulation of the extracellular regulated kinase, ERK2, was suppressed by 2-5A activation of RNase L. Because JNKs are linked to apoptosis and ERK2 to growth or cell survival signals, the result of both activating JNK and inhibiting ERK2 will be to promote cell death. We previously showed that apoptosis by both viral and non-viral agents is deficient in RNase $L^{-/-}$ cells and mice and 2-5A transfection of mammalian cells causes apoptosis (Zhou et al., EMBO J. 16, 6355-6363, 1997). Therefore, the regulation of the JNK and ERK MAP kinases by RNase L is likely to provide some of the cell death signals triggered by IFNs and viral double stranded RNA.

Electrospray Ionization Mass Spectrometry Analysis of Lysophospholipids in Human Ascitic Fluids: Comparison of the Lysophospholipid Contents in Malignant and Non-malignant Ascitic Fluids

Yi-Jin Xiao, Benjamin Schwartz, Monique Washington, Alexander Kennedy, Kenneth Webster, Jerome Berlinson and Yan Xu

Lysophospholipids(lyso-PLs), including various glycerol-based and sphingosine-based lysophospholipids, play important roles in many biochemical, physiological and pathological processes. The classical methods to analyze these lipids involve gas-chromatography and/or high-performance liquid chromatography (HPLC), which are time-consuming, cumbersome and sometimes inaccurate due to the incomplete separation of closely related lipid species. We now describe the quantitative analysis of lyso-PLs in ascites samples from patients with ovarian cancer using electrospray ionization spectrometry (ESI-MS). Three new classes of lyso-PL molecules are detected: alkyl-LPA, alkenyl-LPA and methylated lysophosphatidylethanolamine(LPE). Importantly, the following lysophospholipid species are significantly increased in ascites from patients with ovarian cancer, compared to patients with non-malignant diseases(liver failure): LPA(including acyl-, alkyl- and alkenyl-LPA species), Lysophosphatidylinositol(LPI) and sphingosylphosporylcholing(SPC). Lysophosphorylcholing(LPC) contents are also significantly different among ascitic fluids from the two groups of patients. However, the total phosphate in ascites samples from patients with ovarian cancer are not significantly different compared to that from patients with non-malignant disease.

The Dual Effect of Sphingosine-1-Phosphate on Cell Migration

Guiying Hong and Yan Xu

Sphingosine-1-phosphate (S1P) is a bioactive lysophospholipid that acts as an extracellular and intracellular messenger. We reported previously that S1P modulates both growth and adhesion of ovarian cancer cells (Hong et al.,FEBS Letters, 460,1999, 513-518). In this study, we showed that S1P regulates cell migration/invasion in a cell type specific manner in Boyden chamber assays. S1P (0.2 μM) inhibited chemotactic migration of HEK293 cells (5-fold) and human leukemia Jurkat cells (6-fold), but stimulated the migration/invasion of ovarian cancer cells (HEY and OCC1), although the stimulation was ≤2-fold. The basal levels (chemokinetics) of migration/invasion (when the culture medium and S1P were present in both the upper and lower chambers) of HEY and OCC1 cells were dependent on the composition of the extracellular matrix proteins. HEY cells are more invasive than OCC1 *in vivo*. Nonetheless, HEY and OCC1 cells showed similar rates of migration through laminin-coated membranes. However, HEY cells migrated 1.6-fold and 50-fold faster than OCC1 cells when the Boyden chamber membranes were coated with collagen I and fibronectin, respectively. S1P (0.2 μM) stimulated a 2-fold migration of OCC1 cells through laminin, as compared to the control. Both the basal and S1P-stimulated migration of HEY cells through collagen I, fibronectin, and to a lesser extent, laminin, were inhibited by RGD peptide, suggesting the involvement of RGD-containing integrin(s) in these processes. Since S1P is present in the ascites of patients with ovarian cancer (Hong et al.,FEBS Letters, 460,1999, 513-518), studying the mechanism of S1P-regulated tumor cell invasion will provide important information on ovarian tumor metastasis.

Biological Effects of Alkyl- and Alkenyl-lysophosphatidic Acids in Ovarian Cancer Cells

Jun Lu, Kui Zhu, and Yan Xu

Lysophosphatidic acids (LPAs) are composed of acyl-, alkyl-, and alkenyl-LPA species and they are extracellular signaling molecules acting through G protein-coupled receptors. Our lab recently found that alkyl- and alkenyl-lysophosphatidic acids (alkyl-LPA and alkenyl-LPA) were significantly elevated in ascites from patients with ovarian cancer, compared with patients with non-malignant diseases. In HEY ovarian cancer cells, both alkyl-(16:0) and alkenyl-(16:0/18:0) LPAs induced proliferation, whereas their counterparts, acyl-LPAs (16:0 and 18:0), showed antiproliferative activity at high concentrations (>=5 μM). Alkyl- and alkenyl-LPAs activated Akt2 (protein kinase B) through phosphorylation of Ser 473, which could be inhibited by phosphoinositide 3-kinase (PI3K) inhibitors. In addition, alkyl- and alkenyl-LPAs induced transient increases in intracellular Ca^{2+} in HEY cells. To determine whether acyl-, alkyl- and alkenyl-LPAs activate the same or different receptors, heterologous desensitization was conducted among them by monitoring changes in intracellular Ca^{2+}. While acyl-LPAs (16:0, 18:0, and 18:1) desensitized each other, they did not desensitize the calcium induced by either alkyl or alkenyl-LPAs, suggesting the latter two sub-groups of LPAs may activate different receptors. Together, these results suggest that alkyl- and alkenyl-LPA may play an important role in ovarian cancer development through activating distinct receptor(s) from acyl-LPAs in HEY cells.